THEORETICAL INVESTIGATION ON THE DEVELOPMENT OF NEW AROMATIC SYSTEMS AND THEIR APPLICATIONS

A Thesis submitted to the University of North Bengal

For the Award of

Doctor of Philosophy

in

Chemistry

By

Manoswita Homray

Guide

Prof. Anirban Misra

Department of Chemistry

University of North Bengal

December-2020

DECLARATION

I declare that the thesis entitled **"THEORETICAL INVESTIGATION ON THE DEVELOPMENT OF NEW AROMATIC SYSTEMS AND THEIR APPLICATIONS"** has been prepared by me under the guidance of Dr. Anirban Misra, Professor of Chemistry, University of North Bengal. No part of this thesis has formed the basis for the award of any degree or fellowship previously.

Manoswita Homray

Manoswita Homray
Department of Chemistry,
University of North Bengal,
Darjeeling-734013
West Bengal
India

DATE: 07.12.2020

ENLIGHTENMENT TO PERFECTION

UNIVERSITY OF NORTH BENGAL

Accredited by NAAC with Grade A

DEPARTMENT OF CHEMISTRY

P.O. NORTH BENGAL UNIVERSITY, Raja Rammohunpur, Dist. Darjeeling, West Bengal, India, PIN - 734013.
PHONE : (0353) 2776 381, Fax: (0353) 2699 001

Ref. No..... *Dated.....20.....*

CERTIFICATE

I certify that **MANOSWITA HOMRAY** has prepared the thesis entitled **"THEORETICAL INVESTIGATION ON THE DEVELOPMENT OF NEW AROMATIC SYSTEMS AND THEIR APPLICATIONS"**, for the award of PhD degree of the University of North Bengal, under my guidance. She has carried out the work at Department of Chemistry, University of North Bengal. No part of this thesis has formed the basis for the award of any degree or fellowship previously.

7.12.2020

Dr. Anirban Misra,
Professor,
Department of Chemistry,
University of North Bengal,
Darjeeling-734013
West Bengal
India

Prof. ANIRBAN MISRA
Head Department of Chemistry
University of North Bengal
Darjeeling - 734013, India

URKUND

Urkund Analysis Result

Analysed Document:	Manoswita Homray_Chemistry.pdf (D84591831)
Submitted:	11/10/2020 7:04:00 AM
Submitted By:	nbuplg@nbu.ac.in
Significance:	3 %

Sources included in the report:

https://en.wikipedia.org/wiki/Aromaticity
https://www.researchgate.net/scientific-contributions/38552307_Pratim_Kumar_Chattaraj
https://www.researchgate.net/publication/229981428_Multicenter_bond_indices_as_a_new_measure_of_aromaticity_in_polycyclic_aromatic_hydrocarbons
https://www.researchgate.net/publication/230879951_Molecular_structures_of_M2N22-_M_and_N_B_Al_and_Ga_clusters_using_the_gradient_embedded_genetic_algorithm
https://www.researchgate.net/publication/269042140_A_DFT_Study_on_the_Stability_and_Aromaticity_of_Heterobenzenes_Containing_Group_15_Elements
https://www.researchgate.net/publication/260284723_Chemical_Bonding_in_Coronene_Isocoronene_and_Circumcoronene
https://www.researchgate.net/publication/11645340_Measuring_Aromaticity_by_NMR
https://www.diva-portal.org/smash/get/diva2:1152985/FULLTEXT01.pdf

Instances where selected sources appear:

45

Manoswita Homray
07.12.2020

7.12.2020

Prof. ANIRBAN MISRA
Head Department of Chemistry
University of North Bengal
Darjeeling - 734013, India

ENLIGHTENMENT TO PERFECTION

UNIVERSITY OF NORTH BENGAL

Accredited by NAAC with Grade A

DEPARTMENT OF CHEMISTRY

P.O. NORTH BENGAL UNIVERSITY, Raja Rammohunpur, Dist. Darjeeling, West Bengal, India, PIN - 734013.
PHONE : (0353) 2776 381, Fax: (0353) 2699 001

Ref. No..... *Dated.....20.....*

CERTIFICATE

I certify that **MANOSWITA HOMRAY** has prepared the thesis entitled **"THEORETICAL INVESTIGATION ON THE DEVELOPMENT OF NEW AROMATIC SYSTEMS AND THEIR APPLICATIONS"**, for the award of PhD degree of the University of North Bengal, under my guidance. She has carried out the work at Department of Chemistry, University of North Bengal. No part of this thesis has formed the basis for the award of any degree or fellowship previously.

7.12.2020

Dr. Anirban Misra,
Professor,
Department of Chemistry,
University of North Bengal,
Darjeeling-734013
West Bengal
India

Prof. ANIRBAN MISRA
Head Department of Chemistry
University of North Bengal
Darjeeling - 734013, India

URKUND

Urkund Analysis Result

Analysed Document:	Manoswita Homray_Chemistry.pdf (D84591831)
Submitted:	11/10/2020 7:04:00 AM
Submitted By:	nbuplg@nbu.ac.in
Significance:	3 %

Sources included in the report:

https://en.wikipedia.org/wiki/Aromaticity
https://www.researchgate.net/scientific-contributions/38552307_Pratim_Kumar_Chattaraj
https://www.researchgate.net/publication/229981428_Multicenter_bond_indices_as_a_new_measure_of_aromaticity_in_polycyclic_aromatic_hydrocarbons
https://www.researchgate.net/publication/230879951_Molecular_structures_of_M2N22-_M_and_N_B_Al_and_Ga_clusters_using_the_gradient_embedded_genetic_algorithm
https://www.researchgate.net/publication/269042140_A_DFT_Study_on_the_Stability_and_Aromaticity_of_Heterobenzenes_Containing_Group_15_Elements
https://www.researchgate.net/publication/260284723_Chemical_Bonding_in_Coronene_Isocoronene_and_Circumcoronene
https://www.researchgate.net/publication/11645340_Measuring_Aromaticity_by_NMR
https://www.diva-portal.org/smash/get/diva2:1152985/FULLTEXT01.pdf

Instances where selected sources appear:

45

Manoswita Homray
07.12.2020

7.12.2020

Prof. ANIRBAN MISRA
Head Department of Chemistry
University of North Bengal
Darjeeling - 734013, India

ABSTRACT

The first chapter takes us in a journey of the concept of aromaticity since its inception days. The genesis of the concept of aromaticity, its chronological advancement, the problem with its proper quantification, the different criteria to quantify it and the lack of single unified criteria which makes it an important and relevant field of study is thoroughly discussed. The novel idea of exo-cyclic aromaticity is devised. The idea of aromaticity is extended beyond the domain of organic chemistry to all metal aromatic clusters and how bond stretch isomers plays an important role in these clusters is considered. Importance of aromaticity in DNA nucleobases is highlighted with reference to its biological applications.

The second chapter provides a concise description of the basic theoretical background related to the study of aromaticity. The discussion is centred on the various indices of quantification of aromaticity such as Nucleus Independent Chemical Shifts (NICS), Dissected Canonical Molecular Orbital NICS (CMO-NICS), Multi-centre indices, Electron Localization Function (ELF) and Aromatic Stabilization Energy (ASE) emphasizing on the significance of quantification of aromaticity. A brief background of the stability indices namely the Energy Decomposition Analysis (EDA), Ring Strain Energy (RSE), Adaptive Natural Density Partitioning (AdNDP) Analysis and Atom Centered Density Matrix Propagation (ADMP) is provided. The reactivity parameters involving the conceptual Density Functional Theory including both the global and local reactivity parameters (Fukui functions) are elaborately discussed.

In the third chapter, a mini review study regarding the most important criteria for defining aromaticity i.e., the magnetic criteria is comprehensively covered. Magnetic criteria of aromaticity have been analyzed which are currently the most popular methods, considering the circular delocalization of electrons as the genesis of aromaticity. The various magnetic measures for defining aromaticity such as NMR chemical shifts which include ^{1}H NMR shifts as well as Li^{+} NMR chemical shifts, Magnetic Susceptibility Anisotropy, Current Density Analysis Plots (CDA) and Nucleus Independent Chemical Shifts are explicitly discussed. The NMR chemical shift is explained with the help of the Ring Current Model (RCM) and both experimental and computational applications are also discussed. Magnetic

Susceptibility Anisotropy and its applicability as a magnetic criterion have been elaborated accordingly. A pictorial representation of Current density Analysis Plots and its relevance as a magnetic criterion have also been accounted for. Special attention is given to the NICS criteria, explaining the role of ghost atom, considering it to be the most popular magnetic criterion. Advantages and disadvantages of all the methods along with recent advances are discussed.

The domain of aromaticity spans a wide range of molecules, from polycyclic aromatic hydrocarbons, heterocycles to all-metal systems. So, in the fourth chapter *in silico* we demonstrate the aromaticity in $C_2B_2F_4$, extending beyond the limit of conventional aromatic molecules. This molecule gains the magic number of six π-electrons through an unusual electronic contribution from *exo*-cyclic atoms. The stability of the molecule is established through density functional theory, *ab initio* calculations as well as molecular dynamics simulation.

In the fifth chapter, manifestation of exocyclic aromaticity is further established in novel heteroatomic molecular systems which demonstrate non-conventional aromaticity where the molecules accomplish the *aromatic sextet* and hence stabilization through the conjugation of π-electrons from the exo-cyclic substituents. A considerable σ-aromaticity is also observed which does not involve the exo-cyclic atoms. At first, the stability of these molecular systems is theoretically ascertained through various DFT and *ab initio* calculations along with the Energy Decomposition Analysis (EDA), T1 diagnostic run, estimation of Ring Strain Energy (RSE) and HOMO-LUMO gap which indicate towards the viability of these molecular systems. Then a detailed study of aromaticity with the aid of different computational probes such as Nucleus Independent Chemical Shift (NICS), Dissected canonical molecular orbital NICS (CMO-NICS) analysis, Multi Centre bond Index (MCI), Adaptive Natural Density Partitioning (AdNDP) and theoretical tool as Aromatic Stabilization Energy (ASE) based on a fully *ab initio* approach is performed which establishes unique exo-cyclic aromaticity in these systems.

In the sixth chapter, investigation of the underlying principle behind the occurrence of bond stretch isomerism in Be_3^{2-} is done. The various computational studies of the different isomers are carried out at complete active space self-consistent field (CASSCF) level of theory in addition to B3LYP level in conjunction with 6-311++G(d) basis set. The potential energy surfaces linking the different isomers through transition states and conical intersections are investigated at CASSCF level connecting various geometrical isomers of

Be_3^{2-}. The linear intermediate of the Be_3^{2-} cluster is considered to be of profound importance since its excited state is found to be degenerate and undergoing Renner-Teller effect producing two triangular bond stretch isomers. *Ab initio* molecular dynamics simulation based on Atom Centered Density Matrix Propagation (ADMP) method also further elucidates the phenomenon of isomerization via linear intermediate. The variation of the global reactivity descriptors and free energy profile along the bond stretch isomerization path is also investigated. Estimated aromatic stabilization energy also corroborates the stability ordering of the bond stretch isomers.

In the seventh chapter conceptual density functional theory involving the global and local reactivity parameters is employed to elucidate the process of methylation of aromatic nucleobase cytosine and its subsequent oxidation to its derivatives. The methylation of cytosine to 5-methylcytosine (5mC) is explained with the aid of condensed fukui functions. The active demethylation pathway following the iterative oxidation of 5-methylcytosine (5mC) to 5-(hydroxymethyl) cytosine (5hmC) to 5-formylcytosine (5fC) and finally to 5-carboxycytosine (5caC) is discussed with the help of conceptual density functional parameters such as Frontier Molecular Orbital (FMO) study, chemical hardness and softness, electrophilicity and nucleophilicity. Aromaticity of cytosine and its derivatives employing the Nucleus Independent Shift (NICS) is also employed to ascertain the stability which is in harmony with the hardness profile.

General conclusions of all the chapters are provided in the final chapter comprehensively focusing on the significance of the works done.

PREFACE

The journey of aromaticity from Kekulés definition of benzene has been extensive and the recent developments in this field provide a considerable better insight into the concept. The first chapter thereby provides a crisp discussion about the advancement in the field of aromaticity since its inception days to its recent developments. Any single property based index is unable to wholly describe the event of aromaticity, thereby rendering it to be multidimensional, so a plethora of indices exist to define aromaticity and to ascertain stability of molecules. These various theoretical constructs are discussed in chapter 2 including the reactivity parameters. On the basis of available literature, various criteria have been employed over the years for quantification of aromaticity, but magnetic criteria played an instrumental role in defining the concept of aromaticity. So, a mini review discussing aromaticity in the light of magnetic criteria is done in chapter 3. Although the concept of aromaticity has long been primarily confined to organic chemistry, but the recent advancements in the field of aromaticity made it an important unifying concept to ascertain the bonding and stability in many chemical species such as inorganic radicals, anions, cations and clusters surpassing the domain of organic chemistry. This encouraged us to widen the boundaries of the already existent concept of aromaticity in the fourth chapter where we explored a novel area of exo-cyclic aromaticity in newly designed $C_2B_2F_4$ molecule. Here, we extend beyond the limit of conventional aromatic molecules where the molecule gains the magic number of six π-electrons through an unusual electronic contribution from *exo*-cyclic atoms. This original concept is further manifested in chapter 5 where it is extended to novel three membered heterocyclic moieties. Among different all metal aromatic clusters, research on Be_3^{2-} cluster is prominent due to its structural variety and bond stretch isomerism. Be_3^{2-} is a comprehensively studied system due to the presence of few electrons and accordingly different sophisticated computations are possible. In chapter 6, we illuminate the underlying rationale behind the occurrence of bond stretch isomerism in Be_3^{2-}. Conceptual density functional theory involving the global and local reactivity parameters to elucidate the process of methylation of aromatic nucleobase cytosine and its subsequent oxidation to its derivatives is explored in the seventh chapter. In the final chapter, the essence of preceding chapters and the importance of the present study are surmised. In spite of abundant cultivation of the topic "aromaticity" it still remains an intriguing topic with immense potential as it is aptly said by Schleyer that, "aromaticity has been a time-dependent phenomenon."

TABLE OF CONTENTS

Chapter 1. **Aromaticity** **1-14**

1.1. Introduction
1.1.1. Genesis of the concept of aromaticity 2
1.1.2. Criteria for defining aromaticity 6
1.2. Exo-cyclic aromaticity 8
1.3. All metal-aromatic clusters 9
1.4. Aromatic nucleobases 10
1.5. Objectives of the thesis 11
1.6. References 12

Chapter 2. **Theoretical background** **15-29**

2.1. Quantification of aromaticity
2.1.1. Nucleus Independent Chemical Shifts (NICS) 17
2.1.2. Dissected Canonical Molecular Orbital NICS (CMO-NICS) 18
2.1.3. Multi-centre indices 19
2.1.4. Electron Localization Function (ELF) 20
2.1.5. Aromatic Stabilization Energy (ASE) 21
2.2. Indices of stability
2.2.1. Energy Decomposition Analysis (EDA) 23
2.2.2. Ring Strain Energy (RSE) 24
2.2.3. Adaptive Natural Density Partitioning (AdNDP) Analysis 24
2.2.4. Atom Centered Density Matrix Propagation (ADMP) 25
2.3. Conceptual DFT based reactivity descriptor
2.3.1. Global reactivity descriptors 26
2.3.2. Local reactivity descriptors (Fukui functions) 27
2.4. References 28

Chapter 3. **A mini review article: Aromaticity in the light of magnetic criteria** **30-43**

3.1. Introduction 31
3.2. Criteria for defining aromaticity 32
3.2.1. Chemical behavior 32
3.2.2. Structural pattern 33
3.2.3. Energetic criteria 33
3.2.4. Magnetic criteria
3.2.4.1. NMR chemical shifts 35
3.2.4.2. Magnetic susceptibility anisotropy 36
3.2.4.3. Current Density Analysis Plots (CDA) 37
3.2.4.4. Nucleus Independent Chemical Shift (NICS) 38
3.3. Conclusions 41
3.4. References 41

Chapter 4. **On exo-cyclic aromaticity** **44-62**

4.1. Introduction 45

4.2. Computational details 45
4.2.1. Calculation of Ring Strain Energy(RSE 46
4.2.2. Calculation of Aromatic Stabilization Energy 47
4.3. Results and discussions 48
4.4. Conclusions 60
4.5. References 61

Chapter 5. **Manifestation of exo-cyclic aromaticity in triangular heterocyclic B_2F_2X systems (X = O, S, Se, NH)** **63-86**

5.1. Introduction 64
5.2. Computational details 65
5.3. Results and discussions
5.3.1. Molecular Geometry 66
5.3.2. Ring Strain Energy 71
5.3.3. Molecular orbital analysis 72
5.3.4. Aromaticity analysis employing NICS, CMO-NICS and MCI 73
5.3.5. Adaptive Natural Density Partitioning (AdNDP) Analysis 77
5.3.6. Aromatic Stabilization Energy (ASE) 80
5.4. Conclusions 83
5.5. References 83

Chapter 6. **Bond stretch isomerism in aromatic Be_3^{2-} cluster driven by the Renner-Teller effect** **87-107**

6.1. Introduction 88
6.2. Computational details 90
6.3. Results and discussions 93
6.4. Conclusions 104
6.5. References 105

Chapter 7. **Theoretical elucidation of methylation of cytosine and its subsequent oxidation processes** **108-124**

7.1. Introduction 109
7.2. Computational details 112
7.3. Results and discussions
7.3.1.Condensed fukui functions 116
7.3.2. FMO study 120
7.3.3. Chemical hardness and softness 120
7.3.4. Electrophilicity and Nucleophilicity 121
7.3.5. Aromaticity 121
7.4. Conclusions 122
7.5. References 123

Chapter 8. **Conclusions** **125-129**

Bibliography **130-145**

Index **146-148**

LIST OF TABLES

Table 1.1. Chronological advancement of aromaticity 4
Table 4.1. Optimized bond lengths of $C_2B_2F_4$ 49
Table 4.2. Structural and energy decomposition parameters of $C_2B_2F_4$ 52
Table 4.3. The NICS values of $C_2B_2F_4$ 54
Table 4.4. Optimized geometries, NICS of $C_2B_2F_2H_2$, $C_2B_2Cl_4$, $C_2B_2Br_4$ and $C_2B_2I_4$ 59
Table 4.5. AdNDP orbitals of $C_2B_2Cl_4$ and $C_2B_2Br_4$ 60
Table 5.1. Optimized bond lengths of B_2F_2O 68
Table 5.2. Optimized bond lengths of B_2F_2S 68
Table 5.3. Optimized bond lengths of B_2F_2Se 69
Table 5.4. Optimized bond lengths of B_2F_2NH 69
Table 5.5. Energy decomposition parameters of B_2F_2O, B_2F_2S, B_2F_2Se and B_2F_2NH 70
Table 5.6. The T1 diagnostic values of B_2F_2O, B_2F_2S, B_2F_2Se and B_2F_2NH 70
Table 5.7. The Ring Strain Energy of B_2F_2O, B_2F_2S, B_2F_2Se and B_2F_2NH 72
Table 5.8. HOMO-LUMO gap of B_2F_2O, B_2F_2S, B_2F_2Se and B_2F_2NH 73
Table 5.9. The NICS values of B_2F_2O, B_2F_2S, B_2F_2Se and B_2F_2NH 75
Table 5.10. Population analysis of the orbital which is responsible for σ aromaticity 76
Table 5.11. The ASE of B_2F_2O, B_2F_2S, B_2F_2Se and B_2F_2NH 81
Table 6.1. Optimized geometries of ground state isomers of Be_3^{2-} 93
Table 6.2. Optimized geometries of transition states of Be_3^{2-} 95
Table 6.3. The modes of vibrations of the excited state $D_{\infty h}$ Be_3^{2-} 100
Table 6.4. Aromatic Stabilization Energy of the two D_{3h} isomers 104
Table 7.1. Global reactivity descriptors of derivatives of cytosine in ucam-b3lyp 115
Table 7.2. Global reactivity descriptors of derivatives of cytosine in ub3lyp 116
Table 7.3. Condensed fukui functions for cytosine 117
Table 7.4. Condensed fukui functions for 5mC 118
Table 7.5. Condensed fukui functions for 5hmC 118
Table 7.6. Condensed fukui functions for 5fmC 119
Table 7.7. Condensed fukui functions for 5caC 119
Table 7.8. The NICS values of cytosine and its derivatives 122

LIST OF FIGURES

Figure 1.1. Chronological advancement of aromaticity 5
Figure 1.2. Demonstration of strong diamagnetism of benzene 7
Figure 1.3. Illustration of exo-cyclic aromaticity 8
Figure 1.4. Optimized structure of Be_3^{2-} 10
Figure 1.5. The structure and schematic representation of four nucleobases 11
Figure 2.1. Representation of the ghost atoms placed at the benzene molecule. 18
Figure 2.2. Representation of aromatic systems with localized π-electrons 21
Figure 2.3. The ETS-NOCV difference density plot 24
Figure 2.4. The top-view of the AdNDP orbitals of $C_2B_2F_4$ 25
Figure 3.1. Representation of the Ring Current Model in the case of benzene 35
Figure 3.2. Plot of the current density induced in the plane of the benzene 37
Figure 3.3. Plot of NICS (0) (ppm) *vs.* the ASE (kcal mol^{-1}) 39
Figure 4.1. Optimized structure of $C_2B_2F_4$ 48
Figure 4.2. Geometry convergence during optimization of $C_2B_2F_4$ 50
Figure 4.3. Variation of total energy of $C_2B_2F_4$ 51
Figure 4.4. Variation of kinetic energy of $C_2B_2F_4$ 51
Figure 4.5. Variation of potential energy of $C_2B_2F_4$ 52
Figure 4.6. CMO-NICS analysis of $C_2B_2F_4$ 54
Figure 4.7. The π- (a) and σ- (b) current density vector plots. 55
Figure 4.8. Orbital diagram for six π-electrons in $C_2B_2F_4$ 56
Figure 4.9. The ETS-NOCV difference density 56
Figure 4.10. AdNDP orbitals of $C_2B_2F_4$ 57
Figure 5.1. Optimized structure of B_2F_2O, B_2F_2S, B_2F_2Se andB_2F_2NH 67
Figure 5.2. Orbital representation of the B_2F_2X molecules 71
Figure 5.3. The CMOs with maximum diamagnetic contribution 77
Figure 5.4. The AdNDP orbitals of the studied systems 79
Figure 5.5. Maximally Localized Wannier Functions in B_2F_2O 82
Figure 6.1. Optimized bond lengths of the isomers of Be_3^{2-} 94
Figure 6.2. Optimized structures of the transition states 95
Figure 6.3. IRC plots 96
Figure 6.4. The HOMO and LUMO of the ground state isomers 97
Figure 6.5. FMO diagram for the isomerization pathway 98
Figure 6.6. Schematic representation of the bond stretch isomerism 99
Figure 6.7. The SOMO's of the linear excited state of Be_3^{2-} 99
Figure 6.8. Variation of reactivity parameters from linear to short-bond via TS1 102
Figure 6.9. Variation of reactivity parameters from linear to long-bond via TS2 102
Figure 6.10. Free energy profile 103
Figure 7.1. The structure and schematic representation of cytosine 110

LIST OF APPENDICES

APPENDIX A: LIST OF PUBLICATIONS

PUBLISHED

[1] Goswami, T.; **Homray, M**.; Paul, S.; Bhattacharya, D.; Misra, A. On Exo-Cyclic Aromaticity, *Phys. Chem. Chem. Phys.* **2017**, *19*, 11744-11747.

[2] **Homray, M**.; Misra, A.; Chattaraj, P.K. Aromaticity in the Light of Magnetic Criteria, *Curr. Org. Chem.* **2017**, *21*, 1-6.

[3] **Homray, M**.; Paul, S.; Misra, A Manifestation of exo-cyclic aromaticity in triangular heterocyclic B_2F_2X Systems (X=O, S, Se, NH), *Bull. Mat. Sci*. **2019**, *42*, 46.

[4] **Homray, M**.; Mondal, S.; Misra. A.; Chattaraj, P. K. Bond stretch isomerism in Be_3^{2-} driven by the Renner–Teller effect, *Phys. Chem. Chem. Phys.* **2019**, *21*, 7996- 8003.

[5] Das, S.; **Homray, M**.; Misra, A. A New Approach to Design High Spin Organic Systems: Aromatic Stabilization with Exo-cyclic π Electrons Plays Crucial Role, *ChemistrySelect*, **2020**, *5*, 12586-12589.

COMMUNICATED

[6] **Homray, M**.; Maiti, S.; Misra, A. Theoretical elucidation of methylation of cytosine and its subsequent oxidation processes, Communicated, **2020**.

APPENDIX B: ORAL AND POSTER PRESENTATIONS

Oral Presentation

1. On Exo-cyclic Aromaticity, **Manoswita Homray** and Anirban Misra*, National Seminar on "Frontiers in Chemistry 2017-18", Organized by Department of Chemistry, University of North Bengal, Darjeeling, India.

Poster Presentation

2. Bond stretch isomerism in aromatic Be_3^{2-} cluster driven by the Renner-Teller effect, **Manoswita Homray** and Anirban Misra*, International Seminar on "Frontiers in Chemistry 2018", Organized by Department of Chemistry, University of North Bengal, Darjeeling, India.

APPENDIX C: ACKNOWLEDGEMENTS

In the quest of knowledge, over the years, which led me through the journey of my Ph. D. degree, now I have the opportunity to show my immense gratitude for all those who supported, motivated and inspired me. The person to whom I am indebted the most for guiding me in this voyage is my guide Prof. Anirban Misra for his patience, motivation and continuous support for befitting me for such a pursuit. His undying attitude in the face of adversities motivated me to take up newer challenges and inspired me to reach greater heights to thrive for excellence. His enormous knowledge matched with his dedication for research inspired me. I am grateful to him for his patience in answering my queries and the freedom he provided for academic accomplishments.

I am grateful to my labmates, Dr. Satadal Paul, Dr. Suranjan Shil, Dr. Tamal Goswami, Dr. Banita Sinha, Dr. Manoj Majumder, Dr. Rakesh Kar, Ms Prodipta Sarbadhikary, Ms Tanushree Sutradhar, Mr. Sudip Sarkar and Mr. Soumik Das for their enormous support, invaluable advices and warm camaraderie which made this journey enjoyable. I owe my gratitude to all the fellow research scholars of the department, faculty members and staff at University of North Bengal for providing a cordial environment for research. I would also like to express my warm gratitude to Ma'am (Mrs. Amrita Misra) and affection to Mithi (Miss Anwita Misra).

Last but not the least; I am highly grateful to my parents Mr. Malay Homray and Mrs. Santwana Homray who are the first teachers of my life to instil in me the pursuit for knowledge, without their unwavering support this destination could never have been reached.

CHAPTER 1

Aromaticity

1.1.

INTRODUCTION

1.1.1. Genesis of the Concept of Aromaticity

The term “aromatic” was employed by chemists as early as in the beginning of the 19th century which was used to depict organic substances with a pleasant odor and distinguished them from the straight chain aliphatic compounds. The term “aromaticity” then became intrinsically linked with benzene after it was first isolated and characterized by Michael Faraday in the year 1825.[1] However, the foremost definition of aromaticity was given by Kekulé[2] where he described benzene as “a regular arrangements of the six carbon atoms” in which he suggested oscillating structures where synchronous 1, 2-shifts of the three double bonds occur continually. Emil Erlenmeyer[3] recommended the use of the word "aromatic" for the compounds possessing similar properties to benzene and was the first one to attach reactivity criteria to aromaticity. The deciding reactivity criterion for aromaticity as proposed by him was that the compound should be inclined more towards substitution reactions than towards additional ones. In 1867, Dewar predicted the structure of benzene as one of seven possible isomers[4] and alleged that his experiments involving benzene supported the structure as deduced by Kekulé. Based on the structure constructed by Kekulé, Robinson and Armitt in 1925 represented the benzene by a ring. After the inception of valence bond theory in 1928,[5] the stabilization of the aromatic systems was attributed to the delocalization of π- electrons. A breakthrough in defining the aromaticity of a substance was accomplished by Hückel in 1931. "Hückel's rule" of cyclic 4n+2 π-electron systems enables aromatic and anti-aromatic compounds to be differentiated on the basis of the number of π-electrons. However, this rule is firmly applicable only to conjugated monocyclic systems so an extension of this rule to polycyclic systems was successfully accomplished by Clar in 1972 in the book “*The Aromatic Sextet*”.[6] Clar's rule defines the aromatic π-sextets as six π-electrons localized in a single benzene-like ring divided from adjoining rings by formal CC single bonds which was vital for characterization of properties of polycyclic aromatic hydrocarbons (PAHs) such as naphthalene, anthracene or phenanthrene. The concept of aromaticity was further extended to heteroatoms such as furan, thiophene and pyrolle and to annulenes and their respective ions as tropyliom ions.

The confinement of the concept of aromaticity to the domain of organic chemistry was broken by the inception of the concept of metalloaromaticy by Calvin and Wilson in the year 1945.[7] The opposite pattern of aromatic character to conventional Hückel systems was observed by Heilbroner[8] where a monocyclic array of orbitals in which there is a single out-of-phase overlap (an odd number of out-of-phase overlaps) is stabilized (aromatic) with 4n electrons , whereas with 4n+2 electrons it is destabilized (antiaromatic). The name assigned was Möbius aromaticity which was derived from the topological resemblance of an arrangement of orbitals to a Möbius strip. Discovery of cyclononatetraenyl anion by Katz[9] paved the inclusion of aromatic anions to the realm of aromaticity. Baird's rule further stretches the boundary of aromaticity to the lowest triplet excited state of planar cyclic structures where it is also observed that the Huckel's rule of aromaticity is reversed.[10] Three dimensional aromaticity was first introduced by Aihara in planar boron clusters in the year 1978.[11] The most recent advancement in the field of aromaticity was the characterization of the first all-metal aromatic cluster Al_4^{2-} by Boldyrev, Wang et al.[12] Quoting Boldyrev's words "*Aromaticity has in recent years become an important and powerful unifying concept to describe the stability and bonding in many chemical species beyond organic chemistry, including inorganic cations, anions, radicals, and clusters*.",[13] three dimensional aromaticity involving σ-electrons and multidimensional aromaticity involving *d*-orbitals (δ-aromaticity) or even ϕ-(including *f*-orbitals) have been reported.[14] The chronological advancement in the field of aromaticity is listed in Table 1.1 and illustrated in Figure 1.1.

Table 1.1. Chronological salient contributions to the advancement of the concept of aromaticity

Contributors	Year	Works
M. Faraday	1825	Benzene isolation
A. Kekulé	1865	Cyclic formula of benzene
Erlenmeyer	1866	Reactivity criteria for aromaticity
J. Dewar	1867	Dewar benzene formula
R. Robinson and T. W. Armitt	1925	Aromatic π-sextet
E. Hückel	1931	Hückel molecular orbital theory
Evans, Warhurst	1938	Transition state stabilization by aromaticity
Calvin, Wilson	1945	Aromaticity in metal systems
S. Winstein	1959	Homo-aromaticity
E. Heilbronner	1964	Möbius annulene
T. J. Katz	1965	Aromatic anions
A. L. Chung and M. J. S. Dewar	1965	Anti-aromaticity
Osawa	1970	Superaromaticity
E. Clar	1972	Clar aromatic sextet
Baird	1972	Triplet aromaticity
Aihara	1978	Three-dimensional aromaticity
M. J. S. Dewar	1979	σ-aromaticity
P. v. R. Schleyar	1979	In plane and double aromaticity
H. W. Kroto, R. F. Curl, and R. E. Smalley	1985	Buckminsterfullerene C_{60}
Boldyrev and Wang	2001	All-metal aromaticity
P. v. R. Schleyar	2005	d-orbital aromaticity
Boldyrev and Wang	2007	δ-aromaticity
Tsipis	2008	f-aromaticity

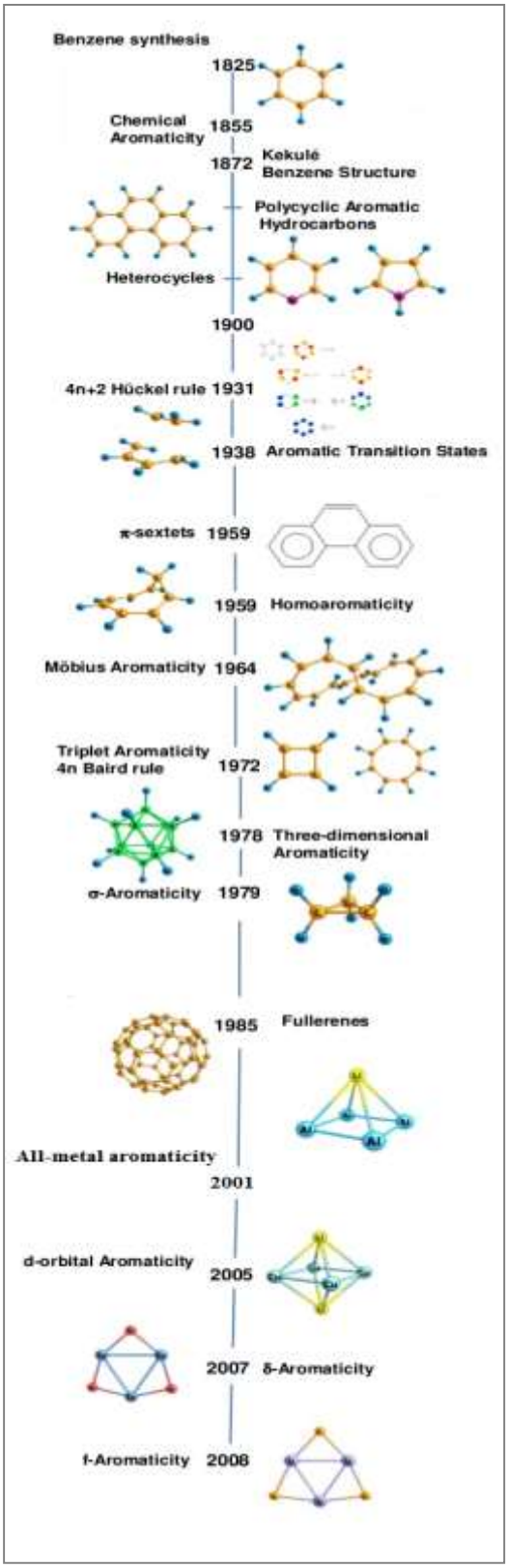

Figure 1.1. Chronological advancement of aromaticity.

The works of Hückel[5] and Pauling[15] explained the role of delocalization of electrons in the stabilization of aromatic systems, using the quantum mechanics based Molecular Orbital (MO) approach and Valence Bond (VB) method respectively. Since then, the circular delocalization of electrons is taken as the genesis of aromaticity. In a VB–type approach to the archetypical aromatic molecule benzene, the circular topology of benzene facilitates a resonance between the wave functions of two complementary sets of localized bond which leads to an extra stabilization of the aromatic moiety. On the other hand, resonance integral or interaction matrix element in circular, planar conjugated hydrocarbons with 4n+2 π-electrons were considered to be the reason behind the additional stabilization in benzene by the MO approach.[5,16] Goldstein and Hoffmann later provided a generalization to other pericyclic topologies.[17]

1.1.2 Criteria for defining aromaticity

A basic definition of aromaticity based on its criteria can be qualitatively described as, "*Aromaticity is a manifestation of electron delocalization in closed circuits, either in two or in three dimensions. This results in energy lowering, often quite substantial, and a variety of unusual chemical and physical properties. These include a tendency toward bond length equalization, unusual reactivity, and characteristic spectroscopic features. Since aromaticity is related to induced ring currents, magnetic properties are particularly important for its detection and evaluation*".[18] The event of aromaticity can be regarded as multidimensional since it cannot be described definitely by any single property based index and all indices do not always give consistent results. Due to all these problems the quantification of aromaticity still remains a challenging and fundamental problem, and ought to be addressed through a precise phenomenological description. On the basis of available literature, the basic criteria for the quantification of aromaticity can be divided into the following categories: (a) Reactivity: electrophilic aromatic substitution reactions are the characteristic reactions of the aromatic systems, (b) Structure: aromatic systems are mainly planar systems, the characteristic property of an aromatic system is that its bond lengths are all equal and π-electrons are delocalized, (c) Energy: aromatic systems have enhanced Resonance Energies (REs) and the Aromatic Stabilization Energies (ASEs), (d) Magnetic Criteria: Magnetic properties are currently the most popular and frequently used criterion for defining aromaticity, the aromatic molecules demonstrate relatively strong diamagnetism when placed in a magnetic field; this is due to the generation of an opposing magnetic field by the induced

ring currents (Figure 1.2). The magnetic criteria of aromaticity are reviewed in detail in Chapter 3.

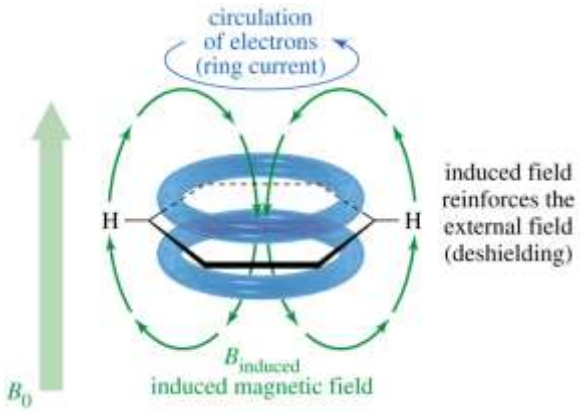

Figure 1.2. Demonstration of relatively strong diamagnetism of archetypical aromatic benzene molecule when placed in a magnetic field due to the generation of an opposing magnetic field by the induced ring currents.

Although aromaticity being the most widely used concept in Chemistry for a long time, the designation of aromaticity is still not unequivocally settled and any of its definition is not unique enough. So quantification of aromaticity is still a major issue to the theoretical and the computational chemists. The ease with which aromaticity bridges the gap between traditional aspects of organic chemistry and latest discoveries in inorganic chemistry are truly fascinating. Aromaticity is not a physically observable quantity so defining it precisely is a challenge till date. Whether aromaticity is a multidimensional phenomenon or can it be defined by a universal single unique criterion is an arguable topic. Aromaticity is perceived differently by chemists of diverse backgrounds in terms of its characteristics and properties. The journey of aromaticity from Kekulés definition of benzene has been extensive and the recent developments in this field provide a considerable better insight into the concept. It is aptly said by Schleyer that, *"aromaticity has been a time-dependent phenomenon."*[19] So, even after two centuries of its existence, this colossal concept is still continually flourishing with increasing vigor and stable novel molecules are enriching the domain of aromaticity.

1.2

EXO-CYCLIC AROMATICTY

Exo-cyclic delocalization at the expense of aromaticity was first used to explain the stability of experimentally observed small ring allenes[20] but after that this domain of aromaticity has remained untouched for a long period of time. In this thesis, a new domain of aromaticity is explored where novel aromatic molecules are theoretically modeled which gains extra stability due to the generation of aromaticity via the back-donation of the substituted ligands attached to the ring (Figure 1.3). The well known back-donation of the π-electrons of the Fluorine ligand to the vacant p_z of Boron is tweaked upon while designing these highly stable aromatic systems. The concept of 2*p*-2*p* orbital interaction or back-donation of fluorine has been well identified in the organic and inorganic domain.[21-23] Both the inductive effect and the resonance or the back-donation effect play a vital role when the non-bonded pair of electrons of fluorine interact with the vacant orbital of the boron atom to which it is attached. The tendency of back-donation by fluorine has been established to be greater than that of the other halogen atoms such as chlorine and bromine, where the order of back-donation is found to be F>Cl>>Br.[24] The degree of back-donation decreases with the increase in the atomic sizes of the halogens since the 2*p*-2*p* interaction is more favorable as compared to the interaction between 3*p* and 4*p* orbital of chlorine and bromine respectively with the vacant 2*p* orbital of boron due to mismatch in the size of the orbitals.

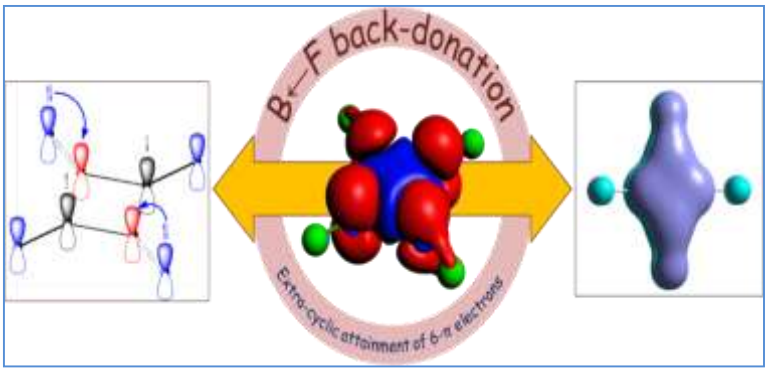

Figure 1.3. Illustration of exo-cyclic aromaticity.

The concept of exo-cyclic aromaticity is further explored to understand and analyze the stability and aromaticity of modeled novel heteroatomic molecular systems where aromaticity in the heteroatomic central ring is achieved through back donation of electrons from the substituted ligands.

1.3

ALL-METAL AROMATIC CLUSTERS

Thorn and Hoffmann[25] predicted in 1979 that some theoretical metallocycles should display delocalized bonding and thereby some aromatic behaviors. In the same year, the term "metalloaromaticity" was introduced by Bursten and Fenske[26] to explain metal complexes of cyclobutadiene - aromatic compounds comprising of a metal atom coordinated to C_4H_4, which can be considered as the archetypal Hückel antiaromatic ($4n\ \pi$ electrons) molecule. However, a coordinated C_4H_4 often behaves as if it were aromatic instead of antiaromatic. The first organometallic compound including an aromatic cycle entirely composed of metal atoms was synthesized by Robinson et al.[27] in the year 1995. Despite of an increasing development in the field of synthesizing aromatic compounds with metal atoms being a part of the aromatic ring, the concept of aromaticity was not extended into gas-phase metal clusters and bulk metal alloys until very recently in 2001 when a series of bimetallic clusters, $LiAl_4^-$, $NaAl_4^-$, and $CuAl_4^-$, in the gas phase and obtained their photoelectron spectra.[12] The theoretical studies revealed that the most stable isomers of these bimetallic clusters all contain a square-planar Al_4^{2-}dianion, which was established to be aromatic moiety. Thus, aromaticity was extended to an all-metal isolated Al_4^{2-} dianion and to bimetallic all-metal $LiAl_4^-$, $NaAl_4^-$, and $CuAl_4^-$ clusters. Since then aromaticity has been reported in a large number of gaseous all-metal or metalloid clusters: XAl_3^- (X = Si, Ge, Sn, Pb),[28-30] M_4^{2-} (M = Ga, In, Tl, Sb, Bi),[31-34] T_5^{6-} (T = Ge, Sn, Pb),[35,36] M_4^{2+} (M = Se, Te),[37-41] M^{3-} (M = Al, Ga),[42-45] Al_6^{2-},[46] Hg_4,[31,34] M_5^-(M = Sb, Bi),[47-49], Au_5Zn^+,[50] Cu_3^{3+},[51] Cu_4^{2-},[52] $[Fe(X_5)]^+$ (X = Sb, Bi).[53]

Apart from the metal systems, the annular system N_4^{2-} is also found to be aromatic.[54] Kuznetsov et al. first studied the M_3^{2-} clusters and explained their stability and aromaticity.[55] These stable anionic clusters X_3^{2-} (X = Mg;[55] Zn, Cd, Hg ;[56] Be[57]), exhibits exclusively pi-aromaticity with no sigma component whatsoever as opposed to other metal clusters like Al_4^{2-} where both σ- and π- aromaticities are present.[28] Some of these anionic cluster molecules are of "fleeting" type[58] and are at the most kinetically stable. Moreover,

there exists a likelihood of "bond-stretch isomerism" in these systems depending on which specific local minima (and/or the global minimum) they are present in.[59] Among different M_3^{2-} clusters, research on Be_3^{2-} cluster (Figure 1.4) is prominent due to its interesting nature of stability, reactivity, aromaticity, structural variety and bond stretch isomerism. Bond Stretch Isomerism (BSI) occurs when the isomers differ in the lengths of certain bonds. The idea of bond stretch isomerism was first proposed by Hoffmann and co-workers in the year 1972 where they had referred to separate stable configurations whose structures vary only in the length of one (or more) chemical bond(s) where the isomers were shown to occupy different minima on their potential energy surface.[60-62] In addition to all these properties Be_3^{2-} is a comprehensively studied system due to the presence of few electrons and accordingly different sophisticated computations are possible.

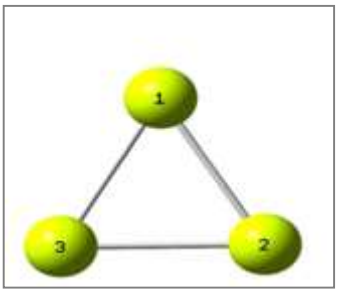

Figure 1.4. Optimized structure of Be_3^{2-}

1.4 AROMATIC NUCLEOBASES

Every multicellular organism includes the DNA which is a significant functional molecule that has evolved to programme and pass on information through generations which play fundamental roles in carrying genetic information in all living things on Earth. DNA has a double helix structure which consists of the four nucleobases adenine (A), cytosine (C), guanine (G) and thymine (T), which is stored within as the primary code and it is the linear sequential arrangement of these four canonical bases that makes up the genetic code (Figure 1.5). They are non-polar and due to their aromaticity, planar. The flat shape of the nucleobases is particularly important when considering their roles as the building blocks of DNA. With respect to the electronic nature of the molecule, aromaticity portrays a closed shell, conjugated system comprising of alternating single and double bonds in a ring. This

arrangement permits pi electron delocalization around the ring, thereby increasing the molecule's stability by resonance.

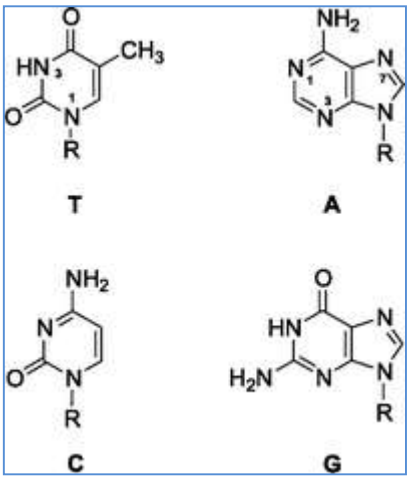

Figure 1.5. The structure and schematic representation of four nucleobases adenine (A), cytosine (C), guanine (G) and thymine (T).

1.5.
OBJECTIVES OF THE THESIS

1. The event of aromaticity can be regarded as multidimensional since it cannot be described definitely by any single property based index and all indices do not always give consistent results. Magnetic criteria are currently the most popular methods and constitute the most frequently used aromaticity indices since magnetic properties provide considerable insight into the concept of aromaticity. Here we make an attempt to review the concept of aromaticity in the light of magnetic criteria in detail.

2. A new domain of aromaticity is explored where novel aromatic molecules are theoretically modeled which gains extra stability due to the generation of aromaticity via the back-donation of the substituted ligands attached to the ring. The well known back-donation of the π-electrons of the Fluorine ligand to the vacant p_z of Boron is tweaked upon while designing these highly stable novel

aromatic systems where the aromaticity is achieved through exo-cyclic conjugation.

3. The concept of exo-cyclic aromaticity is further explored to understand and analyze the stability and aromaticity of modeled novel heteroatomic molecular systems where aromaticity in the heteroatomic central ring is achieved through back donation of electrons from the substituted ligands and to establish the manifestation of exo-cyclic aromaticity in novel designed three-membered heterocyclic moieties.

4. To illuminate the underlying rationale behind the occurrence of bond stretch isomerism in the anionic all-metal aromatic Be_3^{2-} cluster. The primary force behind the presence of two different isomers of the Be_3^{2-} molecule may be the Renner-Teller effect which identifies the prospective of a triatomic molecule present in a degenerate electronic state to split into two when the molecule is bent.

5. In the last part, we make an attempt to provide theoretical elucidation of methylation of aromatic DNA nucleobase cytosine which is an extensively studied DNA modification and its subsequent oxidation processes involving aromatic nucleobases. Here we try to monitor the processes of cytosine modifications using conceptual Density Functional Theory (DFT) based study to compute quantum chemical parameters.

1.6.

REFERENCES

1. Faraday, M. M. *Phil.Trans.Roy.London.* **1825**, *115,* 440.
2. (a) Kekulé, A. *Bull.Soc.Chim.Paris* **1865**, *3,* 98-100. (b) Kekulé, A. *Ann.Chem.Pharm,* **1866**, *137,*129.
3. Erlenmeyer, E. *Ann. Chem. Pharm.* **1866**, *137*, 327.

4. Dewar, J *(1867).* "On the Oxidation of Phenyl Alcohol, and a Mechanical Arrangement adapted to illustrate Structure in the Non-saturated Hydrocarbons". Proc. R. Soc. Edinb. *6: 82–86.*
5. (a) Hückel, E. *Z. Phys* **1931**, *70*, 204. (b) Hückel, *Z.Phys.* **1932**, *76*,628-648. (c) Hückel, E. *Z.Electrochem,Angew. Phys. Chem.* **1937**, *43*, 752-788. (d) Hückel, E. *Z.Electrochem, Angew.Phys.Chem* **1995**, *61*,866-890.
6. Clar, E. The Aromatic Sextet. Wiley & Sons: New York, **1970**.
7. Calvin, M.; Wilson. K. *J. Am. Chem. Soc.* **1945**, *67*, 2003.
8. Heilbronner, E. *Tet Lett* **1964**, *5*, 1923.
9. Katz, T. H; Garratt, P. J. *J. Am. Chem. Soc.* **1963**, *85*, 2852.
10. (a) Colin, B. N. *J. Am. Chem. Soc.* **1972**, *94*, 4941. (b) Henrik, O, *Nat Chem*, **2012**, *4*, 969.
11. Aihara, J. *J. Am. Chem. Soc.* **1978**, *100*, 3339.
12. Li, X.; Kuznetsov, A.; Zhang, H.; Boldyrev, A. Wang, L. *Science* **2001**, *291*, 859.
13. Jose, M. M.; Boldyrev, A. I.; Merino, G.; Ugalde, M. J. *Chem.Soc.Rev.* **2015**, *44*, 6519.
14. Tsipis, A.; Kefalidis, C.; Tsipis, C. *J. Am. Chem. Soc*. **2008**, *130*, 9144.
15. Pauling, L; Wheland, G.W. *J. Chem. Phys.* **1933**, *1*, 362.
16. Pauling, L. In The Nature of the Chemical Bond, 3rd ed., Cornell University Press: Ithaca, New York, 1960.
17. Goldstein. M.J.; Hoffmann, R. *J. Am. Chem. Soc*. **1971**, *93*, 6193.
18. Chen, Z.; Wannere, C. S.; Corminboeuf, C.; Puchta, R.; Schleyer, P. v. R.; *Chem. Rev.* **2005** *105* (10), 3842.
19. Schleyer, P.V.R. Introduction: Aromaticity. *Chem. Rev*. **2001**, *101*, 1115.
20. Fernández, I.; Dyker, C. A.; DeHope, A.; Donnadieu, B.; Frenking, G.; Bertrand, G. *J. Am. Chem. Soc*. **2009** *131*, 11875.
21. Gutowsky, H. S.; McCall, D. W. *J. Phys. Chem.* **1953**, *21*, 279.
22. Onak T. P.; Landesman, H; Williams R E.; Shapiro, I paper presented to the Division of Inorganic Chemistry, 135th National Meeting of the American Chemical Society, Boston, Mass, April 1959.
23. Cotton, F. A.; Wilkinson, G. *"Advanced Inorganic Chemistry,"* Interscience, London, 1966, 256.
24. Olah, G. A.; Mo, Y. K.; Halpern, Y. *J. Am. Chem. Soc.* **1972**, *94*, 3551.
25. Thorn, D. L.; Hoffmann, R. *Nouv. J. Chim.* **1979**, *3*, 39.
26. Bursten, B. E.; Fenske, R. F. *Inorg. Chem.* **1979**, *18*, 1760.
27. Li, X.-W.; Pennington, W. T.; Robinson, G. H. *J. Am. Chem. Soc.* **1995**, *117*, 7578.
28. Li, X.; Zhang, H. F.; Wang, L. S.; Kuznetsov, A. E.; Cannon, N. A.; Boldyrev, A. I. *Angew Chem Int Ed* **2001**, *40*, 1867.
29. Díaz-Cervantes, E.; Poater, J.; Robles, J.; Swart, M.; Solà, M. *J. Phys. Chem. A* 2013, 117, 40, 10462.
30. Kuznetsov, A. E.; Boldyrev, A. I.; Li, X.; Wang, L. S. *J Am Chem Soc* **2001**, *123*, 8825.
31. Twamley, B.; Power, P. P.; *Angew Chem Int Ed* **2000**, *39*, 3500.
32. Cisar, A.; Corbett, J. D. *Inorg Chem* **1977**, *16*, 2482.
33. Critchlow, S. C.; Corbett, J. D. *Inorg Chem* **1984**, *23*, 770.

34. Tuononen, H. M.; Suontamo, R.; Valkonen, J.; Laitinen, R. S. *J Phys Chem A* **2004**, 108, 5670.
35. Todorov, I.; Sevov, S. C. *Inorg Chem* **2004**, *43*, 6490.
36. Todorov, I.; Sevov, S. C. *Inorg Chem* **2005**, *44*, 5361.
37. Gillespie, R. J.; Barr, J.; Kapoor, R.; Malhotra, K. C. *Can J Chem* **1968**, *46*, 149.
38. Gillespie, R. J.; Barr, J.; Crump, D. B.; Kapoor, R.; Ummat, P. K. *Can J Chem* **1968**, *46*, 3607.
39. Barr, J.; Gillespie, R. J.; Kapoor, R.; Pez, G. P. *J Am Chem Soc* **1968**, *90*, 6855.
40. Couch, T. W.; Lokken, D. A.; Corbett, J. D. *Inorg Chem* **1972**, *11*, 357.
41. Burford, N.; Passmore, J.; Sanders, J. C. P. In: Liebman, J. F.; Greenburg, A. (eds) From atoms to polymers. Isoelectronic analogies. VCH, New York, 1989, p 53.
42. Li, X.; Wang, X. B.; Wang, L. S. *Phys Rev Lett* **1998**, *81*, 1909.
43. Wu, H.; Li, X.; Wang, X. B.; Ding, C. F.; Wang, L. S. *J Chem Phys* **1998**, *109*, 449.
44. Baeck, K. K.; Bartlett, R. J.; *J Chem Phys* **1998**, *109*, 1334.
45. Kuznetsov, A. E.; Boldyrev, A. I. *Struct Chem* **2002**, *13*, 141.
46. Kuznetsov, A. E.; Boldyrev, A. I.; Zhai, H. J.; Li, X.; Wang, L. S. *J Am Chem Soc* **2002**, *124*, 11791.
47. Gausa, M.; Kaschner, R.; Lutz, H. O.; Seifert, G.; Meiwes-Broer, K. H. *Chem Phys Lett* **1994**, *230*, 99.
48. Gausa, M.; Kaschner, R.; Seifert, G.; Faehrmann, J. H.; Lutz, H. O.; Meiwes, K. H. B. *J Chem Phys* **1996**, *104*, 9719.
49. Zhai, H. J.; Wang, L.S.; Kuznetsov, A. E.; Boldyrev A. I. *J Phys Chem A* **2002**, *106*, 5600.
50. Tanaka, H.; Neukermans, S.; Janssens, E.; Silverans, R. E.; Lievens. P. *J Am Chem Soc* **2002**, *125*, 2862.
51. Alexandrova, A. N.; Boldyrev, A. I.; Zhai, H. I.; Wang, L. S. *J Phys Chem A* **2005**, *109*, 562 .
52. Wannere, C. S.; Corminboeuf, C.; Wang, Z. X.; Wodrich, M. D.; King, R. B.; Schleyer, P. v. R *J Am Chem Soc* **2005**, *127*, 5701.
53. Lein, M.; Frunzke, J.; Frenking, G. *Angew Chem Int Ed* **2003**, *42*, 1303.
54. Van Zandwijk, G.; Janssen, R. A. J.; Buck, H. M. *J Am Chem Soc* **1990**, *112*, 4155.
55. Kuznetsov, A. E.; Boldyrev, A. I. *Chem. Phys. Lett.* **2004**, *388*, 452.
56. Yong, L.; Chi, X. *Theochem* **2007**, *818*, 93.
57. Roy, D. R.; Chattaraj , P. K. *J Phys Chem A* **2008**, *112*, 1612.
58. Hoffmann, R.; Schleyer, P. v. R.; Schaefer, H. F., III. *Angew Chem Int Ed* **2008**, *47*, 7164.
59. (a) Parkin, G. *Acc Chem Res* **1992**, *25*, 455. (b) Parkin, G. *Chem Rev* **1993**, *93*, 887.
60. Stohrer W. D.; Hoffmann, R. *J. Am. Chem. Soc.* **1972**, *94*, 779.
61. Stohrer W. D.; Hoffmann, R. *J. Am. Chem. Soc.* **1972**, *94*, 1661.
62. Jean, Y.; Lledos, A.; Burdett, J. K.; Hoffmann, R. *J. Am. Chem. Soc.* **1988**, *110*, 4506.

CHAPTER 2

Theoretical background

2.1.

QUANTIFICATION OF AROMATICITY

Aromaticity has been considered as an abstract concept from philosophical point of view by Cryansli et al.[1] Whereas, from another perspective, the event of aromaticity can be regarded as multidimensional since it cannot be described definitely by any single property based index and all indices do not always give consistent results. Due to all these problems the quantification of aromaticity still remains a challenging and fundamental problem. Also, Minkinet al.[2] has described in their book "Aromaticity and Antiaromaticity, Electronic and Structural Aspects", eight different types of aromaticity namely, (i) Aromaticity, (ii) Antiaromaticity, (iii) Homoaromaticity, (iv) Heteroaromaticity, (v) In-plane aromaticity, (vi) Three- dimensional aromaticity and (vii) Spherical aromaticity.

On the basis of available literature, the criteria for the quantification of aromaticity can be divided into the following four basic categories. (1) Chemical behavior: Electrophilic aromatic substitution reactions are the characteristic reactions of the aromatic systems but it is difficult to define aromaticity with the help of the chemical behavior of the molecule. (2) Structural pattern: Aromatic systems are mainly planar systems. The characteristic property of an aromatic system is that its bond lengths are all equal and π-electrons are delocalized. The direct determination of bond lengths gives us valuable information regarding the extent of delocalization. (3) Aromaticity has long been connected to the enhanced resonance energies (REs) and the aromatic stabilization energies (ASEs). Even the (4n+2) π- electron rule of Hückel is based on energetic criterion. The energetic measure of aromaticity and antiaromaticity is based on evaluations of energies relative to the reference systems such as conjugated polyenes or olefins.[3] (4) Magnetic Criteria: The anomalous diamagnetization of benzene has been related to the delocalization of π-electrons since the early days of quantum chemistry. The aromatic molecules demonstrate relatively strong diamagnetism when placed in a magnetic field; this is due to the generation of an opposing magnetic field by the induced ring currents. The magnetic criteria of aromaticity are dependent on the specific reaction of the aromatic compounds to externally applied uniform magnetic field which is placed perpendicular to the molecular plane. This contribution of π-electrons to the magnetic susceptibility component which is placed perpendicular to the molecular plane was chosen as an indicator of aromaticity. While the direction of an induced current in a loop is determined

by the relative orientation of the magnetic field and the loop's movement but the direction of the current in a molecule also depends on the type of the system. Generally in a system containing 4nπ electrons, an external magnetic field induces a paratropic ring current (i.e. in the opposite direction relative to a classic loop) while a system containing (4n+2) π electrons shows a diatropic ring current (i.e. in the same direction as a classic loop).[4] In detail analysis of the magnetic criteria of aromaticity is described in the third chapter in the form of a mini review article.

Aromaticity is not a physically observable quantity so defining it precisely is still a challenge. Quantification of aromaticity is a major challenge to the theoretical and the computational chemists till date. Whether aromaticity is a multidimensional phenomenon or it can be defined by a universal single unique criterion is a debatable topic. The journey of aromaticity from Kekulé's definition of benzene has been extensive and the recent developments in this field provide a considerable better insight into the concept. It is aptly said by Schleyer that, "aromaticity has been a time-dependent phenomenon." The perception of aromaticity is different in terms of its properties and characteristics to chemists with diverse backgrounds

Aromaticity being a multidimensional phenomenon, the effect that aromaticity applies on different structural, energetic, chemical and magnetic properties have led to the development of various aromaticity indices. The different aromaticity indices that have been employed in this thesis are briefly described in the following subsections.

2.1.1. Nucleus Independent Chemical Shifts (NICS)

The most efficient method of quantifying aromaticity is NICS, which was postulated by Schleyer and his co-workers.[6] The negative value of the absolute magnetic shielding gives the definition of NICS. NICS method uses a ghost atom namely Bq (named after the ghost Banquo from Shakespeare's Macbeth), it is devoid of any electrons, protons and neutrons. Initially it was placed at the centre of the system [NICS (0)], then later at a distance of 1 Å above the plane [NICS (1)]. This ghost atom is like a sensor for the magnetic environment at the position at which it is placed. The ghost atom senses this magnetic environment and reports the chemical shielding values through the use of computational technique like GIAO.[7-10] The NICS values are computed by placing the ghost atom at the centre of the ring [NICS (0)] to account for the contribution of the σ-electrons to aromaticity and 1 Å above and below the plane i.e., [NICS (1)] and [NICS (-1)] respectively to estimate the π-

aromaticity of the systems (Figure 2.1). The NICS values were reported with reversed signs, in agreement with NMR chemical shift convention. Positive NICS value indicates a paratropic magnetic field whereas a negative NICS value indicates a diatropic magnetic field, thus a negative NICS value would mean that a system is aromatic and a positive NICS value would correspond to an antiaromatic system. After their initial publication, Schleyer and his co-workers noted the problem in using NICS for 3-membered systems due to the local shielding effects of the neighboring σ-bonds. So they introduced two modifications in the following year.[51] The first modification was that the bq was raised 1 Å above the molecular plane, which was termed as NICS (1). Since σ-contributions are short ranged, so NICS (0) has greater σ-contributions, so by raising the bq by 1 Å, the σ-contributions are effectively reduced. Secondly, the total NICS value was separated into σ and π contributions. Since aromaticity results from π contributions, so NICS (1) is a better aromaticity criterion than NICS (0).

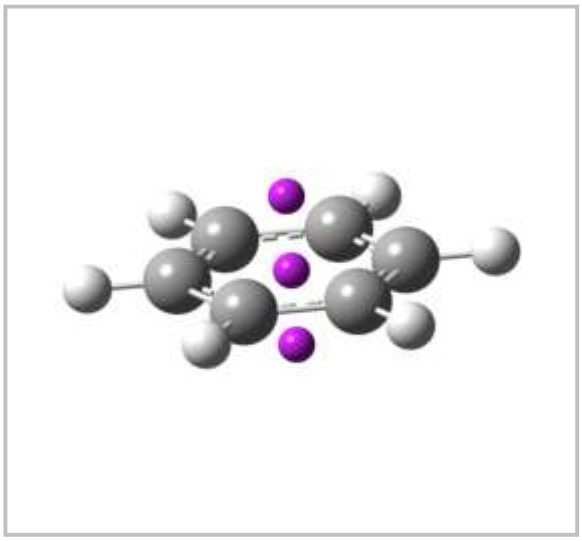

Figure 2.1. Representation of the ghost atoms placed at the centre and 1 Å above and below the plane of the benzene molecule.

2.1.2. Dissected Canonical Molecular Orbital NICS (CMO-NICS)

Later refinement of the original NICS technique offered better understanding of the aromatic systems which include the Dissected NICS technique which consists of the CMO-NICS method. This dissected NICS technique has been termed MO−NICS by Heine et al.,[11] but CMO−NICS is preferable to avoid ambiguity. This method for calculating the dissected NICS rigorously focuses on the employment of canonical MOs. Individual canonical molecular orbital (CMO) contributions to the magnetic shielding of atoms and to

the NICS of aromatic compounds can be calculated by the extensively used GIAO method. CMO−NICS is based on the uncoupled form of current-density functional theory and is limited to purely DFT calculation (i.e., hybrid functional are not used). The shielding tensor is written as a sum of canonical orbital contributions.

Therefore, the NICS dissection into canonical molecular orbital contributions corresponds to the CMO-NICS as expressed in eq (1).

$$\sigma_{tot} = \sum_{i=1}^{occ} \sigma_{CMO_i} \tag{2.1}$$

2.1.3. Multi-centre indices

Giambiagi first developed an index to measure multicenter bonding.[12] The similar expression applied to a molecular ring was represented as I_{ring} to account for aromaticity.[13]

$$I_{ring}(A) = \sum_{i_1, i_2 ..., i_n} S_{i_i i_2}(A_1) .... S_{i_n i_1}(A_n) \tag{2.2}$$

where n_i =[0,1] is the occupancy of the corresponding natural orbital and $S_{ij}(A_1)$ is the atomic overlap matrix (AOM) of atom A_1,

$$S_{ij}(A_1) = \int_{A_1} d_1 \phi_i^*(1) \phi_j(1) \tag{2.3}$$

where $\phi_i(1)$ is a natural orbital. I_{ring} depends on the order of the atoms in the string for n > 3. MCI was suggested by Bultinck et al[14] which is an improvement over I_{ring} that takes into account the delocalization across a ring and is calculated by adding up all the possible I_{ring} contributions obtained from the permutations of the atoms in A,

$$MCI(A) = \frac{1}{2n} \sum_{P(A)} I_{ring}(A) \tag{2.4}$$

where P is an operator acting on A that generates all the n! permutations of its atoms. A higher positive MCI values signifies higher aromaticity in the ring.

2.1.4. Electron Localization Function (ELF)

As electron delocalization constitutes the genesis of aromaticity so another important index for quantifying aromaticity is the ELF. ELF is a measure of the probability of finding an electron in the vicinal area of a reference electron positioned at a given point with a similar spin. So, this quantifies the degree of spatial localization of the reference electron physically and can be applied for the mapping of electron pair probability in multielectronic systems. Its usefulness lies in the fact that it permits the analysis of electron localization in a chemically intuitive manner. The ELF is a mathematical description of the valence shell electron-pair repulsion (VSEPR) theory and was originally defined by Becke and Edgecomb in the year 1990.[15] The first measure of the electron localization as given by them was

$$D_\sigma(r) = \tau_\sigma(r) - \frac{1}{4}\frac{(\nabla_{\rho\sigma}(r))^2}{\rho_\sigma(r)}, \tag{2.5}$$

where ρ represents the electron spin density and τ is the kinetic energy density. *D* is the contribution due to fermions so the second negative term represents the bosonic kinetic energy density. In those regions of space where the probability of finding the localized electrons are high, D is anticipated to have a smaller value. The ratio,

$$\chi_\sigma(r) = \frac{D_\sigma(r)}{D_\sigma^0(r)} \tag{2.6}$$

is a dimensionless localization index, where $D_\sigma(r)$ is the electron localization that has been defined in equation and the uniform electron gas with spin density equal to $\rho(r)$ is given by

$$D_\sigma^0(r) = \frac{3}{5}(6\pi^2)^{2/3}\rho_\sigma^{5/3}(r). \tag{2.7}$$

Then finally the ELF is defined in terms of χ by mapping its values on to the range $0 \leq$ ELF ≤ 1 as

$$ELF(r) = \frac{1}{1+\chi_{\sigma}^{2}(r)} \tag{2.8}$$

The ELF values ranges between 1 and 0, where a perfect localization is in correspondence to an ELF value of 1. The original derivation was based on Hartree–Fock theory. The approach was generalized by Savin in 1992 for Density Functional Theory.[16] The π-component of the electron localization function (ELF_{π}) is normally used as an indicator of aromaticity.

2.1.5. Aromatic Stabilization Energy (ASE)

The aromaticity of the studied systems is calculated using a recently proposed theoretical model where quantification of aromaticity is done with respect to the energy stabilization owing to the circular π-electrons delocalization, termed as the Aromatic Stabilization Energy (ASE).[17] This theoretical model is obtained by localizing unpaired p_z electrons on each individual carbon atom of benzene (Figure 2.2). In this model, the neighbouring antiparallel p_z-spins are in such an orientation so as to spread into one another's non-orthogonal overlapping orbitals stabilizing the entire system. In this theoretical model, ASE is related to the molecular energy stabilization due to electron delocalization in the framework of second order perturbation theory consequential from atom to atom charge transfer.[18-20]

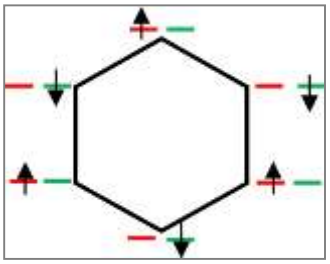

Figure 2.2. A schematic representation of benzenoid aromatic systems with localized π-electrons on the p_z orbitals of carbon atoms. Orbitals for (α) up-spin and (β) down-spin are represented by red and green lines respectively.

The theoretical model proposes the inter-site hopping integral (t_{ij}) and the onsite repulsion energy (U) to be responsible for the electron delocalization. The population of the electrons participating in delocalization is obtained as a product of spin-orbital population ($n_{i\sigma}$

and $n_{j\sigma'}$) within the unrestricted framework and the level of delocalization is projected from electron localization function (ELF) as

$$ASE = \sum_{i,j} \frac{t_{ij}^2}{U} \left(n_{i\sigma} n_{j\sigma'} + n_{i\sigma'} n_{j\sigma} \right) ELF^2 \quad (2.9)$$

As already mentioned, the above equation is applicable for benzene like aromatic molecules, which are different from the studied system in terms of the electronic structure and aromaticity type. In the systems studied in this work, specifically the migration of the lone pair of electrons in between the boron and fluorine completes the loop of electronic circulation and thus makes the pattern of electron delocalization unique and different to conventional aromatic systems. To agree with this representation of electron delocalization, the above equation is divided into two components as

$$ASE = \sum_{B,X} \frac{2t_{ij}^2}{U} \left(n_{B\sigma} n_{X\sigma'} + n_{B\sigma'} n_{X\sigma} \right) ELF^2 + \sum_{F,B} \frac{2t_{ij}^2}{U} \left(n_{F\sigma} n_{B\sigma'} + n_{F\sigma'} n_{B\sigma} \right) ELF^2 \quad (2.10)$$

Here, the first part stands for the electron delocalization within B-X ring, it is multiplied by two to account for two lone pair of electrons of the heteroatom X and the second part quantifies stabilization for electron delocalization within Lewis acid-base pair. The probability of the lone-pair transfer from F to B is taken into consideration by multiplying by two.

Since theoretical study of novel aromatic systems is the main objective of this thesis, so various theoretical indices that could indicate the structural integrity of the proposed molecular systems are discussed in the following as in order to understand function, first we need to comprehend the structure and vouch for its viability.

2.2.

INDICES OF STABILITY

2.2.1. Energy Decomposition Analysis (EDA)

The structural reliability of the molecular systems is established through Energy Decomposition Analysis (EDA) based on the approach of Ziegler and Rauk.[21] The individual atomic fragments are taken into consideration for the EDA. In this method the interaction energy (ΔE_{int}) is divided into three major components namely electrostatic interaction (ΔV_{elstat}), Pauli repulsive orbital interaction (ΔE_{pauli}) and attractive orbital interaction (ΔE_{orb}) as shown,

$$\Delta E_{int}=\Delta V_{elstat}+\Delta E_{pauli}+\Delta E_{orb} \qquad (2.11)$$

Here, the ΔV_{elstat} represents the classical electrostatic interaction between the fragments as they are brought together to form the final complex. ΔE_{pauli} corresponds to the repulsive interaction between the filled orbital, generally termed as steric interaction.[22] ΔE_{orb} corroborates the interactions between the occupied orbitals of one fragment to the unoccupied orbitals of the other fragment and also takes into account the interactions between the occupied and virtual orbitals of the same fragment.

Another important tool to quantitatively analyze chemical bonds, merging the extended transition state (ETS) method[21] for energy decomposition analysis combined with the natural orbitals for chemical valence (NOCV) theory[23] is the extended transition state method and natural orbital for chemical valence scheme (ETS-NOCV).[24]

Here, they have further combined the NOCV and ETS methods in a ETS-NOCV charge and energy decomposition scheme by providing an expression for ΔE_{orb}.

The term ΔE_{orb} is given by:

$$\Delta E_{orb} = E[\rho]-[\rho^0] \qquad (2.12)$$

where $E[\rho]$ is the energy of the final molecule and $E[\rho^0]$ is the energy E^0 associated with the normalized and antisymmetrized wave function Ψ^0. The ETS-NOCV charge and energy

decomposition scheme provides a condensed picture of chemical bond formation within one common theoretical framework as illustrated in the following Figure 2.3.

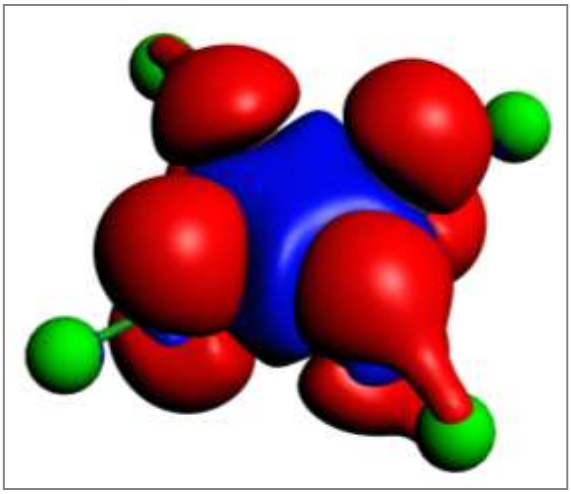

Figure 2.3. The ETS-NOCV difference density plot corresponding to −100 kcal/mol stabilization. The blue and red surfaces represent regions of the electron concentration and electron depletion (isosurface of 0.003 a.u.) respectively.

2.2.2. Ring Strain Energy (RSE)

Ring Strain Energy serves as an important measure for the stability of small ring systems. The ring strain is calculated with the aid of Bader's Quantum theory of Atoms in Molecules (QTAIM)[25] The Lagrange kinetic energy density value G(r) computed at the Ring Critical Point (RCP) can be used to evaluate the ring strain in these small rings, with the application of the Regression equation, RSE= {337.72 × G(r) – 8.115}.[26]

2.2.3. Adaptive Natural Density Partitioning (AdNDP) Analysis

The most important aspect of this thesis is the bonding analysis of the novel aromatic systems and the best way to understand and get a visual illustration of the bonding is the AdNDP method (Figure 2.4). Adaptive Natural Density Partitioning is a theoretical analysis which provides a very proficient and an illustrative method to the understanding of the molecular orbital dependent wave functions. It is a recently developed method which was proposed in the year 2008 by Zubarev and Boldyrev[27] for determining chemical bonding patterns in general molecular systems. This method is based on the simple Lewis concept that describes the chemical bonding with respect to the electron pair thereby characterizing the electronic structures as n-centered-2 electron bonds where the value of n ranges from 1 to the

total number of atoms present in the studied molecular systems. It figure outs the elements responsible for Lewis bonding and also the elements responsible for delocalized bonding which can be correlated with the concepts of aromaticity and antiaromaticity. AdNDP is an overview of NBO analysis as was proposed by Weinhold from a computational view point on the basis of the diagonalization of the blocks of the first order density matrix based on natural atomic orbitals.[28,29] AdNDP bonding patterns are in consonance with the point group symmetry of the molecular systems and resonating structures are generally avoided. The main advantage of this method is that it effortlessly links the Canonical Molecular Orbitals (CMO) and the Natural Bonding Orbitals (NBO).

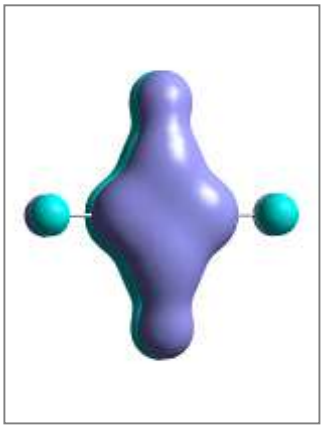

Figure 2.4. The top-view of the AdNDP orbitals of $C_2B_2F_4$.

2.2.4. Atom Centered Density Matrix Propagation (ADMP)

ADMP is based on the theory for an extended Lagrangian molecular dynamics trajectory method that employs atom-centered basis function and density matrix propagation.[30-33] This approach is well fitting for the dynamics of chemical systems such as clusters and gas-phase reactions. For ADMP the Lagrangian for the system can be written as

$$L = \frac{1}{2}Tr\left[V^T MV\right] + \frac{1}{2}Tr\left[\left\{\mu^{1/4} W \mu^{1/4}\right\}^2\right] - E(R,P) - Tr\left[\Lambda(PP-P)\right] \quad (2.13)$$

where R, V, and M are the nuclear positions, velocities and masses; P and W are the density matrix and the density matrix velocity respectively. The fictitious mass for the electronic degrees of freedom, μ, is chosen as a diagonal matrix with larger values for the core orbitals. Constraints on the total number of electrons and the idempotency of the one particle density

matrix enforce *N*-representability and are imposed using the Lagrangian multiplier matrix Λ. The energy is calculated using the McWeeny purification of the density,[34] $\overline{P} = 3P^2 - 2P^3$.

2.3.

CONCEPTUAL DFT BASED REACTIVITY DESCRIPTORS

2.3.1. Global reactivity descriptors

Global reactivity descriptors are an important tool in predicting the structural stability of the molecules. It is established that hardness (η) and electrophilicity (ω) can give us an idea regarding the stability of molecular systems in conjunction with the associated electronic structure principles, viz., the maximum hardness principle (MHP)[35-40] and the minimum electrophilicity principle (MEP).[41-43] The electronegativity (χ),[44-46] hardness (η)[47,48] and electrophilicity (ω)[49] of an *N*-electron system can be defined as follows:

$$\chi = -\mu = -\left(\frac{\partial E}{\partial N}\right)_{\upsilon(\vec{r})} \tag{2.14}$$

$$\eta = \left(\frac{\partial^2 E}{\partial N^2}\right)_{\upsilon(\vec{r})} \tag{2.15}$$

$$\omega = \frac{\mu^2}{2\eta} = \frac{\chi^2}{2\eta} \tag{2.16}$$

E, μ, and $v(\vec{r})$ are the total energy of the *N*-electron system, chemical potential and external potential respectively.

Employing a finite difference approximation to Eqs. 2.14 and 2.15 one can achieve:

$$\chi = \frac{I + A}{2} \tag{2.17}$$

and $$\eta = I - A \tag{2.18}$$

where *I* and *A* indicate the ionization potential and electron affinity of the cluster, respectively, and they are calculated using Koopmans' theorem.[50,51]

2.3.2. Local reactivity descriptors (Fukui functions)

The Fukui functions are employed to describe local electrophilicity and nucleophilicity factors. Removal of an electron from the molecule, called the Fukui function for electrophilic attack, is described as f^- and the Fukui function for *addition* of an electron to the molecule, called the Fukui function for nucleophilic attack is denoted as f^+. The understanding of the quantitative values of the Fukui function is that a large value of f^-, signifies that a molecule *donates* electrons, whereas a larger value of f^+ denotes where a molecule *accepts* electrons. The Fukui functions can be defined using finite differences of the electronic density

$$f^- = \rho(N) - \rho(N-1) \tag{2.19}$$

$$f^+ = \rho(N+1) - \rho(N) \tag{2.20}$$

where the densities of the cation ($N - 1$), the neutral (N), and the anion ($N + 1$) are employed. Here, chemical reactivity is described on an atom-by-atom basis via a "condensed" Fukui function. The condensed Fukui function is computed as

$$f_k^- = q_k(N) - q_k(N-1) \tag{2.21}$$

$$f_k^+ = q_k(N+1) - q_k(N) \tag{2.22}$$

where q_k is the charge at atomic center k.[52-56] Here Hirschfeld charges are used in Multiwfn[57] software.

2.4.

REFERENCES

1. Cryański, M. K.; Krygowski, T. M.; Katritzky, A. R.; Schleyer, P. v. R. *J. Org. Chem* **2002,** *67*, 1333.
2. Minkin, V.; Glukhovtsev, M.; Simkin, B. In *Aromaticity and Antiaromaticity*; Wiley Interscience, New York, **1994**.
3. Schleyer, P. v. R.; Jiao, H. **1996,** *68*, 209.
4. Poranne, G. P.; Stranger, A. *Chem. Soc. Rev.* **2015**, *44*, 6597.
5. Schleyer, P. v. R. *Chem. Rev.* **2001**, *101*, 1115.
6. Schleyer, P. v. R.; Maerke, C.; Dransfeld, A.; Jiao, H.; Hommes, N. J. R. v. E. *J Am Chem Soc* **1996**, *118*, 6317.
7. London, F. *J. Phys. Radiu.* **1937**, *8*, 397.
8. Cheeseman, J. R.; Trucks, G. W.; Keith, T. A.; Frisch, M. J. *J. Chem. Phys.* **1996**, *104*, 5497.
9. Schreckenbach, G.; Ziegler, T. *J. Phys. Chem*. **1995**, *99*, 606.
10. Schreckenbach, G.; Ziegler, T. *Theor. Chem. Acc*. **1998**, *99*, 71.
11. Heine, T.; Schleyer, P. v. R.; Corminboeuf, C.; Seifert, G.; Reviakine, R.; Weber, J. *J. Phys. Chem. A* **2003**, *107*, 6470.
12. Giambiagi, M.; de Giambiagi, M. S.; Mundim, K. C. *Struct. Chem.* **1990**, *1*, 423–427.
13. Giambiagi, M.; de Giambiagi, M. S.; dos Santos Silva, C. D.; de Figuereido, A. P. *Phys. Chem. Chem. Phys*. **2000**, *2*, 3381–3392.
14. Bultinck, P.; Ponec, R.; Van Damme, S. *J. Phys. Org. Chem.* **2005**, *18*, 706–718.
15. Becke A. D.; Edgecomb K. E. *J. Chem. Phys*. **1990**, *92*, 5397-5403.
16. Savin, A.; Jepsen, O.; Flad, J.; Andersen, O. K.; Preuss, H.; von Schnering, H. G. (1992). "Electron localization in solid-state structures of the elements – the diamond structure". *AngewandteChemie International Edition in English*. **31** (2): 187–188.
17. Paul, S.; Goswami, T.; Misra, A. *AIP Advances*, **2015**, ***5***, 107211.
18. Anderson, P. W. *Phys. Rev.* **1950**, *79*, 350.
19. Anderson, P. W. *Phys. Rev.***1959**, *115*, 2.
20. Anderson, P. W. Theory of the magnetic interaction: exchange in insulators and superconductors. In solid state physics; Turnbull, F., Seitz, F., Eds.; Academic Press: New York, 1963; Vol. 14, p 99.
21. Ziegler, T.; Rauk, A. *Theor. Chim. Acta* **1977**, *46*, 1.
22. Pinter, B.; Fievez, T.; Bickelhaupt, F. M.; Geerlings, P.; DeProft, F. *Phys. Chem. Chem. Phys.* **2012**, *14*, 9846.
23. Michalak, A.; Mitoraj, M.; Ziegler, T. *J. Phys. Chem. A* **2008**, *112*, 1933.
24. (a) Mitoraj, M.; Michalak, A. *J. Mol. Model.* **2007**, *13*, 347–355; (b) Mitoraj, M. P.; Michalak, A.; Ziegler, T. *J. Chem. Theory Comput.*, **2009**, *5*, 962–975.
25. Bader, R. F. W. *Atoms in Molecules: A Quantum Theory;* Oxford University Press Oxford UK, 1990.

26. Bauzá, A.; Quiñonero, D.; Deyà, P. M.; Frontera, A. *Chem. Phys. Lett*. **2012**, *536*, 165.
27. Zubarev, D. Yu.; Boldyrev, A. I. *Phys. Chem. Chem. Phys.* **2008**, *10*, 5207.
28. Foster, J. P.; Weinhold, F. *J. Am. Chem. Soc*. **1980**, *102*, 7211.
29. Reed, A. E.; Curtiss, L. A.; Weinhold, F. *Chem. Rev*. **1988**, *88*, 899.
30. Marx, D.; Hutter, J.; J. Grotendorst (Ed.), Proceedings of Modern Methods and Algorithms of Quantum Chemistry, John von Neumann Institute for Computing, Jurich, Germany, 2000.
31. Schlegel, H. B.; Millam, J. M.; Iyengar, S. S.; Voth, G. A.; Daniels, A. D.; Scuseria, G. E.; Frisch, M. J. *J. Chem. Phys.***2011**, *114*, 9758-9763.
32. Iyengar, S. S.; Schlegel, H. B.; Millam, J. M.; Voth, G. A.; Scuseria, G.E.; Frisch, M. J. *J. Chem. Phys.* **2011**, *115*, 10291-10302.
33. Schlegel, H. B.; Iyengar, S. S.; Li, X.; Millam, J. M.; Voth, G. A.; Scuseria, G. E.; Frisch, M. J. *J. Chem. Phys.* **2002**, *117*, 8694-8704.
34. McWeeny, R. *Rev. Mod. Phys*. **1960**, *32*, 335.
35. Pearson, R. G. Recent Advances in the Concept of Hard and Soft Acids and Bases. *J. Chem. Edu.***1987**, *64*, 561-567.
36. Parr, R. G.; Chattaraj, P. K. *J. Am. Chem. Soc*. **1991,** *113*, 1854-1855.
37. Ayers, P. W.; Parr, R. G. *J. Am. Chem. Soc.* **2000**, *122*, 2010-2018.
38. Chattaraj, P. K.; Sengupta, S. *J. Phys. Chem*. **1996**, *100*, 16126-16130.
39. Fuentealba, P.; Simon-Manso, Y.; Chattaraj, P. K. *J. Phys. Chem. A* **2000**, *104*, 3185-3187.
40. Pan, S.; Solà, M.; Chattaraj, P. K. *J. Phys. Chem. A* **2013**, *117*, 1843-1852.
41. Saha, R.; Pan, S.; Chattaraj, P. K. *Molecules* **2016**, *21*, 1477-1493.
42. Chamorro, E.; Chattaraj, P. K.; Fuentealba, P. *J. Phys. Chem. A* **2003**, *107*, 7068-7072.
43. Parthasarathi, R.; Elango, M.; Subramanian, V.; Chattaraj, P. K. *Theo. Chem. Acc.* **2005**, *113*, 257-266.
44. Geerlings, P.; De, P. F.; Langenaeker, W. *Chem. Rev*. **2003**, *103*, 1793-1874.
45. Chattaraj, P. K. *J. Indian. Chem. Soc.* **1992**, *69*, 173-183.
46. Parr, R. G.; Donnelly, R. A.; Levy, M.; Palke, W. E. *J. Chem. Phys.* **1978**, *68*, 3801.
47. Chattaraj, P. K.; Sarkar, U.; Roy, D. R. *Chem. Rev.* **2006**, *106*, 2065-2091.
48. Chattaraj, P. K.; Roy, D. R. *Chem. Rev.* **2007**, *107*, PR46-PR74.
49. Parr, R. G.; Szentpaly, L. v.; Liu, S. *J. Am. Chem. Soc.***1999**, *121*, 1922-1924.
50. Koopmans, T. A. *Physica* **1993**, *1*, 104-113.
51. Janak, J. F. *Phys. Rev. B.* **1978**, *18*, 7165.
52. Roy, R.K.; Pal, S.; Hirao, K. *J. Chem. Phys*. **1999**, *110*, 8236
53. Roy, R.K.; Pal, S.; Hirao, K. *J. Chem. Phys*. **2000**, *113*,1372
54. Ayers, P.W.; Morrisson, R.C.; Roy, R.K. *J. Chem. Phys*. **2002**, 116, 8731.
55. Hocquet, A.; Toro-Labbé, A.; Chermette, H. *J. Mol Struc (THEOCHEM)* **2004**, 686, 213-218.
56. Melin, J.; Aparicio, F.; Subramanian, V.; Galván, M.; Chattaraj, P.K. *J. Phys. Chem. A* **2008**, *108*, 2487-2491.
57. Lu, T.; Chen, F. *J. Comp. Chem.* **2012**, *33*, 580-592.

CHAPTER 3

A mini review article: Aromaticity in the light of magnetic criteria

3.1.

INTRODUCTION

The history of aromaticity, which is a fundamental concept in chemistry, began in 1825 when Michael Faraday[1] isolated benzene for the first time. However, the very first definition of aromaticity was given by Kekulé[2-3] in which he suggested oscillating structures where synchronous 1, 2-shifts of the three double bonds occur perpetually. Then after six decades, the works of Hückel[4-8] and Pauling[9] explained the role of delocalization of electrons in the stabilization of aromatic systems, using the quantum mechanics based Molecular Orbital (MO) approach and Valence Bond (VB) method respectively. Since then, the circular delocalization of electrons is taken as the genesis of aromaticity.

Aromaticity is developed as an important phenomenon for its close relation with chemical reactivity.[10] The increasing interest on aromaticity persuaded a need to attach a quantitative character to it. Consequently, a number of quantitative aromaticity indices have been anticipated starting from the famous (4n+2) π- electron rule of Hückel to the latest Shannon Entropy index.[11] At present, the molecular property based criteria for aromaticity can be broadly divided into four basic categories such as magnetic,[12] structural,[13] electronic,[14] and energetic.[15] Electron density based indices such as para-delocalization index (PDI),[14] fluctuation index (FLU)[16] and multi-centre bond index (MCBI)[17] have also been introduced to characterize aromaticity. Later, Klein and co-workers correlated aromaticity of molecular benzenoids to a unique type of polynomial, [18] as Clar-2-nomial on the basis of Clar's concept of aromatic sextet .[19] Later on, this correlation has been extended for radical benzenoids[20] and more recently on polyacenes and beyond.[21] However, most of the indices do not provide direct measure of aromaticity, as the phenomenon is not directly observable.[22]

After a meticulous revision of structural, energetic and magnetic indices of aromaticity for many aromatic systems, Cyranski et al. concluded aromaticity as an abstract concept from philosophical point of view.[22] Whereas, from another perspective, the event of aromaticity can be regarded as multidimensional since it cannot be described definitely by any single property based index and all indices do not always give consistent results. Due to all these problems the quantification of aromaticity still remains a challenging and fundamental problem, and ought to be addressed through a precise phenomenological description.[23]

3.2.

CRITERIA FOR DEFINING AROMATICITY

3.2.1. Chemical behavior

Electrophilic aromatic substitution reactions are the characteristic reactions of the aromatic systems but it is difficult to define aromaticity with the help of the chemical behavior of the molecule. Since aromaticity is a property of the initial state, and reactivity is the property of the intermediate states so quantifying aromaticity with the help of chemical reactivity is not straightforward. The characteristic electrophilic aromatic substitution reaction also has many exceptions, for example, phenanthrene and anthracene which are aromatic molecules prefer addition of bromine rather than substitution. Also fullerenes (eg, C_{60} or C_{70}) are aromatic compounds but since they are devoid of any hydrogen, they do not undergo aromatic substitution reactions but only undergo addition reactions.[12]

3.2.2 Structural pattern

Aromatic systems are mainly planar systems. The characteristic property of an aromatic system is that its bond lengths are all equal and π-electrons are delocalized. The direct determination of bond lengths gives us valuable information regarding the extent of delocalization. In contrast, in antiaromatic molecules the alternating double and single bond lengths differ significantly, generally over 0.2 Å in length.[24] However, bond length equalization and the symmetry associated with it cannot be used as the only parameter for defining aromaticity because some systems possessing equal bond lengths are not aromatic. Again, borazine which is an isoelectronic system with benzene has roughly equal bond lengths and considered to be weakly aromatic in nature.[12] The degree of aromaticity in borazine has been a topic of some controversy[25] starting soon after its discovery in 1926 by Stock and Pohland.[26] The properties of borazine are in good accordance with a ring structure of six atoms which ‘‘on-the-average’’ correspond to a sp^2 hybridized-carbon.[27] Also, strain effects and other contributing factors provide hindrance in predicting aromaticity with the help of structural criteria.[24]

3.2.3 Energetic criteria

Aromaticity has long been connected to the enhanced resonance energies (REs) and the aromatic stabilization energies (ASEs). Even the (4n+2) π- electron rule of Hückel is based on energetic criterion. The energetic measure of aromaticity and antiaromaticity is based on evaluations of energies relative to the reference systems such as conjugated polyenes or olefins.[24] However, determinations of (REs) and (ASEs) are quite difficult even for simple systems.[12] Since ASE itself is not physically observable, [28] direct experimental determination of ASE is difficult. However, starting from the pioneering work of Pauling and Sherman,[29] various efforts have been made to estimate ASE from experimental data. Also, introduction of isodesmic [30] and homodesmotic reactions, [31] has made it possible to calculate the ASE from the energies of reactants and products, obtained experimentally from calorimetric measurements.[32] In a recent work a phenomenological model is discussed to evaluate ASE without any reference state.[23]

3.2.4. Magnetic criteria

Primarily, aromaticity was restricted to all carbon, coplanar, delocalized conjugated π systems having (4n+2) π electrons according to Huckel's rule of aromaticity.[4-8] Presently aromaticity is not only confined to the organic systems, according to Boldyrev, "Aromaticity has in recent years become an important and powerful unifying concept to describe the stability and bonding in many chemical species beyond organic chemistry, including inorganic cations, anions, radicals, and clusters.",[33] three dimensional aromaticity involving σ-electrons and multidimensional aromaticity involving d-orbitals have been reported. Aromaticity has not been confined to ground states but it has been extended to transition states and excited states. There is possibly no direct way to calculate the aromaticity in a molecule experimentally.

Magnetic criteria are currently the most popular methods and constitute the most frequently used aromaticity indices. There are various criteria for defining aromaticity such as energy, structure, electron density based indices[34] and magnetic properties but we focus our discussions to magnetic properties only. Magnetic properties provide considerable insight into the concept of aromaticity. The anomalous diamagnetization of benzene has been related to the delocalization of π-electrons since the early days of quantum chemistry. The aromatic molecules demonstrate relatively strong diamagnetism when placed in a magnetic field; this is due to the generation of an opposing magnetic field by the induced ring currents. The

magnetic criteria of aromaticity are dependent on the specific reaction of the aromatic compounds to externally applied uniform magnetic field which is placed perpendicular to the molecular plane. This contribution of π-electrons to the magnetic susceptibility component which is placed perpendicular to the molecular plane was chosen as an indicator of aromaticity. While the direction of an induced current in a loop is determined by the relative orientation of the magnetic field and the loop's movement but the direction of the current in a molecule also depends on the type of the system. Generally in a system containing 4nπ electrons, an external magnetic field induces a paratropic ring current (i.e. in the opposite direction relative to a classic loop) while a system containing (4n+2)π electrons shows a diatropic ring current(i.e. in the same direction as a classic loop).[35]

Magnetic properties are necessary but not sufficient to describe a system as aromatic or antiaromatic but magnetic criterion has an advantage over other criterion that we can compare the paratropic and diatropic ring currents to experimental values derived from NMR. Now, the concept of aromaticity is no longer confined to the organic domain but has been found in all-metal clusters systems and the existence of an σ-aromaticity.[36] The most popular and frequently used aromaticity indices are NMR chemical shifts, magnetic susceptibility anisotropy, Nucleus Independent Chemical Shift (NICS), Aromatic Ring Current Shielding (ARCS) and Current Density Analysis (CDA plots).[35]

3.2.4.1. NMR chemical shifts

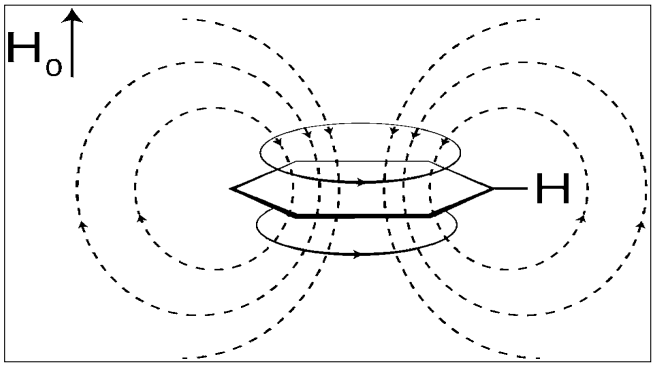

Figure 3.1. Representation of the Ring Current Model in the case of benzene. [35]

The most widely used NMR chemical shifts method is the ^{1}H-NMR method. According to the Ring Current Model (RCM),[37] for a (4n+2) π electrons system, the diatropic ring current will form an induced magnetic field which is opposite in direction to the applied external magnetic field at the centre of the ring as depicted in the above diagram (Figure 3.1). While outside the ring the curved lines of the magnetic field are in the same direction as the applied external field. Thus protons that are inside the ring experience an upfield shift while protons that are outside experience a downfield shift. In the case of a 4nπ electron system, a paratropic ring current is induced, so here the induced magnetic field is in the same direction as the external field at the centre of the ring while outside the ring it is in the opposite direction to the external field, thus here the internal protons experience a downfield shift while the external protons experience an upfield shift, that is the effect is exactly the opposite. Thus, the chemical shifts of protons have been used to characterize aromatic and antiaromatic compounds. The ring current picture has proven to be powerful in justifying the magnetic properties of π electron systems quantitatively. The concept is so visual "that one can almost *feel* when a molecule is subjected to a magnetic field." The ring current is connected to the concept of aromaticity experimentally through anisotropy of magnetic susceptibility or through exaltation of magnetic susceptibility or by chemical shifts methods in a Nuclear Magnetic Resonance experiment and also individual ring current intensities which can be computed.[38]

The rings of most aromatic systems are too small to accommodate inner protons, so the chemical shifts of hydrogen at the bridging positions provide better information regarding the aromaticity and antiaromaticity of the systems. However, this criterion is not general for aromatic systems that are devoid of hydrogen like for example C_{60} and the oxocarbons (30) and ^{13}C chemical shifts in aromatic hydrocarbons are not deshielded.[24]

Other NMR chemical shifts methods are Li^+ and ^3He chemical shifts method. Chemical shifts of ^7Li were used to investigate the electron delocalization. Aromatic and antiaromatic compounds of Li^+ complexes show significant shielding and deshielding respectively of the ^7Li NMR signals due to the induced ring currents.^7Li chemical shifts obtained by modern computations technique match well with the ^7Li NMR chemical shifts that are obtained experimentally. So, one of the advantages of using Li^+ NMR chemical shifts as a computational tool is that it can be compared with the experimental Li NMR data of Li^+ complexes.[24] However, a major drawback is that the ring currents are relatively small. Also, the number of Li^+ complexes is limited therefore the use of Li^+ NMR chemical shifts as a magnetic criterion is also limited. An extension of the use of NMR to assess aromaticity was developed mainly by Mitchell.[39]

3.2.4.2. Magnetic susceptibility anisotropy

This method provides another magnetic criterion of aromaticity. The tensor normal to the aromatic ring is much larger than the average of other tensors and this difference is termed as exaltation. Magnetic susceptibility exaltation (λ) is the difference between the observed bulk magnetic susceptibility value and the susceptibility that is evaluated on the basis of an increment system ($\lambda=\chi_m-\chi_{m'}$). The exaltation of magnetic susceptibility is mainly due to the induced ring currents and is a widely employed magnetic criterion especially for the characterization of metal clusters. In the 1996 review article entitled "What is aromaticity", Schleyer and Jiao suggested that "compounds which exhibit significant exalted diamagnetic susceptibility are aromatic. Those compounds with exalted paramagnetic susceptibility may be antiaromatic."[24]

However, this method is applicable for planar or nearly planar aromatic molecules and is not applicable in the case of spherical systems. Also, in some cases, high magnetic

anisotropy does not necessarily imply aromaticity. In addition, the contribution to the magnetic susceptibility component which is perpendicular to the molecular plane provides a more consistent aromaticity criterion than that which is dependent solely on magnetic anisotropy.[40] This method was popular earlier, but recently it is not much in use because it is difficult to quantify aromaticity using this method. Nowadays, computational methods are more developed and provide a better qualitative and quantitative understanding of the magnetic properties.

It is interesting to note that ring currents and aromaticity are theoretical properties and neither are measurable quantities but both NMR chemical shifts and magnetic susceptibility exaltation methods are experimentally measurable quantities that result from ring currents.

3.2.4.3. Current Density Analysis Plots (CDA)

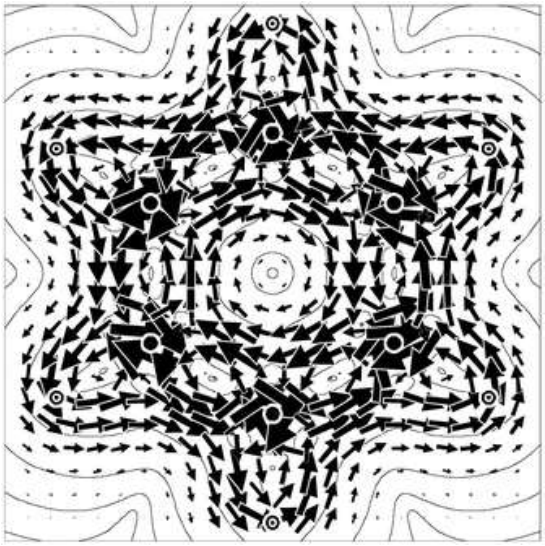

Figure 3.2. Plot of the current density induced in the molecular plane of the benzene by a perpendicular external magnetic field.[56]

This method is purely a computational method. It is the visualization of the ring currents with the help of arrows and the direction of the arrows gives us the idea of whether the ring current is diatropic or paratropic. Clockwise direction represents paratropic ring current while anticlockwise direction represents diatropic ring current. Also the size of the arrows indicates the strength of the ring current. The CDA plot of benzene ring is depicted in the above figure (Figure 3.2).

According to the Ring Current Model (RCM)[37] in the presence of an external magnetic field, a diatropic ring current is generated in aromatic systems and a paratropic ring

current is generated in antiaromatic systems. Thus, the aromaticity of a planar or a nearly planar compound when placed in an external magnetic field perpendicular to the molecular plane can be obtained directly, either by calculating the intensity of the current or by calculating the current density in a given system. New computational methodologies are now developed that provide a visual representation of the current density field induced in a molecule. These current density maps provide relevant information and help in understanding features of aromatic compounds.

The main advantage of this method is that it provides pictorial representation of the ring currents in the systems. However, the major drawback of this method is that it is very difficult to quantify and also the pictures that are obtained through this method are not easily separable into their individual components. Also, in some cases, high magnetic anisotropy does not necessarily imply aromaticity. In addition, second order magnetic properties; such as polarizability, magnetizability, and nuclear shielding were not calculated accurately by the original methods which can generally be obtained by the integration of first order current density. The most popular CDA methods are: Continuous Transformation of Current Density – Diamagnetic Zero (CTOCD-DZS) [41-43] also known as the ipsocentric method.[44-46]

3.2.4.4. Nucleus Independent Chemical Shift (NICS)

It is the most popular method for quantifying the magnetic properties of molecules mainly due to its simplicity and efficiency. NICS has been popularized by Schleyer and his co-workers.[47] NICS is defined as the negative value of the absolute magnetic shielding. NICS method uses a ghost atom namely Bq (named after the ghost Banquo from Shakespeare's Macbeth), it is devoid of any electrons, protons and neutrons. Initially it was placed at the centre of the system [NICS (0)], then later at a distance of 1 Å above the plane [NICS (1)].This ghost atom is like a sensor for the magnetic environment at the position at which it is placed. The ghost atom senses this magnetic environment and reports the chemical shielding values through the use of computational technique like GIAO. [48-49] The NICS values were reported with reversed signs, in agreement with NMR chemical shift convention. Positive NICS value indicates a paratropic magnetic field whereas a negative NICS value indicates a diatropic magnetic field, thus a negative NICS value would mean that a system is aromatic and a positive NICS value would correspond to an antiaromatic system. In some cases, the negative value indicates the 3D-aromaticity of the molecule.[50] The chemical shift is

used as an indicator of the direction and magnitude of the induced magnetic field. From Figure 3.3 it can be noted that NICS corresponds well with the aromatic stabilization energy.[24]

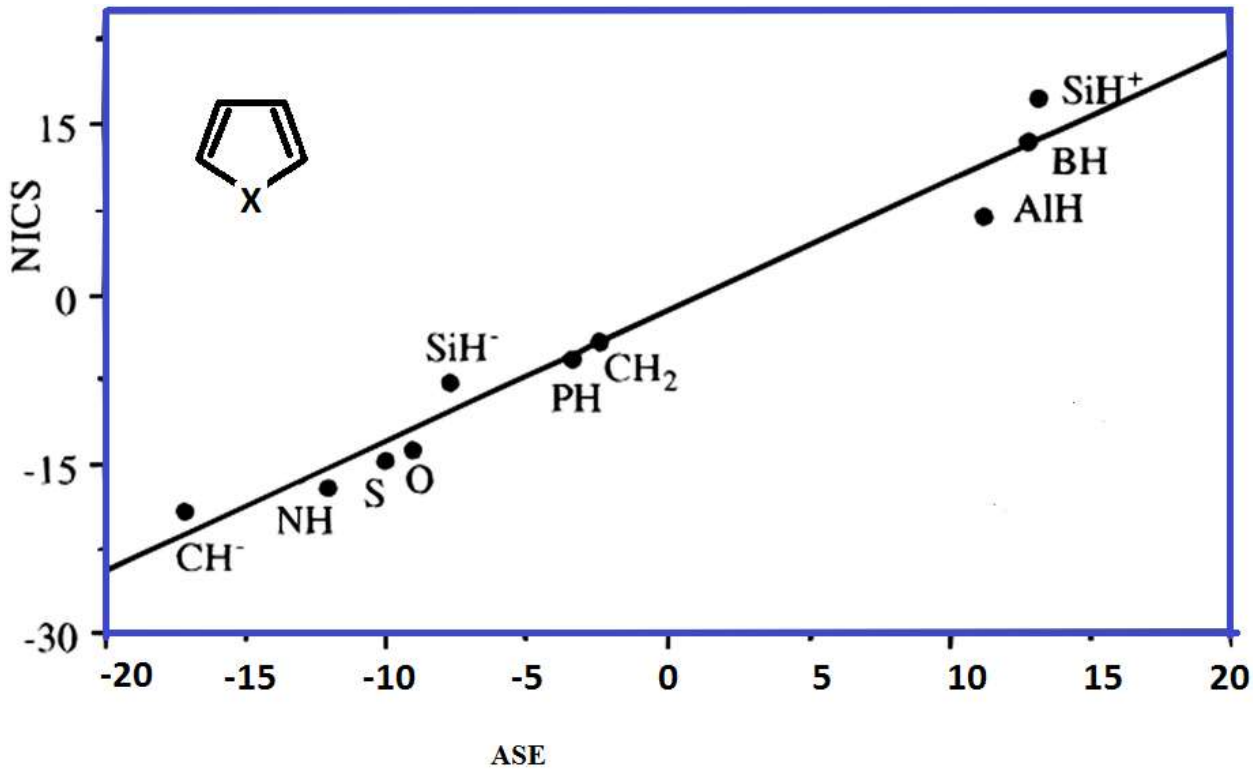

Figure 3.3. Plot of NICS (0) (ppm) *vs.* the ASE (kcal mol^{-1}) for a set of five-membered ring heterocycles, C_4H_4X (X = as shown).[24]

According to an article in 2005 by Schleyer and his coworkers, "NICS has several advantages over many other aromaticity criteria: (i) NICS does not require reference standards, increment schemes, or calibrating (homodesmotic) equations for evaluation. (ii) Unlike λ which depends on the square of the ring area, NICS only shows a modest dependence on the ring size. It does depend on the number of electrons. The 10 π electron systems give significantly higher values than those with six π electrons, for example, the cyclooctatetraenedication and dianion. (iii) Importantly, in several sets of related molecules, NICS correlates well with other aromaticity indexes based on energetic, geometric, and other magnetic criteria (iv) NICS can becomputed easily using standard quantum chemical programs such as Gaussian 09, Gaussian 98, Gaussian 03, ADF, and deMon."[12]

After their initial publication, Schleyer and his co-workers noted the problem in using NICS for 3-membered systems due to the local shielding effects of the neighboring σ-bonds. So they introduced two modifications in the following year. [51] The first modification was that the bq was raised 1 Å above the molecular plane, which was termed as NICS (1). Since σ-contributions are short ranged, so NICS (0) has greater σ-contributions, so by raising the bq by 1 Å, the σ-contributions are effectively reduced. Secondly, the total NICS value was separated into σ and π contributions. Since aromaticity results from π contributions, so NICS (1) is a better aromaticity criterion than NICS (0).

However, the major drawback of NICS is that it reports only a single value at a given position, without any information regarding the magnetic field. Also, there are other magnetic shielding contributions from the local circulation of electrons in bonds, lone pairs and interior electrons, so the reliance on the π-system is not pure. In fact the σ framework of the CC and CH bonds affects the chemical shifts of organic molecules, as a result of this; the NICS value is non-zero for non-aromatic, saturated and unsaturated hydrocarbon rings. Sometimes NICS is considered as a local index rather than a global, aromatic index because contributions from remote parts of molecule are small. Later refinement of the original NICS technique offered better understanding of the aromatic systems which include the Dissected NICS technique which consists of the LMO-NICS method and the CMO-NICS method.[12] Other modifications like NICS rate and NICS scan are also known.

The major difficulty in quantifying aromaticity may be due to the fact that aromaticity is not a property of the ground state energy of molecules but is rather dependent on the excited π electron state. So a recent and a fresh approach, i.e., Quantitative Structure Aromaticity Relationships (QSArR) in relating aromaticity with physico-chemical molecular properties such as chemical hardness and electronegativity are reflected in the works of Putz. His works focuses on the connection of aromaticity with a reactivity index. If successfully applied, "It may provide both conceptual new insight on the aromaticity concept as well as generalization of the chemical reactivity theory and principles grounded on structural indices as electronegativity and chemical hardness that have been intensively considered in the last decades within density functional theory and quantum chemistry." [52-54]

3.3.

CONCLUSIONS

Aromaticity is now no longer confined to the domain of organic chemistry and various inorganic clusters are found to be aromatic considering the delocalization of the π electrons as the genesis of aromaticity. The ease with which aromaticity bridges the gap between traditional aspects of organic chemistry and latest discoveries in inorganic chemistry are truly fascinating. Aromaticity is not a physically observable quantity so defining it precisely is still a challenge. Quantification of aromaticity is a major challenge to the theoretical and the computational chemists till date. Whether aromaticity is a multidimensional phenomenon or it can be defined by a universal single unique criterion is a debatable topic. The journey of aromaticity from Kekulés definition of benzene has been extensive and the recent developments in this field provide a considerable better insight into the concept. It is aptly said by Schleyer that, "aromaticity has been a time-dependent phenomenon." The perception of aromaticity is different in terms of its properties and characteristics to chemists with diverse backgrounds.[55] The magnetic criterion for defining the concept of aromaticity has become very prominent surpassing the other criteria. Various developments in this field have occurred in the recent years and most of the developments were in the magnetic domain. So we can conclude by saying that the magnetic criterion is the most important criterion and provides a plethora of opportunities of future work on aromaticity.

3.4.

REFERENCES

1. Faraday, M. M.*Phil.Trans.Roy.London.* **1825,** *115*, 440-446.
2. Kekulé, A. *Bull.Soc.Chim.Paris* **1865,** *3*, 98-100.
3. Kekulé, A. *Ann.Chem.Pharm* **1866,** *137*,129-196.
4. Hückel, E. *Z. Phys*. **1930,** *60*,423–456.
5. Hückel, E. *Z. Phys.* **1931**, *70*, 204–86.
6. Hückel, E. *Z.Phys.* **1932,** *76*,628-648.
7. Hückel, E. *Z.Electrochem, Angew.Phys.Chem.* **1937,** *43*, 752-788.
8. Hückel, E. *Z.Electrochem, Angew.Phys.Chem* **1995,** *61*,866-890.
9. Pauling, L; Wheland, G.W. *J.Chem.Phys.* **1933**, *1*, 362-374.

10. (a) Balaban, A. T.; Oniciu, D.C.; Katritzky, A.R. *Chem. Rev* **2004**, **104***(5)*, 2777-2812. (b) Chattaraj, P. K.; Sarkar, U.; and Roy, D. R. *J. Chem. Educ*., **2007**, *84*, 354.(c) Chattaraj, P.K.; Roy, D. R.; Elango, M.; and Subramanian, V. *J. Phys. Chem.A* **2005**, *109*, 9590.
11. Noorizadeh, S.; Shakerzadeh, E. *Phys.Chem.Chem.Phys.* **2010**, *12(18)*, 4742-4749.
12. Chen, Z.; Wannere, C. S.; Corminboeuf, C.; Puchta, R.; Schleyer, P. v. R. *Chem.Rev* 2005, *105(10)*, 3842-3888.
13. Krygowski, T. M.; Cyrański, M. K. *Chem. Rev* 2001, **101***(5)*, 1385-1420.
14. Poater, J.; Duran, M.; Solà, M.; Silvi. B. *Chem.Rev* **2005**, *105(10)*, 3911-3947.
15. Cyrański, M. K. *Chem. Rev* 2005, **105***(10)*, 3773-3811.
16. Matito, E.; Duran, M.; Solà, M. *J. Chem. Phys.* 2005, **122***(1)*, 014109.
17. (a)Bultinck, P.; Ponec, R.; Van Damme, S. *J. Phys. Org. Chem* 2005, *18(8)*, 706-718. (b) Roy, D.R.; Bultinck, P.; Subramanium, V.; Chattaraj, P.K. *J. Mol. Struc (THEOCHEM)* 2008, *854(1-3),* 35-39.
18. Misra, A.; Klein, D. J.; Morikawa, T. *J. Phy. Chem. A* **2009,** *113(6),*1151-1158.
19. Clar, E. The Aromatic Sextet. Wiley & Sons: New York, **1970**.
20. Misra, A.; Schmalz, T. G.; Klein, D. J. *J. Chem. Inf. Model* **2009,** *49(12)*, 2670-2676.
21. Bhattacharya, D.; Panda, A.; Misra, A.; Klein, D. J. *J.Phys.Chem.A* **2014,** *118(24)*, 4325-4338.
22. Cryański, M. K.; Krygowski, T. M.; Katritzky, A. R.; Schleyer, P.v.R. *J.Org.Chem* **2002,** *67(4)*, 1333-1338.
23. Paul, S.; Goswami, T.; Misra, A *AIP Advances* **2015**,*5*, 107211.
24. Schleyer, P.v.R.; Jiao, H. *Pure & Appl.Chem.***1996,** *68* 209-218.
25. Islas, R.; Chamorro, E.; Robles, J.; Heine, T.; Santos J.C.; Merino, G. Borazine: to be or not to be aromatic *Struct.Chem.* 2007, *18*, 833.
26. Stock, A.; Pohland, E. Borwasserstoffe, IX.: B3N3H6. *Chem. Ber.*1926, *59B*, 2215.
27. Bhattacharya, D.; Shil, S.; Misra, A.; Bytautasc, L.; Klein, D.J. *Phys. Chem. Chem. Phys.* 2015, *17*, 14223.
28. Mo, Y.; Peyerimhoff, S. D. *J.Chem.Phys.*1998, *109(5)*, 1687-1697.
29. Pauling, L.; Sherman, J. *J. Chem. Phys.* 1933, *1(8)*, 606-617.
30. Hehre, W. J.; Radom, L.; Schleyer,P. v. R.; Pople, J.A. Ab Initio Molecular Orbital Theory, Wiley &Sons: New York, **1986**.
31. Hehre, W. J.; McIver, R.T.; Pople, J.A.; Schleyer,P. v. R. *J. Am. Chem. Soc*. **1974**, *96(22)*, 7162-7163.
32. Pedley, J. B.; Naylor, R. B.; Kirby, S. P.; Thermodynamical Data of Organic Compounds, Chapman & Hall: London, **1986**.
33. Jose, M. M.; Boldyrev, A. I.; Merino, G.; Ugalde, M.J. *Chem.Soc.Rev.* 2015, *44*, 6519.
34. Poater, J.; Fradera, X.; Duran, M.; Solá, *Chem-Eur.J.***2003**, *9(2)*, 400-406.
35. Poranne, G. P.; Stranger, A. *Chem.Soc.Rev.* 2015, *44*, 6597.
36. (a) Dewar, M. J. S.; McKee, M.L *Pure Appl. Chem.*1980, *52*, 1431 – 1441. (b)Dewar, M. J. S. *Bull. Soc. Chim.Belg.* 1979, *88*, 957 – 967.
37. Pople, J. A. *Mol, Phys.*, **1958**, *1*,175-180.
38. Gomes, A. N. F.; Mallion, R. B. *Chem.Rev.* **2001**, *101*, 1349-1384.
39. Mitchell, R. H. *Chem.Rev.* **2001**, *101*, 1301-1315.

40. Benassi, R.; Lazzeretti, P.; Taddei, F. *J.Phys.Chem.* 1975, *79(8)*, 848-851.
41. Coriani, S.; Lazzeretti, P.; Malagoli, M.; Zanasi. R. *Theor.Chim.Acta.* **1994**, *89*,181-192.
42. Lazzeretti, P.; Malagoli, M.; Zanasi, R. *Chem.Phys.Lett.* **1994**, *220*, 299-309.
43. Zanasi, R. *J.Chem.Phys.* 1996, *105*, 1460-1469.
44. Steiner, E.; Fowler, P.W. *J.Phys.Chem.A* 2001, *105*, 9553-9562.
45. Steiner, E.; Fowler, P.W. *Chem.Commun.* **2001**, 2220-2221.
46. Steiner, E.; Fowler, P. W.; Havenith, R. W .A. *J.Phys.Chem.A* 2002, *106*, 7048-7056.
47. Schleyer, P. v. R; Maerker, C.; Dransfeld, A.; Jiao,H.; Hommes, N. J. R. *J.Am.Chem.Soc.* **1996**, *118*, 6317-6318.
48. London, F. *J. Phys. Radium.* **1937**, *8*, 397.
49. (a) Cheeseman, J. R.; Trucks, G. W.; Keith, T. A.; Frisch, M. J. *J. Chem. Phys.* **1996**, *104*, 5497.(b) Schreckenbach, G.; Ziegler, T. *J. Phys. Chem.* **1995**, *99*, 606.(c) Schreckenbach, G.; Ziegler, T. *Theor. Chem. Acc.* **1998**, *99*, 71.
50. Chattaraj, P.K. Aromaticity and Metal Clusters,Taylor & Francis/CRC Press: Florida, **2010**.
51. Schleyer, P. v. R; Jiao, H.; Hommes, N.J.R.; Malkin,V. G.; Malkina, O. *J.Am.Chem.Soc.* **1997**, *119*,12669-12670.
52. Putz, M. V. *MATCH Commun. Math. Comput. Chem*. **2010**, *64*, 391-418.
53. Putz, M. V. *Int. J. Mol. Sci.* 2010, *11*, 1269-1310.
54. Tarko, L.; Putz, M. V. *J.Math.Chem,***2010**, *47(1),*487-495.
55. Schleyer, P. v. R. *Chem.Rev.* 2001, *101*, 1115-1118.
56. Bultinck, P. General discussion. *Faraday Discussions* **2007**, 135, 367-401.

CHAPTER 4

On exo-cyclic aromaticity

4.1.

INTRODUCTION

Unambiguous definition of aromaticity has long been a subject of interest. Aromatic nature is correlated with a varietyof structural and energetic characteristics, such as highly symmetric structure, delocalized electrons, enhanced thermodynamic stability, reduced reactivity as compared to nonaromatic compounds and so on.[1-4] Other prominent indication of aromatic character comes from the properties like down-field shift in proton NMR peak positions resulting from the exaltation of diamagnetic susceptibility.[5,6] However, even after two centuries of existence,[7,8] still there is a scope of defining aromaticity unequivocally,[9] as understood from two legendary examples of complementary topological definition of aromaticity by Hückel[10] and Möbius.[11] The proposition by Hückel that cyclic-planar (4n+2) π-electron characterizes aromatic compounds is taken as gospel by the chemists.[10] Archetypal aromatic molecules contain a planar ring framework with equalized bond lengths. Though, Hückel's (4n+2) π rule is the easiest test to recognize aromaticity, its multidimensional nature often stands in the way of precisely identifying aromatic systems.[12-15] This apparently simple electron count rule was renewed by Dewar's insight of the tropolone structure.[16] In 1922 Crocker noticed that "aromatic structure is observed only in those combinations of elements which furnish six extra or aromatic electrons above those needed to complete a single-bonded ring" and described accurately the "six aromatic electron" structure[17] of benzene, pyridine, and five-membered ring heteroaromatics, earlier than the famous "aromatic sextet" paper by Armit and Robinson.[18]

4.2.

COMPUTATIONAL DETAILS

The minimum energy search was performed in Gaussian 09W suit of software at different DFT and *ab initio* methodologies.[19] ADF program[20] is also used for energy decomposition analysis (EDA) based on the methods of Ziegler and Rauk.[21] The total binding energy ΔE released upon the formation of the molecule from atomic fragments is divided into two major components, namely, ΔE_{prep} and ΔE_{int}, *i.e.*, $\Delta E = \Delta E_{prep} + \Delta E_{int}$. ΔE_{prep} corresponds

to the energy needed to promote the separated fragments from their equilibrium geometry to the final structure in the molecule. The interaction energy ΔE_{int} between the fragments is further decomposed into three physically meaningful terms, $\Delta E_{int} = \Delta E_{elstat} + \Delta E_{Pauli} + \Delta E_{orb}$. Here, ΔE_{elstat} is the classical electrostatic interaction between the promoted fragments as they are brought to their positions in the final complex. ΔE_{Pauli} corresponds to the repulsive Pauli interaction between occupied orbitals on the two fragments in the molecule. ΔE_{orb} represents interactions between the occupied molecular orbitals of one fragment with the unoccupied molecular orbitals of the other fragment and also signifies the mixing of occupied and virtual orbitals within the same fragment.[21] Diradical character y_i was estimated by means of PUHF method with the formula $y_i = 1 - {2T_i}/{1+T_i^2}$. The diradical character is defined by the weight of the doubly excited configuration in multiconfigurational self consistent field (MCSCF) theory and formally expressed by the overlap (T_i) between localized natural orbitals [highest occupied MO (HOMO) − i and lowest unoccupied MO (LUMO) + i], i being the number of MOs.[22] The dissected canonical molecular orbital NICS (CMO-NICS)[23,24] computation is performed using the ADF package. AdNDP is a compact combination of intuitive simplicity of Lewis theory with the flexibility and generality of Canonical Molecular Orbital theory thus providing a perfect description of systems featuring both localized and delocalized bonding without invoking the concept of resonance. AdNDP orbitals are analyzed using Multiwfn−A Multifunctional Wave function Analysis.[25] Molecular dynamics simulations were carried out with CP2K/Quickstep[26] package, which consists Born-Oppenheimer MD (BOMD) BLYP[27,28] GTH pseudopotentials[29,30] with a combined Plane-Wave (280 Ry density cutoff) and TZV2P basis sets.

4.2.1. Calculation of Ring Strain Energy (RSE)

The ring strain energy can be calculated with the help of Bader's Quantum theory of Atoms in Molecules (QTAIM).[31] The kinetic energy density at the ring critical point (3,+1) can be utilized to estimate the ring strain energy.[32] For the calculation of the RSE a regression equation, RSE=337.72×G(r)−8.115, is used as described in Ref. 20. The calculated RSE is found to be 27.98 kcal/mol.

4.2.2. Calculation of Aromatic Stabilization Energy:

The aromaticity of the proposed molecule is deemed to contribute significantly to its inherent stability. Recently, the stabilization in the molecular energy due to electronic mobility has been equated with the aromatic stabilization energy in the frame of second order perturbation theory. The proposed theoretical framework makes use of the inter-site hopping integral (t_{ij}) and the onsite repulsion energy (U) to account for the electron delocalization. The electronic population engaged in delocalization is obtained as a product of spin – orbital population ($n_{i\sigma}$ and $n_{j\sigma'}$) within the unrestricted framework and the degree of delocalization, which is estimated from electron localization function (ELF).

$$\Delta E = \sum_{i,j} \frac{t_{ij}^2}{U} \left(n_{i\sigma} n_{j\sigma'} + n_{i\sigma'} n_{j\sigma}\right) ELF^2 \tag{4.1}$$

However, the above equation had been derived for standard aromatic molecules which differ significantly from the present system with respect to the electronic structure and type of aromaticity. Particularly, the itinerancy of the lone pair of electrons in between the boron and fluorine completes the loop of electronic circulation and thus makes the pattern of electron delocalization unique with respect to traditional aromatic systems. To comply with this picture of electron delocalization, the above equation is split into two parts as follows,

$$\Delta E = \sum_{C,B} \frac{t_{ij}^2}{U} (n_{C\sigma} n_{B\sigma'} + n_{C\sigma'} n_{B\sigma}) ELF^2 + \sum_{F,B} \frac{2t_{ij}^2}{U} (n_{F\sigma} n_{B\sigma'} + n_{F\sigma'} n_{B\sigma}) ELF^2 \tag{4.2}$$

Here, the first part accounts for the electron delocalization within C – B ring, and the second part quantifies stabilization for electron delocalization within Lewis acid-base pair. The probability of both spin transfer from F to B is included by multiplying the stabilization term by two.

4.3.

RESULTS AND DISCUSSION

Aromatic cross-conjugated systems make it apparent that aromaticity must not be restricted only to the completely conjugated cyclic circuits.[33] This inspires us to study a four membered heteroatomic cyclic $C_2B_2F_4$ molecule with D_{2h} symmetry (Figure 4.1). Optimization of this molecule at different level of theory including coupled cluster singles double leads to a planar molecule (Dihedral angle 0.00°, Table 1 which is in agreement with the conclusions drawn in a recent report.[34] Geometry optimization is carried out from two different starting geometries, namely, rectangular and non-planar, to explore the possible existence of any isomer, specifically bond-stretch isomer,[35-37] of the present molecule. The convergence steps along with the energy of the final geometries from two different starting points suggest that both optimizations converge to the same structure depicting a planar as well as square C_2B_2 core (Figure 4.2).

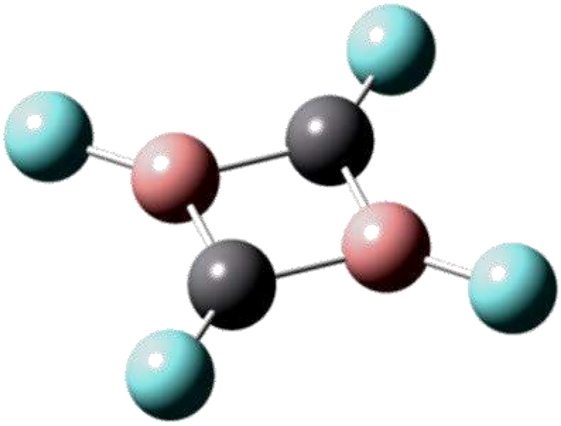

Figure 4.1. Optimized structure of $C_2B_2F_4$ cluster is of D_{2h} symmetry. The gray, pink and cyan spheres represent carbon, boron and fluorine atoms respectively.

Table 4.1. The optimized bond lengths (in Å) at different DFT and *ab initio* methodologies using aug-cc-pVDZ basis set.

Methodology (along with aug-cc-pVDZ basis set)	**B-C bond length (in Å)**	**B-F bond length (in Å)**	**C-F bond length (in Å)**	**∠BCB bond angle (in °)**	**∠CBC bond angle (in °)**	**∠CBBC dihedral angle (in °)**	**Energy (in A.U.)**	**Minimum vibrational frequency (in cm^{-1})**
QCISD*	1.542	1.340	1.319	93.23	86.77	0.00	−524.09	58.58
CISD*	1.527	1.330	1.303	93.18	86.82	0.00	−524.07	52.36
CCSD*	1.541	1.338	1.317	93.22	86.78	0.00	−524.09	57.82
MP2	1.544	1.350	1.331	93.86	86.14	0.00	−524.18	56.54
B3LYP	1.532	1.339	1.322	93.42	86.58	0.00	−525.40	61.90
B3PW91	1.531	1.337	1.317	93.48	86.52	0.00	−525.19	58.27
PBEPBE	1.541	1.347	1.331	93.54	86.46	0.00	−524.86	60.36
BLYP	1.543	1.350	1.340	93.57	86.43	0.00	−525.33	65.22
TPSSH	1.534	1.342	1.326	93.52	86.47	0.00	−525.41	61.65
CAM-B3LYP	1.525	1.334	1.315	93.44	86.56	0.00	−525.23	57.91
M-06	1.526	1.329	1.310	93.42	86.58	0.00	−525.19	60.51

*Computed with cc-pVDZ basis set

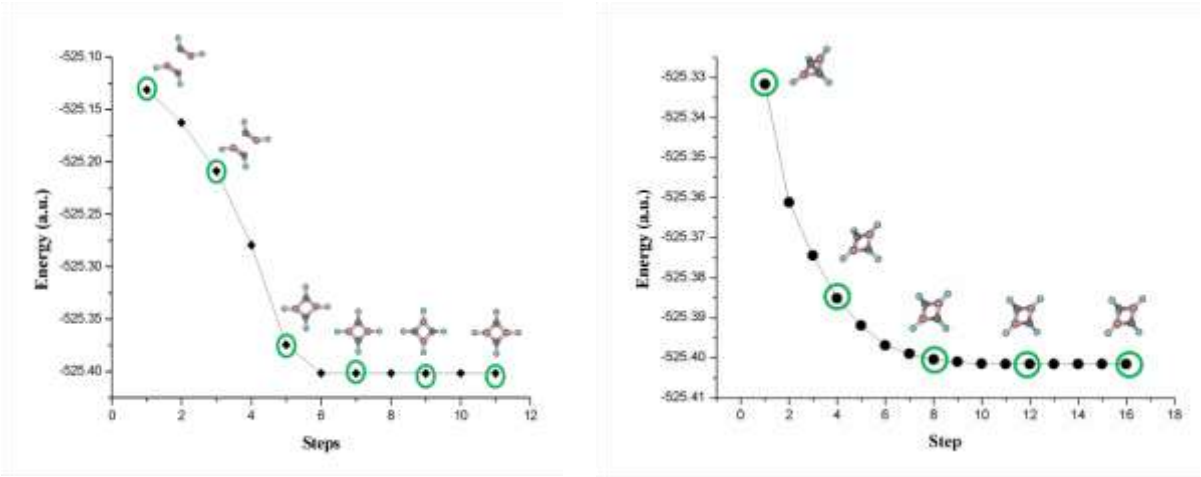

(a) (b)

Final Energy= −525.40156 a.u. **Final Energy**= −525.40156 a.u.

Figure 4.2. Geometry convergence during optimization of $C_2B_2F_4$ from (a) rectangular and (b) non-planar starting geometries and their corresponding final energies at B3LYP/aug-cc-pVDZ level. The points for which the geometries are presented in the plot are circled in green.

The dynamical stability of the molecule is confirmed from the absence of imaginary vibrational frequency (Table 4.1 and also by Molecular dynamics (MD) simulation. No sign of deformation is noted within 5 ps duration in the MD simulation at 300 K (see Figures 4.3, 4.4 and 4.5). The structural stability is often established from the binding energy of the molecule from individual atomic fragments. The larger the value of total binding energy, the more stable is the system. A large total binding energy (−1290.49 kcal/mol) thus advocates for the structural integrity of the system. The total binding energy is decomposed into two major components, namely, ΔE_{prep} and ΔE_{int}, i.e., $\Delta E = \Delta E_{prep} + \Delta E_{int}$, for convenience and ΔE_{int} is further decomposed into three physically meaningful terms, $\Delta E_{int} = \Delta E_{elstat} + \Delta E_{Pauli} + \Delta E_{orb}$. The structural and energy decomposition parameters computed at the B3LYP/aug-cc-pVDZ level are reported in Table 4.2. The reasonably high negative value of the total interaction energy (ΔE_{int}) is also signifies high stability of the molecule. Moreover, the ring strain energy value mentioned in the computational section is also in the range of reportedly stable four membered carbocyles and indicates structural stability. Followed by the validation of structural stability, the internal stability of the wave function is also confirmed with STABLE=OPT keyword implemented in Gaussian 09W.[38] The stable closed-shell electronic structure of the molecule is also indicated by negligibly small diradical character, y_i of

0.006.The closed-shell nature of the molecule is further substantiated by the large HOMO-LUMO gap of 5.2 eV.[39] Hence, the criteria of chemical viability proposed by Hoffmann et al. are persuasively satisfied.[40]

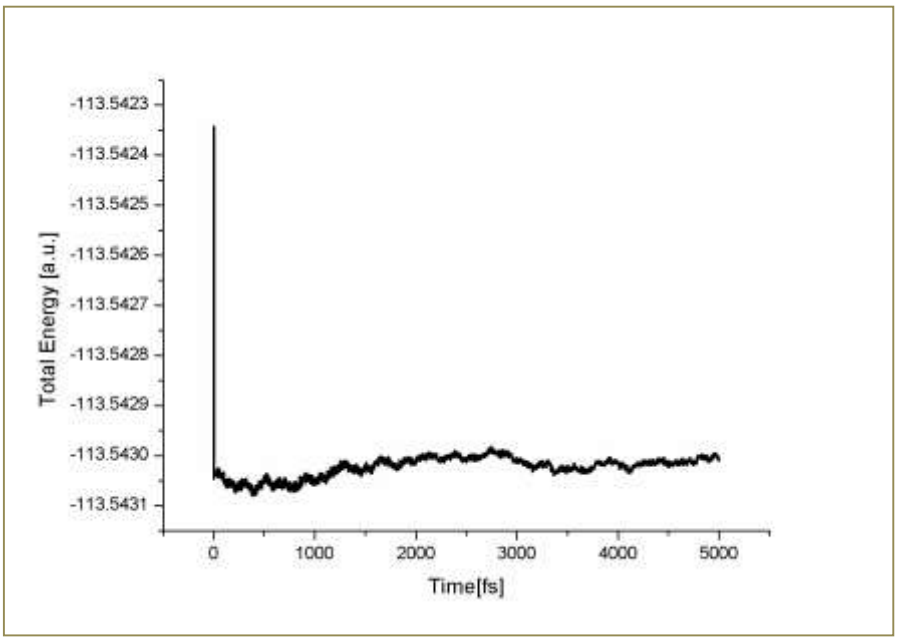

Figure 4.3. Variation of total energy of $C_2B_2F_4$ at T = 300 K along a DFT-based molecular dynamics simulation of 5 ps.

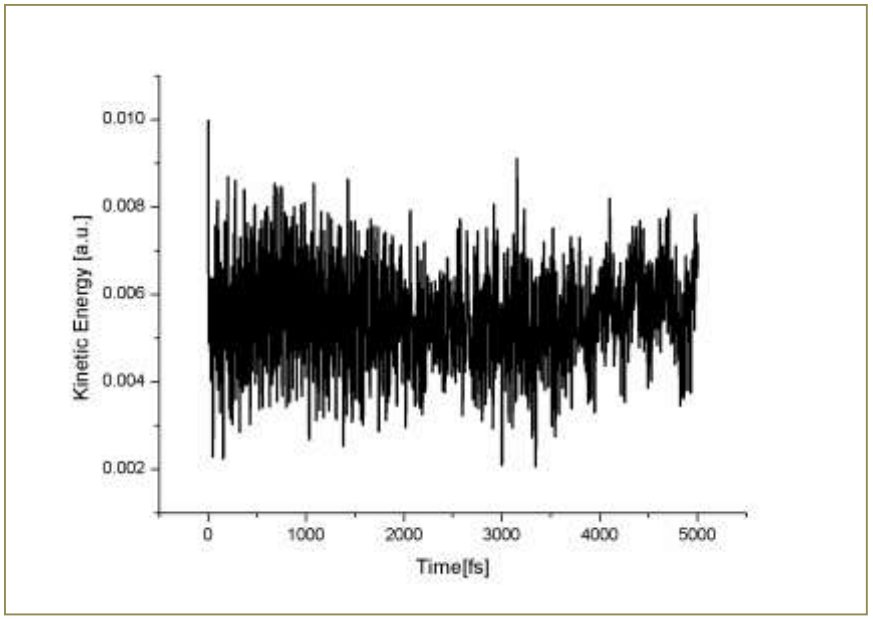

Figure 4.4. Variation of kinetic energy of $C_2B_2F_4$ at T = 300 K along a DFT-based molecular dynamics simulation of 5 ps.

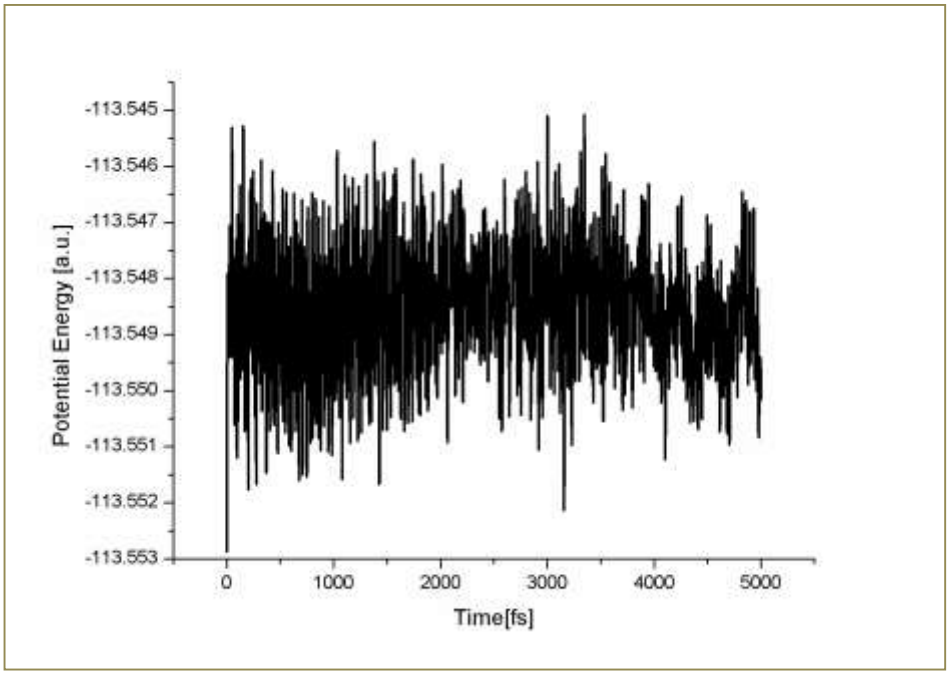

Figure 4.5. Variation of potential energy of $C_2B_2F_4$ at T = 300 K along a DFT-based molecular dynamics simulation of 5 ps.

Table 4.2. Summary of structural and energy decomposition parameters of $C_2B_2F_4$ computed at B3LYP/aug-cc-pVDZ level.

Parameters	Computed Values
B-C bond length (Å)	**1.532**
B-F bond length (Å)	**1.339**
C-F bond length (Å)	**1.322**
ΔE_{Pauli} **(kcal/mol)**	**1812.90**
ΔE_{elstat} **(kcal/mol)**	**−488.57**
ΔE_{orb} **(kcal/mol)**	**−1699.05**
$\Delta E_{int}(=\Delta E_{Pauli} + \Delta E_{elstat} + \Delta E_{orb})$ **(kcal/mol)**	**−374.72**

Satisfactory stability of the ring structure in $C_2B_2F_4$ stimulates to probe the possibility of cyclic electronic delocalization leading to aromaticity. Nucleus-independent chemical shift (NICS) is often considered as one of the superlative descriptors of aromaticity and is computed in terms of isotropic shielding tensor on a dummy atom in GIAO (Gauge Independent Atomic Orbitals) method.[41] A system is defined as aromatic (antiaromatic) based on the negative (positive) sign of the shielding tensor values, implying the presence of a diatropic (paratropic) ring current.[13] To find out the contribution of σ and π electrons to aromaticity, NICS has been calculated both in the center of the ring [NICS (0)], and at 1 Å above the plane [NICS(1)]. The negative values of NICS (0) and NICS (1), computed at different levels of theory (Table 4.3) provides strong indication in favour of the aromatic nature of $C_2B_2F_4$. Dissected canonical molecular orbital NICS (CMO-NICS) analysis is performed to identify orbitals with maximal contribution to NICS and hence to aromaticity. The orbitals that render significant diamagnetic contribution to the total NICS(1), which is found to be −6.33, are presented in Figure 4.6. The CMO-NICS(1) analysis (Figure 4.6) reveals strongest diatropic contribution of the lowest occupied π-orbital (HOMO−10) towards the NICS(1) value compared to modest contribution from higher π-orbitals (HOMO-6 & HOMO). Nevertheless, larger value of NICS(1) compared to NICS(0) suggests a major contribution of π-electrons towards aromaticity. In a recent work, the energy stabilization due to delocalization of π-electron is equated with aromatic stabilization energy (ASE) in the frame of second order perturbation theory.[42] The ASE is found to be 10.84 kcal/mol, which also suggests a substantial stabilization due to aromaticity. Visualization of the induced current density has been proved to be a useful tool for the study of aromaticity.[43] The vector plot of current density for the present molecule (Figure 4.7) exhibits the diatropic ring current for both π- and σ- planes illustrating the aromatic nature of the molecule. The peculiarity of π-electron flow gives rise to ring currents of adaxial-abaxial-adaxial pattern, as visualized in the current density vector map (Figure 4.7).

Table 4.3. The nucleus-independent chemical shift (NICS) values (ppm) in the ring plane [NICS (0)] and 1 Å above the ring plane [NICS (1)] at different DFT and *ab initio* methodologies using aug-cc-pVDZ basis set.

Methodology (along with aug-cc-pVDZ basis set)	NICS (0)	NICS (1)
B3LYP	−5.1673	−7.0986
B3PW91	−4.8444	−7.0370
PBEPBE	−3.3913	−6.2099
BLYP	−3.9376	−6.3329
CAM-B3LYP	−5.5683	−7.3992

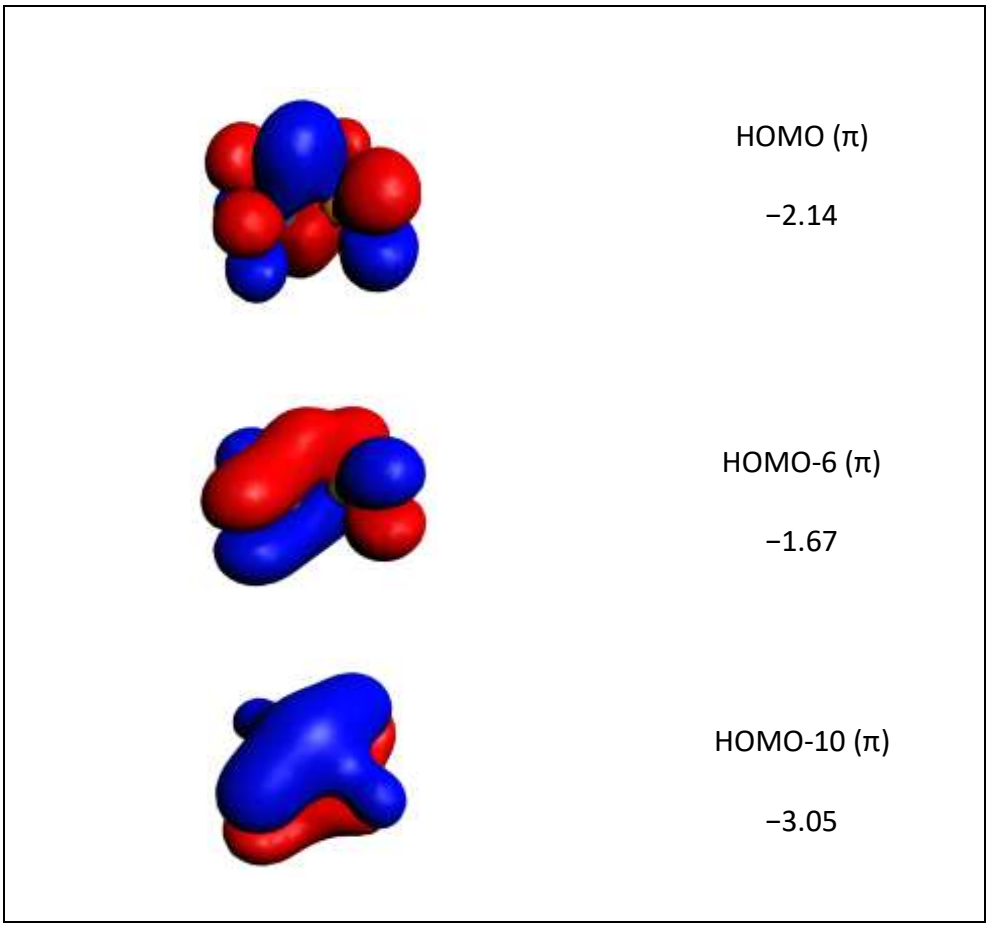

Figure 4.6. CMO-NICS analysis at 1 Å above the ring center of the $C_2B_2F_4$ molecule (D_{2h}).

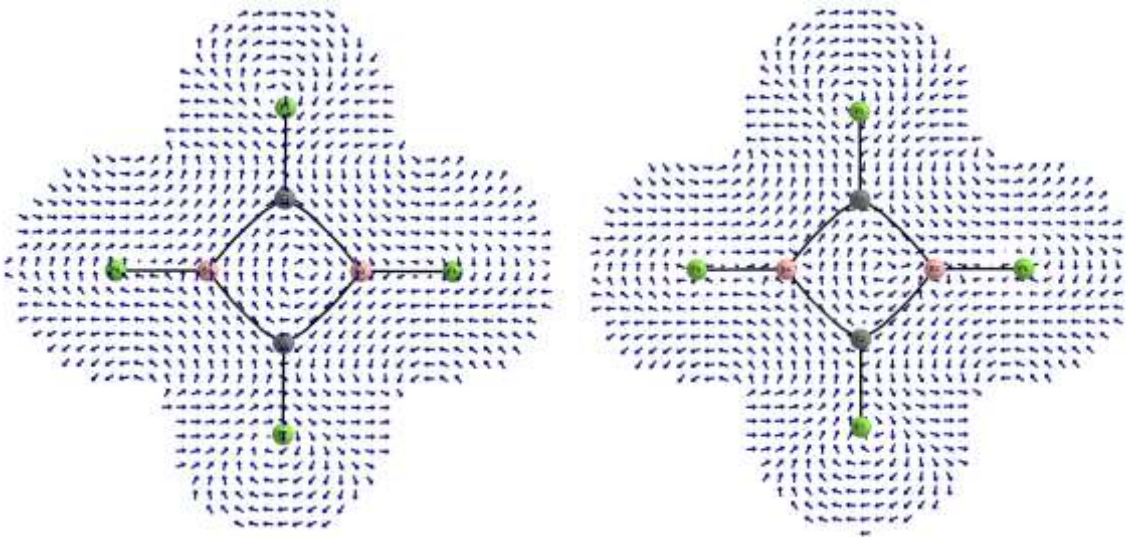

(a) (b)

Figure 4.7. The π- (a) and σ- (b) current density vector plots.

A very interesting fact that shows up in the CMO-NICS analysis is that the MO (HOMO-10 in Figure 4.6) which has the largest contribution towards NICS(1) includes F atoms as a major component. This indicates the involvement of B←F back-donated electrons to the aromatic π-cloud above and below the molecular plane. With these points, we infer that the molecular system is aromatic consisting of six π-electrons. Out of these six π-electrons, two electrons are from the p_z-orbitals of the sp^2 hybridized carbon atoms and the other four electrons are obtained through back-donation of paired electrons from fluorine to locally electron-deficient boron (Figure 4.8). Moreover, the ring current map (Figure 4.7) sustains the present model by displaying the π-density to be extended beyond the parent C_2B_2 ring up to the two B←F units in the molecule.

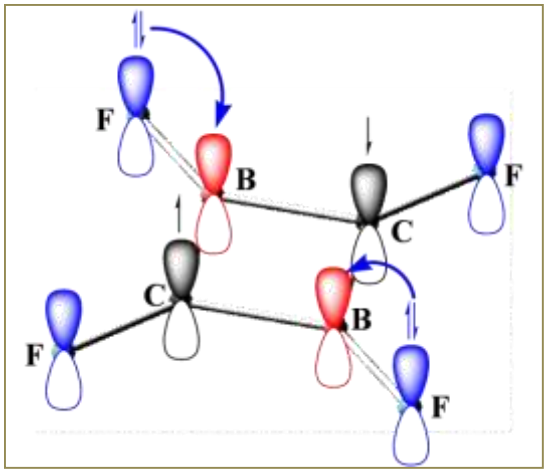

Figure 4.8. Orbital diagram for six π-electrons in $C_2B_2F_4$. The blue arrows indicate the role of the B←F back-bonding electrons to the formation of the aromatic π-cloud.

The key evidence in favor of our model comes from the energy decomposition analysis based on the extended transition state method and natural orbital for chemical valence scheme (ETS-NOCV).[44,45] The difference density, portrayed in Figure 4.9, dictates the involvement of the π-electrons of fluorine attached to boron in forming the aromatic π -electron cloud between the core C_2B_2-ring. Other than the dominant deformation channels corresponding to sigma bond formation between the fragments, a significant stabilization of −100 kcal/mol comes from the channel illustrating the flow of bonding electron pair from fluorine to the vacant $2p_z$-atomic orbitals of boron atoms. It is also noticed from Table 1 that a significant contribution to ΔE_{int} comes from the orbital interaction energy which also supports the current model.

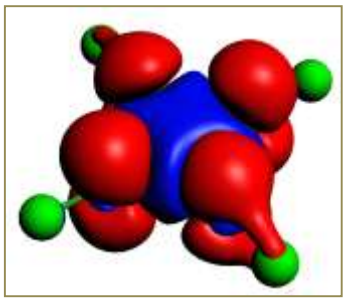

Figure 4.9. The ETS-NOCV difference density plot corresponding to −100 kcal/mol stabilization. The blue and red surfaces represent regions of the electron concentration and electron depletion (isosurface of 0.003 a.u.) respectively.

Adaptive Natural Density Partitioning (AdNDP)[46] is a new tool which can help to visualize the chemical bonding in a molecule in the most general way. AdNDP reveals the delocalized bonding elements related to the notion of aromaticity and antiaromaticity without taking the concept of resonance into account. Treating the electron pairs as the main element of chemical bonding, it models electronic structure of a molecule in terms of n-center-2-electron (nc-2e) bonds. Here, n spans in the interval from one to the total number of atoms in the molecule. Other than the Lewis bonding elements (1c-2e and 2c-2e, corresponding to the core electrons and lone pairs, and two-center two-electron bonds) it also picks up nc-2e delocalized bonding elements. The search for the all-center 2-electron bond in the molecule reveals an unambiguous description of aromaticity in $C_2B_2F_4$. The AdNDP orbital, portrayed in Figure 4.10, predicts the aromatic π-cloud to span fluorine atoms attached to the boron atoms extending the central C_2B_2-ring, thus showing exo-cyclic aromatic conjugation of π-electrons. This doubly occupied 6-centered-2-electron orbital portray the contribution of the said fluorine atoms to the aromatic character. Thus, this description of exo-cyclic aromaticity in the molecule is an extension beyond the classical concept of aromatic molecules with cyclic (4n+2) π conjugated system.

Occupation Number 1.99 Occupation Number 1.99

(a) (b)

Figure 4.10. The top-view of the AdNDP orbitals of $C_2B_2F_4$ (a) and $C_2B_2F_2H_2$ (b) along with their natural occupation numbers.

An *in silico* testing analogous systems with no back donation of 4 π-electrons to the empty $2p_z$-orbital of the boron atom stands necessary to establish the exo-cyclic nature of aromaticity in $C_2B_2F_4$. Thus, we chose to replace the F atoms attached to boron with hydrogen atoms. Harmonic frequency and NICS calculations are performed to judge the stability and aromaticity of the system. The minimum vibrational frequency 29.93 cm^{-1}, lies at a lower range, which evidently questions about its viability compared to $C_2B_2F_4$ at the first instance. Instability in this system also arises out of the σ-antiaromaticity as manifested by the positive values of NICS (0) (Table 4.4). Inspection of the results obtained from AdNDP calculation, performed for $C_2B_2F_2H_2$ reveals the involvement of only 2 π-electrons to the aromatic cloud which is centred only on the C_2B_2-core unlike $C_2B_2F_4$. This fact unambiguously proves the participation of the back donated π-electrons of p_z-orbitals from B←F in $C_2B_2F_4$. *In silico* tests are performed with $C_2B_2Cl_4$, $C_2B_2Br_4$ and $C_2B_2I_4$ systems to examine the effect of B←X back donation on the aromaticity of $C_2B_2X_4$ with X=F, Cl, Br and I. Harmonic frequency and NICS calculations are performed to assess their stability and aromaticity. The results are presented in Table S3. Low values of minimum vibrational frequencies make one sceptic about their viability at the first instance. Additionally the σ-antiaromaticity induces further instability of all these systems as is evident from the positive values of NICS (0). The $C_2B_2X_4$ systems show a decreasing trend in the NICS (1) value from fluorine to iodine (Table 4.4).

It is also to be noted that if B←X back donation is ignored, all the systems including $C_2B_2F_4$ at least posses 2 π-electrons which is capable to maintain the aromaticity in such systems. The AdNDP analyses clearly illustrate that there is no participation of back donated electrons to the aromatic electron cloud (Table 4.5). This observation substantiates the absence of back donation of π-electrons from higher p_z-orbitals of Cl ($3p_z$), Br ($4p_z$) and I ($5p_z$) to the empty $2p_z$-orbital of the boron atom due to energy mismatch. Instead, inspection of the AdNDP orbitals can establish the involvement of only 2 π-electrons to the aromatic cloud unlike $C_2B_2F_4$. The AdNDP analysis for $C_2B_2I_4$ could not be performed due to lack of similar basis set for iodine compared to other atoms.

Table 4.4. The optimized geometries, minimum harmonic frequencies, NICS (0) and NICS (1) values of $C_2B_2F_2H_2$, $C_2B_2Cl_4$, $C_2B_2Br_4$ and $C_2B_2I_4$ at B3LYP/aug-ccpVDZ level*.

Species	Minimum Frequency	NICS (0)	NICS (1)
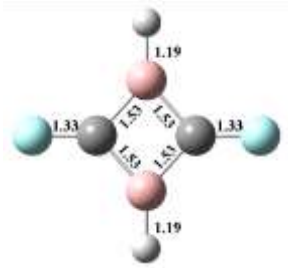	29.93	3.1873	−7.4007
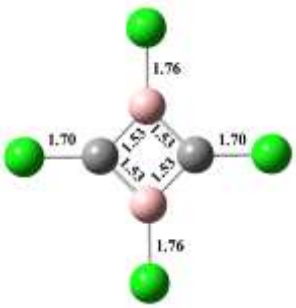	23.52	7.3817	−6.1710
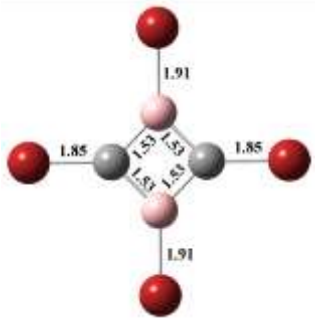	7.97	10.1049	−5.9335
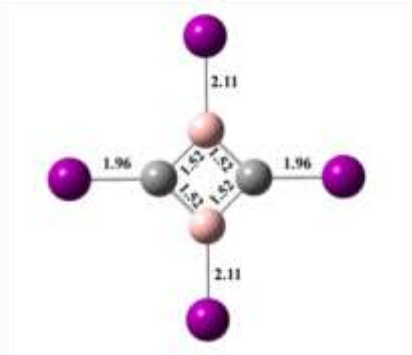	20.30	18.2129	−5.0623

*As the aug-cc-pVDZ basis set is not available for the element I, Sapporo-DKH3-DZP-2012 is applied as an extrabasis on I atoms.

Table 4.5. AdNDP orbitals along with occupations for the designed $C_2B_2Cl_4$ and $C_2B_2Br_4$ systems.

System	Occupation Number	AdNDP Orbital	
		Front View	Side View
$C_2B_2Cl_4$	1.99	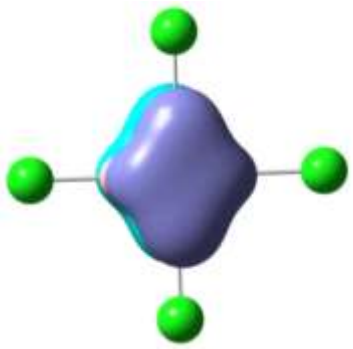	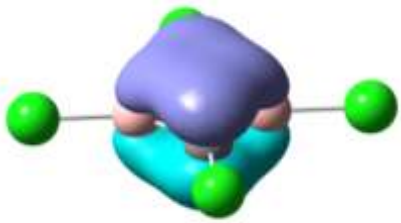
$C_2B_2Br_4$	2.00	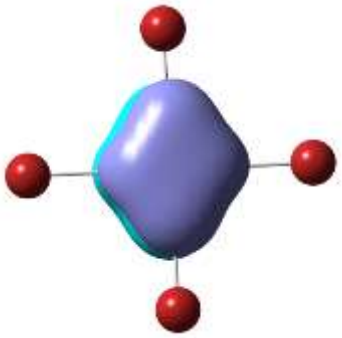	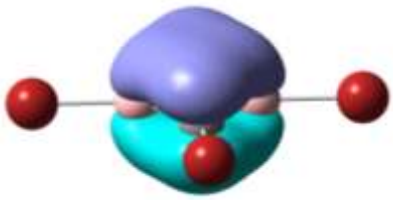

4.4.

CONCLUSIONS

In essence, the molecule $C_2B_2F_4$ acquires aromaticity due to unusual participation of exo-cyclic atoms. Back donation of 4 π-electrons from peripheral fluorine atoms to the electron-deficient boron atoms helps the ring to gain the magic number of 6 π-electrons leading to a unique exo-cyclic aromaticity. Moreover, the existence of molecule with similar C_2B_2 core (compound III/IV in ref. 47) makes us optimistic about the experimental realization of the molecule in near future.

4.5.

REFERENCES

1. Garratt, P. J. *Aromaticity*, John Wiley & Sons, 1986.
2. Minkin, V. I.; Glukhotsev, M. N.; Simkin, B. Y. in Aromaticity and Antiaromaticity: Electronic and Structural Aspects, John Wiley & Sons, Inc., New York, 1994.
3. Bickelhaupt, F.; de Wolf, W. H. *Recl. Trav. Chim. Pays-Bas* **1988**, *107*, 459-478.
4. Kraakman, P. A.; Valk, J.- M.; Niederländer, H. A. G.; Brouwer, D. B. E.; Bickelhaupt, F. M.; de Wolf, W. H.; Bickelhaupt F.; Stam, C. H. *J. Am. Chem. Soc.* **1990**, *112*, 6638-6646.
5. Schleyer P. v. R.; Jiao, H. *J. Pure Appl. Chem*. **1996**, *68*, 209-218.
6. Carey F. A.; Sundberg, R. J. *Advanced Organic Chemistry: Structure And Mechanisms (Part A)*, Springer, 2000.
7. Faraday, M. *Phil. Trans. R. Soc.* **1825**, *115*, 440–466.
8. Kekulé, A. *Bull. Soc. Chim.Fr.* **1865**, *3*, 98-110.
9. Balaban, A. T.; Schleyer P. v. R.; Rzepa, H. S. *Chem. Rev.* **2005**, *105*, 3436-3447.
10. Huckel, E. *Z. Phys.* **1931**, *70*, 204-286.
11. Heilbronner, E. *Tetrahedron Lett.* **1964**, *5*, 1923–1926.
12. Balaban, A. T. *Pure & Appl. Chem.* **1980**, *52*, 1409-1429.
13. Katrizky, A.; Barczymski, P.; Musumarra, G.; Pisano D.; Szafran, M. *J. Am. Chem. Soc.* **1989**, *111*, 7-15.
14. Schleyer, P. v. R.; Maerker, C.; Dransfeld, A.; Jiao, H.; Hommes, N. J. R. v. E. *J. Am. Chem. Soc.* **1996**, *118*, 6317-6318.
15. Misra, A.; Klein, D. J.; Morikawa, T. *J. Phys. Chem. A*, **2009**, *113*, 1151-1158.
16. Dewar, M. J. S. Tropolone. *Nature* **1950**, *166*, 790-791.
17. Crocker, E. C. *J. Am. Chem. Soc.*, **1922**, *44*, 1618-1630.
18. Armit, J. W.; Robinson, R. *J. Chem. Soc.* **1925**, *127*, 1604-1618.
19. Gaussian 09, Revision B.01, Frisch, M. J.; Trucks, G. W.; Schlegel, H. B.; Scuseria, G. E.; Robb, M. A.; Cheeseman, J. R.; Scalmani, G.; Barone, V.; Mennucci, B.; Petersson, G. A.; Nakatsuji, H.; Caricato, M.; Li, X.; Hratchian, H. P.; Izmaylov, A. F.; Bloino, J.; Zheng, G.; Sonnenberg, J. L.; Hada, M.; Ehara, M.; Toyota, K.; Fukuda, R.; Hasegawa, J.; Ishida, M.; Nakajima, T.; Honda, Y.; Kitao, O.; Nakai, H.; Vreven, T.; Montgomery, J. A., Jr.; Peralta, J. E.; Ogliaro, F.; Bearpark, M.; Heyd, J. J.; Brothers, E.; Kudin, K. N.; Staroverov, V. N.; Kobayashi, R.; Normand, J.; Raghavachari, K.; Rendell, A.; Burant, J. C.; Iyengar, S. S.; Tomasi, J.; Cossi, M.; Rega, N.; Millam, J. M.; Klene, M.; Knox, J. E.; Cross, J. B.; Bakken, V.; Adamo, C.; Jaramillo, J.; Gomperts, R.; Stratmann, R. E.; Yazyev, O.; Austin, A. J.; Cammi, R.; Pomelli, C.; Ochterski, J. W.; Martin, R. L.; Morokuma, K.; Zakrzewski, V. G.; Voth, G. A.; Salvador, P.; Dannenberg, J. J.; Dapprich, S.; Daniels, A. D.; Farkas, Ö.; Foresman, J. B.; Ortiz, J. V.; Cioslowski, J.; Fox, D. J. Gaussian, Inc., Wallingford CT, 2009.

20. Amsterdam Density Functional (Theoretical Chemistry, Vrije Universiteit, Amsterdam, The Netherlands, http://www.scm.com).
21. Ziegler, T.; Rauk, A. *Theor. Chim. Acta.* **1977**, *46*, 1-10.
22. Yamaguchi, K. *Self-Consistent Field: Theory and Applications.* (Eds Carbo, R., Klobukowski, M.); Elsevier: Amsterdam, 1990.
23. Corminboeuf, C.; Heine, T.; Weber, J. *Phys. Chem. Chem. Phys.* **2003**, *5*, 246-251.
24. Corminboeuf, C.; King, R. B.; Schleyer, P. v. R. *Chem. Phys. Chem.* **2007**, *8*, 391-398.
25. Lu, T.; Chen, F. *J. Comp. Chem.* **2012**, *33*, 580-592.
26. VandeVondelea, J.; Krackb, M.; Mohamedb, F.; Parrinellob, M.; Chassaingc, T.; Hutter, J. *Comput. Phys. Commun.* **2005**, *167*, 103-128.
27. Becke, A. D. *Phys. Rev. A* **1988**, *38*, 3098-3100.
28. Lee, C.; Yang, W.; Parr, R. G. *Phys. Rev. B* **1988**, *37*, 785-789.
29. Goedecker, S.; Teter, M.; Hutter, J. *Phys. Rev. B* **1996**, *54*, 1703-1710.
30. Hartwigsen, C.; Goedecker, S.; Hutter, J. *Phys. Rev. B* **1998**, *58*, 3641-3662.
31. Bader, R.F.W. *Atoms in Molecules: A Quantum Theory*; Oxford University Press: Oxford, UK, 1990.
32. Bauzá, A.; Quiñonero, D.; Deyà, P. M.; Frontera, A. *Chem. Phys. Lett.* **2012**, *536*, 165–169.
33. Gund, P. *J. Chem. Educ.* **1972**, *49*, 100-103.
34. McKee, W. C.; Wu, J. I.; Hofmann, M.; Berndt A.; Schleyer, P. v. R. *Org. Lett.*, **2012**, *14*, 5712–5715.
35. Goswami, T.; Paul, S.; Mandal, S.; Misra, A.; Anoop, A.; Chattaraj, P. K. *Int. J. Quantum Chem.*, **2015**, *115*, 426-433.
36. Giri, S.; Kumar, R. P. S. A.; Chakraborty A.; Roy, D. R.; Duley, S.; Parthasarathi, R.; Elango, M.; Vijayaraj, R.; Subramanian V.; Merino, G.; Chattaraj, P. K. in *Aromaticity and Metal Clusters*, CRC Press, USA, **2011**.
37. Chattaraj, P. K.; Das, R.; Duley, S.; Vigneresse, J. -L. *Theor. Chem. Acc.*, **2012**, *131*, 1089-1096.
38. Seeger, R.; Pople, J. A. *J. Chem. Phys.* **1977**, *66*, 3045-3050.
39. Dohnert, D.; Koutecky, J. *J. Am. Chem. Soc.*, **1980**, *102*, 1789-1796.
40. Hoffmann, R.; Schleyer, P. v. R.; Schaefer, H. F. *Angew. Chem., Int. Ed.* **2008**, *47*, 7164-7167.
41. Wolinski, K.; Hinton, J. F.; Pulay, P. *J. Am. Chem. Soc.*, **199**
42. Paul, S.; Goswami, T.; Misra, A. *AIP Adv.* **2015**, *5*, 107211.
43. Steiner, E.; Fowler, P. W.; Soncini, A.; Jenneskens, L. W. *Faraday Discuss.*, **2007**, *135*, 309–323.
44. Mitoraj, M.; Michalak, A. *J. Mol. Model.*, **2007**, 13, 347-355.
45. Mitoraj, M. P.; Michalak, A.; Ziegler, T. *J. Chem. Theory Comput.* **2009**, 5, 962-975.
46. Zubarev, D. Y.; Boldyrev, A. I. *Phys. Chem. Chem. Phys.* **2008**, *10*, 5207-5217
47. Bromm, D.; Stalke, D.; Heine, A.; Miller, A. *J. Organomet. Chem.*, **1990**, *386*, 1-7.

CHAPTER 5

Manifestation of exo-cyclic aromaticity in triangular heterocyclic B_2F_2X systems (X = O, S, Se, NH)

5.1.

INTRODUCTION

The idea of aromaticity is an age old concept[1-3] but its purpose and relevance is continually on the rise. Aromaticity can be considered as one of the most intriguing phenomena in chemistry which is evolving with time. The perception of aromaticity is associated with certain specific molecular characteristics such as added stabilization, planarity of the molecular systems, conjugation, electron delocalization[4-7] and most importantly a distinct reaction to applied magnetic field .[8-11] Presently, aromaticity is not the idea involving organic systems only but has incorporated all metal aromatic clusters[12-22] as well. Conjecture of aromaticity in planar π-electron systems by Huckel's (4n+2) rule [23] is one of best recognized and the most functional methods. In recent times, there has been an augmented interest in understanding and development of varied criteria for defining aromaticity.[24-26] Apart from the primary measures for defining aromaticity,[27-29] it has also been explained by electron density based indices.[30-34] Lately, aromaticity has become a significant tool in defining the stability and bonding in various chemical species surpassing the realm of organic chemistry[35-38] extending to inorganic moieties.[20-22] Also acyclic compounds have been found to have aromatic stability[39] thus implying that aromaticity can no longer be confined to the field of classical conjugated organic systems. In a recent theoretical work, it has been shown that exo-cyclic aromaticity is possible in planar systems; i.e., aromaticity is achieved through back-donation of electrons from thesubstituents.[40] The concept of 2p-2p orbital interaction or back-donation of fluorine has been well identified in the organic and inorganic domain.[41-43] Both the inductive effect and the resonance or the back-donation effect play a vital role when the non-bonded pair of electrons of fluorine interact with the vacant orbital of the boron atom to which it is attached. The tendency of back-donation by fluorine has been established to be greater than that of the other halogen atoms such as chlorine and bromine, where the order of back-donation is found to be F>Cl>>Br .[44] The degree of back-donation decreases with the increase in the atomic sizes of the halogens since the 2p-2p interaction is more favorable as compared to the interaction between 3p and 4p orbital of chlorine and bromine respectively with the vacant 2p orbital of boron due to mismatch in the size of the orbitals.

In this work, we theoretically propose novel heteroatomic systems where exo-cyclic aromaticity is observed which is achieved through back-donation of electrons from exo-

cyclic fluorine atoms. The systems studied are cyclic heteroatomic B_2F_2X (where X=O, S, Se, NH) molecules (Figure 5.1). In order to understand the bonding and the structural properties of these systems, a systematic theoretical study has been performed. The molecules are optimized at different levels of theory using various DFT and *ab*-initio methodologies involving coupled-cluster singles and doubles (CCSD). The stability of the molecules isvalidated by the absence of any imaginary frequency, Energy Decomposition Analysis (EDA)[45] computation of the Ring Strain Energy (RSE)[46] and higher HOMO-LUMO gaps.The aromaticity is analyzed and estimated through Nucleus Independent Chemical Shift (NICS),[47] Canonical Molecular Orbital NICS (CMO-NICS)[48] Multi Centre bond Index (MCI),[31] Adaptive Natural Density Partitioning (AdNDP)[49] and Aromatic Stabilization Energy (ASE).[50] As a whole, this work elucidates exo-cyclic aromaticity in novel systems with three-membered heteroatomic rings.

5.2.

COMPUTATIONAL DETAILS

Gaussian 09W suite of software was used for the minimum energy search and frequency calculationat various DFT (UB3LYP, UB3PW91, UPBEPBE, UBLYP and UCAM-B3LYP) and *ab-initio* (UCISD, UQCISD, UCCSD) methodologies using aug-cc-pvdz basis, T1 diagnostic run was carried out at UCCSD(t1diag)/aug-cc-pvdz level, computation of the HOMO-LUMO gap at ub3lyp/ aug-cc-pvdz level and NICS evaluation at various DFT levels (UB3LYP, UB3PW91, UPBEPBE, UBLYP and UCAM-B3LYP) with aug-cc-pvdz basis.[51] The Energy Decomposition Analysis at UB3LYP/aug–ATZP level and the CMO-NICS evaluation at LDA/DZ level are performed by the ADF program.[52] The Ring Strain Energy is calculated by the AIM version program[53] at UB3LYP/ aug-cc-pvdz level. The chemical bonding analysis employing the AdNDP orbitals are visualized and the multicentre bond aromaticity index (MCI) is calculated at UB3LYP/aug-cc-pvdz level using Multiwfn (A Multifunctional Wave function Analysis).[54] For the calculation of ASE, Gaussian 09W suite of software, Multiwfn and OpenMX 3.6 quantum chemistry code[55] are used.

5.3.

RESULTS AND DISCUSSION

5.3.1. Molecular Geometry

The optimized structures of the heteroatomic molecules B_2F_2X (where X=O, S, Se, NH) with their bond lengths in Å and B-X-B bond angles in degrees as computedin uccsd/ aug-cc-pvdz level of theory are given in Figure 5.1. The greater stability of the molecular systems can be accounted from the high minimum frequency value, the viability of the molecules are further substantiated by the absence of an imaginary frequency and the existence of allow ground state minimum energy as provided in Tables 5.1, 5.2, 5.3 and 5.4 for the B_2F_2O, B_2F_2S, B_2F_2Se and B_2F_2NH systems respectively. The structural reliability of the molecular systems is further established through Energy Decomposition Analysis (EDA) based on the approach of Ziegler and Rauk.[45] The individual atomic fragments are taken into consideration for the EDA. In this method the interaction energy (ΔE_{int}) is divided into three major components namely electrostatic interaction (ΔV_{elstat}), Pauli repulsive orbital interaction (ΔE_{pauli}) and attractive orbital interaction (ΔE_{orb}) as shown,

$$\Delta E_{int}=\Delta V_{elstat}+\Delta E_{pauli}+\Delta E_{orb} \qquad (5.1)$$

Here, the ΔV_{elstat} represents the classical electrostatic interaction between the fragments as they are brought together to form the final complex. ΔE_{pauli} corresponds to the repulsive interaction between the filled orbital, generally termed as steric interaction.[56]ΔE_{orb} corroborates the interactions between the occupied orbitals of one fragment to the unoccupied orbitals of the other fragment and also takes into account the interactions between the occupied and virtual orbitals of the same fragment.[45] The rationally high negative value of the total interaction energy as evident from Table 5.5 advocates towards the structural integrity of the molecular systems. Also a T1 diagnostic run from CCSD calculations have been performed to confirm the single-reference character of the molecules studied. The T1 diagnostics of species vary in the range of 0.015-0.017 as evident from Table 5.6 which are less than 0.02 thus advocating towards a single-reference character, as suggested by Lee and Taylor.[57]

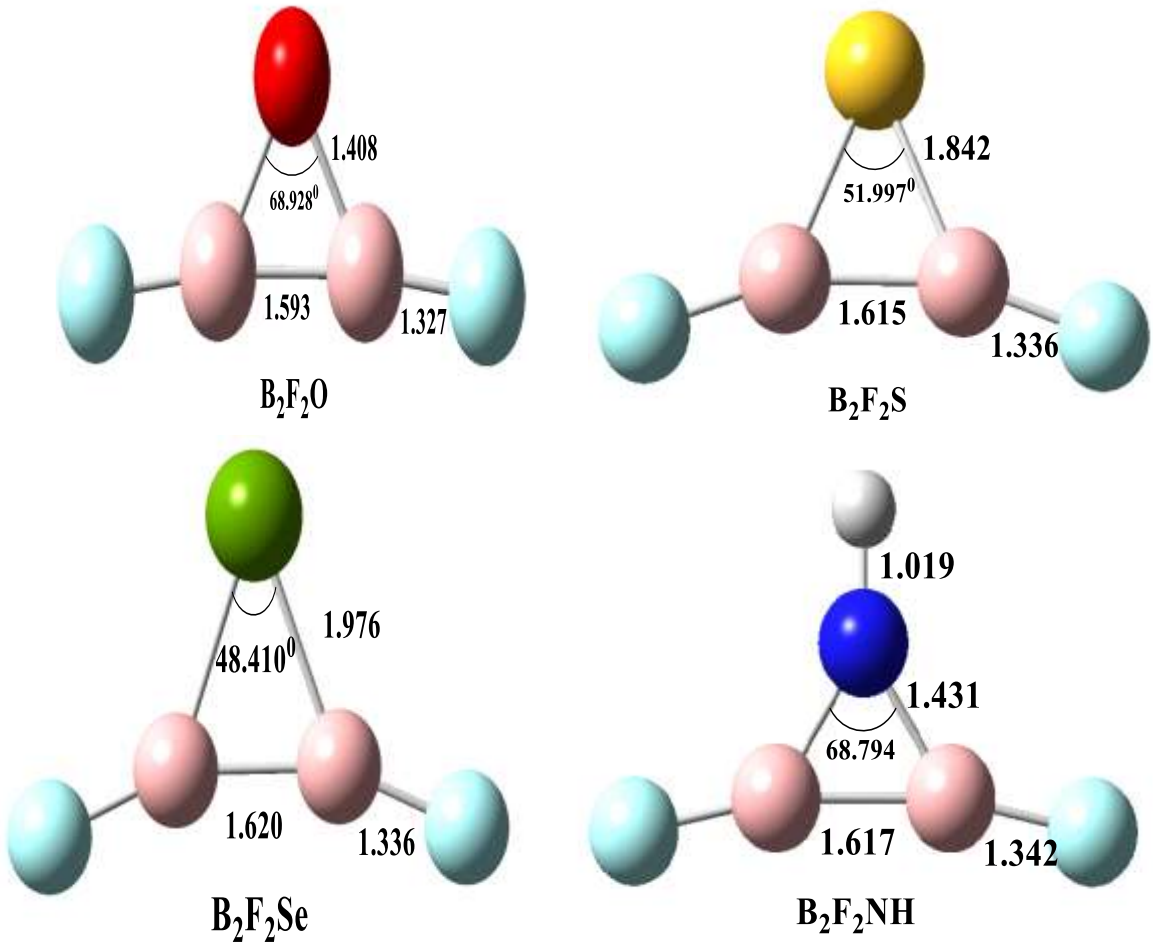

Figure 5.1. Optimized structure of B_2F_2O, B_2F_2S, B_2F_2Se andB_2F_2NH and their bond lengths in Å and the B-X-B bond angles in degree computed in uccsd/aug-cc-pvdz level, theboron, fluorine, oxygen, sulfur, selenium, nitrogen and hydrogen are represented by pink, cyan,red, yellow, green, blueand grey respectively.

Table 5.1. The optimized bond lengths (in Å), bond angles (in °), minimum energy (in a.u.) and minimum frequency (in cm^{-1}) of **B_2F_2O** at different unrestricted DFT and *ab initio* methodologies using aug-cc-pVDZ basis set.

Methodology (along with aug-cc-pvdz)	**B-B bond length(in Å)**	**B-O bond length(in Å)**	**B-F bond length (in Å)**	**< B-O-B (in °)**	**Minimum energy (in a. u.)**	**Minimum frequency(in cm^{-1})**
UCISD	1.58074	1.39251	1.31694	69.16405	-324.00	265.04
UQCISD	1.59440	1.41052	1.32888	68.82957	-324.03	251.94
UCCSD	1.59361	1.40804	1.32725	68.92894	-324.03	254.06
UB3LYP	1.57700	1.39737	1.31793	68.70360	-324.78	248.88
UB3PW91	1.57498	1.39795	1.31700	68.57105	-324.65	248.34
UPBEPBE	1.58413	1.41404	1.32735	68.13154	-324.44	236.47
UBLYP	1.58608	1.41416	1.32954	68.22043	-324.74	237.57
UCAM-B3LYP	1.57211	1.38981	1.31292	68.88600	-324.68	251.03

Table 5.2. The optimized bond lengths (in Å), bond angles (in °), minimum energy (in a.u.) and minimum frequency (in cm^{-1}) of **B_2F_2S** at different DFT and ab initio methodologies using aug-cc-pvdz basis set.

Methodology (along with aug-cc-pvdz)	**B-B bond length(in Å)**	**B-S bond length(in Å)**	**B-F bond length (in Å)**	**< B-S-B (in °)**	**Minimum energy (in a.u)**	**Minimum frequency(in cm^{-1})**
UQCISD	1.61734	1.84560	1.33699	51.97308	-646.63	241.64
UCISD	1.60843	1.82758	1.32538	52.21321	-645.91	252.90
UCCSD	1.61567	1.84290	1.33585	51.99715	-646.63	243.49
UB3LYP	1.59364	1.83892	1.32563	51.35543	-647.74	243.50
UB3PW91	1.59483	1.83306	1.32480	51.57293	-647.59	244.73
UPBEPBE	1.59972	1.84713	1.33504	51.31989	-647.29	236.01
UBLYP	1.59805	1.85851	1.33709	50.92596	-647.68	234.27
UCAM-B3LYP	1.59194	1.82346	1.32090	51.76370	-647.65	247.66

Table 5.3. The optimized bond lengths (in Å), bond angles (in °), minimum energy (in a.u.), and minimum frequency (in cm^{-1}) of **B_2F_2Se** at different DFT and ab initio methodologies using aug-cc-pvdz basis set.

Methodology (along with aug-cc-pvdz)	**B-B bond length(in Å)**	**B-Se bond length(in Å)**	**B-F bond length (in Å)**	**< B-Se-B (in °)**	**Minimum energy (in a.u)**	**Minimum frequency(in cm^{-1})**
UQCISD	1.62129	1.98007	1.33828	48.33459	-2648.91	209.72
UCISD	1.61343	1.96030	1.32573	48.60141	-2648.88	220.07
UCCSD	1.62062	1.97635	1.33655	48.41014	-2648.90	211.17
UB3LYP	1.59634	1.98015	1.32567	47.54242	-2651.08	211.00
UB3PW91	1.59822	1.97064	1.32488	47.84610	-2650.96	212.28
UPBEPBE	1.60132	1.98680	1.33552	47.53059	-2650.43	204.29
UBLYP	1.59910	2.00457	1.33731	47.01442	-2651.08	202.46
UCAM-B3LYP	1.59508	1.95938	1.32111	48.02534	-2651.09	215.41

Table 5.4. The optimized bond lengths (in Å), bond angles (in °), minimum energy (in a.u.) and minimum frequency (in cm^{-1}) of **B_2F_2NH** at different DFT and ab initio methodologies using aug-cc-pvdz basis set.

Methodology (along with aug-cc-pvdz)	**B-B bond length(in Å)**	**B-N bond length(in Å)**	**B-F bond length (in Å)**	**N-H bond length (in Å)**	**< B-N –B (in °)**	**Minimum energy (in A.U)**	**Minimum frequency(in cm^{-1})**
UQCISD	1.61776	1.43222	1.34415	1.01932	68.77968	-304.17	242.64
UCISD	1.60315	1.41842	1.33259	1.01000	68.83053	-303.42	258.39
UCCSD	1.61696	1.43126	1.34265	1.01920	68.79390	-304.17	244.52
UB3LYP	1.59937	1.41923	1.33276	1.01995	68.60454	-304.90	241.78
UB3PW91	1.59786	1.41908	1.33169	1.01886	68.52565	-304.77	242.67
UPBEPBE	1.60707	1.42993	1.34156	1.02902	68.38031	-304.56	229.42
UBLYP	1.61037	1.43073	1.34436	1.02984	68.49682	-304.84	230.59
UCAM-B3LYP	1.59287	1.41320	1.32822	1.01704	68.60613	-304.79	230.59

Table 5.5. Summary of energy decomposition parameters of B_2F_2O, B_2F_2S, B_2F_2Se and B_2F_2NH computed at ub3lyp/aug-cc-pVDZ level.

Molecules	**ΔE_{Pauli} (Kcal/mol)**	**ΔV_{elstat} (Kcal/mol)**	**ΔE_{orb} (Kcal/mol)**	**$\Delta E_{int}(=\Delta E_{Pauli}+\Delta V_{elstat}+\Delta E_{orb}$ (Kcal/mol)**
B_2F_2O	2954.85	-667.25	-2780.13	-492.53
B_2F_2S	2607.85	-612.66	-2419.45	-424.26
B_2F_2Se	2521.45	-602.87	-2380.41	-461.83
B_2F_2NH	3362.75	-717.70	-3265.88	-620.83

Table 5. 6. The T1 diagnostic values computed at the CCSD(t1diag)/aug-cc-pvdz level.

Molecules	**T1(diag)**
B_2F_2O	0.017
B_2F_2S	0.016
B_2F_2Se	0.015
B_2F_2NH	0.016

Evaluation of their structures reveals that these heteroatomic molecules display planar geometry thereby indicating the possibility of aromatic behavior in such systems since planarity of the system is a prerequisite for a molecule to be aromatic. We intuit that these molecules may have achieved the *aromatic sextet* as a consequence of back-donation of paired electrons from the substituent fluorine atoms to the vacant orbitals of the boron atoms as according to the scheme described in Figure 5.2 which agrees with Huckel's (4n+2) rule for aromaticity.

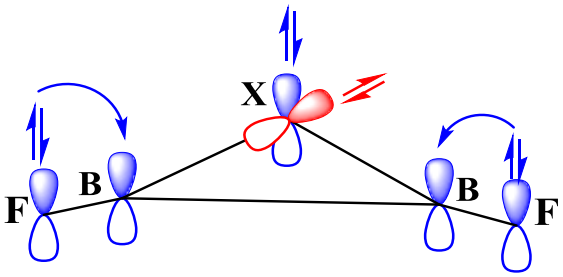

Figure 5.2. Orbital representation of the **B_2F_2X** molecules comprising of 6 π-electrons showing back donation of electrons from the fluorine atom to the vacant orbital of boron forming an aromatic π-cloud.

The B_2F_2X molecular systems possessing the group 16 heteroatom O, S and Se consisting of two lone pair of electrons occupying two orthogonal orbitals, so only one lone pair of electrons represented by blue pair of arrows are likely to be responsible for aromaticity which lies in plane with the plane of the vacant orbital of the boron atoms which are in turn being filled by back donating pair of electrons from the fluorine atoms as depicted in Figure 5.2. The other lone pair of electrons characterized by red pair of arrows of the heteroatom O, S, Se is not involved since it is orthogonal to the π aromatic plane. In B_2F_2X system consisting of the group 15 heteroatom N, two lone pair of electrons are present over the nitrogen atom. Two fluorine atoms donate two lone pairs, i.e., four electrons from fluorine atoms and two electrons are gained from the heteroatom thereby achieving the 6 π-electrons responsible for attaining aromaticity as in accordance to Huckel's(4n+2) rule.

5.3.2. Ring Strain Energy

The molecules studied are planar and cyclic three member rings which are similar to thecyclopropane moiety where ring strain is an important parameter for their stability, so here the ring strain is calculated with the aid of Bader's Quantum theory of Atoms in Molecules (QTAIM).[46] The Lagrange kinetic energy density value G (r) computed at the Ring Critical Point (RCP) can be used to evaluate the ring strain in these small rings, with the application of the Regression equation, RSE= {337.72 × G (r) – 8.115}.[58] The 'atoms in molecules'analysis is carried out by the AIM version program at ub3lyp/ aug-cc-pvdz level of theory. The computed values of the Ring Strain Energy in kcal/mol for our studied systems are given in Table 5.7.

Table 5.7. The Ring Strain Energy in kcal/mol computed at ub3lyp/ aug-cc-pvdz level.

Molecules	RSE (Kcal/mol)
B_2F_2O	29.22
B_2F_2S	21.20
B_2F_2Se	16.52
B_2F_2NH	28.49

The computed Ring Strain Energy values are in parity with the Ring Strain Energy values of experimentally observed stable three member cyclic systems[59-61] thereby indicating towards the structural stability and viability of the studied molecular systems. It also hints towards the presence of sigma aromaticity in the systems[62] which accounts for the reduced strain energy in the three-member planar rings. The stability of the three member planar cyclic ring structure encourages the prospect of circular electronic delocalization which is the genesis of aromaticity.

5.3.3. Molecular Orbital Analysis

The HOMO-LUMO gap can be considered as a direct measurement of kinetic stability[63-70] as a greater HOMO-LUMO gap would mean a higher kinetic stability. The molecules studied have a reasonably high HOMO-LUMO gap (Table 5.8) and since an appreciable HOMO-LUMO separation should be present for the molecules to be viable[71] thereby indicating that our systems are stable and also suggests of the closed shell nature of the molecules. This is a clear indication of the fact that these systems may have (4n+2) π aromatic electrons where all π-electrons are paired in bonding molecular orbitals.

Table 5.8. HOMO- LUMO gap in eV computed in ub3lyp/ aug-cc-pvdz methodology.

Molecules	HOMO-LUMO gap (eV)
B_2F_2O	4.43
B_2F_2S	6.637
B_2F_2Se	4.717
B_2F_2NH	6.593

The above analysis shows that these molecular three- member ring structures are reasonably stable thereby encouraging us to explore the possibility of circular electronic delocalization which direct towards aromaticity.

5.3.4. Aromaticity analysis employing NICS, CMO-NICS and MCI

Quantifying aromaticity is a challenge due to its multidimensional nature, [72-74] but the most efficient method of quantifying aromaticity is NICS, which was postulated by Schleyer and his co-workers.[47] The negative value of the absolute magnetic shielding gives the definition of NICS. A ghost atom is used for the determination of NICS through computational methodologies like GIAO.[75-78] In this work, the NICS values for the heterocyclic B_2F_2X systems are computed using UB3LYP, UB3PW91, UPBEPBE, UBLYP and UCAM-B3LYP methodology along with aug-cc-pvdz basis set which are represented in Table 5.9. The NICS values are computed by placing the ghost atom at the centre of the ring [NICS(0)] to account for the contribution of the σ-electrons to aromaticity and 1 Å above and below the plane i.e.,[NICS (1)] and [NICS(-1)] respectively to estimate the π-aromaticity of the systems. In harmony with NMR chemical shift principle, the NICS values are reported with negative signs. Positive NICS value signifies a paratropic magnetic field corresponding to antiaromatic systems whereas a negative NICS value signifies a diatropic magnetic field which correlates to aromatic systems.

The NICS (0) and NICS (1) computed for our systems are highly negative which indicates that the heterocyclic B_2F_2X systems are strongly aromatic. If we compare for the negative NICS (1) values, elements (O, S and Se) containing B_2F_2X systems than it is observed that thetrend is O<S<Se since the order of electronegativity is just the opposite so oxygen attracts the electrons more towards itself as compared to sulphur then selenium so the

order of electron delocalization is highest for Se, then S and then O. The NICS (1) value of nitrogen is also comparatively less owing to its higher electronegativity. The observation is in accordance to the notion that aromaticity increases with the decrease in the electronegativity difference between a heteroatom and its neighbouring atoms.[79]

Dissected Canonical Molecular Orbital NICS (CMO-NICS) analysis of B_2F_2O system is carried out to classify the orbitals contributing to σ and π aromaticity respectively. CMO-NICS calculations for B_2F_2O yield orbital contributions of −8.82 ppm from π, -17.422 ppm from valence σ towards the total of −26.242 ppm. From the orbital picture of the CMO contributing towards π-aromaticity {Figure 5.3(a)} it is apparent that the p_z orbitals of all the atoms including the exo-cyclic Flourine atoms are involved in formation of the π-cloud over the molecular plane.The orbital picture of the CMO contributing towards σ aromaticity {Figure 5.3(b)} reveals that the hybridized orbitals of the threeatoms i.e., the heteroatom and the two boron atoms are involved in the formation of this canonical molecular orbital. It is also to be noted that fluorine atoms do not contribute to the σ aromaticity at all. The picture becomes much clearer if we consider the population analysis provided in Table 5.10, where a 3-centred bond is present with the involvement of two sp^2 hybridised orbitals of boron and a pure in-plane p- orbital of the heteroatom (oxygen). So the σ aromaticity arises due to the delocalization of electrons across the trigonal ring through the planar heteroatom-bonds with the participation of two sp^2 hybridised orbitals of boron and an in-plane pure p-orbital of oxygen without the involvement of the flourine atoms. The trend of σ aromaticity is opposite to that of the trend followed by π aromaticity, it is highest for the heteroatom that are comparatively smaller in size, i.e., the systems containing the heteroatom oxygen and nitrogen have higher NICS (0) values implying higher σ aromaticity which is also supported by the CMO-NICS analysis. A shorter bond distance between the heteroatom (N and O) and the boron atom facilitates a greater in-plane delocalization thereby accounting for a higher σ aromaticity in B_2F_2O and B_2F_2NH systems. As the size of the heteroatom gradually increases down the group the bond distance between the heteroatom and the boron atom consequently increases as evident from Figure 5.1 thereby reducing the in-plane delocalization and correspondingly the σ aromaticity in B_2F_2S and B_2F_2Se systems. From the observation it is apparent that there exists an antagonistic relationship between σ and π aromaticity. This σ aromaticity accounts for the reduced strain energy in the three-member rings.[62]

Table 5.9. The nucleus-independent chemical shift (NICS) values in ppm at the plane of the ring (NICS (0)) and at 1 Å above the plane of the ring (NICS (1)) in different DFT methodologies using aug-cc-pVDZ basis set.

Molecules	**Methodology (along with aug-cc-pvdz)**	**NICS(0)**	**NICS(1)**
	UB3LYP	-25.8965	-9.3217
	UB3PW91	-25.4372	-9.3164
B_2F_2O	UPBEPBE	-24.9269	-9.3870
	UBLYP	-25.1485	-9.3241
	UCAM-B3LYP	-26.2475	-9.3766
	UB3LYP	-12.0535	-10.8361
	UB3PW91	-11.4657	-10.7858
B_2F_2S	UPBEPBE	-11.5345	-10.5561
	UBLYP	-12.0159	-10.5518
	UCAM-B3LYP	-12.1434	-11.0275
	UB3LYP	-10.0864	-11.2460
	UB3PW91	-9.5752	-11.1972
B_2F_2Se	UPBEPBE	-9.8592	-10.9167
	UBLYP	-10.2615	-10.8969
	UCAM-B3LYP	-9.9759	-11.4983
	UB3LYP	-23.7343	-8.5054
	UB3PW91	-23.4382	-8.4983
B_2F_2NH	UPBEPBE	-23.2253	-8.4073
	UBLYP	-30.1548	-9.1237
	UCAM-B3LYP	-23.7884	-8.5914

Table 5.10. Population analysis of the orbital which is responsible for σ aromaticity involving three centre bonds.

(Occupancy) Bond orbital/ Coefficients/ Hybrids

(1.98942) 3C*(1) B 1- B 2- O 3

(9.43%) 0.3070* B 1 s(32.75%)p 2.03(66.48%)d 0.02(0.76%)

-0.0003 0.5714 -0.0283 0.0166 0.0000

0.0000 -0.2477 -0.0716 -0.7690 0.0838

0.0000 0.0000 0.0547 -0.0199 0.0652

(9.43%) -0.3070* B 2 s(32.75%)p 2.03(66.48%)d 0.02(0.76%)

-0.0003 0.5714 -0.0283 0.0166 0.0000

0.0000 0.2477 0.0716 -0.7690 0.0838

0.0000 0.0000 -0.0547 -0.0199 0.0652

(81.15%) -0.9008* O 3 s(0.00%)p 1.00(98.94%)d 0.01(1.06%)

0.0000 0.0000 0.0000 0.0000 0.0000

0.0000 -0.9947 -0.0004 0.0000 0.0000

0.0000 0.0000 -0.1031 0.0000 0.0000

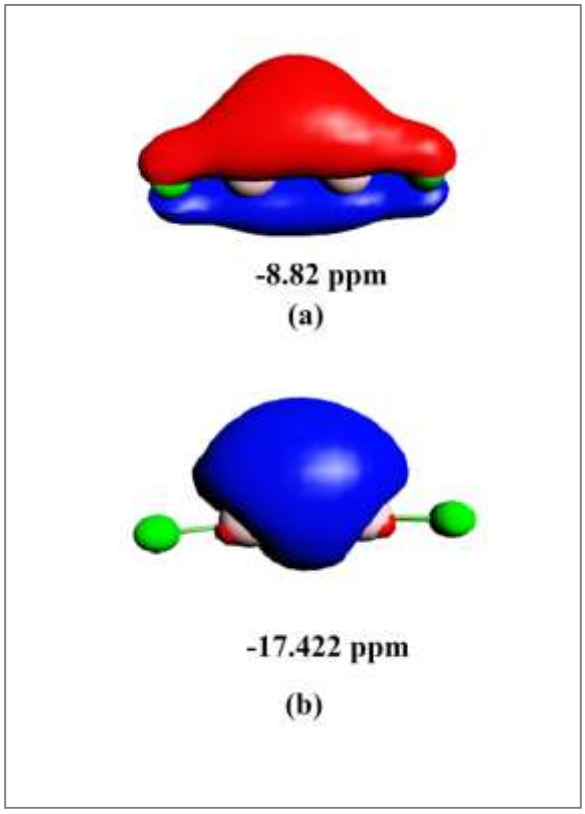

Figure 5.3. The CMOs with maximum diamagnetic contribution to π and σ aromaticity in (a) and (b)respectively, obtained through CMO-NICS analysis at the ring centre of the B_2F_2O molecule.

Apart from NICS, we also performed calculations using the Multiwfn program[54] to generate the multicentre bond aromaticity index (MCI). The MCI data for the studied molecular systems are provided in Table S6 of the Supplementary Information. The MCI values are in the range of 0.45-0.52 which strongly indicates the presence of aromaticity in these heterocyclic moieties.

5.3.5. Adaptive Natural Density Partitioning (*AdNDP) Analysis*

Adaptive Natural Density Partitioning is a theoretical analysis which provides a very proficient and an illustrative method to the understanding of the molecular orbital dependent wave functions. It is a recently developed method which was proposed in the year 2008 by Zubarev and Boldyrev[49] for determining chemical bonding patterns in general molecular systems. This method is based on the simple Lewis concept that describes the chemical bonding with respect to the electron pair thereby characterizing the electronic structures as n-centered-2 electron bonds where the value of n ranges from 1 to the total number of atoms present in the studied molecular systems. It figure outs the elements responsible for Lewis

bonding and also the elements responsible for delocalized bonding which can be correlated with the concepts of aromaticity and antiaromaticity. AdNDP is an overview of NBO analysis as was proposed by Weinhold[80,81] from a computational view point on the basis of the diagonalization of the blocks of the first order density matrix based on natural atomic orbitals. AdNDP bonding patterns are in consonance with the point group symmetry of the molecular systems and resonating structures are generally avoided. The main advantage of this method is that it effortlessly links the Canonical Molecular Orbitals (CMO) and the Natural Bonding Orbitals (NBO). AdNDP orbitals for our systems are investigated using Multiwfn (A Multifunctional Wave function Analysis program).[54]

The AdNDP analysis has been performed for all our systems as presented in Figure 5.4.The quest for the all-centre-2 electron bond whose natural occupation number ranges from 1.99-2.00|e| indicates a strong aromatic character in the studied systems. The visualization of the AdNDP orbitals reveals that the aromatic π cloud hovers over the molecular moiety comprising of the heteroatom (O, S, Se and N) along with the boron and the fluorine atom thereby indicating that the fluorine atoms are involved in aromaticity. This portrayal of the 5-centered 2-electron AdNDP orbital signifies the role of the substituent fluorine atoms in developing aromaticity thus strongly establishing our notion of exo-cyclic aromaticity in these systems (Figure 5.4).

B_2F_2O	 **B_2F_2O** Occupation No. 1.99
B_2F_2S	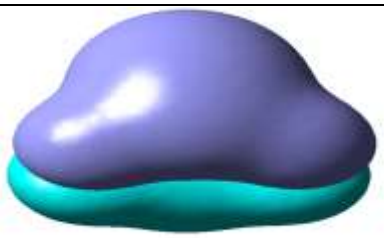 **B_2F_2S** Occupation No. 1.99
B_2F_2Se	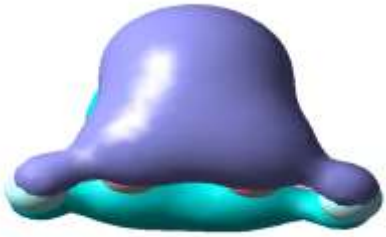 **B_2F_2Se** Occupation No. 1.99
B_2F_2NH	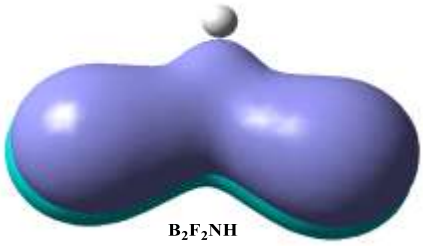 **B_2F_2NH** Occupation No. 2.00

Figure 5.4. The AdNDP orbitals of the studied systems from top view with their natural occupation numbers.

5.3.6. Aromatic Stabilization Energy(ASE)

In a recent work, aromaticity is quantified with respect to the energy stabilization due to circular π-electrons delocalization, termed as the Aromatic Stabilization Energy (ASE).[50] The expression for ASE for conventional benzene like systems was derived[54] to be

$$ASE = \sum_{i,j} \frac{t_{ij}^2}{U} \left(n_{i\sigma} n_{j\sigma'} + n_{i\sigma'} n_{j\sigma}\right) ELF^2 \quad (5.2)$$

Therefore, from Eq. (2), we can relate the π-electron delocalization energy (ASE) to the inter-site hopping integral (t_{ij}) and the onsite repulsion energy (U). The electronic population engaged in delocalization is obtained as a product of spin – orbital population ($n_{i\sigma}$ and $n_{j\sigma'}$) within the unrestricted framework and the degree of delocalization, which is estimated from electron localization function (ELF).

As already mentioned, the above equation is applicable for benzene like aromatic molecules, which are different from the studied system in terms of the electronic structure and aromaticity type.In the systems studied here, specifically the migration of the lone pair of electrons in between the boron and fluorine completes the loop of electronic circulation and thus makes the pattern of electron delocalization unique and different to conventional aromatic systems. To agree with this representation of electron delocalization, the above equation is divided into two components as

$$ASE = \sum_{B,X} \frac{2t_{ij}^2}{U} (n_{B\sigma} n_{X\sigma'} + n_{B\sigma'} n_{X\sigma}) ELF^2 + \sum_{F,B} \frac{2t_{ij}^2}{U} (n_{F\sigma} n_{B\sigma'} + n_{F\sigma'} n_{B\sigma}) ELF^2 \quad (5.3)$$

Here, the first part stands for the electron delocalization within B-X ring, it is multiplied by two to account for two lone pair of electrons of the heteroatom X and the second part quantifies stabilization for electron delocalization within Lewis acid-base pair. The probability of the lone-pair transfer from F to B is taken into consideration by multiplying by two.

TABLE 5.11. The Aromatic Stabilization Energy (ASE) of the studied molecular systems in kcal/mol.

MOLECULES	ASE(kcal/mol)
B_2F_2O	**17.1**
B_2F_2S	**22.8**
B_2F_2Se	**34.6**
B_2F_2NH	**21.1**

The high values of ASE as evident from Table 11 also advocate towards a significant stabilization of the molecules as a result of aromaticity. It can also be observed thatthe ASE values obtained are also in accordance and are in correlation to the NICS values. The values computed are comparable to highly stable classical aromatic systems[82, 83] thereby further accentuating the viability of these molecular systems. A method to localize Wannier function was given by Marzari and Vanderbilt named as Maximally Localized Wannier Function [MLWF] [84] which provides an enhanced bonding picture.

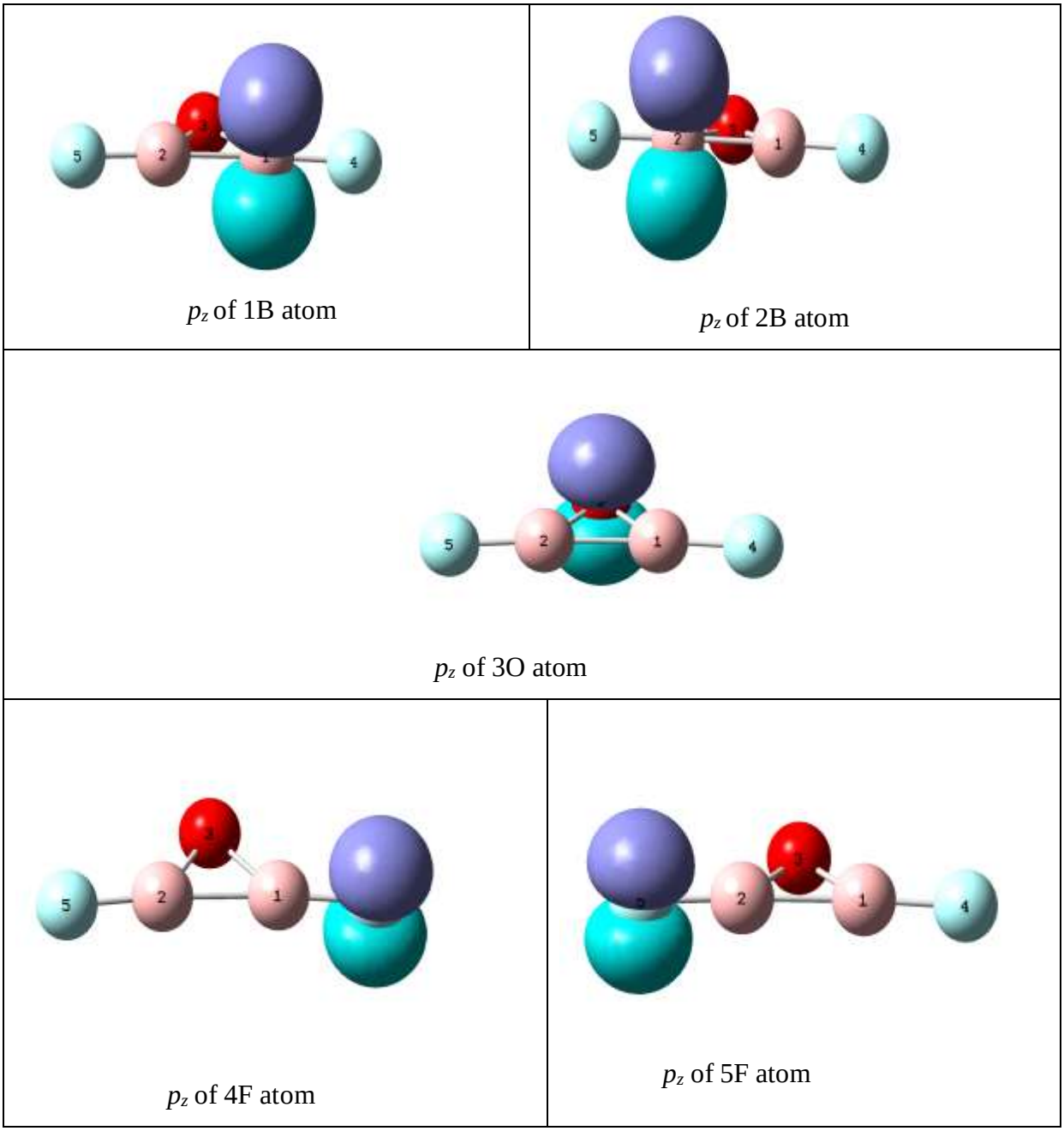

Figure 5.5. Maximally Localized Wannier Functions in B_2F_2O

The Maximally Localized Wannier Functions (MLWFs) obtained through OpenMX 3.6 quantum chemistry code[55] (Figure 5.5) provide a vivid picture that the p_z orbitals perpendicular to the molecular plane of all the atoms including the exo-cyclic atoms are involved in aromaticity as in accordance to our scheme described in Fig.2. thereby establishing our notion of exo-cyclic aromaticity where aromaticity is achieved through back donation of electrons of the fluorine atoms to the electron-deficient p_z orbitals of the boron atoms.

5.4.

CONCLUSIONS

The observation of unique aromaticity obtained through back donation of 4π-electrons from substituent exo-cyclic flourineatoms to the vacantp_z orbitals of the boron atomsmake the study of these proposed novel three-membered heterocyclic planar systems an interesting addition to the domain of aromaticity. Rigorous computational study involving DFT and *ab initio* calculations along with Energy Decomposition Analysis (EDA), the evaluation of Ring Strain Energy and HOMO-LUMO gap indicate towards the viability of the systems. The aromaticity of the molecule is evaluated through some standard criteria, specifically Nucleus Independent Chemical Shift (NICS) and Multi Centre bond Index (MCI). The dissected NICS analysis (CMO-NICS) presents a clear picture of the molecular orbitals contributing towards σ and π aromaticity respectively. A coherent picture of the exo-cyclic nature of the aromatic π-cloud is viewed with the AdNDP analysis. The Aromatic Stabilization Energy (ASE) based on a fully *ab initio* approach is also reported which renders the proposed heterocyclic molecules to be remarkable 6 π -aromatic systems where the *magic number* is attained through an 'exo-cyclic' conjugation. These proposed molecules are unique and distinctive due to the presence of both the σ and the π aromaticity and the antagonistic relationship existing between them makes the systems aremarkable addition to the class of aromatic molecules and provide a significant scope of future study. The high stability of the molecular systems as apparent from the various computational analysis makes us hopeful regarding the investigational reality of these molecules.

5.5.

REFERENCES

1. Faraday, M. *M.Phil.Trans.Roy.London* **1825**, *115*, 440.
2. Kekulé, A. .*Bull.Soc.Chim.Paris* **1865**, *3*, 98.
3. Kekulé, A. *Ann.Chem.Pharm* **1866**, *137*, 129.
4. Garratt, P. J. *Aromaticity*; John Wiley & Sons, 1986.
5. Minkin, V. I.; Glukhotsev, M. N.; Simkin, B. Y. *Aromaticity and antiaromaticity: electronic and structural aspects;* John Wiley & Sons, Inc., New York, **1994**.
6. Bickelhaupt, F.; de Wolf, W. H. *Recl. Trav. Chim. Pays-Bas.* **1988**, *107*, 459

7. Kraakman, P. A.; Valk, J. M.; Niederla¨nder, H. A. G.; Brouwer, D. B. E.; Bickelhaupt, F. M.; de Wolf, W. H.; Bickelhaupt, F.; Stam, C. H. *J. Am. Chem. Soc.***1990**, *112*, 6638.
8. Schleyer, P. V. R.; Jiao, H. *J. Pure Appl. Chem.* **1996**, *68*, 209.
9. Schleyer, P. V. R.; Jiao, H.; Hommes, N. J. R. v. E.; Malkin, V.G.; Malkina, O. L. *J. Am. Chem. Soc.***1997**,*119*, 12669.
10. Poranne, G.P.; Stranger, A. *Magnetic and structural aspects*; Wiley: New York, **1994**.
11. Homray, M.; Misra, A.; Chattaraj, P. K. *Curr. Org. Chem.***2017**, *21*, 2699.
12. Katritzky, A. R. *Chem. Rev.* **2004**, *104*, 2125.
13. Aihara, J. I. *Pure Appl. Chem*. **1982**, *54*, 1115.
14. Graovac, A.; Trinajstic, N.International symposiumon aromaticity, Dubrovnik, 1979.
15. Nyulaszi, L. *Chem. Rev.* **2001**, *101*, 1229.
16. Minkin, V. I.; Minyaev, R. M. *Chem. Rev.***2001**, *101*, 1247.
17. Katritzky, A. R.; Jug, K.; Oniciu, D. C. *Chem. Rev.***2001**, *101*, 1421.
18. Li,X.; Kuznetsov, A.; Zhang, H.; Boldyrev, A. I.; Wang, L. *Science,***2001**, 291, 859.
19. Kuznetsov, A. E.; Birch, K. A.; Boldyrev, A. I.; Li, X.; Zhai, H.; Wang, L. *Science*, **2003**, *300*, 622.
20. Boldyrev, A. I.; Wang, L .*Chem. Rev.* **2005**, *105*, 3716.
21. Paul, S.; Misra, A. *Inorg Chem* **2011,** *50*, 3234.
22. Chattaraj, P. K.; Roy, D. R.; Duley, S. *Chem.Phys.Lett.* 2008, *460*,382.
23. Huckel,E. *Z. Phys*. **1931**, *70*, 204.
24. Hehre, W. J.; Radom,L.; Schleyer,P. v. R.; Pople, J. A. *Ab Initio molecular orbital theory*; Wiley, New York, 1986.
25. Xie, Y.; Schaefer III, H. F.; Thrasher, J. S. *J. Mol. Struct. Theochem.*, **1991**, *234*, 247.
26. Shaik, S.; Shurki, A.; Danovich, D.; Hiberty, P. C. *J. Mol. Struct.Theochem* **1997**, *398*, 155.
27. Krygowski, T. M.; Cyraski, M. K., *Chem. Rev.* **2001**, ***101***, 1385.
28. Poater, J.; Duran, M.; Solà, M.; Silvi, B. *Chem. Rev.* **2005**, *105*, 3911.
29. Cyraski, M. K. *Chem. Rev.* **2005**, *105*, 3773.
30. Matito, E.; Duran, M.; Solà, M. *J. Chem. Phys.* **2005**, *122*, 014109.
31. Bultinck, P.; Ponec, R.; Van Damme,S. *J. Phys.Org. Chem*. **2005**, *18*, 706.
32. Feixas, F.; Matito, E.;Poater, J.;Solà, M. On the performance of some aromaticity indices: A critical assessment using a test set. *J. Comput. Chem.* 2008, 29, 1543-1554.
33. Roy, D. R.; Bultinck, P.; Subramanium, V.; P. K. Chattaraj, J. Mol. Struc., **2008**, *854*, 35.
34. Feixas, F.; Matito, E.; Poater, J.; Solà, M. *Chem. Soc. Rev*. **2015**, *44*, 6434.
35. Misra, A.; Klein, D. J.; Morikawa,T. J. Phys. Chem. A **2009***, 113*, 1151.
36. Clar, E. *The Aromatic Sextet*; Wiley & Sons: New York, **1970**.
37. Misra, A.; Schmalz, T. G.; Klein, D. J. *J.Chem. Inf.Model*, **2009**, *49*, 2670.
38. Bhattacharya, D.; Panda, A.; Misra, A.; Klein, D. J. *J. Phys. Chem. A*, **2014**, *118*, 4325.
39. Gund, P. *J. Chem. Educ.* **1972**, *49*, 100.
40. Goswami, T.; Homray, M.; Paul, S.;Bhattacharya, D.; Misra, A. *Phys. Chem. Chem. Phys.* **2017**, *19*, 11744.
41. Gutowsky, H. S.; McCall, D. W. *J. Phys. Chem.* **1953**, *21*, 279.

42. Onak, T. P.; Landesman, H.; Williams, R. E.; Shapiro, I. paper presented to the Division of Inorganic Chemistry, 135th NationalMeeting of the American Chemical Society, Boston, Mass., April **1959**.
43. Cotton, F. A.; Wilkinson,G. *"Advanced Inorganic Chemistry,"*Interscience, London, **1966**, 256.
44. Olah, G. A.; Mo, Y. K.; Halpern, Y. *J Am Chem Soc* **1972**, *94*, 3551.
45. Ziegler, T.; Rauk, A. 1**977**, *46*, 1.
46. Bader, R. F. W. *Atoms in Molecules: A Quantum Theory;* Oxford University Press, Oxford, UK, **1990**.
47. Schleyer, P. v. R.;Maerke, C.; Dransfeld, A.; Jiao, H.; Hommes, N. J. R. v. E. *J Am Chem Soc*, **1996**, *118*, 6317.
48. Heine, T.; Schleyer, P. v. R.; Corminboeuf, C.; Seifert, G.; Reviakine, R.; Weber, J. *J. Phys. Chem. A* **2003**, *107*, 6470.
49. Zubarev, D. Yu.; Boldyrev, A. I. *Phys. Chem. Chem. Phys*. **2008**, *10*, 5207.
50. Paul,S.; Goswami, T.; Misra, A. *AIP Advances*, **2015**, *5*, 107211.
51. Gaussian 09, Revision B.01, Frisch, M. J.; Trucks, G. W.; Schlegel, H. B.; Scuseria, G. E.; Robb, M. A.; Cheeseman, J. R.; Scalmani, G.; Barone, V.; Petersson, G. A.; Nakatsuji, H.; Li, X.; Caricato, M.; Marenich, A. V.; Bloino, J.; Janesko, B. G.; Gomperts, R.; Mennucci, B.; Hratchian, H. P.; Ortiz, J. V.; Izmaylov, A. F.; Sonnenberg, J. L.; Williams-Young, D.; Ding, F.; Lipparini, F.; Egidi, F.; Goings, J.; Peng, B.; Petrone, A.; Henderson, T.; Ranasinghe, D.; Zakrzewski, V. G.; Gao, J.; Rega, N.; Zheng, G.; Liang, W.; Hada, M.; Ehara, M.; Toyota, K.; Fukuda, R.; Hasegawa, J.; Ishida, M.; Nakajima, T.; Honda, Y.; Kitao, O.; Nakai, H.; Vreven, T.; Throssell, K.; Montgomery, J. A., Jr.; Peralta, J. E.; Ogliaro, F.; Bearpark, M. J.; Heyd, J. J.; Brothers, E. N.; Kudin, K. N.; Staroverov, V. N.; Keith, T. A.; Kobayashi, R.; Normand, J.; Raghavachari, K.; Rendell, A. P.; Burant, J. C.; Iyengar, S. S.; Tomasi, J.; Cossi, M.; Millam, J. M.; Klene, M.; Adamo, C.; Cammi, R.; Ochterski, J. W.; Martin, R. L.; Morokuma, K.; Farkas, O.; Foresman, J. B.; Fox, D. J. Gaussian, Inc., Wallingford CT, 2009.
52. Amsterdam Density Functional (Theoretical Chemistry, Vrije Universitiet, Amsterdam, The Netherlands, http://www.scm.com).
53. AIMAll (Version 17.01.25), Todd A. Keith, TK Gristmill Software, Overland Park KS, USA, 2017
54. Lu, T.; Chen, F. Multiwfn: A multifunctional wavefunction analyzer*J. Comp. Chem*.**2012**, 33, 580-592.
55. The DFT code, OPENMX, is available at http://www.openmx-square.org under the GNU General Public License.
56. Pinter, B.; Fievez, T.; Bickelhaupt, F. M.; Geerlings, P.; F. DeProft, *Chem. Chem. Phys.***2012**, *14*, 9846.
57. Lee, J. T.; Taylor, P. R. *Int. J. Quantum Chem.***1989**, *36*, 199.
58. Bauzá, A.; Quiñonero, D.; Deyà, P. M.; Frontera, A. *Chem. Phys. Lett*., **2012**, *536*, 165.
59. Cox, J. D.; Pilcher, G.; *Thermochemistry of organic and Organometallic compounds;* Academic: London, 1970.
60. Benson, S. W. *Thermochemical Kinetics;* Wiley: New York, 1976.
61. Inagaki, S.; Ishitani, Y.; Kakefu, T. *J. Am. Chem. Soc.* **1994**, *116*, 13.

62. Dewar, M. J. S. *J. Am. Chem. Soc.* **1984**, *106*, 669.
63. Aihara, J. *J. Phys. Chem. A* **1999**, *103*, 7487.
64. Aihara, J. *Theor. Chem. Acc.***1999**, *102*, 134.
65. Aihara, J. *Phys. Chem. Chem. Phys.* **1999**, *1*, 227.
66. Parr, R. G.; Zhou, Z.; *Acc. Chem. Res*. **1993**, *26*, 256.
67. Liu, X.; Schmalz, T. G.; Klien, D. J. *Chem. Phys. Lett.* **1992**, *188*, 550.
68. Haddon, R. C.; Fukunaga, T. *Tetrahedron Lett.* **1980**, *21*, 1191.
69. Pearson, R. G. *Hard and soft acids and bases*; Dowden, Hutchinson and Ross: Stroudsburg, PA, 1973.
70. Manolopoulos, D. E.; May, J. C.; Down, S. *Chem. Phys. Lett.***1991**, *181*, 105.
71. Hoffmann, R.; Schleyer, P. V. R.; Schaefer, H. F. *Angew. Chem., Int. Ed.* **2008**, *47*, 7164.
72. Katrizky, A.; Barczymski, P.; Musumarra, G.; Pisano, D.; Szafran, M. *J. Am. Chem. Soc* **1989**, *111*, 7.
73. Schleyer, P. V. R.; Manoharan, M.; Jiao, H.; Stahl, F. *Org Lett.* **2001**, *3*, 3643.
74. Chen, Z.; Wannere, C. S.; Corminboeuf, C.; Puchta, R.; Schleyer, P. V. R. *Chem Rev.* **2005**, *105*, 3842.
75. London, F. *J. Phys. Radium.* **1937**, *8*, 397.
76. Cheeseman, J. R.; Trucks, G. W.; Keith, T. A.; Frisch, M. J. *J. Chem. Phys.* **1996**, *104*, 5497.
77. Schreckenbach, G.; Ziegler,T.; *J. Phys. Chem*. 1995, *99*, 606.
78. Schreckenbach, G.; Ziegler,T.; *Theor. Chem. Acc.*1998, *99*, 71.
79. Simkin, B. Y.; Minkin, V.I.; Glukhotsev, M.N. *Adv. Heterocyclic Chem*.**1993**, *56*, 304.
80. Foster, J. P.; Weinhold, F. *J. Am. Chem. Soc*. **1980**, *102*, 7211.
81. Reed, A. E.; Curtiss, L. A.;Weinhold, F. *Chem. Rev.***1988**, *88*, 899.
82. Katrizky, A.; Barczymski, P.; Musumarra, G.; Pisano, D.; Szafran, M. *J. Am. Chem. Soc* **1984**, *111*, 7.
83. Radhakrishnan, S.; Anathakrishnan, S. J.; Somanathan, N. *Bull. Mater. Sci.* **2011**, *34*, 713.
84. Marzari, N.;Vanderbilt, D. *Phys. Rev. B* **1997**, *56(20)*, 12847.

CHAPTER 6

Bond stretch isomerism in aromatic Be_3^{2-} cluster driven by the Renner-Teller effect

6.1.

INTRODUCTION

Bond Stretch Isomerism (BSI) occurs when the isomers differ in the lengths of certain bonds. This phenomenon is intriguing due to the fact that the inter conversion between the two isomers requires only a simple compression or elongation of a bond. The idea of bond stretch isomerism was first proposed by Hoffmann and co-workers in the year 1972 where they had referred to separate stable configurations whose structures vary only in the length of one (or more) chemical bond(s) where the isomers were shown to occupy different minima on their potential energy surface.[1-3] Experimental evidence of BSI was however reported in the year 1970 by Chatt,[4] prior to the theoretical proposition. Since then a range of compounds have been shown to exhibit BSI[5-8] which was theoretically rationalized later in the year 1988.[3] In spite of increasing illustrations of BSI, both theoretically and experimentally, lack of a proper explanation behind the existence of bond stretch isomers makes the event unclear.[9-12] Despite the vagueness surrounding this phenomenon, there are a number of occurrences where BSI undoubtedly exist[13-15] but an appropriate elucidation of the phenomenon still remains a major challenge, which sets up the objective of this present work.

BSI has been established recently in $Be_3^{2-}$and its unique bonding pattern is extensively discussed.[16] $Be_3^{2-}$is a comprehensively studied system in the field of all-metal aromatic clusters in terms of stability, aromaticity, hardness, etc. It has been shown to exist in a range of structural isomers including cyclic (D_{3h}, C_{2v}) and linear ($D_{\infty h}$) forms[17-24] however, a correlation between the different isomers is yet to be realized. In numerous works, the short-bond isomer of the Be_3^{2-} with D_{3h} symmetry is reported to have a bond length of 2.078Å;[18] on the other hand, Sola and co-workers obtained the long-bond isomer with the same D_{3h} symmetry with an optimized bond length of 2.156Å.[24] It has been established that they lie on entirely different potential energy surfaces occupying two different minima corresponding to short- and long-bond isomers respectively, since the existence of BSI requires both a double minimum on a potential energy surface and a considerable barrier between these two minima.[16] The existence of BSI is further emphasized due to the reversal of the frontier molecular orbitals where HOMO of the short-bond isomer is observed to be the LUMO of the long-bond isomer and vice-versa. Hybridization isomerism, due to the change in hybridization on one atom and Jahn-Teller distortions may be subtly distinguished from

BSI.[25] The potential energy surfaces of these two isomers may have an intersecting point representing the Conical Intersection (CI) to obtain a degenerate state. All these factors instigate the present study to find a connection between the two D_{3h} BSIs in Be_3^{2-}. In this paper we try to understand the underlying mechanism which leads to the presence of two bond stretch isomers. The primary force behind the presence of two different isomers of the Be_3^{2-} molecule may be the Renner-Teller effect[26-28] which identifies the prospective of a triatomic molecule present in a degenerate electronic state to split into two when the molecule is bent. Renner-Teller effect occurs in its simplest form in open shell linear triatomic molecule (Scheme 6.1). The Be_3^{2-} molecule has a linear geometrical isomer possessing $D_{\infty h}$ symmetry; as a result the electronic states may be two-fold degenerate, thereby causing the breakdown of the adiabatic (Born-Oppenheimer) approximation which lifts the degeneracy of a linear molecule. The linear triatomic molecule is electronically non-degenerate in its ground state, but its excited state is degenerate thereby forces bending of the linear structure to produce two lower energy ground state equilateral triangular D_{3h} bond stretch isomers via conical intersections.

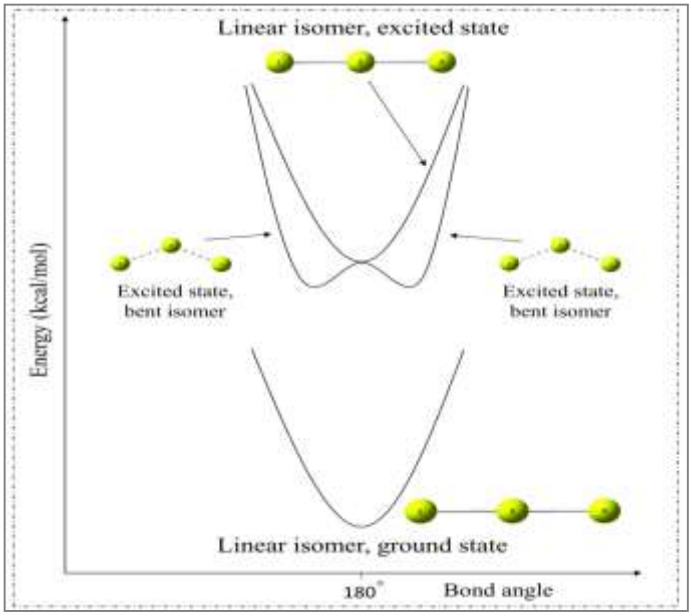

Scheme 6.1

6.2.

COMPUTATIONAL DETAILS

According to our previously reported results,[16, 23] all the isomers of Be_3^{2-}cluster are modeled in this work. For the preparation and study of different input and output geometries, graphical software GaussView 5[29] is used. All the optimizations, frequency calculations and molecular dynamics simulations are done using the Gaussian 09 package.[30] As Beryllium exhibits multi-reference behavior (due to the near degeneracy of *s* and *p* orbitals), T_1 diagnostic of the system to check the multireference issue was done in a previous work.[23] Here it was shown that the values of T_1 are 0.08496, 0.08827 and 0.08108 for D_{3h}, C_{2v} and $D_{\infty h}$ isomers respectively which are much greater than the 0.02 threshold. The occupation of higher energy molecular states is preferential due to the presence of two additional electrons in the Be_3 moiety. Higher influence of non-dynamical electron correlation account for the higher values of T_1. Large values of T_1 evidently point towards the insufficiency of single-reference methods which suggests the requirements of muli-reference methods to predict the energy and equilibrium structure of Be_3^{2-} more precisely. The modeled structures are optimized at complete active space self-consistent field (CASSCF) level of theory in addition to B3LYP levelin conjunction with6-311++G(d) basis set.[23] Harmonic vibrational frequencies are computed at the same level of theories, and the obtained results confirm that the structures correspond to minima on the potential energy surfaces for the cyclic (D_{3h}) and linear ($D_{\infty h}$) isomers. The transition state search, excited state search, conical intersections search and intrinsic reaction coordinate (IRC) calculations are carried out at different theoretical levels and mentioned in appropriate places. During the CASSCF calculations, all the valence electrons are taken into active space considerations due to the smaller size of the molecule. CASSCF (8,6) takes into account 8 electrons in the active space and 6 orbitals in the active space. The σ MOs corresponding to the 1s orbitals of the constituent Be atoms are not assigned to the active space. The σ and π MOs resultant to the 2s and 2p orbitals of the Be atoms are assigned to the active space. Since the CASSCF method lacks of dynamic correlation, an MP2 level electron correlation correction to the CASSCF energy is computed which incorporates the dynamic correlation.[31-33]

Dynamics of the Be_3^{2-}isomers are studied through an Atom Centered Density Matrix Propagation (ADMP)[34-37] technique as included in Gaussian 09 program package.

Simulations are done at B3LYP/6-311++G(d) level of theory at several temperatures and it is noted that at 700 K the short-bond Be_3^{2-}isomerizes to form the long-bond analogue via linear $D_{\infty h}$ isomer. Boltzmann distribution is used to generate the initial nuclear kinetic energy of the systems. Temperature is maintained throughout the simulation by using a velocity scaling thermostat. Simulation is carried out keeping the fictitious electronic mass as 0.1 amu.

The variation of hardness (η) and electrophilicity (ω) along the isomerization path is evaluated at B3LYP/6-311++G(d) level of theory. It is established that η and ω can predict the stability of molecular systems in conjunction with the associated electronic structure principles, viz., the maximum hardness principle (MHP)[38-43] and the minimum electrophilicity principle (MEP).[43-46]The electronegativity (χ),[47-49] hardness (η)[50,51] and electrophilicity (ω)[52] of an *N*-electron system can be defined as follows:

$$\chi = -\mu = -\left(\frac{\partial E}{\partial N}\right)_{\upsilon(\vec{r})} \tag{6.1}$$

$$\eta = \left(\frac{\partial^2 E}{\partial N^2}\right)_{\upsilon(\vec{r})} \tag{6.2}$$

$$\omega = \frac{\mu^2}{2\eta} = \frac{\chi^2}{2\eta} \tag{6.3}$$

E, μ, and $v(\vec{r})$ are the total energy of the *N*-electron system, chemical potential and external potential respectively.

Employing a finite difference approximation to Eqs.1 and 2 one can achieve:

$$\chi = \frac{I + A}{2} \tag{6.4}$$

and

$$\eta = I - A \tag{6.5}$$

where *I* and *A* indicate the ionization potential and electron affinity of the cluster, respectively, and they are calculated using Koopmans' theorem.[53,54]

The aromaticity of the two cyclic D_{3h} BSIs is calculated using a recently proposed theoretical model[55-57] where quantification of aromaticity is done with respect to the energy stabilization owing to the circular π-electrons delocalization, termed as the Aromatic Stabilization Energy (ASE). In this theoretical model, ASE is related to the molecular energy stabilization due to electron delocalization in the framework of second order perturbation theory consequential from atom to atom charge transfer.[58-61]

The theoretical model proposes the inter-site hopping integral (t_{ij}) and the onsite repulsion energy (U) to be responsible for the electron delocalization. The population of the electronsparticipatingin delocalization is obtained as a product of spin-orbital population ($n_{i\sigma}$ and $n_{j\sigma'}$) within the unrestricted framework and the level of delocalization is projected from electron localization function (ELF) as

$$ASE = \sum_{i,j} \frac{t_{ij}^2}{U} \left(n_{i\sigma} n_{j\sigma'} + n_{i\sigma'} n_{j\sigma} \right) ELF^2 \tag{6.6}$$

For the estimation of ASE, Gaussian 09 suite of software is used to calculate the onsite repulsion energy (U) and the spin-orbital population ($n_{i\sigma}$ and $n_{j\sigma'}$). The ELF value is obtained utilizing the Multiwfn code[62] and OpenMX 3.6 quantum chemistry code[63] are used to estimate the inter-site hopping integral (t_{ij}).

6.3.

RESULTS AND DISCUSSION

Optimized structures of the two cyclic BSIs and linear Be_3^{2-} are given in Figure 6.1 along with their varying bond lengths. The energies and bond lengths of the ground state (short-bond isomer, linear isomer and the long-bond isomer) are given in Table 6.1. All the optimized structures are devoid of any imaginary frequency but the linear isomer has higher ground state energy compared to the cyclic isomers as anticipated from the perspective of aromaticity at various levels of theory.[23]

Table 6.1. Energy (*E* in a.u.) and bond length (*r* in Å) of the ground state isomers of Be_3^{2-} at DFT, CASSCF and CASSCF MP2 level of theory and their relative stability in kcal/mol with respect to the lower energy long bond isomer are also reported.

Ground State	**B3LYP/6-311++G(d)**	**Relative stability (kcal/mol) B3LYP/6-311++G(d)**	**CASSCF/6-311++G(d)**	**Relative stability (kcal/mol) CASSCF/6-311++G(d)**	**CASSCF MP2**	**Relative stability (kcal/mol) CASSCF MP2**
Short-bond isomer	*E* = -44.00343 *r* = 2.078	4.4	*E* = -43.66049 *r* = 2.220	5.9	*E* = -43.80883 *r* = 2.218	4.3
Linear isomer	*E* = -43.98421 *r* = 2.124	16.4	*E* = -43.65011 *r* = 2.158	12.5	*E* = -43.79084 *r* = 2.159	15.6
Long-bond isomer	*E* = -44.01043 *r* = 2.156	0	*E* = -43.67001 *r* = 2.312	0	*E* = -43.81582 *r* = 2.320	0

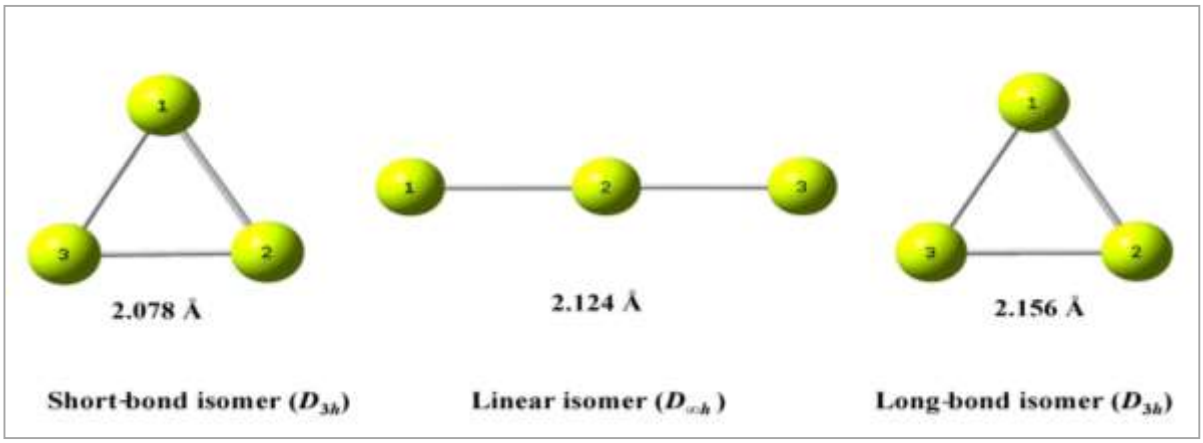

Figure 6.1. Optimized bond lengths of the short-bond, linear and the long-bond isomers at B3LYP/6-311++g(d) level of theory.

A transition state[64] search reveals the presence of an optimized C_{2v} transition state (TS1) connecting the D_{3h} short-bond isomer to a linear $D_{\infty h}$ Be_3^{2-}intermediate. The TS1 has one imaginary frequency and from the atomic displacement vectors it is evident that the TS1 facilitates the formation of the linear intermediate from the short-bond isomer. Similar C_{2v} transition state (TS2) is also observed to be present and connecting the linear $D_{\infty h}$ intermediate to the D_{3h} long-bond isomer with one negative frequency and showing atomic displacement vectors in a direction which indicates the formation of the long-bond isomer from the linear intermediate. Both the C_{2v} transition states satisfy the aforementioned criteria and their optimized structures are given in Figure 6.2. The energies and the bond lengths of the transition states (TS1 and TS2) are given in Table 2. The Intrinsic Reaction Coordinate (IRC) plots showing the path from the short-bond isomer to the linear intermediate via TS1 and the path from the linear intermediate to the long-bond isomer via TS2 are given in Figure 6.3. From these observations, one can infer that the linear intermediate is a vital connector between the two bond-stretch isomers. Similar observation is also made using *ab initio* molecular dynamics simulation through ADMP technique. In a five *pico* second simulation run at 700 K, it is noted that the D_{3h} short-bond form of Be_3^{2-} isomerizes to the $D_{\infty h}$ structure at 3387 *femto* second which thereafter passes through a TS2 like geometry to form the long-bond isomer.

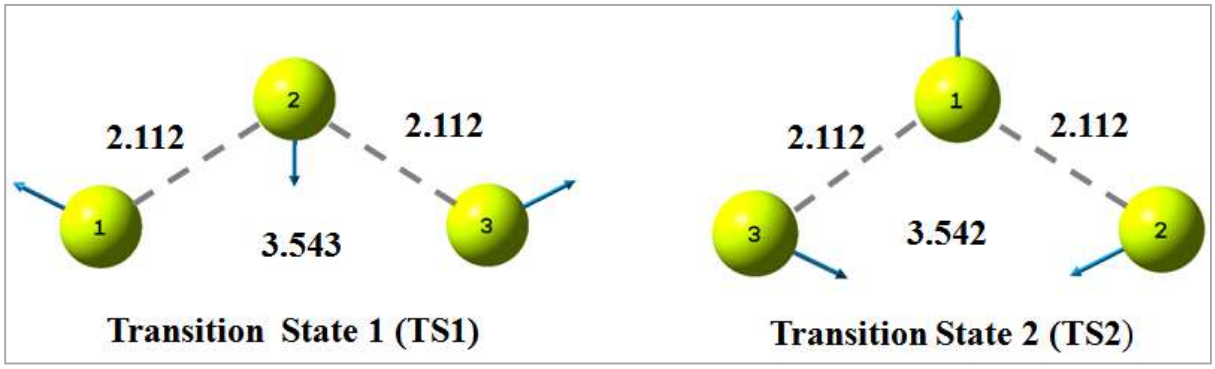

Figure 6.2. Optimized structures of the transition states with their atomic displacement vectors and the respective bond lengths in Å at B3LYP/6-311++g(d) level of theory.

Table 6.2. Energy (*E* in a.u.) and bond length (*r* in Å) of the transition states of Be_3^{2-} at DFT, CASSCF and CASSCF MP2 level of theory and their relative stability in kcal/mol with respect to the lower energy TS2 are also reported.

Transition State	B3LYP/6-311++G(d)	Relative stability (kcal/mol) B3LYP/6-311++G(d)	CASSCF/6-311++G(d)	Relative stability (kcal/mol) CASSCF/6-311++G(d)	CASSCF MP2	Relative stability (kcal/mol) CASSCF MP2
TS1	*E* = -43.97723 *r*[Be(1)-Be(2), Be(2)-Be(3)] = 2.112 *r*[Be(1)-Be(3)] = 3.543	0.5	*E* = -43.62712 *r*[Be(1)-Be(2), Be(2)-Be(3)] = 2.118 *r*[Be(1)-Be(3)] = 3.452	5.2	*E* = -43.78339 *r*[Be(1)-Be(2), Be(2)-Be(3)] = 2.172 *r*[Be(1)-Be(3)] = 3.574	5.7
TS2	*E* = -43.97801 *r*[Be(1)-Be(2), Be(1)-Be(3)] = 2.112 *r*[Be(2)-Be(3)] = 3.542	0	*E* = -43.63542 *r*[Be(1)-Be(2), Be(1)-Be(3)] = 2.118 *r*[Be(2)-Be(3)] = 3.451	0	*E* = -43.79254 *r*[Be(1)-Be(2), Be(1)-Be(3)] = 2.170 *r*[Be(2)-Be(3)] = 3.572	0

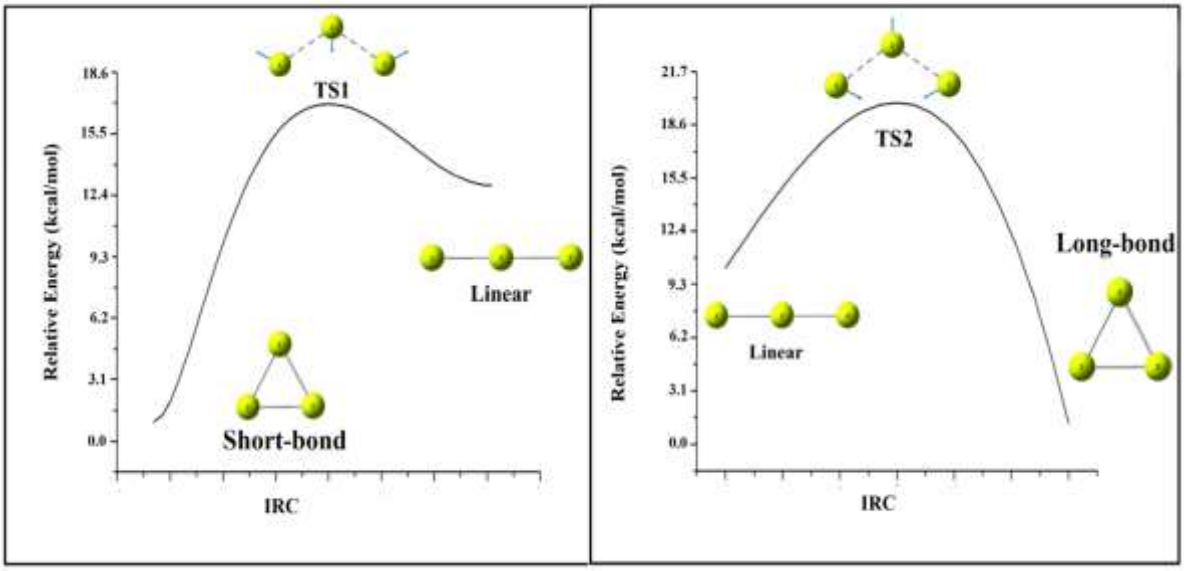

Figure 6.3. IRC plots showing the path from the short-bond isomer to the linear intermediate via TS1 and linear intermediate to long-bond isomer via TS2 at UB3LYP/6-311++G(d) level of theory.

From the molecular orbital analysis, a MO flip was observed for the two minima equilateral structures as reported in one earlier work,[16] where the HOMO(LUMO) of the short-bond(long-bond) isomer is mainly comprised of p_z orbitals of Be atoms and the LUMO(HOMO) of short-bond (long-bond) isomer is composed of p_x and p_y orbitals as is given in Figure 6.4. Moreover, the Frontier Molecular Orbital (FMO) diagram[65] indicates that there is a reversal of the highest occupied and lowest unoccupied molecular orbitals during the passage from the short-bond isomer to the long-bond isomer via linear intermediate (Figure 6.5). So, there must be a point where the HOMO and the LUMO become degenerate, that point of degeneracy was observed at the first excited state of the linear isomer which is very similar to the ground state, possessing $D_{\infty h}$ symmetry. The major difference between them is a shrinkage in the Be-Be bond length in the excited state, from 2.158 Å to 2.140 Å and the energy difference between the two structures is about 9.2 kcal/molat CASSCF(8,6)/6-311++G(d) level of theory where the excited state energy is −43.63545 a.u.(Figure 6.6). At the CASSCF MP2 level, there is also a reduction of bond-length from 2.159 Å to 2.157 Å at the excited state and here the excited state energy considering the dynamic correlation is −43.78145 a.u. So the difference in energy between the two structures in CASSCF MP2 level

is 6.3 kcal/mol. The degenerate orbitals of the excited state are given in Figure 6.7. The different modes of vibration of the linear excited $D_{\infty h}$ state are provided in Table 6.3. The bending mode at a frequency of 198.15 cm^{-1} is responsible for the Renner-Teller effect. The total energy of linear molecules with three or more atoms is reduced by bending the molecule so that the degeneracy is lifted to produce two non-degenerate components.[66] Here, the breakdown of the Born-Oppenheimer approximation is the Renner-Teller effect[26] which lifts the degeneracy as the molecule bends. This leads to a conical intersection which ultimately forms two bond stretch isomers via their respective transition states. The conical intersections have slightly bent structures with an angle of 167.65°, Be-Be bond length at 2.141 Å and energy of −43.63462 a.u.at CASSCF(8,6)/6-311++G(d) level of theory. At the CASSCF MP2 level the energy computed is -43.78145 a.u. considering the dynamic correlations with an angle of 172.02° and bond length of 2.138 Å respectively. The schematic representation of the phenomenon is provided in Figure 6.6.

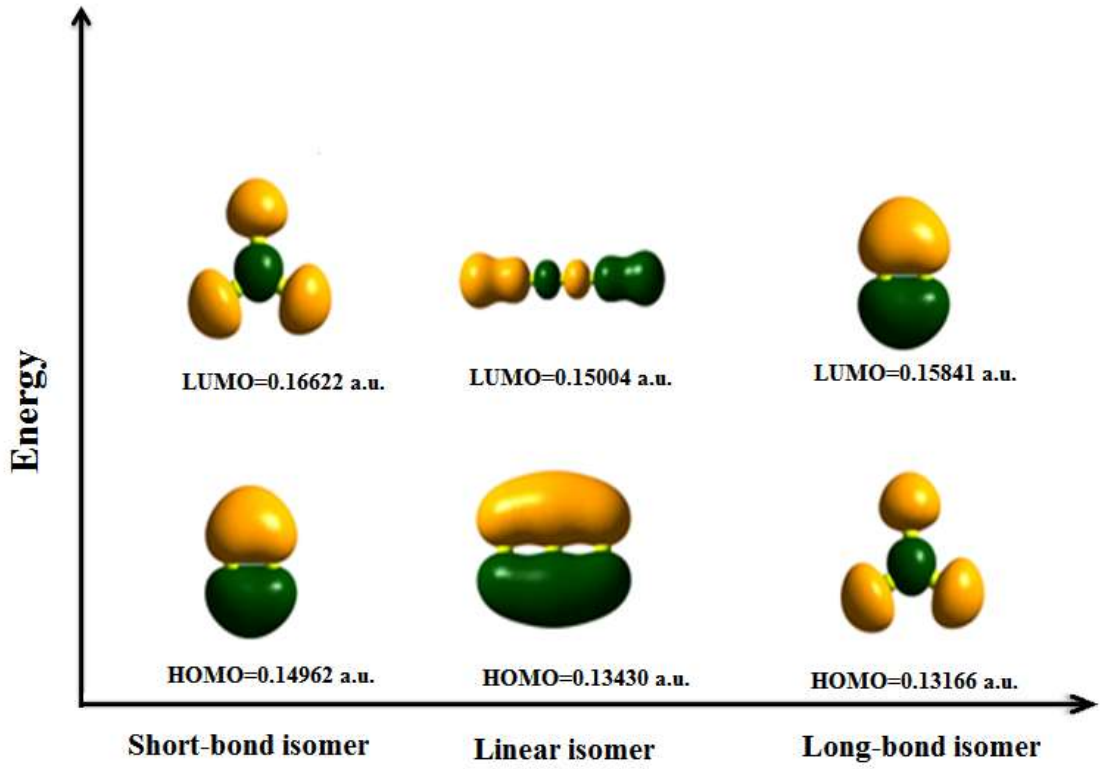

Figure 6.4. The HOMO and LUMO of the ground state isomers along with their energy eigen values obtained at UB3LYP/6-311++G(d) level of theory.

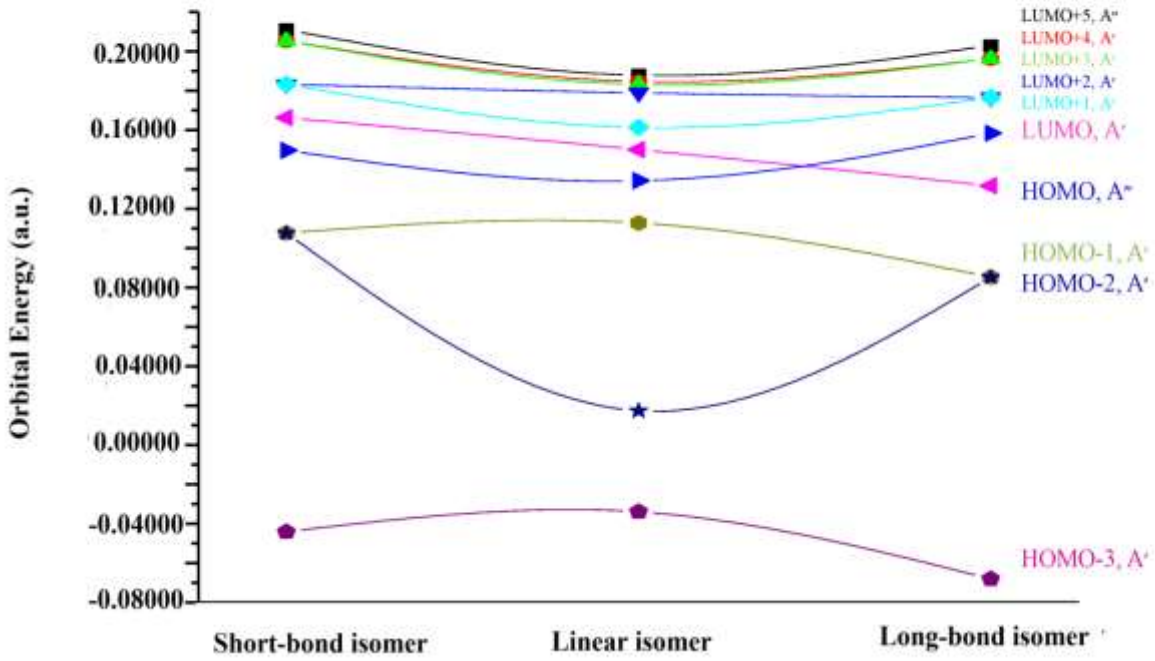

Figure 6.5. Frontier Molecular Orbital (FMO) diagram for the isomerization pathway, D_{3h} short-bond isomer to linear $D_{\infty h}$ Be_3^{2-} intermediate to D_{3h} long-bond isomer at UB3LYP/6-311++G(d) level of theory.

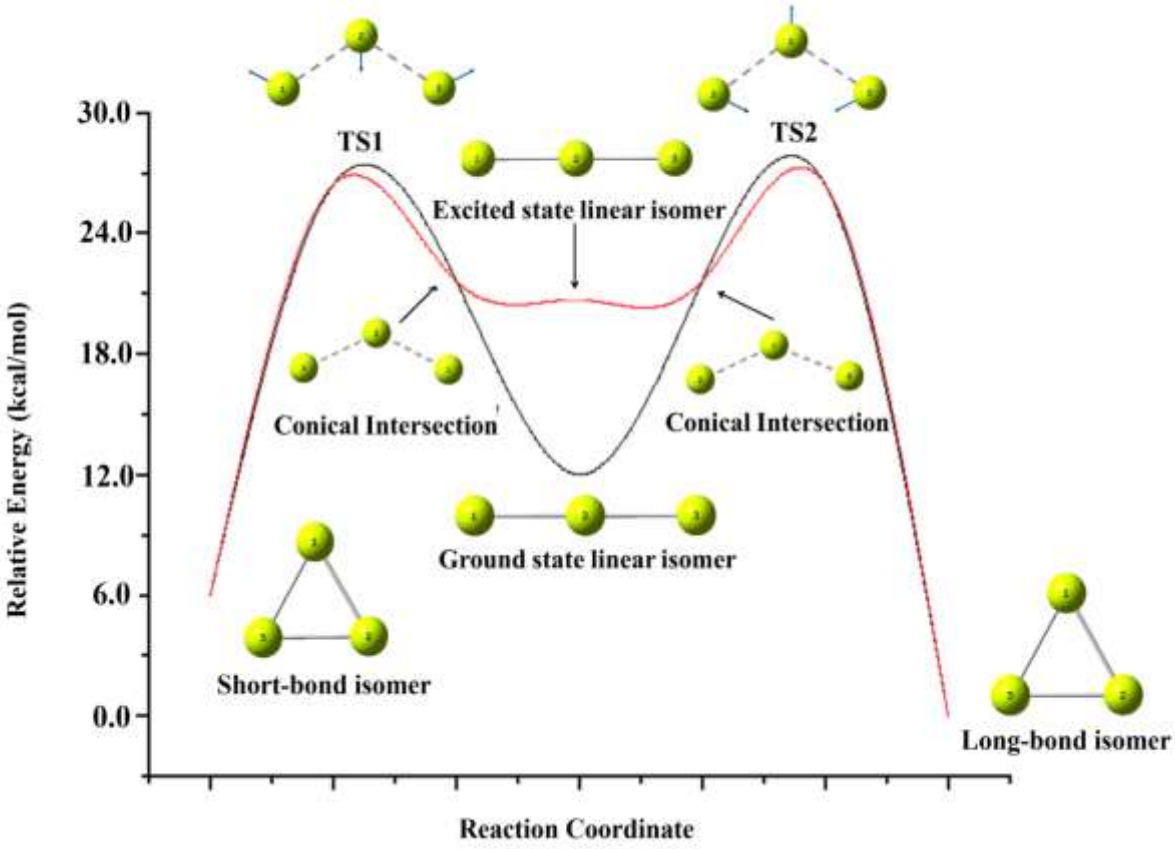

Figure 6.6. Schematic representation of the bond stretch isomerism in Be_3^{2-} molecule at CASSCF(8,6)/6-311++G(d) level of theory.

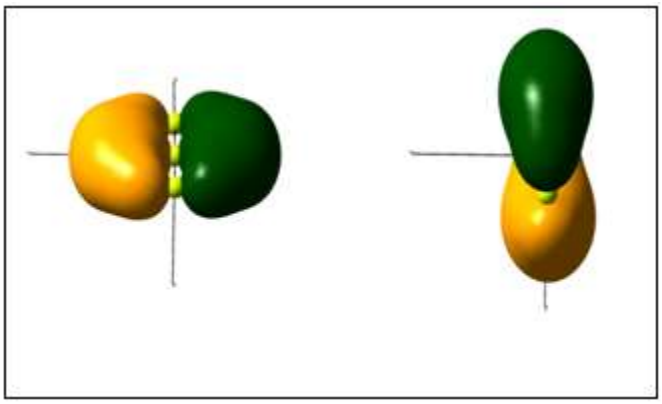

Figure 6.7 The SOMO's of the linear excited state of Be_3^{2-}.

Table 6.3. The modes of vibrations of the excited state $D_{\infty h}$ Be_3^{2-} along with the vibrational energy in cm^{-1} obtained at CASSCF/6-311++G(d) level.

Energy of the vibration of linear $D_{\infty h}$ in cm^{-1}	Assignment of the vibration
198.15	**BENDING**
433.29	**SYMMETRIC STRETCHING**
721.31	**ASYMMETRIC STRETCHING**

The intermediate linear isomer is non-degenerate in its ground state (Figure 6.4) but the excited state is found to possess a degenerate HOMO and LUMO as shown in Figure 6.7, which goes through slightly bent geometries at the conical intersections to reach the ground state potential energy surface. So this explains the underlying mechanism for the presence of two bond stretch isomers in Be_3^{2-} which had remained an intriguing question since the observation of the phenomenon of bond stretch isomerism in Be_3^{2-} molecule.

Variation of hardness(η), electrophilicity(ω), chemical potential(μ) and relative energy(ΔE) is studied along the conversion pathway from the short-bond isomer to the linear isomer via TS1 and from linear to long-bond via TS2. It is noted that hardness and electrophilicity are not minimum and maximum, respectively, at TS1 and TS2.The conversions from reactant to intermediate and intermediate to product via TS1 and TS2 are not through the constant chemical potential path,[50, 67] thus they are not corroborating MHP and MEP. Isomerization processes are often accompanied by drastic change in external potential as well. Moreover, it is reported that the pseudo Jahn-Teller effect is the reason behind several exceptions found to the MHP[68, 69] and here the bond stretch isomerism in the molecule arises due to Renner-Teller effect which is a specific case of Jahn-Teller effect. Thus, the divergence from MHP and MEP is not unexpected here; rather this deviation, in turn, corroborates the occurrence of the Renner-Teller effect. However, in both the above cases it is evident that these indices are rapidly varying near the stationary points[70], (Figure 6.8 and Figure 6.9). Free energy profile of the isomerization process (Figure 6.10) shows the schematic path from the short-bond isomer to the linear intermediate via TS1 and the path from the linear intermediate to the long-bond isomer via TS2. From this plot we can infer that the energy barrier between the short-bond isomer and the intermediate is comparatively smaller than the energy gap between the long-bond isomer and the intermediate.

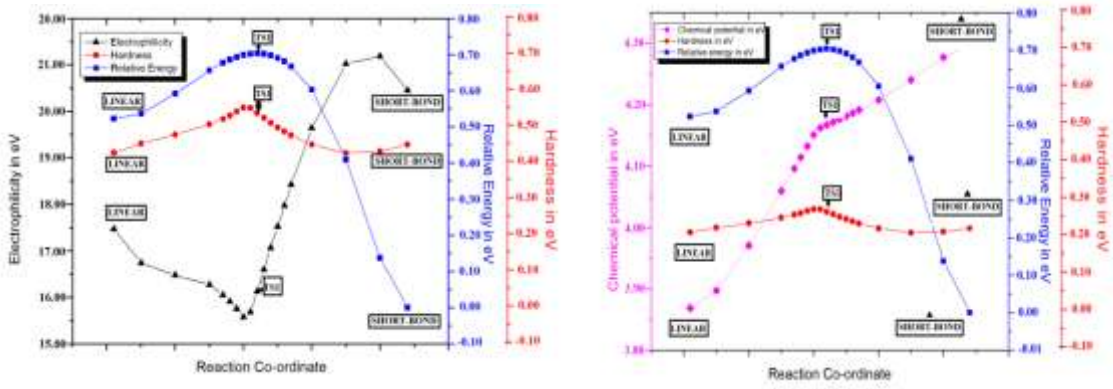

Figure 6.8. Variation of hardness, electrophilicity, relative energy and chemical potential along the isomerization path from linear to short-bond via TS1.

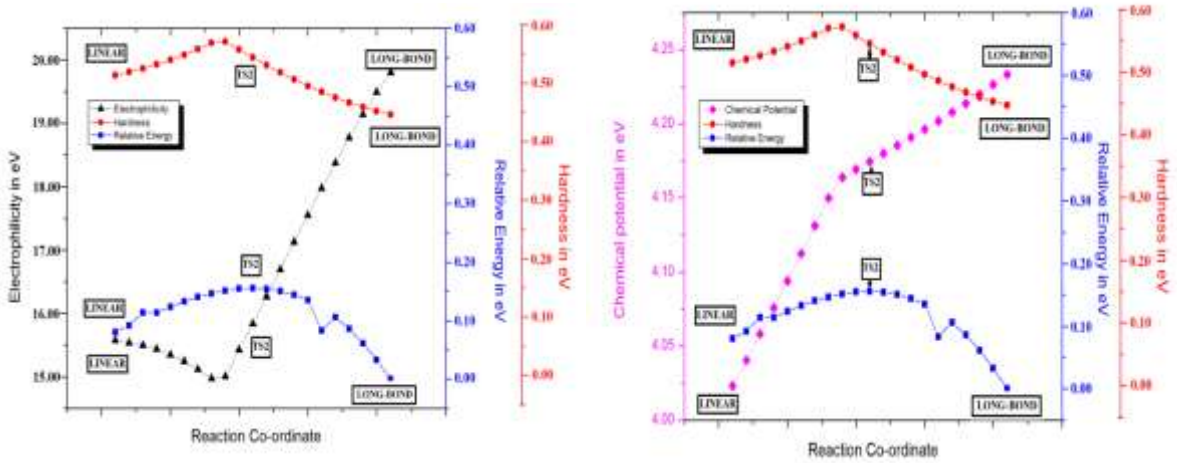

Figure 6.9. Variation of hardness, electrophilicity, relative energy and chemical potential along the isomerization path from linear to long-bond via TS2.

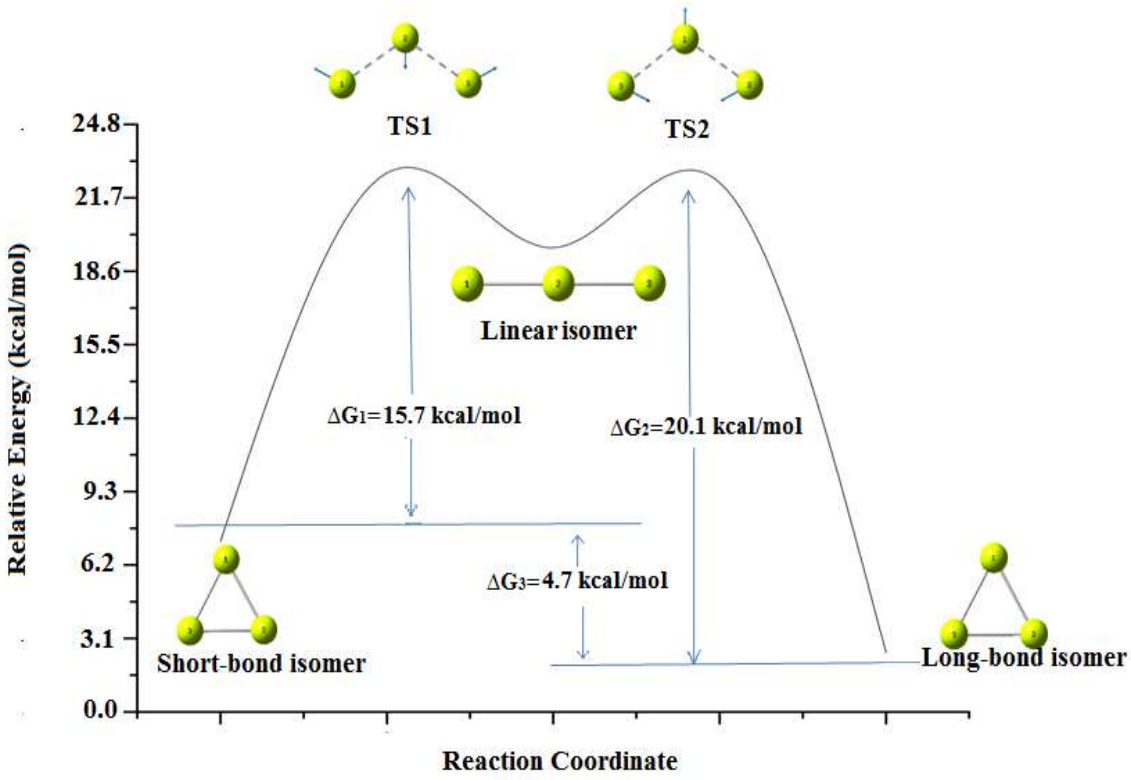

Figure 6.10. Free energy profile showing the path from the short-bond isomer to the intermediate via TS1 and from the intermediate to the long-bond isomer via TS2.

Aromaticity of a molecule is inherently associated with its stability. As Be_3^{2-} is a simple aromatic moiety with 2-electron aromaticity, the aromatic stabilization energies of the two D_{3h} isomers are calculated (Table 6.4) using a recently proposed theoretical model.[55-57]The long-bond isomer has been computed to have a higher ASE as compared to the short-bond isomer thereby correlating to the order of the ground state stability of the respective D_{3h} bond stretch isomers.

Table 6.4. Aromatic Stabilization Energy of the two D_{3h} isomers in kcal/mol.

ASE for short-bond isomer of Be_3^{2-} (kcal/mol)	ASE for long-bond isomer of Be_3^{2-} (kcal/mol)
8.5	9.7

6.4.

CONCLUSIONS

In the present work, comprehension of the inter-conversion between the bond stretch isomers of Be_3^{2-} is unveiled. We illuminate the underlying rationale for the phenomenon of bond stretch isomerism in Be_3^{2-} and suggest that the Renner-Teller effect of the degenerate excited state linear intermediate is the main driving force behind the occurrence of bond stretch isomerism in Be_3^{2-}. The potential energy surfaces connecting different isomers through transition states and conical intersections are elucidated. Simulation based on ADMP method supports the fact of isomerization through the linear intermediate. Hardness and electrophilicity profiles also support the occurrence of Renner-Teller effect in this bond stretch isomerism. Stability ordering of the bond stretch isomers is in consonance with the calculated aromatic stabilization energy.Thus, as a whole this work provides an explanation to the intriguing phenomenon of bond stretch isomerism in Be_3^{2-}.

6.5.

REFERENCES

1. Stohrer, W. D.; Hoffmann, R. *J. Am. Chem. Soc.* **1972**, *94*, 779-786.
2. Stohrer, W. D.; Hoffmann, R. *J. Am. Chem. Soc.***1972**, *94*, 1661-1668.
3. Jean, Y.; Lledos, A.; Burdett, J. K.; Hoffmann, R. *J. Am. Chem. Soc.***1988**, *110*, 4506-4516.
4. Butcher, A. V.; Chatt, J. *J. Chem. Soc. A*, **1970**, *0*, 2652-2656.
5. Goodgame, M. M.; Goddard III, W. A. *Phys. Rev. Lett*. **1985**, *54*, 661.
6. Moskovits, M.; Limm, W.; T. Mejean. *J. Chem. Phys.* **1985**, *82*, 4875.
7. Rohmer, M. M.; Benard, M. *Chem. Soc. Rev.* **2001**, *30*, 340-354.
8. Wieghardt, K.; Backes-Dahmann, G.; Nuber, B.; Weiss, J. *Angew. Chem., Int. Ed. Engl.* **1985**, *24*, 777-778.
9. Parkin, G. *Acc. Chem. Res.* **1992**, *25*, 455-460.
10. Parkin, G. *Chem. Rev.* **1993**, *93*, 887-912.
11. Rohmer, M. M.; Strich, A.; Benard, M.; Malrieu, J. P. *J. Am. Chem. Soc.* **2001**, *123*, 9126-9134.
12. Song, J; Hall, M. B. *Inorg. Chem.* **1991**, *30*, 4433-4437.
13. Comba, P.; Hauser, A.; Kerscher, M.; H. Pritzkow. *Angew. Chem.* **2003**, *42*, 4536-4540.
14. Antol, I.; Eckert-Maksic´, M.; Lischka, H.; Maksic´, Z. B. *Chem. Phys. Chem.* **2004**, *5*, 975-981.
15. Petrov, K. T.; Pinter, B.; Veszpremi, T. *J. Organomet. Chem.* **2012**, *706*, 84-88.
16. Goswami, T.; Paul, S.; Mandal, S.; Misra, A.; Anoop, A.; Chattaraj P. K. *Int. J. Quantum Chem.* **2015**, *115*, 426-433.
17. Chattaraj, P. K.; Roy, D. R.; Elango, M.; Subramanian, V. *J. Phys. Chem. A* **2005**, *109*, 9590-9597.
18. Chattaraj, P. K.; Giri, S. *J. Mol. Struct. (THEOCHEM)* **2008**, *865*, 53-56.
19. Giri, S.; Roy, D. R.; Duley, S.; Chakraborty, A.; Parthasarathi, R.; Elango, M.; Vijayaraj, R.; Subramanian, V.; Islas, R.; Merino, G.; Chattaraj, P. K. *J. Comp. Chem.* **2010**, *31*, 1815-1821.
20. Roy, D. R.; Chattaraj, P. K. *J. Phys. Chem. A* **2008**, *112*, 1612-1621.
21. Brito, B. G. A.; Hai, G. Q.; Candido, L. *Chem. Phys. Lett.* **2013**, *586*, 108-110.
22. Paul, S.; Misra, A. *Inorg. Chem.* 2011, *50*, 3234-3246.
23. Mondal, S.; Chattaraj, P. K. *Chem. Phys. Lett.* **2014**, *593*, 128-131.
24. Jiménez-Halla, J. O. C.; Matito, E.; Blancafort, L.; Robles, J.; Solà, M. *J. Comput. Chem.* **2011**, *32*, 372-373.
25. Di Nicola, F. P.; Lanzi, M.; Marchetti, F.; Pampaloni, G.; Zacchini, S. *Dalton Trans.* **2015**, *44*, 12653-12659.
26. Renner, R. *Z. Phys.* **1934**, *92*, 172-193.
27. Herzberg, G.; Teller, E. *Z. Phys. Chemie B.* **1933**, *21*, 410-446.

28. Herzberg, G. *Molecular Spectra and Molecular Structure* (Reprint Edition, Krieger, Malabar, (1991) Vol. III.
29. GaussView, Version 5, R. Dennington, T. Keith, J. Millam, *Semichem Inc.* Shawnee Mission KS. 2009.
30. Gaussian 09, Revision C.01, Frisch, M. J.; Trucks, G. W.; Schlegel, H. B.; Scuseria, G. E.; Robb, M. A.; Cheeseman, J. R.; Scalmani, G.; Barone, V.; Petersson, G. A.; Nakatsuji, H.; Li, X.; Caricato, M.; Marenich, A. V.; Bloino, J.; Janesko, B. G.; Gomperts, R.; Mennucci, B.; Hratchian, H. P.; Ortiz, J. V.; Izmaylov, A. F.; Sonnenberg, J. L.; Williams-Young, D.; Ding, F.; Lipparini, F.; Egidi, F.; Goings, J.; Peng, B.; Petrone, A.; Henderson, T.; Ranasinghe, D.; Zakrzewski, V. G.; Gao, J.; Rega, N.; Zheng, G.; Liang, W.; Hada, M.; Ehara, M.; Toyota, K.; Fukuda, R.; Hasegawa, J.; Ishida, M.; Nakajima, T.; Honda, Y.; Kitao, O.; Nakai, H.; Vreven, T.; Throssell, K.; Montgomery, J. A., Jr.; Peralta, J. E.; Ogliaro, F.; Bearpark, M. J.; Heyd, J. J.; Brothers, E. N.; Kudin, K. N.; Staroverov, V. N.; Keith, T. A.; Kobayashi, R.; Normand, J.; Raghavachari, K.; Rendell, A. P.; Burant, J. C.; Iyengar, S. S.; Tomasi, J.; Cossi, M.; Millam, J. M.; Klene, M.; Adamo, C.; Cammi, R.; Ochterski, J. W.; Martin, R. L.; Morokuma, K.; Farkas, O.; Foresman, J. B.; Fox, D. J. Gaussian, Inc., Wallingford CT, 2010.
31. McDouall, J. J.; Peasley, K.; Robb, M. A. *Chem. Phys. Lett.*, **1988**, *148*, 183-189.
32. Bernardi, F.; Bottoni, A.; Field, M. J.; Guest, M. F.; Hillier, I. H.; Robb, M. A.; Venturini, A. *J. Am. Chem. Soc.*, **1988**, *110*, 3050-3055.
33. Tonachini, G.; Schlegel, H. B.; Bernardi, F.; Robb, M. A. *J. Am. Chem. Soc.*, **1990**, *112*, 483-491
34. Marx, D.; Hutter, J.; Grotendorst, J. (Ed.), Proceedings of Modern Methods and Algorithms of Quantum Chemistry, John von Neumann Institute for Computing, Jurich, Germany (2000).
35. Schlegel, H. B.; Millam, J. M.; Iyengar, S. S.; Voth, G. A.; Daniels, A. D.; Scuseria, G. E.; Frisch, M. J. *J. Chem. Phys.***2011**, *114*, 9758-9763.
36. Iyengar, S. S.; Schlegel, H. B.; Millam, J. M.; Voth, G. A.; Scuseria, G.E.; Frisch, M. J. *J. Chem. Phys.* **2011**, *115*, 10291-10302.
37. Schlegel, H. B.; Iyengar, S. S.; Li, X.; Millam, J. M.; Voth, G. A.; Scuseria, G. E.; Frisch, M. J. *J. Chem. Phys.* **2002**, *117*, 8694-8704.
38. Pearson, R. G. Recent Advances in the Concept of Hard and Soft Acids and Bases. *J. Chem. Edu.***1987**, *64*, 561-567.
39. Parr, R. G.; Chattaraj, P. K. *J. Am. Chem. Soc.* **1991,** *113*, 1854-1855.
40. Ayers P. W.; Parr, R. G. *J. Am. Chem. Soc.* **2000**, *122*, 2010-2018.
41. Chattaraj, P. K.; Sengupta, S. *J. Phys. Chem.* **1996**, *100*, 16126-16130.
42. Fuentealba, P.; Simon-Manso, Y.; Chattaraj, P. K. *J. Phys. Chem. A* **2000**, *104*, 3185-3187.
43. Pan, S.; Solà, M.; Chattaraj, P. K. *J. Phys. Chem. A* **2013**, *117*, 1843-1852.
44. Saha, R.; Pan, S.; Chattaraj, P. K. *Molecules* **2016**, *21*, 1477-1493.
45. Chamorro, E.; Chattaraj, P. K.; Fuentealba, P. *J. Phys. Chem. A* **2003**, *107*, 7068-7072.
46. Parthasarathi, R.; Elango, M.; Subramanian, V.; Chattaraj, P. K. *Theo. Chem. Acc.* **2005**, *113*, 257-266.

47. Geerlings, P.; De, P. F.; Langenaeker, W. *Chem. Rev*. **2003**, *103*, 1793-1874.
48. Chattaraj, P. K. *J. Indian. Chem. Soc.* **1992**, *69*, 173-183.
49. Parr, R. G.; Donnelly, R. A.; Levy, M.; Palke, W. E. *J. Chem. Phys.***1978**, *68*, 3801.
50. Chattaraj, P. K.; Sarkar, U.; Roy, D. R. *Chem. Rev.* **2006**, *106*, 2065-2091.
51. Chattaraj, P. K.; Roy, D. R. *Chem. Rev.* **2007**, *107*, PR46-PR74.
52. Parr, R. G.; Szentpaly, L. v.; Liu, S. *J. Am. Chem. Soc*.**1999**, *121*, 1922-1924.
53. T. A. Koopmans, *Physica* **1993**, *1*, 104-113.
54. Janak, J. F. *Phys. Rev. B.* **1978**, *18*, 7165.
55. Paul, S.; Goswami, T.; Misra, A. *AIP Advances*, **2015**, *5*, 107211.
56. Goswami, T.; Homray, M.; Paul, S.; Bhattacharya, D.; Misra, A. *Phys. Chem. Chem. Phys.* **2017**, *19*, 11744-11747.
57. Homray, M.; Paul, S.; Misra, A. *Bull Mater Sci.*, **2019**, *42*, 46.
58. Anderson, P.W. *Phys, Rev.* **1950**, *79*, 350.
59. Anderson, P. W. *Phys. Rev.***1959**, *115*, 2.
60. Anderson, P. W. Theory of the magnetic interaction: exchange in insulators and superconductors .In solid state physics; Turnbull, F., Seitz, F., Eds.; Academic Press: New York, **1963**; Vol. 14, p 99.
61. Paul, S.; Misra, A. *J. Chem. Theory Comput*. **2012**, *8*,843-853.
62. Lu, T.; Chen, F. *J. Comp. Chem.* **2012**, *33*, 580-592.
63. The DFT code, OPENMX, is available at http://www.openmx-square.org under the GNU General Public License.
64. Dewar, M. J. S.; Healy, E. F.; Stewart, J. J. P. *J. Chem. Soc*., *Faraday Trans. 2***, 1984**, *80*, 227-233.
65. Walsh, A. D. *J. Chem. Soc.* **1953,** *0*, 2260-2266.
66. Peric, M.; Engles, E.; Peyerimhoff, S. D. *In Quantum Mechanical Electronic Structure Calculations with Chemical Accuracy*; Langhoff, S. R., Ed., Kluwer: Dordrecht, 1995, p 261.
67. Kar, T.; Scheiner, S. *J. Phys. Chem.***1995**, *99*, 8121-8124.
68. Torrent-Sucarrat, M.; Blancafort, L.; Duran, M.; Luis, J.; Solà, M. *In Theoretical Aspects of Chemical Reactivity;* Toro-Labbe, A., Ed. Elsevier: Amsterdam, 2007.
69. Torrent-Sucarrat, M.; Luis, J. M.; Duran, M.; Solà, M. *J. Chem. Phys.* **2002**, *117*, 10561.
70. Chattaraj, P. K.; Pérez, P.; Zevallos, J.; Toro-Labbé, A. *J. Phys. Chem. A* **2001**, *105*, 4272-4283.

CHAPTER 7

Theoretical elucidation of methylation of cytosine and its subsequent oxidation processes

7.1.

INTRODUCTION

Every multicellular organism includes the DNA which is a significant functional molecule that has evolved to programme and pass on information through generations. DNA consists of the four nucleobases adenine (A), cytosine (C), guanine (G) and thymine (T), which is stored within as the primary code and it is the linear sequential arrangement of these four canonical bases that makes up the genetic code. The first modification of a canonical nucleobase to be discovered was the 5-methylcytosine (5mC).[1] More than 17 modified DNA bases have been reported[2] since the discovery of 5mC in the year 1898. The Watson–Crick pairing is not hindered by the introduction of these characteristic modifications but rather introduces chemical functionality into the major groove of the double helix structure. This additional functionality in the major groove will definitely change or block protein recognition which can be effectively applied in bacterial warfare. In bacterial warfare, methylation of specific sequence sites in the host genome, described as restriction methylation, safeguards self-cleavage by special nucleases. Cytosine methylation is an extensively studied DNA modification. Johnson and Coghill confirmed its existence in the year 1925, recognizing it as a hydrolysis product of tuberculinic acid.[3] Mammalian DNA methylation (5mC) is ascertained by de novo DNA methyltransferases DNMT3A/3B, and the patterns of 5mC are maintained by DNMT1. In mammals, DNA methylation is concerned with the preservation of cellular functions and genomic stability, as well as is involved in procedures of X-chromosome inactivation, genomic imprinting and transposon silencing.[4–7] The active demethylation pathway probably involves the iterative oxidation of 5-methylcytosine (5mC) to5-(hydroxymethyl)cytosine (5hmC), 5-formylcytosine(5fC) and 5-carboxycytosine (5caC) by the ten-eleven translocation (TET) enzymes (namely, TET1, TET2 and TET3), which are 2-oxoglutarate (2-OG)- and Fe(II)-dependent dioxygenases (Scheme 7.1).

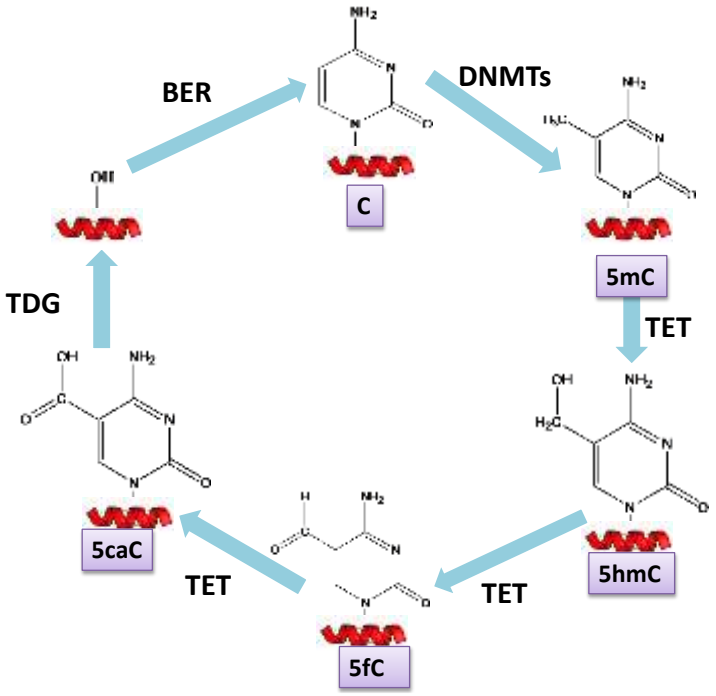

Scheme 7.1. DNA methylation (5mC) is established by de novo DNA methyltransferases DNMT3A/3B, and the patterns of 5mC are sustained by DNMT1. TET enzymes successively oxidize 5mC to 5hmC, 5fC, and 5caC.

Cytosine (C)

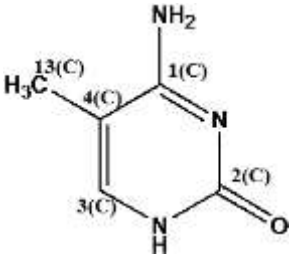

5-methylcytosine (5mC)

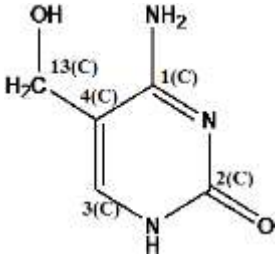

5-(hydroxymethyl)cytosine (5hmC)

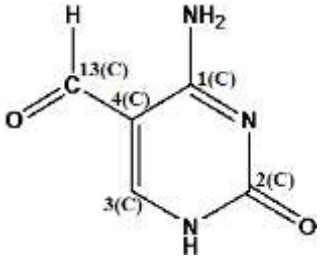

5-formylcytosine (5fC)

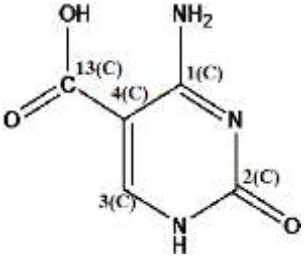

5-carboxycytosine (5caC)

Figure 7.1. The structure and schematic representation of cytosine molecule and its derivatives. The numbering of Carbons are according to their fukui function calculations.

The chemical and physical properties of modified DNA bases differ substantially despite the similarity in the chemical structure of their unmodified counterpart. It is clear that base modifications cause changes in the reactivity, structure and base-pairing interactions of DNA. DNA base modifications also influence DNA metabolism and DNA repair. Consequently, the understanding of chemical and physical properties of modified molecules becomes extremely important to decipher the role of modified bases in biological events. However, studies towards understanding the chemical and physical properties of modified bases are limited in literature. In past few decades the density functional theory (DFT) has successfully been used as a general tool to investigate the structure and properties of atoms and molecules. Employing this theory, the properties of a many-electron system can be determined by the suitable use of proper functionals, i.e., functions of another function, which is the spatially dependent electron density. DFT is one of the most accepted and resourceful methods available in computational chemistry. However, the popularity of DFT emerged when the approximations used in the theory were greatly sophisticated to better model the exchange and correlation interactions. Computational costs are relatively low when compared to conventional methods, such as exchange only Hartree–Fock theory and its descendants that include electron correlation. Several qualitative and semiquantitative methods have since been developed for predicting how and whether a reaction will take place. The most popular method of prediction is frontier molecular orbital theory (FMO) which uses the shapes and symmetries of the highest occupied molecular orbital (HOMO) and the lowest unoccupied molecular orbital (LUMO) to assign whether a reaction will take place or not. If the HOMO of the electron donor and the LUMO of the electron acceptor have similar shape and phase, then electron transfer from the HOMO of the first molecule to the LUMO of the second is facilitated, often forming a bond between them. One of the most significant qualities of the density functional theory is its appropriateness for elucidating vital chemical concepts of molecular structure and reactivity. In the late 1970s and early 1980s Parr developed the "conceptual DFT"[8] which is a subfield of DFT where information is obtained from the electron density relevant concepts and principles thus making it possible to comprehend and predict the chemical behaviour of a molecule. Parr and co-workers, along with a large community of theoretical chemists, have been able to give precise definitions for chemical concepts, thus providing their calculations with a quantitative value. Recently, conceptual DFT has been successfully employed as a powerful predictive tool in understanding the structure, property and reactivity of DNA bases and their assemblies.[9,10]

Herein, the most relevant indices defined within the conceptual for the study of the organic reactivity of cytosine and its modifications are discussed.

So, here we try to monitor the processes of cytosine modifications using conceptual Density Functional Theory (DFT) based study to compute quantum chemical parameters such as highest occupied molecular orbital (HOMO), lowest unoccupied molecular orbital (LUMO), electrophilicity, electronegativity, chemical potential, chemical hardness, and nucleophilicity which give considerable insight towards defining reactivity of the cytosine modifications. The conceptual DFT based global reactivity and the local reactivity descriptors are constructive measures of comprehending the global reactivity and the local site selectivity, respectively. In this study, we have computed the global reactivity descriptors for the four cytosine modifications: 5-methylcytosine, 5(hydroxylmethyl) cytosine, 5-formylcytosine and 5-carboxylcytosine (Figure 7.1) and compared it with the unmodified cytosine and also the ability of these descriptors to predict the electrophilic attack on cytosine to produce the 5mC. The subsequent oxidation from 5mC to 5hmC, 5fC, and 5caC is explained with the help of these global and local reactivity parameters. In addition to this, we also quantify the aromaticity of the rings in all these compounds and correlate it with the stability of these molecules.

6.2.

COMPUTATIONAL DETAILS

Conceptual density functional theory based methods are widely used to predict reactivity of molecules. In this study, the inputs of studied molecules are prepared with Gauss View.[11] Calculations are performed by using Gaussian 16,[12] at b3lyp level and cam-b3lyp level of theory. The results obtained from cam-b3lyp are used for discussion in this manuscript because it includes the Handy and coworkers long-range-corrected version of b3lyp via the Coulomb-attenuating method[13] which gives better insight into the conceptual DFT results. The Chemical reactivity descriptors include E_{HOMO}, E_{LUMO}, ΔE (HOMO–LUMO energy gap), electronegativity (χ), chemical potential (μ), chemical hardness (η), electrophilicity (ω), nucleophilicity (ε) and global softness (σ). Electronegativity, global softness, and chemical hardness have pertained to ionization energy (I) and electron affinity (A) values of molecules obtaining the following equations. It is well

established that the negative value of the highest occupied molecular orbital energy and the negative value of the lowest unoccupied molecular orbital energy were attached to the ionization energy and electron affinity, respectively ($-E_{HOMO} = I$ and $-E_{LUMO} = A$). The electronegativity (χ),[14-16] hardness (η)[17,18] and electrophilicity (ω)[19] of an N-electron system can be defined as follows,

$$\chi = -\mu = -\left(\frac{\partial E}{\partial N}\right)_{\upsilon(\vec{r})} \tag{7.1}$$

$$\eta = \left(\frac{\partial^2 E}{\partial N^2}\right)_{\upsilon(\vec{r})} \tag{7.2}$$

$$\omega = \frac{\mu^2}{2\eta} = \frac{\chi^2}{2\eta} \tag{7.3}$$

where E, μ, and $v(\vec{r})$ are the total energy of the N-electron system, chemical potential and external potential respectively.

Employing a finite difference approximation to Eqs.1 and 2 one can achieve

$$\chi = \frac{I + A}{2} \tag{7.4}$$

and

$$\eta = I - A \tag{7.5}$$

where I and A indicate the ionization potential and electron affinity of the cluster respectively, and they are calculated using Koopmans' theorem.[20,21]

The Fukui functions are employed to describe local electrophilicity and nucleophilicity factors. Removal of an electron from the molecule, called the Fukui function for electrophilic attack, is described as f^- and the Fukui function for *addition* of an electron to the molecule, called the Fukui function for nucleophilic attack is denoted as f^+. The understanding of the quantitative values of the Fukui function is that a large value of f^-, signifies that a molecule *donates* electrons, whereas a larger value of f^+ denotes where a

molecule *accepts* electrons. The Fukui functions can be defined using finite differences of the electronic density

$$f^{-}=\rho(N)-\rho(N-1) \tag{7.6}$$

$$f^{+}=\rho(N+1)-\rho(N) \tag{7.7}$$

where the densities of the cation ($N-1$), the neutral (N), and the anion ($N+1$) are employed. Here, chemical reactivity is described on an atom-by-atom basis via a "condensed" Fukui function. The condensed Fukui function is computed as

$$f_k^{-}=q_k(N)-q_k(N-1) \tag{7.8}$$

$$f_k^{+}=q_k(N+1)-q_k(N) \tag{7.9}$$

where q_k is the charge at atomic center k.[22-25] Here Hirschfeld charges are used in Multiwfn[27] software.

7.3.

RESULTS AND DISCUSSION

The quantum chemical parameters such as the HOMO, LUMO, hardness, electronegativity, nucleophilicity, softness, HOMO-LUMO gap and chemical potential of the nucleobase cytosine and its derivatives such as 5-methylcytosine, 5(hydroxylmethyl) cytosine, 5-formylcytosine and 5-carboxylcytosine are calculated and compared using the conceptual DFT based approach (Table 7.1 and Table 7.2).

Table 7.1. Global reactivity descriptors of derivatives of cytosine in ucam-b3lyp /6-311++g(d,p) methodology.

Molecule	HOMO Energy (eV)	LUMO Energy (eV)	HOMO-LUMO gap(eV)	Hardness (eV)	Softness (eV.)	Electrophilicity (eV)	Nucleophilicity (eV)
5-methylcytosine (5mC)	–0.287	–0.001	7.808	7.808	0.128	0.983	1.017
5-(hydroxylmethyl)cytosine (5hmC)	–0.293	–0.003	7.882	7.881	0.126	1.027	0.973
5-formylcytosine (5fC)	–0.315	–0.042	7.455	7.455	0.134	1.582	0.632
5-carboxylcytosine (5caC)	–0.319	–0.039	7.641	7.641	0.130	1.562	0.640

Table 7.2. Global reactivity descriptors of nucleobase cytosine and its derivatives in ub3lyp/6-311++g(d,p) methodology.

Molecule	HOMO Energy (eV)	LUMO Energy (eV)	HOMO-LUMO gap (eV)	Softness (eV.)	Electrophilicity (eV)	Nucleophilicity (eV)
5-methylcytosine	–0.234	–0.046	5.117	0.195	1.423	0.702
5-(hydroxylmethyl)cytosine	–0.239	–0.050	5.137	0.194	1. 510	0.662
5-formylcytosine	–0.263	–0.090	4.710	0.212	2.460	0.406
5-carboxylcytosine	–0.262	–0.082	4.881	0.205	2.249	0.445
cytosine	–0.242	–0.048	5.285	5.284	1.479	0.676

7.3.1 Condensed fukui functions employed to explain the methylation of cytosine

From the electrophilicity value we can say that the nucleobase cytosine is highly electrophilic which is apparent from the electrophilicity value of 1.479 eV, so is prone towards electrophilic addition to form 5-methyl cytosine. The highest electrophilic site of cytosine is at the 4-C centre as is described by the f^- value (0.142451), (Table 7.3) so the electrophilic attack occurs at the 4-C position to form 5-methyl cytosine. The numbering of the Carbon sites are given in Figure 7.1. Thus, the DNA modification involving the

methylation of the cytosine centre to form 5-methyl cytosine at the 4-C position can be theoretically ascertained from the conceptual DFT based electrophilicity value.

Table 7.3. Condensed fukui functions for cytosine

Atoms	f^-	f^+
1C	0.090071	-0.09007
2C	0.038033	-0.03803
3C	0.04374	-0.04374
4C	0.142451	-0.14245
5H	0.049219	-0.04922
6H	0.053832	-0.05383
7N	-0.00208	0.00208
8H	0.013769	-0.01377
9H	0.005771	-0.00577
10N	0.146118	-0.14612
11N	0.113676	-0.11368
12O	0.247402	-0.2474
13H	0.057552	-0.05755

The global reactivity descriptors for the four cytosine modifications: 5-methylcytosine, 5(hydroxylmethyl)cytosine, 5-formylcytosine and 5-carboxylcytosine are also calculated and is used to explain the subsequent oxidation from 5mC to 5hmC to 5fC to 5caC. The comparative study is described in detail in the following paragraphs. The condensed fukui functions for the cytosine modifications are used to describe the local reactivity factors such as electrophilicity and nucleophilicity describing the oxidation process in the subsection below and the condensed fukui values for 5mC, 5hmC, 5fC and 5caC are given in Table 7.4, 7.5, 7.6 and 7.7 respectively.

Table 7.4. Condensed fukui functions for 5mC

Atoms	f^-	f^+
1C	0.075667	-0.07567
2C	0.049557	-0.04956
3C	0.026808	-0.02681
4C	0.119714	-0.11971
5H	0.042504	-0.0425
6H	0.047027	-0.04703
7N	0.041219	-0.04122
8H	0.026466	-0.02647
9H	0.032453	-0.03245
10N	0.09116	-0.09116
11N	0.09006	-0.09006
120	0.220735	-0.22074
13C	0.029629	-0.02963
14H	0.039748	-0.03975
15H	0.039718	-0.03972
16H	0.02727	-0.02727

Table 7.5. Condensed fukui functions for 5hmC

Atoms	f^-	f^+
1C	0.0866	-0.0866
2C	0.041203	-0.0412
3C	0.039291	-0.03929
4C	0.115557	-0.11556
5H	0.038565	-0.03857
6H	0.054213	-0.05421
7N	0.004223	-0.00422
8H	0.022313	-0.02231
9H	0.011895	-0.0119
10N	0.134653	-0.13465
11N	0.110706	-0.11071
12O	0.236262	-0.23626
13C	0.024515	-0.02452
14O	0.029134	-0.02913
15H	0.032423	-0.03242
16H	-0.00263	0.002628
17H	0.029253	-0.02925

Table 7.6. Condensed fukui functions for 5fmC

Atoms	f^-	f^+
1C	0.062529	-0.06253
2C	0.030542	-0.03054
3C	0.032086	-0.03209
4C	0.115754	-0.11575
5H	0.03659	-0.03659
6H	0.047198	-0.0472
7N	-0.00409	0.004095
8H	0.019013	-0.01901
9H	0.003749	-0.00375
10N	0.13975	-0.13975
11N	0.100452	-0.10045
120	0.223286	-0.22329
13C	0.039735	-0.03974
14O	0.104238	-0.10424
15H	0.048661	-0.04866

Table 7.7. Condensed fukui functions for 5caC

Atoms	f^-	f^+
1C	0.054344	-0.05434
2C	0.028213	-0.02821
3C	0.028391	-0.02839
4C	0.058567	-0.05857
5H	-0.56288	0.56288
6H	0.042599	-0.0426
7N	0.087213	-0.08721
8H	0.051076	-0.05108
9H	0.02216	-0.02216
10N	-0.68013	0.68013
11N	0.084189	-0.08419
12O	0.172475	-0.17248
13C	0.028692	-0.02869
140	0.043475	-0.04348
15H	0.008592	-0.00859
16O	0.124051	-0.12405

7.3.2 FMO Study

The frontier molecular orbital study can predict the reactivity of the nucleobase cytosine and its derivatives and thus can serve as an important predictive tool for the iterative oxidation process of 5mC to 5hmC, 5fC, and 5caC. The energy of HOMO is related to the electron donating ability of the molecules. The molecules possessing higher HOMO energy show the tendency to donate the electrons to appropriate acceptor molecules. Oxidation involves loss of electrons from the HOMO, so higher the energy of HOMO, greater will be the tendency for oxidation. If we compare the HOMO energy of cytosine and its derivatives, the order followed is 5caC<5fC<5hmC<5mC. So, from the order of HOMO energy, we can predict that 5mC has a greater tendency to be oxidised to 5hmC and subsequently to 5fC and then to 5caC. Similarly energy levels of LUMO can predict electron accepting abilities following the trend 5fC<5caC<5hmC<5mC. So the trend for subsequent oxidation process is similar with slight mismatch in 5fC and 5caC. The HOMO-LUMO energy gap can be considered as a direct indicator of stability. The trend followed by cytosine and its derivatives is 5fC<5caC<5mC<5hmC. 5hmC is relatively abundant amongst the other oxidised derivatives and this is evident from the higher HOMO-LUMO gap of the 5hmC (Table 7.1).

7.3.3 Chemical hardness and softness

Chemical hardness is described as the measure of the resistance of a chemical species to changes in its inherent electronic configuration. Thus, hardness serves as an indicator of reactivity and stability of molecules. If we compare the hardness profile, the order of increasing hardness is 5fC<5caC<5mC<5hmC. The hardness value of 5hmC is highest. This theoretical interpretation is further strengthened by the experimental observations where employing the methylation-insensitive restriction enzyme MspI and a TLC assay, Tahiliani et al. (2009) reported that the 5hmC level in mouse ES cells is ;0.03% of total nucleotides. Utilising a two-dimensional (2D) TLC method and nearest- neighbor analysis, Kriaucionis and Heintz (2009) accounted 5hmC level of 0.6% and 0.2% of total nucleotides in Purkinje and granule neurons, respectively. Thus, these experimental results further validate the abundance of 5hmC as compared to the other oxidized products, as is predicted by its highest hardness value amongst the other substituents. Thus, the hardness profile is in consonance

with its experimental abundance. Softness is defined as the reciprocal of hardness. So, the trend followed by cytosine derivatives is just the opposite to the trend followed by chemical hardness i.e., 5hmC<5mC<5caC<5fC.

7.3.4 Electrophilicity and Nucleophilicity

Electrophilicity predicts the attraction of a molecule towards electron rich centres; from the electrophilicity values we can predict the tendency of a molecule towards electrophilic substitution reactions. On the other hand, nucleophilicity values give us an idea regarding the attraction of a molecule towards electron deficient centres thereby predicting whether the molecule is prone towards nucleophilic substitution or not. The trend of global electrophilicity followed by cytosine derivatives is 5mC<5hmC<5caC<5fC and that of nucleophilicity is 5fC<5caC<5hmC<5mC which is just the opposite of the trend followed by the electrophilicity values as expected. The local electrophilicity and nucleophilicity values for each atom centres for the individual cytosine derivatives are calculated based on condensed fukui functions and are given in Table 7.4, 7.5, 7.6 and 7.7.

7.3.5 Aromaticity

Nucleobases are non- polar and due to their aromaticity, planar. The flat shape due to the virtue of aromaticity is of particularly important when considering their roles as building blocks of DNA. Cytosine and its derivatives are aromatic molecules comprising one aromatic ring. With respect to the electronic nature of the molecule, aromaticity portrays a conjugated system comprising of alternating single and double bonds in a ring. This arrangement permits pi electron delocalization around the ring, thereby increasing the molecule's stability by resonance. Thus, aromaticity can be directly linked to the inherent stability of the molecules. Aromaticity is quantified here with the help of Nucleus Independent Chemical Shifts (NICS) which was postulated by Schleyer and his co-workers.[28] The negative value of the absolute magnetic shielding provides the definition of NICS. The NICS values are computed by placing the ghost atom at the centre of the ring [NICS(0)] to account for the contribution of the σ-electrons to aromaticity and 1 Å above and below the plane i.e., [NICS (1)] and [NICS(-1)] respectively to estimate the π-aromaticity of the systems. In harmony with NMR chemical shift principle, the NICS values are reported with negative signs. Positive NICS value signifies a paratropic magnetic field corresponding to antiaromatic systems whereas a negative NICS value signifies a diatropic magnetic field which correlates to aromatic systems. The NICS values for cytosine and its derivatives are given in Table 7.8. As

aromaticity is an indicator of stability higher the aromaticity, greater will be its stability. So, the trend followed by both σ and π aromaticity for the cytosine derivatives are similar to the trend followed by hardness, i.e., 5fC<5caC<5mC<5hmC. So, 5hmC has already been established as the most stable molecule among the cytosine derivatives from its hardness value owing to its higher abundance from experimental observations. From quantitative evaluation of aromaticity also, it is observed that it has a higher NICS value thereby is in harmony with its higher stability as was predicted from the hardness profile.

Table 7.8. The nucleus-independent chemical shift (NICS) values in ppm at the plane of the ring (NICS (0)) and at 1 Å above the plane of the ring (NICS (1)) in cam-b3lyp methodologies using 6-311++g(d,p) basis set.

Molecule	**NICS(0)**	**NICS(1)**	**NICS(–1)**
Cytosine	0.7346	2.5725	2.5734
5Mc	1.2683	2.8656	2.8601
5hmC	1.3124	2.8414	3.0726
5f	0.6990	2.6796	2.6775
5caC	0.9457	2.6726	2.5231

7.4.

CONCLUSIONS

The conceptual DFT based global and local reactivity parameters serve as an important chemical intuitive and predictive tool to elucidate the process of DNA modification i.e., the methylation of cytosine and its subsequent oxidation. Cytosine is one of the most essential DNA nucleobases which makes up the genetic code and its methylation is one of the widely studied DNA modifications. The following successive active demethylation pathway involving the iterative oxidation of 5-methylcytosine (5mC) to5-(hydroxymethyl)cytosine (5hmC), 5-formylcytosine(5fC) and 5-carboxycytosine (5caC) is explained with the constructive methods of conceptual DFT based approach such as frontier molecular orbital study, chemical hardness and softness, local reactivity descriptors such as electrophilicity and

nucleophilicity which provide considerable insight into the reaction pathway. Aromaticity descriptor NICS also offers a significant understanding of the stability of cytosine and its derivatives as stability is intricately related to chemical reactivity.

7.5.

REFERENCES

1. Ruppel, W. G. *Z. Physiol. Chem.* **1899**, *26*, 218–232.
2. Gommers-Ampt, J. H.; Borst, P. *FASEB J.* **1995**, *9*, 1034–1042.
3. Johnson, T. B.; Coghill, R. D. *J. Am. Chem. Soc.***1925**, *47*, 2838–2844.
4. Wyatt, G. R. *Nature* **1950**, *166*, 237–238.
5. Bird, A. *Genes Dev.* **2002**, *16*, 6–21.
6. Deaton, A.; Bird, A. *Genes Dev.* **2011**, *25*, 1010–1022.
7. Jones, P. A. *Nat. Rev. Genet.* **2012**, *13*, 484–492.
8. Kohn, W.; Sham, L. J. Phys. Rev. B **1965**, *140*, A1133–A1138.
9. Varsano, D.; Di Felice, R.; Marques, M. A. L.; Rubio, A. *J. Phys. Chem. B* **2006**, *110*, 7129-7138.
10. Dkhissi, A.; Blossey, R. *J. Phys. Chem. B* 2008, 112, 9182–918.
11. GaussView, Version 5, R. Dennington, T. Keith, J. Millam, *Semichem Inc.* Shawnee Mission KS. 2009.
12. Gaussian 09, Revision C.01, Frisch, M. J.; Trucks, G. W.; Schlegel, H. B.; Scuseria, G. E.; Robb, M. A.; Cheeseman, J. R.; Scalmani, G.; Barone, V.; Petersson, G. A.; Nakatsuji, H.; Li, X.; Caricato, M.; Marenich, A. V.; Bloino, J.; Janesko, B. G.; Gomperts, R.; Mennucci, B.; Hratchian, H. P.; Ortiz, J. V.; Izmaylov, A. F.; Sonnenberg, J. L.; Williams-Young, D.; Ding, F.; Lipparini, F.; Egidi, F.; Goings, J.; Peng, B.; Petrone, A.; Henderson, T.; Ranasinghe, D.; Zakrzewski, V. G.; Gao, J.; Rega, N.; Zheng, G.; Liang, W.; Hada, M.; Ehara, M.; Toyota, K.; Fukuda, R.; Hasegawa, J.; Ishida, M.; Nakajima, T.; Honda, Y.; Kitao, O.; Nakai, H.; Vreven, T.; Throssell, K.; Montgomery, J. A., Jr.; Peralta, J. E.; Ogliaro, F.; Bearpark, M. J.; Heyd, J. J.; Brothers, E. N.; Kudin, K. N.; Staroverov, V. N.; Keith, T. A.; Kobayashi, R.; Normand, J.; Raghavachari, K.; Rendell, A. P.; Burant, J. C.; Iyengar, S. S.; Tomasi, J.; Cossi, M.; Millam, J. M.; Klene, M.; Adamo, C.; Cammi, R.; Ochterski, J. W.; Martin, R. L.; Morokuma, K.; Farkas, O.; Foresman, J. B.; Fox, D. J. Gaussian, Inc., Wallingford CT, 2010.
13. Yanai,T.;Tew, D.P.; Handy, N.C. *ChemPhysLett* **2004**, *393*, 51-57.
14. Geerlings, P.; De, P. F.; Langenaeker, W. *Chem. Rev.* **2003**, *103*, 1793-1874.
15. Chattaraj, P. K. *J. Indian. Chem. Soc.* **1992**, *69*, 173-183.
16. Parr, R. G.; Donnelly, R. A.; Levy, M.; Palke, W. E. *J. Chem. Phys.***1978**, *68*, 3801.

17. Chattaraj, P. K.; Sarkar, U.; Roy, D. R. *Chem. Rev.* **2006**,*106*, 2065-2091.
18. Chattaraj, P. K.; Roy, D. R. *Chem. Rev.* **2007**, *107*, PR46-PR74.
19. Parr, R. G.; Szentpaly, L. v.; Liu, S. *J. Am. Chem. Soc.***1999**, *121*, 1922-1924.
20. Koopmans, T. A. *Physica* **1993**, *1*, 104-113.
21. Janak, J. F. *Phys. Rev. B.* **1978**, *18*, 7165.
22. Roy, R. K.; Pal, S.; Hirao, K.*J. Chem. Phys*. **1999**, *110*, 8236
23. Roy, R. K.; Pal, S.; Hirao, K. *J. Chem. Phys*. **2000**, *113*,1372
24. Ayers, P.W.; Morrisson, R.C.; Roy, R. K. *J. Chem. Phys*. **2002**, 116, 8731.
25. Hocquet, A.; Toro-Labbé, A.; Chermette, H. *J.Mol Struc(THEOCHEM)* **2004**, 686, 213-218.
26. Melin, J.; Aparicio, F.; Subramanian, V.; Galván, M.; Chattaraj, P.K. *J.Phys. Chem. A* **2008**, *108*, 2487-2491.
27. Lu, T.; Chen, F. *J. Comp. Chem.* **2012**, *33*, 580-592.
28. Schleyer, P. v. R.;Maerke, C.; Dransfeld, A.; Jiao, H.; Hommes, N. J. R. v. E. *J. Am. Chem. Soc.*, 1996, *118*, 6317.

CHAPTER 8

Conclusions

This final chapter presents a comprehensive and a general conclusion of all the previous chapters. In the first chapter, a brief introduction to the origin and the chronological advancements of the concept of aromaticity through the course of history is extensively presented. The development of the theory of aromaticity and the advent of the synthesis of novel materials is discussed. A short summary of the different criteria for defining aromaticity based on energetic, magnetic and structural properties are described and the problem of unambiguously defining the concept of aromaticity is addressed. The concept of exo-cyclic aromaticity is introduced and how it has been an essential tool in stabilizing novel small ringed aromatic molecules is explored. Finally, the origin and development of the all-metal aromatic clusters are elaborated and the phenomenon of bond stretch isomerism that exists on a particular three membered all-metal aromatic cluster is analysed.

The second chapter provides an intricate detail of the different theoretical backgrounds that have been employed in defining aromaticity in this thesis. The quantification of aromaticity based on the chemical behavior, structural pattern, energetic and magnetic criteria is elaborately discussed. Aromaticity being a multidimensional phenomenon, the different indices of aromaticty that are utilized in this thesis to quantify aromaticity have been explained in detail. Since theoretical study of novel aromatic systems is the main objective of this thesis, so various theoretical indices that are employed in this thesis that could indicate the structural integrity of the proposed molecular systems are thoroughly elucidated. Finally, the theoretical background behind the popular global reactivity descriptors such as hardness, electrophilicity and electronegativity which give us an idea regarding the stability of molecular systems is explicitly discussed.

The third chapter offers a mini review of defining the concept of aromaticity in the light of magnetic criteria. Aromaticity is now no longer confined to the domain of organic chemistry and various inorganic clusters are found to be aromatic considering the delocalization of the electrons as the genesis of aromaticity. The ease with which aromaticity bridges the gap between traditional aspects of organic chemistry and latest discoveries in inorganic chemistry are truly fascinating. Aromaticity is not a physically observable quantity so defining it precisely is still a challenge. Quantification of aromaticity is a major challenge to the theoretical and the computational chemists till date. Whether aromaticity is a multidimensional phenomenon or it can be defined by a universal criterion is a debatable

topic. The journey of aromaticity from Kekulés definition of benzene has been extensive and the recent developments in this field provide a considerable better insight into the concept. It is aptly said by Schleyer that, "aromaticity has been a time-dependent phenomenon." The perception of aromaticity is different in terms of its properties and characteristics to chemists with diverse backgrounds. The magnetic criterion for defining the concept of aromaticity has become very prominent surpassing the other criteria. Various developments in this field have occurred in the recent years and most of the developments were in the magnetic domain. So we can conclude by saying that the magnetic criterion is the most important criterion and provides a plethora of opportunities of future work on aromaticity.

The concept of exo-cyclic aromaticity in a novel aromatic moleulule is introduced in chapter four. Aromatic cross-conjugated systems make it apparent that aromaticity must not be restricted only to the completely conjugated cyclic circuits. This inspires us to study a four membered heteroatomic cyclic $C_2B_2F_4$ molecule with D_{2h} symmetry which stretches the boundary of the concept of aromaticity by incorporating the idea of exo-cyclic aromaticity in the fourth chapter. In essence, the molecule $C_2B_2F_4$ acquires aromaticity due to unusual participation of exo-cyclic atoms. Back donation of 4 π-electrons from peripheral fluorine atoms to the electron-deficient boron atoms helps the ring to gain the magic number of 6 π-electrons leading to a unique exo-cyclic aromaticity. Moreover, the existence of molecule with similar C_2B_2 core makes us optimistic about the experimental realization of the molecule in near future.

The observation of unique aromaticity obtained through back donation of 4 π-electrons from substituent exo-cyclic flourine atoms to the vacant p_z orbitals of the boron atoms is further studied on proposed novel three-membered heterocyclic planar systems which are an interesting addition to the domain of aromaticity is studied in chapter five. Rigorous computational study involving DFT and *ab initio* calculations along with Energy Decomposition Analysis (EDA), the evaluation of Ring Strain Energy and HOMO-LUMO gap indicate towards the viability of the systems. The aromaticity of the molecule is evaluated through some standard criteria, specifically Nucleus Independent Chemical Shift (NICS) and Multi Centre bond Index (MCI). The dissected NICS analysis (CMO-NICS) presents a clear picture of the molecular orbitals contributing towards σ and π aromaticity respectively. A coherent picture of the exo-cyclic nature of the aromatic π-cloud is viewed with the AdNDP analysis. The Aromatic Stabilization Energy (ASE) based on a fully *ab initio* approach is also reported which renders the proposed heterocyclic molecules to be

remarkable 6 π-aromatic systems where the *magic number* is attained through an 'exo-cyclic' conjugation. These proposed molecules are unique and distinctive due to the presence of both the σ and the π aromaticity and the antagonistic relationship existing between them makes the systems a remarkable addition to the class of aromatic molecules and provide a significant scope of future study. The high stability of the molecular systems as apparent from the various computational analysis makes us hopeful regarding the investigational reality of these molecules.

Comprehension of the inter-conversion between the bond stretch isomers of an all-metal aromatic Be_3^{2-} is unveiled in the sixth chapter. We illuminate the underlying rationale for the phenomenon of bond stretch isomerism in Be_3^{2-} and suggest that the Renner-Teller effect of the degenerate excited state linear intermediate is the main driving force behind the occurrence of bond stretch isomerism in Be_3^{2-}. The potential energy surfaces connecting different isomers through transition states and conical intersections are elucidated. Simulation based on ADMP method supports the fact of isomerization through the linear intermediate. Hardness and electrophilicity profiles also support the occurrence of Renner-Teller effect in this bond stretch isomerism. Stability ordering of the bond stretch isomers is in consonance with the calculated aromatic stabilization energy. Thus, as a whole this work provides an explanation to the intriguing phenomenon of bond stretch isomerism in Be_3^{2-}.

In the 7th chapter, the conceptual DFT based global and local reactivity parameters serve as an important chemical intuitive and predictive tool to elucidate the process of DNA modification i.e., the methylation of cytosine and its subsequent oxidation. Cytosine is one of the most essential DNA nucleobases which makes up the genetic code and its methylation is one of the widely studied DNA modifications. The following successive active demethylation pathway involving the iterative oxidation of 5-methylcytosine (5mC) to5-(hydroxymethyl)cytosine (5hmC), 5-formylcytosine(5fC) and 5-carboxycytosine (5caC) is explained with the constructive methods of conceptual DFT based approach such as frontier molecular orbital study, chemical hardness and softness, local reactivity descriptors such as electrophilicity and nucleophilicity which provide considerable insight into the reaction pathway. Since the DNA nucleobases are aromatic molecules, aromaticity descriptor NICS also offers a significant understanding of the stability of cytosine and its derivatives as stability is intricately related to chemical reactivity.

So, this thesis provides a wholesome account of the concept of aromaticity including a review of the magnetic criteria for defining aromaticity. The concept of exo-cyclic aromaticity in novel molecular systems is introduced and is further established in novel three-membered heteroatomic aromatic systems. It explains the phenomenon of bond stretch isomerism in an important all-metal aromatic cluster. Finally, it provides theoretical elucidation of methylation of cytosine and its subsequent oxidation processes involving aromatic nucleobases.

BIBLIOGRAPHY

Chapter 1

1. Faraday, M. M. *Phil.Trans.Roy.London.* **1825,** *115*, 440.
2. (a) Kekulé, A. *Bull.Soc.Chim.Paris* **1865,** *3*, 98-100. (b) Kekulé, A. *Ann.Chem.Pharm*, **1866**, *137*,129.
3. Erlenmeyer, E. *Ann. Chem. Pharm.* **1866**, *137*, 327.
4. Dewar, J *(1867).* "On the Oxidation of Phenyl Alcohol, and a Mechanical Arrangement adapted to illustrate Structure in the Non-saturated Hydrocarbons". Proc. R. Soc. Edinb. *6: 82–86.*
5. (a) Hückel, E. *Z. Phys* **1931**, *70*, 204. (b) Hückel, *Z.Phys.* **1932,** *76*,628-648. (c) Hückel, E. *Z.Electrochem, Angew.Phys.Chem.* **1937,** *43*, 752-788. (d)Hückel, E. *Z.Electrochem, Angew.Phys.Chem* **1995,** *61*,866-890.
6. Clar, E. The Aromatic Sextet. Wiley & Sons: New York, **1970**.
7. Calvin, M.; Wilson. K. *J. Am. Chem. Soc.* **1945**, *67*, 2003.
8. Heilbronner, E. *Tet Lett* **1964**, *5*, 1923.
9. Katz, T. H; Garratt, P. J. *J. Am. Chem. Soc.* **1963,** *85*, 2852.
10. (a) Colin, B. N. *J. Am. Chem. Soc.* **1972**, *94*, 4941. (b) Henrik, O, *Nat Chem*, **2012**, *4*, 969.
11. Aihara, J. *J. Am. Chem. Soc.* **1978**, *100*, 3339.
12. Li, X.; Kuznetsov, A.; Zhang, H.; Boldyrev, A. Wang, L. *Science* **2001**, *291*, 859.
13. Jose, M. M.; Boldyrev, A. I.; Merino, G.; Ugalde, M. J. *Chem.Soc.Rev.* **2015**, *44*, 6519.
14. Tsipis, A.; Kefalidis, C.; Tsipis, C. *J. Am. Chem. Soc*. **2008**, *130*, 9144.
15. Pauling, L; Wheland, G.W. *J. Chem. Phys.* **1933**, *1*, 362.
16. Pauling, L. In The Nature of the Chemical Bond, 3rd ed., Cornell University Press: Ithaca, New York, 1960.
17. Goldstein. M.J.; Hoffmann, R. *J. Am. Chem. Soc*. **1971**, *93*, 6193.
18. Chen, Z.; Wannere, C. S.; Corminboeuf, C.; Puchta, R.; Schleyer, P. v. R.; *Chem. Rev.* **2005** *105* (10), 3842.
19. Schleyer, P.V.R. Introduction: Aromaticity. *Chem. Rev*. **2001**, *101*, 1115.
20. Fernández, I.; Dyker, C. A.; DeHope, A.; Donnadieu, B.; Frenking, G.; Bertrand, G. *J. Am. Chem. Soc*. **2009**, *131*, 11875.
21. Gutowsky, H. S.; McCall, D. W. *J. Phys. Chem.* **1953**, *21*, 279.
22. Onak T. P.; Landesman, H; Williams R E.; Shapiro, I paper presented to the Division of Inorganic Chemistry, 135th National Meeting of the American Chemical Society, Boston, Mass, April 1959.
23. Cotton, F. A.; Wilkinson, G. *"Advanced Inorganic Chemistry,"* Interscience, London, 1966, 256.

24. Olah, G. A.; Mo, Y. K.; Halpern, Y. *J. Am. Chem. Soc.* **1972**, *94*, 3551.
25. Thorn, D. L.; Hoffmann, R. *Nouv. J. Chim.* **1979**, *3*, 39.
26. Bursten, B. E.; Fenske, R. F. *Inorg. Chem.* **1979**, *18*, 1760.
27. Li, X.-W.; Pennington, W. T.; Robinson, G. H. *J. Am. Chem. Soc.* **1995**, *117*, 7578.
28. Li, X.; Zhang, H. F.; Wang, L. S.; Kuznetsov, A. E.; Cannon, N. A.; Boldyrev, A. I. *Angew Chem Int Ed* **2001**, *40*, 1867.
29. Díaz-Cervantes, E.; Poater, J.; Robles, J.; Swart, M.; Solà, M. *J. Phys. Chem. A* **2013**, 117, 40, 10462.
30. Kuznetsov, A. E.; Boldyrev, A. I.; Li, X.; Wang, L. S. *J Am Chem Soc* **2001**, *123*, 8825.
31. Twamley, B.; Power, P. P.; *Angew Chem Int Ed* **2000**, *39*, 3500.
32. Cisar, A.; Corbett, J. D. *Inorg Chem* **1977**, *16*, 2482.
33. Critchlow, S. C.; Corbett, J. D. *Inorg Chem* **1984**, *23*, 770.
34. Tuononen, H. M.; Suontamo, R.; Valkonen, J.; Laitinen, R. S. *J Phys Chem A* **2004**, 108, 5670.
35. Todorov, I.; Sevov, S. C. *Inorg Chem* **2004**, *43*, 6490.
36. Todorov, I.; Sevov, S. C. *Inorg Chem* **2005**, *44*, 5361.
37. Gillespie, R. J.; Barr, J.; Kapoor, R.; Malhotra, K. C. *Can J Chem* **1968**, *46*, 149.
38. Gillespie, R. J.; Barr, J.; Crump, D. B.; Kapoor, R.; Ummat, P. K. *Can J Chem* **1968,** *46*, 3607.
39. Barr, J.; Gillespie, R. J.; Kapoor, R.; Pez, G. P. *J Am Chem Soc* **1968**, *90*, 6855.
40. Couch, T. W.; Lokken, D. A.; Corbett, J. D. *Inorg Chem* **1972**, *11*, 357.
41. Burford, N.; Passmore, J.; Sanders, J. C. P. In: Liebman, J. F.; Greenburg, A. (eds) From atoms to polymers. Isoelectronic analogies. VCH, New York, 1989, p 53.
42. Li, X.; Wang, X. B.; Wang, L. S. *Phys Rev Lett* **1998**, *81*, 1909.
43. Wu, H.; Li, X.; Wang, X. B.; Ding, C. F.; Wang, L. S. *J Chem Phys* **1998**, *109*, 449.
44. Baeck, K. K.; Bartlett, R. J.; *J Chem Phys* **1998**, *109*, 1334.
45. Kuznetsov, A. E.; Boldyrev, A. I. *Struct Chem* **2002**, *13*, 141.
46. Kuznetsov, A. E.; Boldyrev, A. I.; Zhai, H. J.; Li, X.; Wang, L. S. *J Am Chem Soc* **2002**, *124*, 11791.
47. Gausa, M.; Kaschner, R.; Lutz, H. O.; Seifert, G.; Meiwes-Broer, K. H. *Chem Phys Lett* **1994**, *230*, 99.
48. Gausa, M.; Kaschner, R.; Seifert, G.; Faehrmann, J. H.; Lutz, H. O.; Meiwes, K. H. B. *J Chem Phys* **1996**, *104*, 9719.
49. Zhai, H. J.; Wang, L.S.; Kuznetsov, A. E.; Boldyrev A. I. *J Phys Chem A* **2002**, *106*, 5600.
50. Tanaka, H.; Neukermans, S.; Janssens, E.; Silverans, R. E.; Lievens. P. *J Am Chem Soc* **2002**, *125*, 2862.
51. Alexandrova, A. N.; Boldyrev, A. I.; Zhai, H. I.; Wang, L. S. *J Phys Chem A* **2005**, *109*, 562 .

52. Wannere, C. S.; Corminboeuf, C.; Wang, Z. X.; Wodrich, M. D.; King, R. B.; Schleyer, P. v. R *J Am Chem Soc* **2005**, *127*, 5701.
53. Lein, M.; Frunzke, J.; Frenking, G. *Angew Chem Int Ed* **2003**, *42*, 1303.
54. Van Zandwijk, G.; Janssen, R. A. J.; Buck, H. M. *J Am Chem Soc* **1990**, *112*, 4155.

55. Kuznetsov, A. E.; Boldyrev, A. I. *Chem. Phys. Lett.* **2004**, *388*, 452.
56. Yong, L.; Chi, X. *Theochem* **2007**, *818*, 93.
57. Roy, D. R.; Chattaraj , P. K. *J Phys Chem A* **2008**, *112*, 1612.
58. Hoffmann, R.; Schleyer, P. v. R.; Schaefer, H. F., III. *Angew Chem Int Ed* **2008**, *47*, 7164.
59. (a) Parkin, G. *Acc Chem Res* **1992**, *25*, 455. (b) Parkin, G. *Chem Rev* **1993**, *93*, 887.
60. Stohrer W. D.; Hoffmann, R. *J. Am. Chem. Soc.* **1972**, *94*, 779.
61. Stohrer W. D.; Hoffmann, R. *J. Am. Chem. Soc.* **1972**, *94*, 1661.
62. Jean, Y.; Lledos, A.; Burdett, J. K.; Hoffmann, R. *J. Am. Chem. Soc.* **1988**, *110*, 4506.

Chapter 2

1. Cryański, M. K.; Krygowski, T. M.; Katritzky, A. R.; Schleyer, P. v. R. *J. Org. Chem* **2002,** *67*, 1333.
2. Minkin, V.; Glukhovtsev, M.; Simkin, B. In *Aromaticity and Antiaromaticity*; Wiley Interscience, New York, **1994**.
3. Schleyer, P. v. R.; Jiao, H. **1996,** *68*, 209.
4. Poranne, G. P.; Stranger, A. *Chem. Soc. Rev.* **2015**, *44*, 6597.
5. Schleyer, P. v. R. *Chem. Rev.* **2001**, *101*, 1115.
6. Schleyer, P. v. R.; Maerke, C.; Dransfeld, A.; Jiao, H.; Hommes, N. J. R. v. E. *J Am Chem Soc* **1996**, *118*, 6317.
7. London, F. *J. Phys. Radiu.* **1937**, *8*, 397.
8. Cheeseman, J. R.; Trucks, G. W.; Keith, T. A.; Frisch, M. J. *J. Chem. Phys.* **1996**, *104*, 5497.
9. Schreckenbach, G.; Ziegler, T. *J. Phys. Chem*. **1995**, *99*, 606.
10. Schreckenbach, G.; Ziegler, T. *Theor. Chem. Acc*. **1998**, *99*, 71.
11. Heine, T.; Schleyer, P. v. R.; Corminboeuf, C.; Seifert, G.; Reviakine, R.; Weber, J. *J. Phys. Chem. A* **2003**, *107*, 6470.
12. Giambiagi, M.; de Giambiagi, M. S.; Mundim, K. C. *Struct. Chem.* **1990**, *1*, 423–427.
13. Giambiagi, M.; de Giambiagi, M. S.; dos Santos Silva, C. D.; de Figuereido, A. P. *Phys. Chem. Chem. Phys*. **2000**, *2*, 3381–3392.
14. Bultinck, P.; Ponec, R.; Van Damme, S. *J. Phys. Org. Chem.* **2005**, *18*, 706–718.
15. Becke A. D.; Edgecomb K. E. *J. Chem. Phys*. **1990**, *92*, 5397-5403.
16. Savin, A.; Jepsen, O.; Flad, J.; Andersen, O. K.; Preuss, H.; von Schnering, H. G. (1992). "Electron localization in solid-state structures of the elements – the diamond structure". *AngewandteChemie International Edition in English*. **31** (2): 187–188.
17. Paul, S.; Goswami, T.; Misra, A. *AIP Advances*, **2015**, ***5***, 107211.
18. Anderson, P. W. *Phys. Rev.* **1950**, *79*, 350.
19. Anderson, P. W. *Phys. Rev.***1959**, *115*, 2.

20. Anderson, P. W. Theory of the magnetic interaction: exchange in insulators and superconductors. In solid state physics; Turnbull, F., Seitz, F., Eds.; Academic Press: New York, 1963; Vol. 14, p 99.
21. Ziegler, T.; Rauk, A. *Theor. Chim. Acta* **1977**, *46*, 1.
22. Pinter, B.; Fievez, T.; Bickelhaupt, F. M.; Geerlings, P.; DeProft, F. *Phys. Chem. Chem. Phys.* **2012**, *14*, 9846.
23. Michalak, A.; Mitoraj, M.; Ziegler, T. *J. Phys. Chem. A* **2008**, *112*, 1933.
24. (a) Mitoraj, M.; Michalak, A. *J. Mol. Model.* **2007**, 13, 347–355; (b) Mitoraj, M. P.; Michalak, A.; Ziegler, T. *J. Chem. Theory Comput.*, **2009**, 5, 962–975.
25. Bader, R. F. W. *Atoms in Molecules: A Quantum Theory;* Oxford University Press Oxford UK, 1990.
26. Bauzá, A.; Quiñonero, D.; Deyà, P. M.; Frontera, A. *Chem. Phys. Lett*. **2012**, *536*, 165.
27. Zubarev, D. Yu.; Boldyrev, A. I. *Phys. Chem. Chem. Phys.* **2008**, *10*, 5207.
28. Foster, J. P.; Weinhold, F. *J. Am. Chem. Soc*. **1980**, *102*, 7211.
29. Reed, A. E.; Curtiss, L. A.; Weinhold, F. *Chem. Rev*. **1988**, *88*, 899.
30. Marx, D.; Hutter, J.; J. Grotendorst (Ed.), Proceedings of Modern Methods and Algorithms of Quantum Chemistry, John von Neumann Institute for Computing, Jurich, Germany, 2000.
31. Schlegel, H. B.; Millam, J. M.; Iyengar, S. S.; Voth, G. A.; Daniels, A. D.; Scuseria, G. E.; Frisch, M. J. *J. Chem. Phys.***2011**, *114*, 9758-9763.
32. Iyengar, S. S.; Schlegel, H. B.; Millam, J. M.; Voth, G. A.; Scuseria, G.E.; Frisch, M. J. *J. Chem. Phys.* **2011**, *115*, 10291-10302.
33. Schlegel, H. B.; Iyengar, S. S.; Li, X.; Millam, J. M.; Voth, G. A.; Scuseria, G. E.; Frisch, M. J. *J. Chem. Phys.* **2002**, *117*, 8694-8704.
34. McWeeny, R. *Rev. Mod. Phys*. **1960**, *32*, 335.
35. Pearson, R. G. Recent Advances in the Concept of Hard and Soft Acids and Bases. *J. Chem. Edu.***1987**, *64*, 561-567.
36. Parr, R. G.; Chattaraj, P. K. *J. Am. Chem. Soc*. **1991,** *113*, 1854-1855.
37. Ayers, P. W.; Parr, R. G. *J. Am. Chem. Soc*. **2000**, *122*, 2010-2018.
38. Chattaraj, P. K.; Sengupta, S. *J. Phys. Chem.* **1996**, *100*, 16126-16130.
39. Fuentealba, P.; Simon-Manso, Y.; Chattaraj, P. K. *J. Phys. Chem. A* **2000**, *104*, 3185-3187.
40. Pan, S.; Solà, M.; Chattaraj, P. K. *J. Phys. Chem. A* **2013**, *117*, 1843-1852.
41. Saha, R.; Pan, S.; Chattaraj, P. K. *Molecules* **2016**, *21*, 1477-1493.
42. Chamorro, E.; Chattaraj, P. K.; Fuentealba, P. *J. Phys. Chem. A* **2003**, *107*, 7068-7072.
43. Parthasarathi, R.; Elango, M.; Subramanian, V.; Chattaraj, P. K. *Theo. Chem. Acc.* **2005**, *113*, 257-266.
44. Geerlings, P.; De, P. F.; Langenaeker, W. *Chem. Rev*. **2003**, *103*, 1793-1874.
45. Chattaraj, P. K. *J. Indian. Chem. Soc.* **1992**, *69*, 173-183.
46. Parr, R. G.; Donnelly, R. A.; Levy, M.; Palke, W. E. *J. Chem. Phys.* **1978**, *68*, 3801.
47. Chattaraj, P. K.; Sarkar, U.; Roy, D. R. *Chem. Rev.* **2006**, *106*, 2065-2091.
48. Chattaraj, P. K.; Roy, D. R. *Chem. Rev*. **2007**, *107*, PR46-PR74.
49. Parr, R. G.; Szentpaly, L. v.; Liu, S. *J. Am. Chem. Soc.***1999**, *121*, 1922-1924.
50. Koopmans, T. A. *Physica* **1993**, *1*, 104-113.

51. Janak, J. F. *Phys. Rev. B.* **1978**, *18*, 7165.
52. Roy, R.K.; Pal, S.; Hirao, K. *J. Chem. Phys.* **1999**, *110*, 8236
53. Roy, R.K.; Pal, S.; Hirao, K. *J. Chem. Phys.* **2000**, *113*,1372
54. Ayers, P.W.; Morrisson, R.C.; Roy, R.K. *J. Chem. Phys.* **2002**, 116, 8731.
55. Hocquet, A.; Toro-Labbé, A.; Chermette, H. *J.Mol Struc(THEOCHEM)***2004**, 686, 213-218.
56. Melin, J.; Aparicio, F.; Subramanian, V.; Galván, M.; Chattaraj, P.K. *J.Phys. Chem. A* **2008**, *108*, 2487-2491.
57. Lu, T.; Chen, F. *J. Comp. Chem.* **2012**, *33*, 580-592.

Chapter 3

1. Faraday, M. M.*Phil.Trans.Roy.London.* 1825, *115*, 440-446.
2. Kekulé, A. *Bull.Soc.Chim.Paris* **1865,** *3*, 98-100.
3. Kekulé, A. *Ann.Chem.Pharm* ***1866,*** *137*,129-196.
4. Hückel, E. *Z. Phys.* **1930,** *60*,423–456.
5. Hückel, E. *Z. Phys.* **1931**, *70*, 204–86.
6. Hückel, E. *Z.Phys.* **1932,** *76*,628-648.
7. Hückel, E. *Z.Electrochem, Angew.Phys.Chem.* **1937,** *43*, 752-788.
8. Hückel, E. *Z.Electrochem, Angew.Phys.Chem* **1995,** *61*,866-890.
9. Pauling, L; Wheland, G.W. *J.Chem.Phys.* **1933**, *1*, 362-374.
10. (a) Balaban, A. T.; Oniciu, D.C.; Katritzky, A.R. *Chem. Rev* **2004**, ***104****(5)*, 2777-2812. (b) Chattaraj, P. K.; Sarkar, U.; and Roy, D. R. *J. Chem. Educ.*, **2007**, *84*, 354.(c) Chattaraj, P.K.; Roy, D. R.; Elango, M.; and Subramanian, V. *J. Phys. Chem.A* **2005**, *109*, 9590.
11. Noorizadeh, S.; Shakerzadeh, E. *Phys.Chem.Chem.Phys.* **2010**, *12(18)*, 4742-4749.
12. Chen, Z.; Wannere, C. S.; Corminboeuf, C.; Puchta, R.; Schleyer, P. v. R. *Chem.Rev* 2005, *105(10)*, 3842-3888.
13. Krygowski, T. M.; Cyrański, M. K. *Chem. Rev* 2001,***101****(5)*, 1385-1420 .
14. Poater, J.; Duran, M.; Solà, M.; Silvi. B. *Chem.Rev* **2005**, *105(10)*, 3911-3947.
15. Cyrański, M. K. *Chem. Rev* 2005, ***105****(10)*, 3773-3811.
16. Matito, E.; Duran, M.; Solà, M. *J. Chem. Phys.* 2005, ***122****(1)*, 014109 .
17. (a)Bultinck, P.; Ponec, R.; Van Damme, S. *J.Phys.Org.Chem* 2005, *18(8)*, 706-718. (b) Roy, D.R.; Bultinck, P.; Subramanium, V.; Chattaraj, P.K. *J.Mol.Struc(THEOCHEM)* 2008, *854(1-3)*, 35-39.
18. Misra, A.; Klein, D.J. ; Morikawa, T. *J.Phy.Chem.A* **2009,** *113(6)*,1151-1158.
19. Clar, E. The Aromatic Sextet. Wiley & Sons: New York, **1970**.
20. Misra, A.; Schmalz, T. G.; Klein, D. J. *J.Chem.Inf.Model* **2009,** *49(12)*, 2670-2676.

21. Bhattacharya, D.; Panda, A.; Misra, A .; Klein,D.J. *J.Phys.Chem.A* **2014,** *118(24),* 4325-4338.
22. Cryański, M. K.; Krygowski, T. M.; Katritzky, A. R.; Schleyer, P.v.R. *J.Org.Chem* **2002,** *67(4),* 1333-1338.
23. Paul, S.; Goswami, T.; Misra, A *AIP Advances* **2015**,*5*, 107211.
24. Schleyer, P.v.R.; Jiao, H. *Pure &Appl.Chem.***1996,** *68* 209-218.
25. Islas, R.; Chamorro, E.; Robles, J.; Heine, T.; Santos J.C.; Merino, G. *Struct.Chem.* 2007, *18*, 833.
26. Stock, A.; Pohland, E. Borwasserstoffe, IX.: B3N3H6. *Chem. Ber.*1926, *59B*, 2215.
27. Bhattacharya, D.; Shil, S.; Misra, A.; Bytautasc, L.; Klein, D.J. *Phys. Chem. Chem. Phys.* 2015, *17*, 14223.
28. Mo, Y.; Peyerimhoff, S. D. *J.Chem.Phys.*1998, *109(5)*, 1687-1697.
29. Pauling, L.; Sherman, J. *J. Chem. Phys.* 1933, *1(8)*, 606-617.
30. Hehre, W. J.; Radom, L.; Schleyer, P. v. R.; Pople, J.A. Ab Initio Molecular Orbital Theory, Wiley &Sons: New York, **1986**.
31. Hehre, W. J.; McIver, R.T.; Pople, J.A.; Schleyer,P. v. R. *J. Am. Chem. Soc*. **1974**, *96(22),* 7162-7163.
32. Pedley, J. B.; Naylor, R. B.; Kirby, S. P.; Thermodynamical Data of Organic Compounds, Chapman & Hall: London, **1986**.
33. Jose, M. M.; Boldyrev, A. I.; Merino, G.; Ugalde, M.J. *Chem.Soc.Rev.* 2015, *44*, 6519.
34. Poater, J.; Fradera, X.; Duran, M.; Solá, *Chem-Eur.J.***2003**, *9(2),* 400-406.
35. Poranne, G. P.; Stranger, A. *Chem.Soc.Rev.* 2015, *44*, 6597.
36. (a) Dewar,M. J. S.; McKee, M.L *Pure Appl. Chem.*1980, *52*, 1431 – 1441. (b)Dewar, M. J. S. *Bull. Soc. Chim.Belg.* 1979, *88*, 957 – 967.
37. Pople, J. A. *Mol,Phys.*, **1958**, *1*,175-180.
38. Gomes, A. N. F.; Mallion, R. B. *Chem.Rev.* **2001**, *101*, 1349-1384.
39. Mitchell, R. H. *Chem.Rev.* **2001**, *101*, 1301-1315.
40. Benassi, R.;Lazzeretti, P.; Taddei, F. *J.Phys.Chem.* 1975, *79(8)*, 848-851.
41. Coriani, S.; Lazzeretti, P.; Malagoli, M.; Zanasi. R. *Theor.Chim.Acta.* **1994**, *89*,181-192.
42. Lazzeretti, P.; Malagoli, M.; Zanasi, R. *Chem.Phys.Lett.* **1994**, *220*, 299-309.
43. Zanasi, R. *J.Chem.Phys.* 1996, *105*, 1460-1469.
44. Steiner, E.; Fowler, P.W. *J.Phys.Chem.A* 2001, *105*, 9553-9562.
45. Steiner, E.; Fowler, P.W. *Chem.Commun.* **2001**, 2220-2221.
46. Steiner, E.; Fowler, P. W.; Havenith, R. W .A. *J.Phys.Chem.A* 2002, *106*, 7048-7056.
47. Schleyer, P. v. R; Maerker, C.; Dransfeld, A.; Jiao,H.; Hommes, N. J. R. *J.Am.Chem.Soc.* **1996**, *118*, 6317-6318.
48. London, F. *J. Phys. Radium.* **1937**, *8*, 397.
49. (a) Cheeseman, J. R.; Trucks, G. W.; Keith, T. A.; Frisch, M. J. *J. Chem. Phys.* **1996**, *104*, 5497.(b) Schreckenbach, G.; Ziegler, T. *J. Phys. Chem.* **1995**, *99*, 606.(c) Schreckenbach, G.; Ziegler, T. *Theor. Chem. Acc.* **1998**, *99*, 71.
50. Chattaraj, P.K. Aromaticity and Metal Clusters,Taylor & Francis/CRC Press: Florida, **2010**.
51. Schleyer, P. v. R; Jiao, H.; Hommes, N. J. R.; Malkin,V. G.; Malkina, O. *J.Am.Chem.Soc.* **1997**, *119*,12669-12670.

52. Putz, M. V. *MATCH Commun. Math. Comput. Chem*. **2010**, *64*, 391-418.
53. Putz, M. V. *Int. J. Mol. Sci.* 2010, *11*, 1269-1310.
54. Tarko, L.; Putz, M. V. *J.Math.Chem,***2010**, *47(1),*487-495.
55. Schleyer, P. v. R. *Chem.Rev.* 2001, *101*, 1115-1118.
56. Bultinck, P. General discussion. *Faraday Discussions* **2007**, 135, 367-401.

Chapter 4

1. Garratt, P. J. *Aromaticity*, John Wiley & Sons, 1986.
2. Minkin, V. I.; Glukhotsev, M. N.; Simkin, B. Y. in Aromaticity and Antiaromaticity: Electronic and Structural Aspects, John Wiley & Sons, Inc., New York, 1994.
3. Bickelhaupt, F.; de Wolf, W. H. *Recl. Trav. Chim. Pays-Bas* **1988**, *107*, 459-478.
4. Kraakman, P. A.; Valk, J.- M.; Niederländer, H. A. G.; Brouwer, D. B. E.; Bickelhaupt, F. M.; de Wolf, W. H.; Bickelhaupt F.; Stam, C. H. *J. Am. Chem. Soc.* **1990**, *112*, 6638-6646.
5. Schleyer P. v. R.; Jiao, H. *J. Pure Appl. Chem*. **1996**, *68*, 209-218.
6. Carey F. A.; Sundberg, R. J. *Advanced Organic Chemistry: Structure And Mechanisms (Part A)*, Springer, 2000.
7. Faraday, M. *Phil. Trans. R. Soc.* **1825**, *115*, 440–466.
8. Kekulé, A. *Bull. Soc. Chim.Fr.* **1865**, *3*, 98-110.
9. Balaban, A. T.; Schleyer P. v. R.; Rzepa, H. S. *Chem. Rev.* **2005**, *105*, 3436-3447.
10. Huckel, E. *Z. Phys.* **1931**, *70*, 204-286.
11. Heilbronner, E. *Tetrahedron Lett.* **1964**, *5*, 1923–1926.
12. Balaban, A. T. *Pure & Appl. Chem.* **1980**, *52*, 1409-1429.
13. Katrizky, A.; Barczymski, P.; Musumarra, G.; Pisano D.; Szafran, M. *J. Am. Chem. Soc.* **1989**, *111*, 7-15.
14. Schleyer, P. v. R.; Maerker, C.; Dransfeld, A.; Jiao, H.; Hommes, N. J. R. v. E. *J. Am. Chem. Soc.* **1996**, *118*, 6317-6318.
15. Misra, A.; Klein, D. J.; Morikawa, T. *J. Phys. Chem. A*, **2009**, *113*, 1151-1158.
16. Dewar, M. J. S. Tropolone. *Nature* **1950**, *166*, 790-791.
17. Crocker, E. C. *J. Am. Chem. Soc.*, **1922**, *44*, 1618-1630.
18. Armit, J. W.; Robinson, R. *J. Chem. Soc.* **1925**, *127*, 1604-1618.
19. Gaussian 09, Revision B.01, Frisch, M. J.; Trucks, G. W.; Schlegel, H. B.; Scuseria, G. E.; Robb, M. A.; Cheeseman, J. R.; Scalmani, G.; Barone, V.; Mennucci, B.; Petersson, G. A.; Nakatsuji, H.; Caricato, M.; Li, X.; Hratchian, H. P.; Izmaylov, A. F.; Bloino, J.; Zheng, G.; Sonnenberg, J. L.; Hada, M.; Ehara, M.; Toyota, K.; Fukuda, R.; Hasegawa, J.; Ishida, M.; Nakajima, T.; Honda, Y.; Kitao, O.; Nakai, H.; Vreven, T.; Montgomery, J. A., Jr.; Peralta, J. E.; Ogliaro, F.; Bearpark, M.; Heyd, J. J.; Brothers, E.; Kudin, K. N.; Staroverov, V. N.; Kobayashi, R.; Normand, J.; Raghavachari, K.; Rendell, A.; Burant, J.

C.; Iyengar, S. S.; Tomasi, J.; Cossi, M.; Rega, N.; Millam, J. M.; Klene, M.; Knox, J. E.; Cross, J. B.; Bakken, V.; Adamo, C.; Jaramillo, J.; Gomperts, R.; Stratmann, R. E.; Yazyev, O.; Austin, A. J.; Cammi, R.; Pomelli, C.; Ochterski, J. W.; Martin, R. L.; Morokuma, K.; Zakrzewski, V. G.; Voth, G. A.; Salvador, P.; Dannenberg, J. J.; Dapprich, S.; Daniels, A. D.; Farkas, Ö.; Foresman, J. B.; Ortiz, J. V.; Cioslowski, J.; Fox, D. J. Gaussian, Inc., Wallingford CT, 2009.

20. Amsterdam Density Functional (Theoretical Chemistry, Vrije Universiteit, Amsterdam, The Netherlands, http://www.scm.com).
21. Ziegler, T.; Rauk, A. *Theor. Chim. Acta.* **1977**, *46*, 1-10.
22. Yamaguchi, K. *Self-Consistent Field: Theory and Applications.* (Eds Carbo, R., Klobukowski, M.); Elsevier: Amsterdam, 1990.
23. Corminboeuf, C.; Heine, T.; Weber, J. *Phys. Chem. Chem. Phys.* **2003**, *5*, 246-251.
24. Corminboeuf, C.; King, R. B.; Schleyer, P. v. R. *Chem. Phys. Chem.* **2007**, *8*, 391-398.
25. Lu, T.; Chen, F. *J. Comp. Chem.* **2012**, *33*, 580-592.
26. VandeVondelea, J.; Krackb, M.; Mohamedb, F.; Parrinellob, M.; Chassaingc, T.; Hutter, J. *Comput. Phys. Commun.* **2005**, *167*, 103-128.
27. Becke, A. D. *Phys. Rev. A* **1988**, *38*, 3098-3100.
28. Lee, C.; Yang, W.; Parr, R. G. *Phys. Rev. B* **1988**, *37*, 785-789.
29. Goedecker, S.; Teter, M.; Hutter, J. *Phys. Rev. B* **1996**, *54*, 1703-1710.
30. Hartwigsen, C.; Goedecker, S.; Hutter, J. *Phys. Rev. B* **1998**, *58*, 3641-3662.
31. Bader, R.F.W. *Atoms in Molecules: A Quantum Theory*; Oxford University Press: Oxford, UK, 1990.
32. Bauzá, A.; Quiñonero, D.; Deyà, P. M.; Frontera, A. *Chem. Phys. Lett.* **2012**, *536*, 165–169.
33. Gund, P. *J. Chem. Educ.* **1972**, *49*, 100-103.
34. McKee, W. C.; Wu, J. I.; Hofmann, M.; Berndt A.; Schleyer, P. v. R. *Org. Lett.*, **2012**, *14*, 5712–5715.
35. Goswami, T.; Paul, S.; Mandal, S.; Misra, A.; Anoop, A.; Chattaraj, P. K. *Int. J. Quantum Chem.*, **2015**, *115*, 426-433.
36. Giri, S.; Kumar, R. P. S. A.; Chakraborty A.; Roy, D. R.; Duley, S.; Parthasarathi, R.; Elango, M.; Vijayaraj, R.; Subramanian V.; Merino, G.; Chattaraj, P. K. *Aromaticity and Metal Clusters*, CRC Press, USA, **2011**.
37. Chattaraj, P. K.; Das, R.; Duley, S.; Vigneresse, J. -L. *Theor. Chem. Acc.*, **2012**, *131*, 1089-1096.
38. Seeger, R.; Pople, J. A. *J. Chem. Phys.* **1977**, *66*, 3045-3050.
39. Dohnert, D.; Koutecky, J. *J. Am. Chem. Soc.*, **1980**, *102*, 1789-1796.
40. Hoffmann, R.; Schleyer, P. v. R.; Schaefer, H. F. *Angew. Chem., Int. Ed.* **2008**, *47*, 7164-7167.
41. Wolinski, K.; Hinton, J. F.; Pulay, P. *J. Am. Chem. Soc.*, **199**
42. Paul, S.; Goswami, T.; Misra, A. *AIP Adv.* **2015**, *5*, 107211.
43. Steiner, E.; Fowler, P. W.; Soncini, A.; Jenneskens, L. W. *Faraday Discuss.*, **2007**, *135*, 309–323.
44. Mitoraj, M.; Michalak, A. *J. Mol. Model.*, **2007**, 13, 347-355.
45. Mitoraj, M. P.; Michalak, A.; Ziegler, T. *J. Chem. Theory Comput.* **2009**, 5, 962-975.

46. Zubarev, D. Y.; Boldyrev, A. I. *Phys. Chem. Chem. Phys.* **2008**, *10*, 5207-5217
47. Bromm, D.; Stalke, D.; Heine, A.; Miller, A. *J. Organomet. Chem.*, **1990**, *386*, 1-7.

Chapter 5

1. Faraday, M. *M.Phil.Trans.Roy.London* 1825, *115*, 440.
2. Kekulé, A. *Bull.Soc.Chim.Paris* **1865**, *3*, 98.
3. Kekulé, A. *Ann.Chem.Pharm* **1866**, *137*, 129.
4. Garratt, P. J. *Aromaticity*; John Wiley & Sons, 1986.
5. Minkin, V. I.; Glukhotsev, M. N.; Simkin, B. Y. *Aromaticity and antiaromaticity: electronic and structural aspects;* John Wiley & Sons, Inc., New York, **1994**.
6. Bickelhaupt, F.; de Wolf, W. H. *Recl. Trav. Chim. Pays-Bas.* **1988**, *107*, 459
7. Kraakman, P. A.; Valk, J. M.; Niederla¨nder, H. A. G.; Brouwer, D. B. E.; Bickelhaupt, F. M.; de Wolf, W. H.; Bickelhaupt, F.; Stam, C. H. *J. Am. Chem. Soc.***1990**, *112*, 6638.
8. Schleyer, P. V. R.; Jiao, H. *J. Pure Appl. Chem.* **1996**, *68*, 209.
9. Schleyer, P. V. R.; Jiao, H.; Hommes, N. J. R. v. E.; Malkin, V.G.; Malkina, O. L. *J. Am. Chem. Soc.* **1997**,*119*, 12669.
10. Poranne, G.P.; Stranger, A. *Magnetic and structural aspects*; Wiley: New York, **1994**.
11. Homray, M.; Misra, A.; Chattaraj, P. K. *Curr. Org. Chem.* **2017**, *21*, 2699.
12. Katritzky, A. R. *Chem. Rev.* **2004**, *104*, 2125.
13. Aihara, J. I. *Pure Appl. Chem*. **1982**, *54*, 1115.
14. Graovac, A.; Trinajstic, N.International symposiumon aromaticity, Dubrovnik, **1979**.
15. Nyulaszi, L. *Chem. Rev.* **2001**, *101*, 1229.
16. Minkin, V. I.; Minyaev, R. M. *Chem. Rev.***2001**, *101*, 1247.
17. Katritzky, A. R.; Jug, K.; Oniciu, D. C. *Chem. Rev.***2001**, *101*, 1421.
18. Li,X.; Kuznetsov, A.; Zhang, H.; Boldyrev, A. I.; Wang, L. *Science,***2001**, 291, 859.
19. Kuznetsov, A. E.; Birch, K. A.; Boldyrev, A. I.; Li, X.; Zhai, H.; Wang, L. *Science*, **2003**, *300*, 622.
20. Boldyrev, A. I.; Wang, L .*Chem. Rev.* **2005**, *105*, 3716.
21. Paul, S.; Misra, A. *Inorg Chem* **2011,** *50*, 3234.
22. Chattaraj, P. K.; Roy, D. R.; Duley, S. *Chem.Phys.Lett.* 2008, *460*,382.
23. Huckel, E. *Z. Phys*. **1931**, *70*, 204.
24. Hehre, W. J.; Radom,L.; Schleyer,P. v. R.; Pople, J. A. *Ab Initio molecular orbital theory*; Wiley, New York, 1986.
25. Xie, Y.; Schaefer III, H. F.; Thrasher, J. S. *J. Mol. Struct. Theochem.*, **1991**, *234*, 247.
26. Shaik, S.; Shurki, A.; Danovich, D.; Hiberty, P. C. *J. Mol. Struct.Theochem* **1997**, *398*, 155.
27. Krygowski, T. M.; Cyraski, M. K., *Chem. Rev.* 2001, ***101***, 1385.
28. Poater, J.; Duran, M.; Solà, M.; Silvi, B. *Chem. Rev.* **2005**, *105*, 3911.
29. Cyraski, M. K. *Chem. Rev.* **2005**, *105*, 3773.

30. Matito, E.; Duran, M.; Solà, M. *J. Chem. Phys.* **2005**, *122*, 014109.
31. Bultinck, P.; Ponec, R.; Van Damme,S. *J. Phys.Org. Chem*. **2005**, *18*, 706.
32. Feixas, F.; Matito, E.;Poater, J.;Solà, M. On the performance of some aromaticity indices: A critical assessment using a test set. *J. Comput. Chem.* 2008, 29, 1543-1554.
33. Roy, D. R.; Bultinck, P.; Subramanium, V.; P. K. Chattaraj, J. Mol. Struc., **2008**, *854*, 35.
34. Feixas, F.; Matito, E.; Poater, J.; Solà, M. *Chem. Soc. Rev*. **2015**, *44*, 6434.
35. Misra, A.; Klein, D. J.; Morikawa,T. J. Phys. Chem. A **2009**, *113*, 1151.
36. Clar, E. *The Aromatic Sextet*; Wiley & Sons: New York, **1970**.
37. Misra, A.; Schmalz, T. G.; Klein, D. J. *J.Chem. Inf.Model*, **2009**, *49*, 2670.
38. Bhattacharya, D.; Panda, A.; Misra, A.; Klein, D. J. *J. Phys. Chem. A*, **2014**, *118*, 4325.
39. Gund, P. *J. Chem. Educ.* **1972**, *49*, 100.
40. Goswami, T.; Homray, M.; Paul, S.;Bhattacharya, D.; Misra, A. *Phys. Chem. Chem. Phys*. **2017**, *19*, 11744.
41. Gutowsky, H. S.; McCall, D. W. *J. Phys. Chem.* **1953**, *21*, 279.
42. Onak, T. P.; Landesman, H.; Williams, R. E.; Shapiro, I. paper presented to the Division of Inorganic Chemistry, 135th NationalMeeting of the American Chemical Society, Boston, Mass., April **1959**.
43. Cotton, F. A.; Wilkinson,G. *"Advanced Inorganic Chemistry,"*Interscience, London, **1966**, 256.
44. Olah, G. A.; Mo, Y. K.; Halpern, Y. *J Am Chem Soc* **1972**, *94*, 3551.
45. Ziegler, T.; Rauk, A. 1**977**, *46*, 1.
46. Bader, R. F. W. *Atoms in Molecules: A Quantum Theory;* Oxford University Press, Oxford, UK, **1990**.
47. Schleyer, P. v. R.;Maerke, C.; Dransfeld, A.; Jiao, H.; Hommes, N. J. R. v. E. *J Am Chem Soc*, **1996**, *118*, 6317.
48. Heine, T.; Schleyer, P. v. R.; Corminboeuf, C.; Seifert, G.; Reviakine, R.; Weber, J. *J. Phys. Chem. A* **2003**, 107, 6470.
49. Zubarev, D. Yu.; Boldyrev, A. I. *Phys. Chem. Chem. Phys*. **2008**, *10*, 5207.
50. Paul,S.; Goswami, T.; Misra, A. *AIP Advances*, **2015**, *5*, 107211.
51. Gaussian 09, Revision B.01, Frisch, M. J.; Trucks, G. W.; Schlegel, H. B.; Scuseria, G. E.; Robb, M. A.; Cheeseman, J. R.; Scalmani, G.; Barone, V.; Petersson, G. A.; Nakatsuji, H.; Li, X.; Caricato, M.; Marenich, A. V.; Bloino, J.; Janesko, B. G.; Gomperts, R.; Mennucci, B.; Hratchian, H. P.; Ortiz, J. V.; Izmaylov, A. F.; Sonnenberg, J. L.; Williams-Young, D.; Ding, F.; Lipparini, F.; Egidi, F.; Goings, J.; Peng, B.; Petrone, A.; Henderson, T.; Ranasinghe, D.; Zakrzewski, V. G.; Gao, J.; Rega, N.; Zheng, G.; Liang, W.; Hada, M.; Ehara, M.; Toyota, K.; Fukuda, R.; Hasegawa, J.; Ishida, M.; Nakajima, T.; Honda, Y.; Kitao, O.; Nakai, H.; Vreven, T.; Throssell, K.; Montgomery, J. A., Jr.; Peralta, J. E.; Ogliaro, F.; Bearpark, M. J.; Heyd, J. J.; Brothers, E. N.; Kudin, K. N.; Staroverov, V. N.; Keith, T. A.; Kobayashi, R.; Normand, J.; Raghavachari, K.; Rendell, A. P.; Burant, J. C.; Iyengar, S. S.; Tomasi, J.; Cossi, M.; Millam, J. M.; Klene, M.; Adamo, C.; Cammi, R.; Ochterski, J. W.; Martin, R. L.; Morokuma, K.; Farkas, O.; Foresman, J. B.; Fox, D. J. Gaussian, Inc., Wallingford CT, 2009.

52. Amsterdam Density Functional (Theoretical Chemistry, Vrije Universitiet, Amsterdam, The Netherlands, http://www.scm.com).
53. AIMAll (Version 17.01.25), Todd A. Keith, TK Gristmill Software, Overland Park KS, USA, 2017
54. Lu, T.; Chen, F. Multiwfn: A multifunctional wavefunction analyzer *J. Comp. Chem*. **2012**, 33, 580-592.
55. The DFT code, OPENMX, is available at http://www.openmx-square.org under the GNU General Public License.
56. Pinter, B.; Fievez, T.; Bickelhaupt, F. M.; Geerlings, P.; F. DeProft, *Chem. Chem. Phys.* **2012**, *14*, 9846.
57. Lee, J. T.; Taylor, P. R. *Int. J. Quantum Chem.* **1989**, *36*, 199.
58. Bauzá, A.; Quiñonero, D.; Deyà, P. M.; Frontera, A. *Chem. Phys. Lett*., **2012**, *536*, 165.
59. Cox, J. D.; Pilcher, G.; *Thermochemistry of organic and Organometallic compounds;* Academic: London, 1970.
60. Benson, S. W. *Thermochemical Kinetics;* Wiley: New York, 1976.
61. Inagaki, S.; Ishitani, Y.; Kakefu, T. *J. Am. Chem. Soc.* **1994**, *116*, 13.
62. Dewar, M. J. S. *J. Am. Chem. Soc.* **1984**, *106*, 669.
63. Aihara, J. *J. Phys. Chem. A* **1999**, *103*, 7487.
64. Aihara, J. *Theor. Chem. Acc.* **1999**, *102*, 134.
65. Aihara, J. *Phys. Chem. Chem. Phys.* **1999**, *1*, 227.
66. Parr, R. G.; Zhou, Z.; *Acc. Chem. Res*. **1993**, *26*, 256.
67. Liu, X.; Schmalz, T. G.; Klien, D. J. *Chem. Phys. Lett.* **1992**, *188*, 550.
68. Haddon, R. C.; Fukunaga, T. *Tetrahedron Lett.* **1980**, *21*, 1191.
69. Pearson, R. G. *Hard and soft acids and bases*; Dowden, Hutchinson and Ross: Stroudsburg, PA, 1973.
70. Manolopoulos, D. E.; May, J. C.; Down, S. *Chem. Phys. Lett.* **1991**, *181*, 105.
71. Hoffmann, R.; Schleyer, P. V. R.; Schaefer, H. F. *Angew. Chem., Int. Ed.* **2008**, *47*, 7164.
72. Katrizky, A.; Barczymski, P.; Musumarra, G.; Pisano, D.; Szafran, M. *J. Am. Chem. Soc* **1989**, *111*, 7.
73. Schleyer, P. V. R.; Manoharan, M.; Jiao, H.; Stahl, F. *Org Lett.* **2001**, *3*, 3643.
74. Chen, Z.; Wannere, C. S.; Corminboeuf, C.; Puchta, R.; Schleyer, P. V. R. *Chem Rev.* **2005**, *105*, 3842.
75. London, F. *J. Phys. Radium.* **1937**, *8*, 397.
76. Cheeseman, J. R.; Trucks, G. W.; Keith, T. A.; Frisch, M. J. *J. Chem. Phys.* **1996**, *104*, 5497.
77. Schreckenbach, G.; Ziegler,T.; *J. Phys. Chem*. 1995, *99*, 606.
78. Schreckenbach, G.; Ziegler,T.; *Theor. Chem. Acc*.1998, *99*, 71.
79. Simkin, B. Y.; Minkin, V.I.; Glukhotsev, M.N. *Adv. Heterocyclic Chem*.**1993**, *56*, 304.
80. Foster, J. P.; Weinhold, F. *J. Am. Chem. Soc*. **1980**, *102*, 7211.
81. Reed, A. E.; Curtiss, L. A.;Weinhold, F. *Chem. Rev*.**1988**, *88*, 899.
82. Katrizky, A.; Barczymski, P.; Musumarra, G.; Pisano, D.; Szafran, M. *J. Am. Chem. Soc* **1984**, *111*, 7.
83. Radhakrishnan, S.; Anathakrishnan, S. J.; Somanathan, N. *Bull. Mater. Sci.* **2011**, *34*, 713.

84. Marzari, N.;Vanderbilt, D. *Phys. Rev. B* **1997**, *56(20)*, 12847.

Chapter 6

1. Stohrer, W. D.; Hoffmann, R. *J. Am. Chem. Soc.* **1972**, *94*, 779-786.
2. Stohrer, W. D.; Hoffmann, R. *J. Am. Chem. Soc.***1972**, *94*, 1661-1668.
3. Jean, Y.; Lledos, A.; Burdett, J. K.; Hoffmann, R. *J. Am. Chem. Soc.***1988**, *110*, 4506-4516.
4. Butcher, A. V.; Chatt, J. *J. Chem. Soc. A*, **1970**, *0*, 2652-2656.
5. Goodgame, M. M.; Goddard III, W. A. *Phys. Rev. Lett*. **1985**, *54*, 661.
6. Moskovits, M.; Limm, W.; T. Mejean. *J. Chem. Phys.* **1985**, *82*, 4875.
7. Rohmer, M. M.; Benard, M. *Chem. Soc. Rev*. **2001**, *30*, 340-354.
8. Wieghardt, K.; Backes-Dahmann, G.; Nuber, B.; Weiss, J. *Angew. Chem., Int. Ed. Engl.* **1985**, *24*, 777-778.
9. Parkin, G. *Acc. Chem. Res.* **1992**, *25*, 455-460.
10. Parkin, G. *Chem. Rev*. **1993**, *93*, 887-912.
11. Rohmer, M. M.; Strich, A.; Benard, M.; Malrieu, J. P. *J. Am. Chem. Soc.* **2001**, *123*, 9126-9134.
12. Song, J; Hall, M. B. *Inorg. Chem.* **1991**, *30*, 4433-4437.
13. Comba, P.; Hauser, A.; Kerscher, M.; H. Pritzkow. *Angew. Chem.* **2003**, *42*, 4536-4540.
14. Antol, I.; Eckert-Maksic´, M.; Lischka, H.; Maksic´, Z. B. *Chem. Phys. Chem.* **2004**, *5*, 975-981.
15. Petrov, K. T.; Pinter, B.; Veszpremi, T. *J. Organomet. Chem.* **2012**, *706*, 84-88.
16. Goswami, T.; Paul, S.; Mandal, S.; Misra, A.; Anoop, A.; Chattaraj P. K. *Int. J. Quantum Chem.* **2015**, *115*, 426-433.
17. Chattaraj, P. K.; Roy, D. R.; Elango, M.; Subramanian, V. *J. Phys. Chem. A* **2005**, *109*, 9590-9597.
18. Chattaraj, P. K.; Giri, S. *J. Mol. Struct. (THEOCHEM)* **2008**, *865*, 53-56.
19. Giri, S.; Roy, D. R.; Duley, S.; Chakraborty, A.; Parthasarathi, R.; Elango, M.; Vijayaraj, R.; Subramanian, V.; Islas, R.; Merino, G.; Chattaraj, P. K. *J. Comp. Chem.* **2010**, *31*, 1815-1821.
20. Roy, D. R.; Chattaraj, P. K. *J. Phys. Chem. A* **2008**, *112*, 1612-1621.
21. Brito, B. G. A.; Hai, G. Q.; Candido, L. *Chem. Phys. Lett.* **2013**, *586*, 108-110.
22. Paul, S.; Misra, A. *Inorg. Chem.* 2011, *50*, 3234-3246.
23. Mondal, S.; Chattaraj, P. K. *Chem. Phys. Lett.* **2014**, *593*, 128-131.
24. Jiménez-Halla, J. O. C.; Matito, E.; Blancafort, L.; Robles, J.; Solà, M. *J. Comput. Chem.* **2011**, *32*, 372-373.
25. Di Nicola, F. P.; Lanzi, M.; Marchetti, F.; Pampaloni, G.; Zacchini, S. *Dalton Trans.* **2015**, *44*, 12653-12659.

26. Renner, R. *Z. Phys.* **1934**, *92*, 172-193.
27. Herzberg, G.; Teller, E. *Z. Phys. Chemie B.* **1933**, *21*, 410-446.
28. Herzberg, G. *Molecular Spectra and Molecular Structure* (Reprint Edition, Krieger, Malabar, (1991) Vol. III.
29. GaussView, Version 5, R. Dennington, T. Keith, J. Millam, *Semichem Inc.* Shawnee Mission KS. 2009.
30. Gaussian 09, Revision C.01, Frisch, M. J.; Trucks, G. W.; Schlegel, H. B.; Scuseria, G. E.; Robb, M. A.; Cheeseman, J. R.; Scalmani, G.; Barone, V.; Petersson, G. A.; Nakatsuji, H.; Li, X.; Caricato, M.; Marenich, A. V.; Bloino, J.; Janesko, B. G.; Gomperts, R.; Mennucci, B.; Hratchian, H. P.; Ortiz, J. V.; Izmaylov, A. F.; Sonnenberg, J. L.; Williams-Young, D.; Ding, F.; Lipparini, F.; Egidi, F.; Goings, J.; Peng, B.; Petrone, A.; Henderson, T.; Ranasinghe, D.; Zakrzewski, V. G.; Gao, J.; Rega, N.; Zheng, G.; Liang, W.; Hada, M.; Ehara, M.; Toyota, K.; Fukuda, R.; Hasegawa, J.; Ishida, M.; Nakajima, T.; Honda, Y.; Kitao, O.; Nakai, H.; Vreven, T.; Throssell, K.; Montgomery, J. A., Jr.; Peralta, J. E.; Ogliaro, F.; Bearpark, M. J.; Heyd, J. J.; Brothers, E. N.; Kudin, K. N.; Staroverov, V. N.; Keith, T. A.; Kobayashi, R.; Normand, J.; Raghavachari, K.; Rendell, A. P.; Burant, J. C.; Iyengar, S. S.; Tomasi, J.; Cossi, M.; Millam, J. M.; Klene, M.; Adamo, C.; Cammi, R.; Ochterski, J. W.; Martin, R. L.; Morokuma, K.; Farkas, O.; Foresman, J. B.; Fox, D. J. Gaussian, Inc., Wallingford CT, 2010.
31. McDouall, J. J.; Peasley, K.; Robb, M. A. *Chem. Phys. Lett.*, **1988**, *148*, 183-189.
32. Bernardi, F.; Bottoni, A.; Field, M. J.; Guest, M. F.; Hillier, I. H.; Robb, M. A.; Venturini, A. *J. Am. Chem. Soc.*, **1988**, *110*, 3050-3055.
33. Tonachini, G.; Schlegel, H. B.; Bernardi, F.; Robb, M. A. *J. Am. Chem. Soc.*, **1990**, *112*, 483-491
34. Marx, D.; Hutter, J.; Grotendorst, J. (Ed.), Proceedings of Modern Methods and Algorithms of Quantum Chemistry, John von Neumann Institute for Computing, Jurich, Germany (2000).
35. Schlegel, H. B.; Millam, J. M.; Iyengar, S. S.; Voth, G. A.; Daniels, A. D.; Scuseria, G. E.; Frisch, M. J. *J. Chem. Phys.***2011**, *114*, 9758-9763.
36. Iyengar, S. S.; Schlegel, H. B.; Millam, J. M.; Voth, G. A.; Scuseria, G.E.; Frisch, M. J. *J. Chem. Phys.* **2011**, *115*, 10291-10302.
37. Schlegel, H. B.; Iyengar, S. S.; Li, X.; Millam, J. M.; Voth, G. A.; Scuseria, G. E.; Frisch, M. J. *J. Chem. Phys.* **2002**, *117*, 8694-8704.
38. Pearson, R. G. Recent Advances in the Concept of Hard and Soft Acids and Bases. *J. Chem. Edu.***1987**, *64*, 561-567.
39. Parr, R. G.; Chattaraj, P. K. *J. Am. Chem. Soc.* **1991,** *113*, 1854-1855.
40. Ayers P. W.; Parr, R. G. *J. Am. Chem. Soc.* **2000**, *122*, 2010-2018.
41. Chattaraj, P. K.; Sengupta, S. *J. Phys. Chem.* **1996**, *100*, 16126-16130.
42. Fuentealba, P.; Simon-Manso, Y.; Chattaraj, P. K. *J. Phys. Chem. A* **2000**, *104*, 3185-3187.
43. Pan, S.; Solà, M.; Chattaraj, P. K. *J. Phys. Chem. A* **2013**, *117*, 1843-1852.
44. Saha, R.; Pan, S.; Chattaraj, P. K. *Molecules* **2016**, *21*, 1477-1493.

45. Chamorro, E.; Chattaraj, P. K.; Fuentealba, P. *J. Phys. Chem. A* **2003**, *107*, 7068-7072.
46. Parthasarathi, R.; Elango, M.; Subramanian, V.; Chattaraj, P. K. *Theo. Chem. Acc.* **2005**, *113*, 257-266.
47. Geerlings, P.; De, P. F.; Langenaeker, W. *Chem. Rev.* **2003**, *103*, 1793-1874.
48. Chattaraj, P. K. *J. Indian. Chem. Soc.* **1992**, *69*, 173-183.
49. Parr, R. G.; Donnelly, R. A.; Levy, M.; Palke, W. E. *J. Chem. Phys.* **1978**, *68*, 3801.
50. Chattaraj, P. K.; Sarkar, U.; Roy, D. R. *Chem. Rev.* **2006**, *106*, 2065-2091.
51. Chattaraj, P. K.; Roy, D. R. *Chem. Rev.* **2007**, *107*, PR46-PR74.
52. Parr, R. G.; Szentpaly, L. v.; Liu, S. *J. Am. Chem. Soc.***1999**, *121*, 1922-1924.
53. T. A. Koopmans, *Physica* **1993**, *1*, 104-113.
54. Janak, J. F. *Phys. Rev. B.* **1978**, *18*, 7165.
55. Paul, S.; Goswami, T.; Misra, A. *AIP Advances*, **2015**, *5*, 107211.
56. Goswami, T.; Homray, M.; Paul, S.; Bhattacharya, D.; Misra, A. *Phys. Chem. Chem. Phys.* **2017**, *19*, 11744-11747.
57. Homray, M.; Paul, S.; Misra, A. *Bull Mater Sci.,* **2019**, *42*, 46.
58. Anderson, P.W. *Phys, Rev.* **1950**, *79*, 350.
59. Anderson, P. W. *Phys. Rev.***1959**, *115*, 2.
60. Anderson, P. W. Theory of the magnetic interaction: exchange in insulators and superconductors .In solid state physics; Turnbull, F., Seitz, F., Eds.; Academic Press: New York, **1963**; Vol. 14, p 99.
61. Paul, S.; Misra, A. *J. Chem. Theory Comput*. **2012**, *8*,843-853.
62. Lu, T.; Chen, F. *J. Comp. Chem.* **2012**, *33*, 580-592.
63. The DFT code, OPENMX, is available at http://www.openmx-square.org under the GNU General Public License.
64. Dewar, M. J. S.; Healy, E. F.; Stewart, J. J. P. ***J****. Chem. Soc., Faraday Trans. 2***, 1984,** *80***,** 227-233.
65. Walsh, A. D. *J. Chem. Soc.* **1953,** *0*, 2260-2266.
66. Peric, M.; Engles, E.; Peyerimhoff, S. D. *In Quantum Mechanical Electronic Structure Calculations with Chemical Accuracy*; Langhoff, S. R., Ed., Kluwer: Dordrecht, 1995, p 261.
67. Kar, T.; Scheiner, S. *J. Phys. Chem.***1995**, *99*, 8121-8124.
68. Torrent-Sucarrat, M.; Blancafort, L.; Duran, M.; Luis, J.; Solà, M. *In Theoretical Aspects of Chemical Reactivity;* Toro-Labbe, A., Ed. Elsevier: Amsterdam, 2007.
69. Torrent-Sucarrat, M.; Luis, J. M.; Duran, M.; Solà, M. *J. Chem. Phys.* **2002**, *117*, 10561.
70. Chattaraj, P. K.; Pérez, P.; Zevallos, J.; Toro-Labbé, A. *J. Phys. Chem. A* **2001**, *105* ,4272-4283.

Chapter 7

1. Ruppel, W. G. *Z. Physiol. Chem.* **1899**, *26*, 218–232.
2. Gommers-Ampt, J. H.; Borst, P. *FASEB J.* **1995**, *9*, 1034–1042.
3. Johnson, T. B.; Coghill, R. D. *J. Am. Chem. Soc.***1925**, *47*, 2838–2844.
4. Wyatt, G. R. *Nature* **1950**, *166*, 237–238.
5. Bird, A. *Genes Dev.* **2002**, *16*, 6–21.
6. Deaton, A.; Bird, A. *Genes Dev.* **2011**, *25*, 1010–1022.
7. Jones, P. A. *Nat. Rev. Genet.* **2012**, *13*, 484–492.
8. Kohn, W.; Sham, L. J. Phys. Rev. B **1965**, *140*, A1133–A1138.
9. Varsano, D.; Di Felice, R.; Marques, M. A. L.; Rubio, A. *J. Phys. Chem. B* **2006**, *110*, 7129-7138.
10. Dkhissi, A.; Blossey, R. *J. Phys. Chem. B* 2008, 112, 9182–918.
11. GaussView, Version 5, R. Dennington, T. Keith, J. Millam, *Semichem Inc.* Shawnee Mission KS. 2009.
12. Gaussian 09, Revision C.01, Frisch, M. J.; Trucks, G. W.; Schlegel, H. B.; Scuseria, G. E.; Robb, M. A.; Cheeseman, J. R.; Scalmani, G.; Barone, V.; Petersson, G. A.; Nakatsuji, H.; Li, X.; Caricato, M.; Marenich, A. V.; Bloino, J.; Janesko, B. G.; Gomperts, R.; Mennucci, B.; Hratchian, H. P.; Ortiz, J. V.; Izmaylov, A. F.; Sonnenberg, J. L.; Williams-Young, D.; Ding, F.; Lipparini, F.; Egidi, F.; Goings, J.; Peng, B.; Petrone, A.; Henderson, T.; Ranasinghe, D.; Zakrzewski, V. G.; Gao, J.; Rega, N.; Zheng, G.; Liang, W.; Hada, M.; Ehara, M.; Toyota, K.; Fukuda, R.; Hasegawa, J.; Ishida, M.; Nakajima, T.; Honda, Y.; Kitao, O.; Nakai, H.; Vreven, T.; Throssell, K.; Montgomery, J. A., Jr.; Peralta, J. E.; Ogliaro, F.; Bearpark, M. J.; Heyd, J. J.; Brothers, E. N.; Kudin, K. N.; Staroverov, V. N.; Keith, T. A.; Kobayashi, R.; Normand, J.; Raghavachari, K.; Rendell, A. P.; Burant, J. C.; Iyengar, S. S.; Tomasi, J.; Cossi, M.; Millam, J. M.; Klene, M.; Adamo, C.; Cammi, R.; Ochterski, J. W.; Martin, R. L.; Morokuma, K.; Farkas, O.; Foresman, J. B.; Fox, D. J. Gaussian, Inc., Wallingford CT, 2010.
13. Yanai,T.;Tew, D.P.; Handy, N.C. *ChemPhysLett* **2004**, *393*, 51-57.
14. Geerlings, P.; De, P. F.; Langenaeker, W. *Chem. Rev.* **2003**, *103*, 1793-1874.
15. Chattaraj, P. K. *J. Indian. Chem. Soc.* **1992**, *69*, 173-183.
16. Parr, R. G.; Donnelly, R. A.; Levy, M.; Palke, W. E. *J. Chem. Phys.***1978**, *68*, 3801.
17. Chattaraj, P. K.; Sarkar, U.; Roy, D. R. *Chem. Rev.* **2006**,*106*, 2065-2091.
18. Chattaraj, P. K.; Roy, D. R. *Chem. Rev.* **2007**, *107*, PR46-PR74.
19. Parr, R. G.; Szentpaly, L. v.; Liu, S. *J. Am. Chem. Soc.***1999**, *121*, 1922-1924.
20. Koopmans, T. A. *Physica* **1993**, *1*, 104-113.
21. Janak, J. F. *Phys. Rev. B.* **1978**, *18*, 7165.
22. Roy, R. K.; Pal, S.; Hirao, K.*J. Chem. Phys*. **1999**, *110*, 8236
23. Roy, R. K.; Pal, S.; Hirao, K. *J. Chem. Phys*. **2000**, *113*,1372
24. Ayers, P.W.; Morrisson, R.C.; Roy, R. K. *J. Chem. Phys*. **2002**, 116, 8731.

25. Hocquet, A.; Toro-Labbé, A.; Chermette, H. *J.Mol Struc(THEOCHEM)* **2004**, 686, 213-218.
26. Melin, J.; Aparicio, F.; Subramanian, V.; Galván, M.; Chattaraj, P.K. *J.Phys. Chem. A* **2008**, *108*, 2487-2491.
27. Lu, T.; Chen, F. *J. Comp. Chem.* **2012**, *33*, 580-592.
28. Schleyer, P. v. R.;Maerke, C.; Dransfeld, A.; Jiao, H.; Hommes, N. J. R. v. E. *J. Am. Chem. Soc.*, 1996, *118*, 6317.

INDEX

A

All-metal aromatic systems, 9
Antiaromatic, 3
Aromatic, 1
Aromatic nucleobases, 10
Aromatic stabilization energy, 21

B

Bond stretch isomerism, 88
Born-Oppenhiemer approximation, 89

C

Chemical potential, 91
Clusters, 3
Conceptual DFT, 26
Conical intersection, 89
Current density analysis plots (CDA), 37

D

Degeneracy, 89
Diatropic ring current, 17
Diradical, 46
Dissected Canonical Molecular Orbital NICS (CMO-NICS), 18
DNA methylation, 109
Dummy atom, 53

E

Electron Localization Function (ELF), 20
Electrophilicity, 26
Exo-cyclic, 8
Extended transition state, 23

F

Frontier molecular orbital, 120
Fukui functions, 27

G

GIAO, 38

H

Hardness, 120
Hirschfeld charges, 27
Hopping integral, 21
Huckel's rule, 33

I

Intrinsic Reaction Coordinate (IRC), 94
Ionization potential, 27

J

Jahn-Teller distortions, 88

K

Kinetic energy, 71
Koopman's theorem, 27

L

Lagrange, 71
Lagrangian molecular dynamics, 25
Ligand, 8

M

Magnetic field, 7
Metalloaromaticity, 9
Möbius aromaticity, 3
Multi-centre indices, 19

N

NMR, 18
Nucleophilicity, 112
Nucleus Independent Chemical Shifts (NICS), 17

O

Oxidation, 109

P

Paratropic ring current, 17
Pauli repulsive orbital interaction, 23
Potential Energy Surface, 88

Q

Quantum theory of atoms in molecules (QTAIM), 24

R

Renner- Teller effect, 89
Ring Current Model (RCM), 35
Ring Strain Energy (RSE), 24

S

Schleyer, 17
Softness, 112

T

TET enzymes, 110
Three- dimensional aromaticity, 3
Transition state, 95

V

Vibrational energy, 100

Z

Ziegler, 23

REPRINTS OF PUBLISHED PAPERS IN CONNECTION TO THIS THESIS

[1] **Homray, M**.; Misra, A.; Chattaraj, P.K. Aromaticity in the Light of Magnetic Criteria, *Curr. Org. Chem.* **2017**, *21*, 1-6. (**Chapter 3**)

[2] Goswami, T.; **Homray, M**.; Paul, S.; Bhattacharya, D.; Misra, A. On Exo-Cyclic Aromaticity, *Phys. Chem. Chem. Phys.* **2017**, *19*, 11744-11747. (**Chapter 4**)

[3] **Homray, M**.; Paul, S.; Misra, A Manifestation of exo-cyclic aromaticity in triangular heterocyclic B_2F_2X Systems (X=O, S, Se, NH), *Bull. Mat. Sci*. **2019**, *42*, 46. (**Chapter 5**)

[4] **Homray, M**.; Mondal, S.; Misra. A.; Chattaraj, P. K. Bond stretch isomerism in $Be32^{-}$ driven by the Renner–Teller effect, *Phys. Chem. Chem. Phys.* **2019**, *21*, 7996- 8003. (**Chapter 6**)

Send Orders for Reprints to reprints@benthamscience.ae

Current Organic Chemistry, 2017, *21*, 2699-2704

REVIEW ARTICLE

Aromaticity in the Light of Magnetic Criteria

Manoswita Homray[†], Anirban Misra[†,*] and Pratim K. Chattaraj[‡]

[†]*Department of Chemistry, University of North Bengal, Darjeeling 734013, India;* [‡]*Department of Chemistry and Centre for Theoretical Studies, Indian Institute of Technology, Kharagpur, 721302, India*

ARTICLE HISTORY

Received: July 26, 2016
Revised: December 30, 2016
Accepted: February 15, 2017

DOI:
10.2174/1385272821666170428124343

Abstract: Magnetic criteria of aromaticity have been analyzed which are currently the most popular methods, considering the circular delocalization of electrons as the genesis of aromaticity. The concept of aromaticity as was visualized by Kekulé to the latest development in the field has been discussed. The other criteria for defining aromaticity such as the chemical behavior, the structural behavior and the energetic criteria are briefly defined keeping the main focus on the magnetic criteria. The various magnetic measures for defining aromaticity such as NMR chemical shifts which include ^{1}H NMR shifts as well as Li^{+} NMR chemical shifts, Magnetic Susceptibility Anisotropy, Current Density Analysis Plots (CDA) and Nucleus Independent Chemical Shifts are explicitly discussed. The NMR chemical shift is explained with the help of the Ring Current Model (RCM) and its both experimental and computational applications are also discussed. Magnetic Susceptibility Anisotropy and its applicability as a magnetic criterion have been elaborated accordingly. A pictorial representation of Current density Analysis Plots and its relevance as a magnetic criterion have also been accounted for. Special attention is given to the NICS criteria, explaining the role of ghost atom, considering it to be the most popular magnetic criterion. Advantages and disadvantages of all the methods along with recent advances are discussed.

Keywords: Aromaticity, magnetic criteria, ring current, NMR chemical shifts, NICS, CDA.

Personal Use Only
Not For Distribution

1. INTRODUCTION

The history of aromaticity, which is a fundamental concept in chemistry, began in 1825 when Michael Faraday [1] isolated benzene for the first time. However, the very first definition of aromaticity was given by Kekulé [2, 3] in which he suggested oscillating structures where synchronous 1, 2-shifts of the three double bonds occur perpetually. Then after six decades, the works of Hückel [4-8] and Pauling [9] explained the role of delocalization of electrons in the stabilization of aromatic systems, using the quantum mechanics based Molecular Orbital (MO) approach and Valence Bond (VB) method respectively. Since then, the circular delocalization of electrons is taken as the genesis of aromaticity.

Aromaticity is developed as an important phenomenon for its close relation with chemical reactivity [10]. The increasing interest on aromaticity persuaded a need to attach a quantitative character to it. Consequently, a number of quantitative aromaticity indices have been anticipated starting from the famous (4n+2) π-electron rule of Hückel to the latest Shannon Entropy index [11]. At present, the molecular property based criteria for aromaticity can be broadly divided into four basic categories such as magnetic [12], structural [13], electronic [14], and energetic [15], Electron density based indices such as para-delocalization index (PDI) [14], fluctuation index (FLU) [16] and multi-centre bond index (MCBI) [17] have also been introduced to characterize aromaticity. Later, Klein and co-workers correlated aromaticity of molecular benzenoids to a unique type of polynomial [18], as Clar-*2-nomial* on the basis of Clar's concept of aromatic sextet [19]. Later on, this correlation has been extended for radical benzenoids [20] and more recently on polyacenes and beyond [21].However, most of the indices do not provide direct measure of aromaticity, as the phenomenon is not directly observable [22].

After a meticulous revision of structural, energetic and magnetic indices of aromaticity for many aromatic systems, Cyranski *et al*. concluded aromaticity as an abstract concept from philosophical point of view [22]. Whereas, from another perspective, the event of aromaticity can be regarded as multidimensional since it cannot be described definitely by any single property based index and all indices do not always give consistent results. Due to all these problems the quantification of aromaticity still remains a challenging and fundamental problem, and ought to be addressed through a precise phenomenological description [23]. On the basis of available literature, the criteria for the quantification of aromaticity can be divided into the following four basic categories.

2. CHEMICAL BEHAVIOR

Electrophilic aromatic substitution reactions are the characteristic reactions of the aromatic systems but it is difficult to define aromaticity with the help of the chemical behavior of the molecule. Since aromaticity is a property of the initial state, and reactivity is the property of the intermediate states so quantifying aromaticity with the help of chemical reactivity is not straightforward. The characteristic electrophilic aromatic substitution reaction also has many exceptions, for example, phenanthrene and anthracene which

*Address for correspondence to this author at the Department of Chemistry, University of North Bengal, Darjeeling 734013, India; Tel: +919434228745;
E-mail: anirbanmisra@yahoo.com

1875-5348/17 $58.00+.00 © 2017 Bentham Science Publishers

Current Organic Chemistry

are aromatic molecules prefer the addition of bromine rather than substitution. Also fullerenes (eg, C_{60} or C_{70}) are aromatic compounds but since they are devoid of any hydrogen, they do not undergo aromatic substitution reactions but only undergo addition reactions [12].

3. STRUCTURAL PATTERN

Aromatic systems are mainly planar systems. The characteristic property of an aromatic system is that its bond lengths are all equal and π-electrons are delocalized. The direct determination of bond lengths gives us valuable information regarding the extent of delocalization. In contrast, in antiaromatic molecules the alternating double and single bond lengths differ significantly, generally over 0.2 Å in length [24]. However, bond length equalization and the symmetry associated with it cannot be used as the only parameter for defining aromaticity because some systems possessing equal bond lengths are not aromatic. Again, borazine which is an isoelectronic system with benzene has roughly equal bond lengths and considered to be weakly aromatic in nature [12]. The degree of aromaticity in borazine has been a topic of some controversy [25] starting soon after its discovery in 1926 by Stock and Pohland [26]. The properties of borazine are in good accordance with a ring structure of six atoms which ''on-the-average'' correspond to an sp^2 hybridized-carbon [27]. Also, strain effects and other contributing factors provide hindrance in predicting aromaticity with the help of structural criteria [24].

4. ENERGETIC CRITERIA

Aromaticity has long been connected to the enhanced resonance energies (REs) and the aromatic stabilization energies (ASEs). Even the (4n+2) π- electron rule of Hückel is based on energetic criterion. The energetic measure of aromaticity and antiaromaticity is based on evaluations of energies relative to the reference systems such as conjugated polyenes or olefins [24]. However, determinations of (REs) and (ASEs) are quite difficult even for simple systems [12]. Since ASE itself is not physically observable [28], direct experimental determination of ASE is difficult. However, starting from the pioneering work of Pauling and Sherman [29], various efforts have been made to estimate ASE from experimental data. Also, introduction of isodesmic [30] and homodesmotic reactions [31], has made it possible to calculate the ASE from the energies of reactants and products, obtained experimentally from calorimetric measurements [32]. In a recent work a phenomenological model is discussed to evaluate ASE without any reference state [23].

5. MAGNETIC CRITERIA

Primarily, aromaticity was restricted to all carbon, coplanar, delocalized conjugated π systems having (4n+2) π electrons according to Huckel's rule of aromaticity [4-8]. Presently aromaticity is not only confined to the organic systems, according to Boldyrev, "Aromaticity, in recent years has become an important and powerful unifying concept to describe the stability and bonding in many chemical species beyond organic chemistry, including inorganic cations, anions, radicals, and clusters" [33], three dimensional aromaticity involving σ-electrons and multidimensional aromaticity involving d-orbitals have been reported. Aromaticity has not been confined to ground states but it has been extended to transition states and excited states. There is possibly no direct way to calculate the aromaticity in a molecule experimentally.

Magnetic criteria are currently the most popular methods and constitute the most frequently used aromaticity indices. There are various criteria for defining aromaticity such as energy, structure, electron density based indices [34] and magnetic properties but we focus our discussions to magnetic properties only. Magnetic properties provide considerable insight into the concept of aromaticity. The anomalous diamagnetization of benzene has been related to the delocalization of π-electrons since the early days of quantum chemistry. The aromatic molecules demonstrate relatively strong diamagnetism when placed in a magnetic field; this is due to the generation of an opposing magnetic field by the induced ring currents. The magnetic criteria of aromaticity are dependent on the specific reaction of the aromatic compounds to externally applied uniform magnetic field which is placed perpendicular to the molecular plane. This contribution of π-electrons to the magnetic susceptibility component which is placed perpendicular to the molecular plane was chosen as an indicator of aromaticity. While the direction of an induced current in a loop is determined by the relative orientation of the magnetic field and the loop's movement but the direction of the current in a molecule also depends on the type of the system. Generally in a system containing 4nπ electrons, an external magnetic field induces a paratropic ring current (*i.e.* in the opposite direction relative to a classic loop)while a system containing (4n+2)π electrons shows a diatropic ring current (*i.e.* in the same direction as a classic loop) [35].

Magnetic properties are necessary but not sufficient to describe a system as aromatic or antiaromatic but magnetic criterion has an advantage over other criterion that we can compare the paratropic and diatropic ring currents to experimental values derived from NMR. Now, the concept of aromaticity is no longer confined to the organic domain but has been found in all-metal clusters systems and the existence of an σ-aromaticity [36]. The most popular and frequently used aromaticity indices are NMR chemical shifts, magnetic susceptibility anisotropy, Nucleus Independent Chemical Shift (NICS), Aromatic Ring Current Shielding (ARCS) and Current Density Analysis (CDA plots) [35].

6. NMR CHEMICAL SHIFTS

The most widely used NMR chemical shifts method is the ^{1}H-NMR method. According to the Ring Current Model (RCM) [37], for a (4n+2) π electrons system, the diatropic ring current will form an induced magnetic field which is opposite in direction to the applied external magnetic field at the centre of the ring as depicted in the above diagram (Fig. **1**). While outside the ring the curved lines of the magnetic field are in the same direction as the applied external field. Thus protons that are inside the ring experience an upfield shift while protons that are outside experience a downfield shift. In the case of a 4nπ electron system, a paratropic ring current is induced, so here the induced magnetic field is in the same direction as the external field at the centre of the ring while outside the ring it is in the opposite direction to the external field, thus here the internal protons experience a downfield shift while the external protons experience an upfield shift, that is the effect is exactly the opposite. Thus, the chemical shifts of protons have been used to characterize aromatic and antiaromatic compounds. The ring current picture has proven to be powerful in justifying the magnetic properties of π electron systems quantitatively. The concept is so visual "that one can almost *feel* when a molecule is subjected to a magnetic field." The ring current is connected to the concept of aromaticity experimentally through anisotropy of magnetic susceptibility or through exaltation of magnetic susceptibility or by chemical shifts methods

Personal Use Only
Not For Distribution

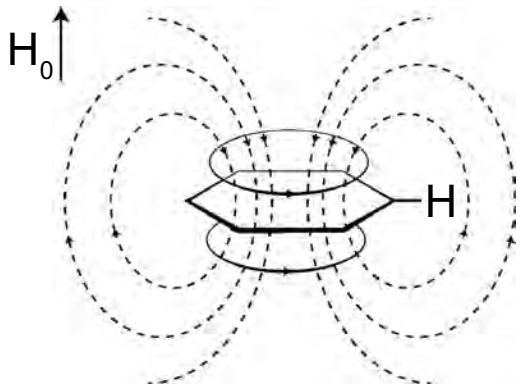

Fig. (1). Representation of the Ring Current Model in the case of benzene [35].

in a Nuclear Magnetic Resonance experiment and also individual ring current intensities which can be computed [38].

The rings of most aromatic systems are too small to accommodate inner protons, so the chemical shifts of hydrogen at the bridging positions provide better information regarding the aromaticity and antiaromaticity of the systems. However, this criterion is not general for aromatic systems that are devoid of hydrogen like for example C_{60} and the oxocarbons (30) and ^{13}C chemical shifts in aromatic hydrocarbons are not deshielded [24].

Other NMR chemical shifts methods are Li^+ and ^3He chemical shifts method. Chemical shifts of ^7Li were used to investigate the electron delocalization. Aromatic and antiaromatic compounds of Li^+ complexes show significant shielding and deshielding respectively of the ^7Li NMR signals due to the induced ring currents. ^7Li chemical shifts obtained by modern computations technique match well with the ^7Li NMR chemical shifts that are obtained experimentally. So, one of the advantages of using Li^+ NMR chemical shifts as a computational tool is that it can be compared with the experimental Li NMR data of Li^+ complexes [24]. However, a major drawback is that the ring currents are relatively small. Also, the number of Li^+ complexes is limited therefore the use of Li^+ NMR chemical shifts as a magnetic criterion is also limited. An extension of the use of NMR to assess aromaticity was developed mainly by Mitchell [39].

7. MAGNETIC SUSCEPTIBILITY ANISOTROPY

This method provides another magnetic criterion of aromaticity. The tensor normal to the aromatic ring is much larger than the average of other tensors and this difference is termed as exaltation. Magnetic susceptibility exaltation (λ) is the difference between the observed bulk magnetic susceptibility value and the susceptibility that is evaluated on the basis of an increment system ($\lambda=\chi_m-\chi_{m'}$). The exaltation of magnetic susceptibility is mainly due to the induced ring currents and is a widely employed magnetic criterion especially for the characterization of metal clusters. In the 1996 review article entitled "What is aromaticity", Schleyer and Jiao suggested that "compounds which exhibit significant exalted diamagnetic susceptibility are aromatic. Those compounds with exalted paramagnetic susceptibility may be antiaromatic" [24].

However, this method is applicable for planar or nearly planar aromatic molecules and is not applicable in the case of spherical systems. Also, in some cases, high magnetic anisotropy does not necessarily imply aromaticity. In addition, the contribution to the magnetic susceptibility component which is perpendicular to the molecular plane provides a more consistent aromaticity criterion than that which is dependent solely on magnetic anisotropy [40]. This method was popular earlier, but recently it is not much in use because it is difficult to quantify aromaticity using this method. Nowadays, computational methods are more developed and provide a better qualitative and quantitative understanding of the magnetic properties.

It is interesting to note that ring currents and aromaticity are theoretical properties and neither are measurable quantities but both NMR chemical shifts and magnetic susceptibility exaltation methods are experimentally measurable quantities that result from ring currents.

8. CURRENT DENSITY ANALYSIS PLOTS (CDA)

This method is purely a computational method. It is the visualization of the ring currents with the help of arrows and the direction of the arrows gives us the idea of whether the ring current is diatropic or paratropic. Clockwise direction represents paratropic ring current while anticlockwise direction represents diatropic ring current. Also the size of the arrows indicates the strength of the ring current. The CDA plot of benzene ring is depicted in the figure below (Fig. **2**).

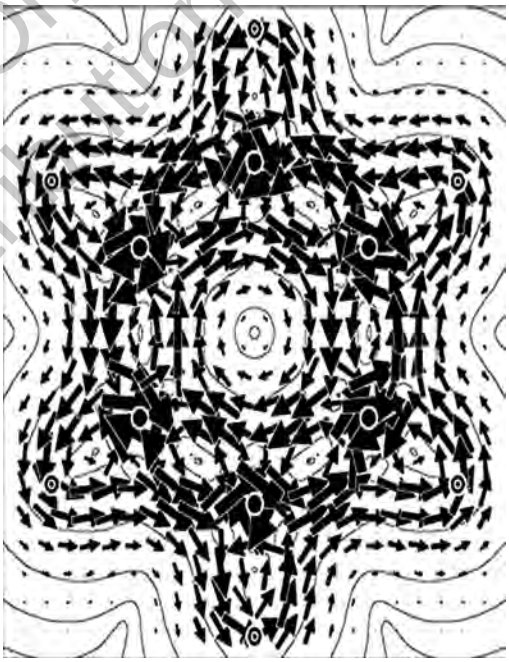

Fig. (2). Plot of the current density induced in the molecular plane of the benzene by a perpendicular external magnetic field [56].

According to the Ring Current Model (RCM) [37] in the presence of an external magnetic field, a diatropic ring current is generated in aromatic systems and a paratropic ring current is generated in antiaromatic systems. Thus, the aromaticity of a planar or a nearly planar compound when placed in an external magnetic field perpendicular to the molecular plane can be obtained directly, either by calculating the intensity of the current or by calculating the current density in a given system. New computational methodologies are now developed that provide a visual representation of the current density field induced in a molecule. These current density maps provide relevant information and help in understanding features of aromatic compounds.

The main advantage of this method is that it provides pictorial representation of the ring currents in the systems. However, the

Personal Use Only
Not For Distribution

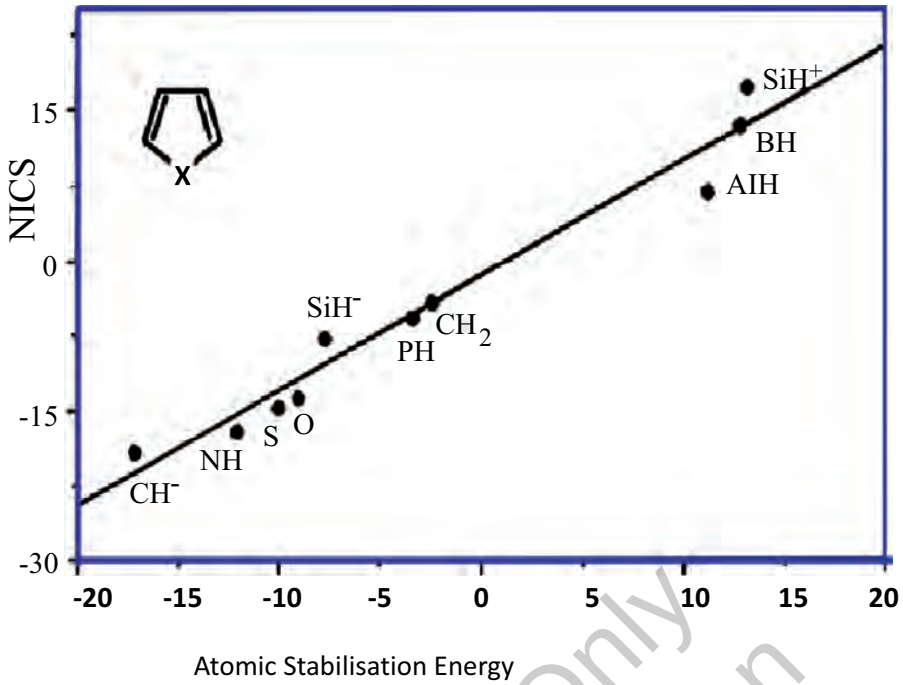

Fig. (3). Plot of NICS (0) (ppm) *vs*. the ASE (kcal mol^{-1}) for a set of five-membered ring heterocycles, C_4H_4X (X = as shown) [24].

major drawback of this method is that it is very difficult to quantify and also the pictures that are obtained through this method are not easily separable into their individual components. Also, in some cases, high magnetic anisotropy does not necessarily imply aromaticity. In addition, second order magnetic properties; such as polarizability, magnetizability, and nuclear shielding were not calculated accurately by the original methods which can generally be obtained by the integration of first order current density. The most popular CDA methods are: Continuous Transformation of Current Density - Diamagnetic Zero (CTOCD-DZS) [41-43] also known as the ipsocentric method [44-46].

9. NUCLEUS INDEPENDENT CHEMICAL SHIFT (NICS)

It is the most popular method for quantifying the magnetic properties of molecules mainly due to its simplicity and efficiency. NICS has been popularized by Schleyer and his co-workers [47]. NICS is defined as the negative value of the absolute magnetic shielding. NICS method uses a ghost atom namely Bq(named after the ghost Banquo from Shakespeare's Macbeth),it is devoid of any electrons, protons and neutrons. Initially it was placed at the centre of the system [NICS (0)], then later at a distance of 1 Å above the plane [NICS (1)]. This ghost atom is like a sensor for the magnetic environment at the position at which it is placed. The ghost atom senses this magnetic environment and reports the chemical shielding values through the use of computational technique like GIAO [48, 49]. The NICS values were reported with reversed signs, in agreement with NMR chemical shift convention. Positive NICS value indicates a paratropic magnetic field whereas a negative NICS value indicates a diatropic magnetic field, thus a negative NICS value would mean that a system is aromatic and a positive NICS value would correspond to an antiaromatic system. In some cases, the negative value indicates the 3D-aromaticity of the molecule [50]. The chemical shift is used as an indicator of the direction and magnitude of the induced magnetic field. From Fig. (**3**), it can be noted that NICS corresponds well with the aromatic stabilization energy [24].

According to an article in 2005 by Schleyer and his coworkers, "NICS has several advantages over many other aromaticity criteria: (i) NICS does not require reference standards, increment schemes, or calibrating (homodesmotic) equations for evaluation. (ii) Unlike λ which depends on the square of the ring area, NICS only shows a modest dependence on the ring size. It does depend on the number of electrons. The 10 π electron systems give significantly higher values than those with six π electrons, for example, the cyclooctatetraenedication and dianion. (iii) Importantly, in several sets of related molecules, NICS correlates well with other aromaticity indexesbased on energetic, geometric, and other magnetic criteria (iv) NICS can becomputed easily using standard quantum chemical programs such as Gaussian 09, Gaussian 98, Gaussian 03, ADF, and deMon" [12].

After their initial publication, Schleyer and his co-workers noted the problem in using NICS for 3-membered systems due to the local shielding effects of the neighboring σ-bonds. So they introduced two modifications in the following year [51]. The first modification was that the bq was raised 1 Å above the molecular plane, which was termed as NICS (1). Since σ-contributions are short ranged, so NICS (0) has greater σ-contributions, so by raising the bq by 1 Å, the σ-contributions are effectively reduced. Secondly, the total NICS value was separated into σ and π contributions. Since aromaticity results from π contributions, so NICS (1) is a better aromaticity criterion than NICS (0).

However, the major drawback of NICS is that it reports only a single value at a given position, without any information regarding the magnetic field. Also, there are other magnetic shielding contributions from the local circulation of electrons in bonds, lone pairs and interior electrons, so the reliance on the π-system is not pure. In fact the σ framework of the CC and CH bonds affects the chemical shifts of organic molecules, as a result of this; the NICS value is non-zero for non-aromatic, saturated and unsaturated hydrocarbon rings. Sometimes NICS is considered as a local index rather than a global, aromatic index because contributions from remote parts of molecule are small. Later refinement of the original NICS tech-

Personal Use Only
Not For Distribution

nique offered better understanding of the aromatic systems which include the Dissected NICS technique which consists of the LMO-NICS method and the CMO-NICS method [12]. Other modifications like NICS rate and NICS scan are also known.

The major difficulty in quantifying aromaticity may be due to the fact that aromaticity is not a property of the ground state energy of molecules but is rather dependent on the excited π electron state. So a recent and a fresh approach, i.e., Quantitative Structure Aromaticity Relationships (QSArR) in relating aromaticity with physico-chemical molecular properties such as chemical hardness and electronegativity are reflected in the works of Putz. His works focuses on the connection of aromaticity with a reactivity index. If successfully applied, "It may provide both conceptual new insight on the aromaticity concept as well as generalization of the chemical reactivity theory and principles grounded on structural indices as electronegativity and chemical hardness that have been intensively considered in the last decades within density functional theory and quantum chemistry" [52-54].

CONCLUSION

Aromaticity is now no longer confined to the domain of organic chemistry and various inorganic clusters are found to be aromatic considering the delocalization of the π electrons as the genesis of aromaticity. The ease with which aromaticity bridges the gap between traditional aspects of organic chemistry and latest discoveries in inorganic chemistry are truly fascinating. Aromaticity is not a physically observable quantity so defining it precisely is still a challenge. Quantification of aromaticity is a major challenge to the theoretical and the computational chemists till date. Whether aromaticity is a multidimensional phenomenon or it can be defined by a universal single unique criterion is a debatable topic. The journey of aromaticity from Kekulés definition of benzene has been extensive and the recent developments in this field provide a considerable better insight into the concept. It is aptly said by Schleyer that, "aromaticity has been a time-dependent phenomenon." The perception of aromaticity is different in terms of its properties and characteristics to chemists with diverse backgrounds [55]. The magnetic criterion for defining the concept of aromaticity has become very prominent surpassing the other criteria. Various developments in this field have occurred in the recent years and most of the developments were in the magnetic domain. So we can conclude by saying that the magnetic criterion is the most important criterion and provides a plethora of opportunities of future work on aromaticity.

CONSENT FOR PUBLICATION

Not applicable.

CONFLICT OF INTEREST

The authors declare no conflict of interest, financial or otherwise.

ACKNOWLEDGEMENTS

Manoswita Homray and Pratim K. Chattaraj would like to thank CSIR, India for financial support and PKC would like to thank DST, New Delhi for the J. C. Bose National Fellowship.

REFERENCES

[1] Faraday, M. On new compounds of carbon and hydrogen, and on certain other products obtained during the decomposition of oil by heat. *Phil. Trans. R. Soc. Lond*., **1825**, *115*, 440-446.

[2] Kekulé, A. Sur la constitution des substances aromatiques. *Bull. Soc. Chim. Paris*, **1865**, *3*, 98-100.

[3] Kekulé, A. Ueber einige Condensations producte de Aldehyds. *Ann. Chem. Pharm*., **1866**, *137*, 129-196.

[4] Hückel, E. Zur quantentheorie der doppelbindung. *Z. Phys*., **1930**, *60*, 423-456.

[5] Hückel, E. Quantum-theoretical contributions to the benzene problem. I. The electron configuration of benzene and related compounds. *Z. Phys*., **1931**, *70*, 204-286.

[6] Hückel, E. Quantum theoretical contributions to the problem of aromatic and non-saturated compounds. *Z. Phys*., **1932**, *76*, 628-648.

[7] Hückel, E. The theory of unsaturated and aromatic compounds. *Z. Electrochem. Angew. Phys. Chem*., **1937**, *43*, 752-788.

[8] Hückel, E. Theory of the magnetism of so-called biradicals. *Z. Electrochem. Angew. Phys. Chem*., **1995**, *61*, 866-890.

[9] Pauling, L.; Wheland, G.W. The nature of the chemical bond. V. The quantum-mechanical calculation of the resonance energy of benzene and naphthalene and the hydrocarbon free radicals. *J. Chem. Phys*., **1933**, *1*, 362-374.

[10] (a) Balaban, A.T.; Oniciu, D.C.; Katritzky, A.R. Aromaticity as a cornerstone of heterocyclic chemistry. *Chem. Rev*., **2004**, *104*(5), 2777-2812. (b) Chattaraj, P.K.; Sarkar, U.; Roy, D.R.; Electronic structure principles and aromaticity. *J. Chem. Educ*., **2007**, *84*, 354.(c) Chattaraj, P.K.; Roy, D.R.; Elango, M.; Subramanian, V. Stability and reactivity of all-metal aromatic and antiaromatic systems in the light of the principles of maximum hardness and minimum polarizability. *J. Phys. Chem. A*, **2005**, *109*, 9590-9597.

[11] Noorizadeh, S.; Shakerzadeh, E. Shannon entropy as a new measure of aromaticity, Shannon aromaticity. *Phys. Chem. Chem. Phys*., **2010**, *12*(18), 4742-4749.

[12] Chen, Z.; Wannere, C.S.; Corminboeuf, C.; Puchta, R.; Schleyer, P.V.R. Nucleus-independent chemical shifts (NICS) as an aromaticity criterion. *Chem. Rev*., **2005**, *105*(10), 3842-3888.

[13] Krygowski, T.M.; Cyrański, M.K. Structural aspects of aromaticity. *Chem. Rev*., **2001**, *101*(5), 1385-1420.

[14] Poater, J.; Duran, M.; Solà, M.; Silvi, B. Theoretical evaluation of electron delocalization in aromatic molecules by means of atoms in molecules (AIM) and electron localization function (ELF) topological approaches. *Chem. Rev*., **2005**, *105*(10), 3911-3947.

[15] Cyrański, M.K. Energetic aspects of cyclic pi-electron delocalization: Evaluation of the methods of estimating aromatic stabilization energies. *Chem. Rev*., **2005**, *105*(10), 3773-3811.

[16] Matito, E.; Duran, M.; Solà, M. The aromatic fluctuation index (FLU): A new aromaticity index based on electron delocalization. *J. Chem. Phys*., **2005**, *122*(1), 014109.

[17] (a) Bultinck, P.; Ponec, R.; Van Damme, S. Multicenter bond indices as a new measure of aromaticity in polycyclic aromatic hydrocarbons. *J. Phys. Org. Chem*., **2005**, *18*(8), 706-718. (b) Roy, D.R.; Bultinck, P.; Subramanium, V.; Chattaraj, P.K. Bonding, reactivity and aromaticity in the light of the multicenter indices. *J. Mol. Struc*., **2008**, *854*(1-3), 35-39.

[18] Misra, A.; Klein, D.J.; Morikawa, T. Clar theory of molecular benzenoids. *J. Phy. Chem. A*, **2009**, *113*(6), 1151-1158.

[19] Clar, E. *The Aromatic Sextet*; Wiley & Sons: New York, **1970**.

[20] Misra, A.; Schmalz, T.G.; Klein, D.J. Clar theory of radical benzenoids. *J. Chem. Inf. Model*, **2009**, *49*(12), 2670-2676.

[21] Bhattacharya, D.; Panda, A.; Misra, A.; Klein, D.J. Clar theory extended for polyacenes and beyond. *J. Phys. Chem. A*, **2014**, *118*(24), 4325-4338.

[22] Cryański, M.K.; Krygowski, T.M.; Katritzky, A.R.; Schleyer, P.V.R. To what extent can aromaticity be defined uniquely? *J. Org. Chem*., **2002**, *67*(4), 1333-1338.

[23] Paul, S.; Goswami, T.; Misra, A. Noncomparative scaling of aromaticity through electron itinerancy. *AIP Adv*., **2015**, *5*, 107211.

[24] Schleyer, P.V.R.; Jiao, H. What is aromaticity? *Pure Appl. Chem*., **1996**, *68*, 209-218.

[25] Islas, R.; Chamorro, E.; Robles, J.; Heine, T.; Santos, J.C.; Merino, G. Borazine: To be or not to be aromatic. *Struct. Chem*., **2007**, *18*, 833-839.

[26] Stock, A.; Pohland, E. Borwasserstoffe, IX. B3N3H6. *Chem. Ber*., **1926**, *59B*, 2215-2223.

[27] Bhattacharya, D.; Shil, S.; Misra, A.; Bytautasc, L.; Klein, D.J. A perspective on designing chiral organic magnetic molecules with unusual behavior in magnetic exchange coupling. *Phys. Chem. Chem. Phys*., **2015**, *17*, 14223.

[28] Mo, Y.; Peyerimhoff, S.D. Theoretical analysis of electronic delocalization. *J. Chem. Phys*., **1998**, *109*(5), 1687-1697.

[29] Pauling, L.; Sherman, J. The nature of the chemical bond. VI. The calculation from thermochemical data of the energy of resonance of molecules among several electronic structures. *J. Chem. Phys*., **1933**, *1*(8), 606-617.

[30] Hehre, W.J.; Radom, L.; Schleyer, P.V.R.; Pople, J.A. *Ab Initio Molecular Orbital Theory*; Wiley & Sons: New York, **1986**.

[31] Hehre, W.J.; McIver, R.T.; Pople, J.A.; Schleyer, P.V.R. Alkyl substituent effects on the stability of protonated benzene *J. Am. Chem. Soc*., **1974**, *96*(22), 7162-7163.

[32] Pedley, J.B.; Naylor, R.B.; Kirby, S.P. *Thermodynamical Data of Organic Compounds*; Chapman & Hall: London, **1986**.

[33] Jose, M.M.; Boldyrev, A.I.; Merino, G.; Ugalde, M.J. Recent developments and future prospects of all-metal aromatic compounds. *Chem. Soc. Rev*., **2015**, *44*, 6519-6534.

Personal Use Only
Not For Distribution

[34] Poater, J.; Fradera, X.; Duran, M.; Solá, M. The delocalization index as an electronic aromaticity criterion: Application to a series of planar polycyclic aromatic hydrocarbons. *Chem-Eur. J.*, **2003**, *9*(2), 400-406.

[35] Poranne, G.P.; Stranger, A. Magnetic criteria of aromaticity. *Chem. Soc. Rev.*, **2015**, *44*, 6597- 6615.

[36] (a) Dewar, M.J.S.; McKee, M.L. σ-Aromaticity in hexa-group 16 atom-substituted benzene dications: A theoretical study. *Pure Appl. Chem.*, **1980**, *52*, 1431-1441. (b) Dewar, M.J.S. σ-Conjugation and σ-aromaticity. *Bull. Soc. Chim. Belg.*, **1979**, *88*, 957-967.

[37] Pople, J.A. Molecular orbital theory of aromatic ring currents. *Mol. Phys.*, **1958**, *1*, 175-180.

[38] Gomes, A.N.F.; Mallion, R.B. Aromaticity and ring currents. *Chem. Rev.*, **2001**, *101*, 1349-1384.

[39] Mitchell, R.H. Measuring aromaticity by NMR. *Chem. Rev.*, **2001**, *101*, 1301-1315.

[40] Benassi, R.; Lazzeretti, P.; Taddei, F. Magnetic criteria for aromaticity. *J. Phys. Chem.*, **1975**, *79*(8), 848-851.

[41] Coriani, S.; Lazzeretti, P.; Malagoli, M.; Zanasi, R. On CHF calculations of second-order magnetic properties using the method of continuous transformation of origin of the current density. *Theor. Chim. Acta*, **1994**, *89*, 181-192.

[42] Lazzeretti, P.; Malagoli, M.; Zanasi, R. Computational approach to molecular magnetic properties by continuous transformation of the origin of the current density. *Chem. Phys. Lett.*, **1994**, *220*, 299-309.

[43] Zanasi, R. Coupled Hartree-Fock calculations of molecular magnetic properties annihilating the transverse paramagnetic current density. *J. Chem. Phys.*, **1996**, *105*, 1460-1469.

[44] Steiner, E.; Fowler, P.W. Patterns of ring currents in conjugated molecules: A few-electron model based on orbital contributions. *J. Phys. Chem. A*, **2001**, *105*, 9553-9562.

[45] Steiner, E.; Fowler, P.W. Four- and two-electron rules for diatropic and paratropic ring currents in monocyclic π systems. *Chem. Commun.*, **2001**, (21), 2220-2221.

[46] Steiner, E.; Fowler, P.W.; Havenith, R.W.A. Current densities of localized and delocalized electrons in molecules. *J. Phys. Chem. A*, **2002**, *106*, 7048-7056.

[47] Schleyer, P.V.R; Maerker, C.; Dransfeld, A.; Jiao, H.; Hommes, N.J.R. Nucleus-independent chemical shifts: A simple and efficient aromaticity probe. *J. Am. Chem. Soc.*, **1996**, *118*, 6317-6318.

[48] London, F. Théorie quantique des courants interatomiques dans les combinaisons aromatiques. *J. Phys. Radium.*, **1937**, *8*, 397.

[49] a) Cheeseman, J.R.; Trucks, G.W.; Keith, T.A.; Frisch, M.J. A comparison of models for calculating nuclear magnetic resonance shielding tensors. *J. Chem. Phys.*, **1996**, *104*, 5497. (b) Schreckenbach, G.; Ziegler, T. Calculation of NMR shielding tensors using Gauge-Including Atomic Orbitals and modern density functional theory. *J. Phys. Chem.*, **1995**, *99*, 606-611. (c) Schreckenbach, G.; Ziegler, T. Density functional calculations of NMR chemical shifts and ESR g-tensors. *Theor. Chem. Acc.*, **1998**, *99*, 71-82.

[50] Chattaraj, P.K. *Aromaticity and Metal Clusters*; CRC Press: Florida, **2010**.

[51] Schleyer, P.V.R; Jiao, H.; Hommes, N.J.R.; Malkin, V.G.; Malkina, O. An evaluation of the aromaticity of inorganic rings: Refined evidence from magnetic properties. *J. Am. Chem. Soc.*, **1997**, *119*, 12669-12670.

[52] Putz, M.V. On absolute aromaticity within electronegativity and chemical hardness reactivity pictures. *MATCH Commun. Math. Comput. Chem.*, **2010**, *64*, 391-418.

[53] Putz, M.V. Compactness aromaticity of atoms in molecules. *Int. J. Mol. Sci.*, **2010**, *11*, 1269-1310.

[54] Tarko, L.; Putz, M.V. On electronegativity and chemical hardness relationships with aromaticity. *J. Math. Chem.*, **2010**, *47*(1), 487-495.

[55] Schleyer, P.V.R. Introduction: Aromaticity. *Chem. Rev.*, **2001**, *101*, 1115-1118.

[56] Bultinck, P. General discussion. *Faraday Discussions*, **2007**, *135*, 367-401.

Personal Use Only
Not For Distribution

PCCP

COMMUNICATION

View Article Online
View Journal | View Issue

Check for updates

Cite this: *Phys. Chem. Chem. Phys.*, 2017, **19**, 11744

Received 29th March 2017,
Accepted 18th April 2017

DOI: 10.1039/c7cp02031g

rsc.li/pccp

Published on 18 April 2017. Downloaded by University of North Bengal on 3/4/2019 11:25:14 AM.

On *exo*-cyclic aromaticity†

Tamal Goswami, Manoswita Homray, Satadal Paul, Debojit Bhattacharya and Anirban Misra *

The domain of aromaticity spans a wide range of molecules, from polycyclic aromatic hydrocarbons, heterocycles to all-metal systems. Here, *in silico* we demonstrate the aromaticity in $C_2B_2F_4$, extending beyond the limit of conventional aromatic molecules. This molecule gains the magic number of six π-electrons through an unusual electronic contribution from *exo*-cyclic atoms. The stability of the molecule is established through density functional theory, *ab initio* calculations as well as molecular dynamics simulation.

The unequivocal definition of aromaticity has long been a subject to delve into. The aromatic nature is correlated with a multitude of structural and energetic characteristics, such as highly symmetric structures, delocalized electrons, enhanced thermodynamic stability, and reduced reactivity as compared to nonaromatic compounds and so on.[1–4] Another prominent indication of the aromatic character comes from the properties like down-field shift in proton NMR peak positions resulting from the exaltation of diamagnetic susceptibility.[5,6] However, even after two centuries of existence,[7,8] still there is scope for defining aromaticity unambiguously,[9] as understood from two legendary examples of the complementary topological definition of aromaticity by Hückel[10] and Möbius.[11] The proposition by Hückel that a cyclic-planar $(4n + 2)$ π-electron characterizes aromatic compounds is taken as gospel by chemists.[10] Archetypal aromatic molecules contain a planar ring framework with equalized bond lengths. Though, Hückel's $(4n + 2)$ π rule is the easiest test to recognize aromaticity, its multidimensional nature often stands in the way of precisely identifying aromatic systems.[12–15] This apparently simple electron count rule was renewed by Dewer's insight into the tropolone structure.[16] In 1922 Crocker noticed that the "aromatic structure is observed only in those combinations of elements which furnish six extra or aromatic electrons above those needed to complete a single-bonded ring" and described accurately the "six aromatic electron" structure[17] of benzene, pyridine, and five-membered ring heteroaromatics, earlier than the famous "aromatic sextet" paper by Armit and Robinson.[18]

Aromatic cross-conjugated systems make it apparent that aromaticity must not be restricted only to the completely conjugated cyclic circuits.[19] This inspires us to study a four membered heteroatomic cyclic $C_2B_2F_4$ molecule with D_{2h} symmetry (Fig. 1). Optimization of this molecule at different levels of theory including coupled-cluster singles, doubles (CCSD) leads to a planar molecule (dihedral angle 0.00°, Table S1 of the ESI†), which is in agreement with the conclusions drawn in a recent report.[20] Geometry optimization is carried out from two different starting geometries, namely, rectangular and non-planar, to explore the possible existence of any isomer, specifically a bond-stretch isomer,[21–23] of the present molecule. The convergence steps along with the energy of the final geometries from two different starting points suggest that both optimizations converge to the same structure depicting a planar as well as square C_2B_2 core (Fig. S1 of the ESI†). The details of the computational methodology employed in the present work are given in the ESI.†

The dynamical stability of the molecule is confirmed from the absence of imaginary vibrational frequency (Table S1 of the ESI†) and also by molecular dynamics (MD) simulation. No sign

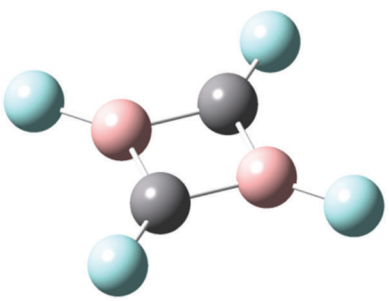

Fig. 1 Optimized structure of the $C_2B_2F_4$ cluster with D_{2h} symmetry. The gray, pink and cyan spheres represent carbon, boron and fluorine atoms respectively.

Department of Chemistry, University of North Bengal, Darjeeling 734013, India. E-mail: anirbanmisra@yahoo.com; Tel: +919434228745

† Electronic supplementary information (ESI) available: Experimental procedures. See DOI: 10.1039/c7cp02031g

This journal is © the Owner Societies 2017

Published on 18 April 2017. Downloaded by University of North Bengal on 3/4/2019 11:25:14 AM.

Table 1 Summary of structural and energy decomposition parameters of $C_2B_2F_4$ computed at the B3LYP/aug-cc-pVDZ level

Parameters	Computed values
B–C bond length (Å)	1.532
B–F bond length (Å)	1.339
C–F bond length (Å)	1.322
ΔE_{Pauli} (kcal mol^{-1})	1812.90
ΔE_{elstat} (kcal mol^{-1})	−488.57
ΔE_{orb} (kcal mol^{-1})	−1699.05
ΔE_{int} (=ΔE_{Pauli} + ΔE_{elstat} + ΔE_{orb}) (kcal mol^{-1})	−374.72

of deformation is noted within 5 ps duration in the MD simulation at 300 K (see Fig. S2–S4 of the ESI†). The structural stability is often established from the binding energy of the molecule from individual atomic fragments. The larger the total binding energy, the more stable is the system. A large total binding energy (−1290.49 kcal mol^{-1}) thus advocates for the structural integrity of the system. The total binding energy is decomposed into two major components, namely, ΔE_{prep} and ΔE_{int}, *i.e.*, $\Delta E = \Delta E_{prep} + \Delta E_{int}$, for convenience and ΔE_{int} is further decomposed into three physically meaningful terms, $\Delta E_{int} = \Delta E_{elstat} + \Delta E_{Pauli} + \Delta E_{orb}$ (see the ESI† for details). The structural and energy decomposition parameters computed at the B3LYP/aug-cc-pVDZ level are reported in Table 1. The reasonably high negative value of the total interaction energy (ΔE_{int}) also signifies high stability of the molecule. Moreover, the ring strain energy value (see the ESI† for details) is also in the range of reportedly stable four membered carbocycles and indicates structural stability. Followed by the validation of structural stability, the internal stability of the wave function is also confirmed with STABLE = OPT keyword implemented in Gaussian 09W.[24] The stable closed-shell electronic structure of the molecule is also indicated by a negligibly small diradical character, y_i of 0.006 (see the ESI†). The closed-shell nature of the molecule is further substantiated by the large HOMO–LUMO gap of 5.2 eV.[25] Hence, the criteria of chemical viability proposed by Hoffmann *et al.* are convincingly fulfilled.[26]

Satisfactory stability of the ring structure in $C_2B_2F_4$ stimulates to probe the possibility of cyclic electronic delocalization leading to aromaticity. Nucleus-independent chemical shift (NICS) is often considered as one of the superlative descriptors of aromaticity and is computed in terms of the isotropic shielding tensor on a dummy atom in the GIAO (Gauge Independent Atomic Orbitals) method.[27] A system is defined as aromatic (antiaromatic) based on the negative (positive) sign of the shielding tensor values, implying the presence of a diatropic (paratropic) ring current.[13] To find out the contribution of σ and π electrons to aromaticity, NICS has been calculated both in the center of the ring [NICS (0)], and at 1 Å above the plane [NICS(1)]. The negative values of NICS (0) and NICS(1), computed at different levels of theory (Table S2 of the ESI†) provide strong indication in favour of the aromatic nature of $C_2B_2F_4$. Dissected canonical molecular orbital NICS (CMO-NICS) analysis is performed to identify orbitals with maximal contribution to NICS and hence to aromaticity. The orbitals that render significant diamagnetic contribution to the total NICS(1), which is found to be −6.33, are presented in Fig. 2. The CMO-NICS(1) analysis (Fig. 2) reveals the strongest diatropic contribution of the lowest occupied π-orbital (HOMO−10) towards the NICS(1) value compared to modest contribution from higher π-orbitals (HOMO−6 & HOMO). Nevertheless, a larger value of NICS(1) compared to NICS(0) suggests a major contribution of π-electrons to aromaticity. In a recent work, the energy stabilization due to delocalization of π-electrons is equated with aromatic stabilization energy (ASE) in the frame of second order perturbation theory (see the ESI† for details).[28] The ASE is found to be 10.84 kcal mol^{-1}, which also suggests a substantial stabilization due to aromaticity. Visualization of the induced current density has been proved to be a useful tool for the study of aromaticity.[29] The vector plot of current density for the present molecule (Fig. S5 of the ESI†) exhibits the diatropic ring current for both π- and σ-planes illustrating the aromatic nature of the molecule. The peculiarity of π-electron flow gives rise to ring currents of the adaxial–abaxial–adaxial pattern, as visualized in the current density vector map (Fig. S5 of the ESI†).

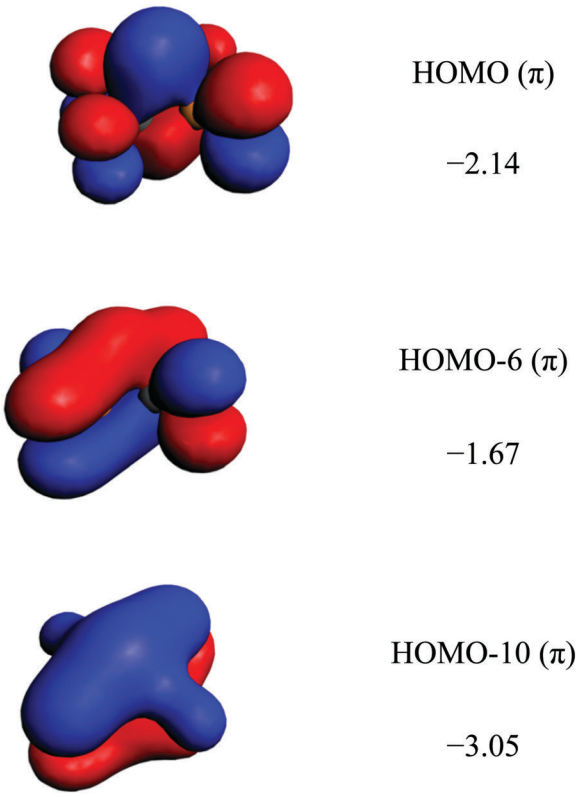

Fig. 2 CMO-NICS analysis at 1 Å above the ring center of the $C_2B_2F_4$ molecule (D_{2h}).

A very interesting fact that shows up in the CMO-NICS analysis is that the MO (HOMO−10 in Fig. 2) which has the largest contribution to NICS(1) includes F atoms as a major component. This indicates the involvement of B←F back-donated electrons to the aromatic π-cloud above and below the molecular plane. With these points, we infer that the molecular system is aromatic consisting of six π-electrons. Out of these six π-electrons, two electrons are from the p_z-orbitals of the sp^2

Published on 18 April 2017. Downloaded by University of North Bengal on 3/4/2019 11:25:14 AM.

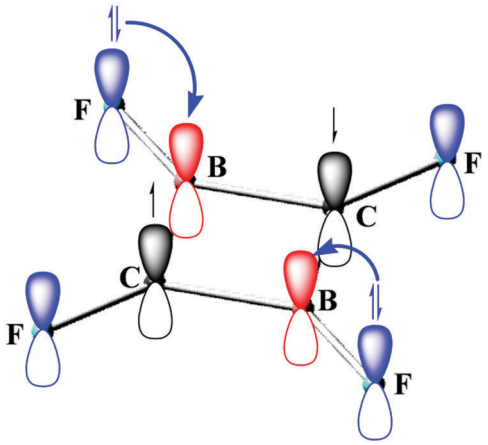

Fig. 3 Orbital diagram for six π-electrons in $C_2B_2F_4$. The blue arrows indicate the role of the B←F back-bonding electrons to the formation of the aromatic π-cloud.

hybridized carbon atoms and the other four electrons are obtained through back-donation of paired electrons from fluorine to locally electron-deficient boron (Fig. 3). Moreover, the ring current map (Fig. S5 of the ESI†) sustains the present model by displaying the π-density to be extended beyond the parent C_2B_2 ring up to the two B←F units in the molecule.

The key evidence in favor of our model comes from the energy decomposition analysis based on the extended transition state method and natural orbital for chemical valence scheme (ETS-NOCV).[30,31] The difference density, portrayed in Fig. 4, dictates the involvement of the π-electrons of fluorine attached to boron in forming the aromatic π-electron cloud between the core C_2B_2-rings. Other than the dominant deformation channels corresponding to sigma bond formation between the fragments, a significant stabilization of −100 kcal mol^{-1} comes from the channel illustrating the flow of bonding electron pair from fluorine to the vacant $2p_z$-atomic orbitals of boron atoms. It is also noticed from Table 1 that a significant contribution to ΔE_{int} comes from the orbital interaction energy which also supports the current model.

Adaptive Natural Density Partitioning (AdNDP)[32] is a new tool which can help to visualize the chemical bonding in a molecule in the most general way. AdNDP reveals the delocalized bonding elements related to the notion of aromaticity and antiaromaticity without taking the concept of resonance into account. Treating the electron pairs as the main element of chemical bonding, it models an electronic structure of a molecule in terms of *n*-center–2-electron (*nc*–2e) bonds. Here, *n* spans in the interval from one to the total number of atoms in the molecule. Other than the Lewis bonding elements (1c–2e and 2c–2e, corresponding to the core electrons and lone pairs, and two-center two-electron bonds) it also picks up *nc*–2e delocalized bonding elements. The search for the all-center 2-electron bond in the molecule reveals an unambiguous description of aromaticity in $C_2B_2F_4$. The AdNDP orbital, portrayed in Fig. 5a, predicts the aromatic π-cloud to span fluorine atoms attached to the boron atoms extending the central C_2B_2-ring, thus showing an *exo*-cyclic aromatic conjugation of π-electrons. This doubly occupied 6-centered-2-electron orbital portrays the contribution of the said fluorine atoms to the aromatic character. Thus, this description of *exo*-cyclic aromaticity in the molecule is an extension beyond the classical concept of aromatic molecules with a cyclic $(4n + 2)$ π conjugated system.

An *in silico* testing of analogous systems with no back donation of 4 π-electrons to the empty $2p_z$-orbital of the boron atom stands necessary to establish the *exo*-cyclic nature of aromaticity in $C_2B_2F_4$. Thus, we chose to replace the F atoms attached to boron with hydrogen atoms. Harmonic frequency and NICS calculations are performed to judge the stability and aromaticity of the system. The minimum vibrational frequency of 29.93 cm^{-1} lies at a lower range, which evidently questions about its viability compared to $C_2B_2F_4$ at the first instance. Instability in this system also arises out of the σ-antiaromaticity as manifested by the positive values of NICS (0) (Table S3 of the ESI†). Inspection of the results obtained from AdNDP calculations, performed for $C_2B_2F_2H_2$, reveals the involvement of only 2 π-electrons in the aromatic cloud which is centred only on the C_2B_2-core unlike $C_2B_2F_4$. This fact unambiguously proves the participation of the back donated π-electrons of p_z-orbitals from B←F in $C_2B_2F_4$. Similar tests with $C_2B_2Cl_4$, $C_2B_2Br_4$ and $C_2B_2I_4$ are also performed and it can be concluded that such systems will also be very unstable and will be 2 π-electron aromatic (Tables S3 and S4 and subsequent discussions in the ESI†).

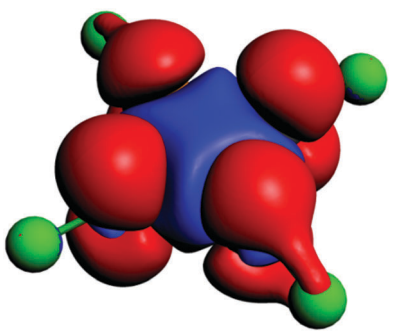

Fig. 4 The ETS-NOCV difference density plot corresponding to −100 kcal mol^{-1} stabilization. The blue and red surfaces represent regions of the electron concentration and electron depletion (isosurface of 0.003 a.u.) respectively.

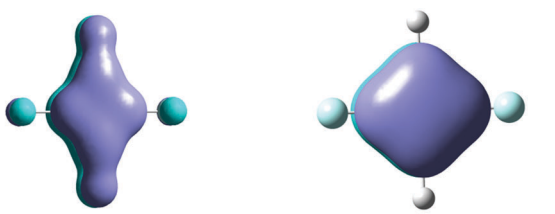

Fig. 5 The top-view of the AdNDP orbitals of $C_2B_2F_4$ (a) and $C_2B_2F_2H_2$ (b) along with their natural occupation numbers.

This journal is © the Owner Societies 2017

Published on 18 April 2017. Downloaded by University of North Bengal on 3/4/2019 11:25:14 AM.

In essence, the $C_2B_2F_4$ molecule acquires aromaticity due to unusual participation of *exo*-cyclic atoms. Back donation of 4 π-electrons from peripheral fluorine atoms to the electron-deficient boron atoms helps the ring to gain the magic number of 6 π-electrons leading to a unique *exo*-cyclic aromaticity. Moreover, the existence of a molecule with a similar C_2B_2 core (compound III/IV in ref. 33) makes us optimistic about the experimental realization of the molecule in near future.

Acknowledgements

Financial support from CSIR, India, is thankfully acknowledged. We also thank Prof. Souvik Maiti of the Institute of Genomics and Integrative Biology, New Delhi, India, for providing access to computational facility for molecular dynamics calculations. The authors are thankful to Prof. Basudeb Basu, University of North Bengal, for fruitful discussions. This work is dedicated to Prof. D. J. Klein of Texas A&M University of Galveston, on the occasion of his forthcoming 75th birthday.

References

1 P. J. Garratt, *Aromaticity*, John Wiley & Sons, 1986.
2 V. I. Minkin, M. N. Glukhotsev and B. Y. Simkin, *Aromaticity and Antiaromaticity: Electronic and Structural Aspects*, John Wiley & Sons, Inc., New York, 1994.
3 F. Bickelhaupt and W. H. de Wolf, *Recl. Trav. Chim. Pays-Bas*, 1988, **107**, 459–478.
4 P. A. Kraakman, J.-M. Valk, H. A. G. Niederländer, D. B. E. Brouw-er, F. M. Bickelhaupt, W. H. de Wolf, F. Bickelhaupt and C. H. Stam, *J. Am. Chem. Soc.*, 1990, **112**, 6638–6646.
5 P. V. R. Schleyer and H. Jiao, *J. Pure Appl. Chem.*, 1996, **68**, 209–218.
6 F. A. Carey and R. J. Sundberg, *Advanced Organic Chemistry: Structure And Mechanisms (Part A)*, Springer, 2000.
7 M. Faraday, *Philos. Collect. R. Soc. London*, 1825, **115**, 440–466.
8 A. Kekulé, *Bull. Soc. Chim. Fr.*, 1865, **3**, 98–110.
9 A. T. Balaban, P. V. R. Schleyer and H. S. Rzepa, *Chem. Rev.*, 2005, **105**, 3436–3447.
10 E. Huckel, *Z. Phys.*, 1931, **70**, 204–286.
11 E. Heilbronner, *Tetrahedron Lett.*, 1964, **5**, 1923–1926.
12 A. T. Balaban, *Pure Appl. Chem.*, 1980, **52**, 1409–1429.
13 A. Katrizky, P. Barczymski, G. Musumarra, D. Pisano and M. Szafran, *J. Am. Chem. Soc.*, 1989, **111**, 7–15.
14 P. V. R. Schleyer, C. Maerker, A. Dransfeld, H. Jiao and N. J. R. V. E. Hommes, *J. Am. Chem. Soc.*, 1996, **118**, 6317–6318.
15 A. Misra, D. J. Klein and T. Morikawa, *J. Phys. Chem. A*, 2009, **113**, 1151–1158.
16 M. J. S. Dewar, *Nature*, 1950, **166**, 790–791.
17 E. C. Crocker, *J. Am. Chem. Soc.*, 1922, **44**, 1618–1630.
18 J. W. Armit and R. Robinson, *J. Chem. Soc.*, 1925, **127**, 1604–1618.
19 P. Gund, *J. Chem. Educ.*, 1972, **49**, 100–103.
20 W. C. McKee, J. I. Wu, M. Hofmann, A. Berndt and P. V. R. Schleyer, *Org. Lett.*, 2012, **14**, 5712–5715.
21 T. Goswami, S. Paul, S. Mandal, A. Misra, A. Anoop and P. K. Chattaraj, *Int. J. Quantum Chem.*, 2015, **115**, 426–433.
22 S. Giri, R. P. S. A. Kumar, A. Chakraborty, D. R. Roy, S. Duley, R. Parthasarathi, M. Elango, R. Vijayaraj, V. Subramanian, G. Merino and P. K. Chattaraj, *Aromaticity and Metal Clusters*, CRC Press, USA, 2011.
23 P. K. Chattaraj, R. Das, S. Duley and J.-L. Vigneresse, *Theor. Chem. Acc.*, 2012, **131**, 1089–1096.
24 R. Seeger and J. A. Pople, *J. Chem. Phys.*, 1977, **66**, 3045–3050.
25 D. Dohnert and J. Koutecky, *J. Am. Chem. Soc.*, 1980, **102**, 1789–1796.
26 R. Hoffmann, P. V. R. Schleyer and H. F. Schaefer, *Angew. Chem., Int. Ed.*, 2008, **47**, 7164–7167.
27 K. Wolinski, J. F. Hinton and P. Pulay, *J. Am. Chem. Soc.*, 1990, **112**, 8251–8260.
28 S. Paul, T. Goswami and A. Misra, *AIP Adv.*, 2015, **5**, 107211.
29 E. Steiner, P. W. Fowler, A. Soncini and L. W. Jenneskens, *Faraday Discuss.*, 2007, **135**, 309–323.
30 M. Mitoraj and A. Michalak, *J. Mol. Model.*, 2007, **13**, 347–355.
31 M. P. Mitoraj, A. Michalak and T. Ziegler, *J. Chem. Theory Comput.*, 2009, **5**, 962–975.
32 D. Y. Zubarev and A. I. Boldyrev, *Phys. Chem. Chem. Phys.*, 2008, **10**, 5207–5217.
33 D. Bromm, D. Stalke, A. Heine and A. Miller, *J. Organomet. Chem.*, 1990, **386**, 1–7.

Bull. Mater. Sci. (2019) 42:46
https://doi.org/10.1007/s12034-018-1718-8

© Indian Academy of Sciences

Check for updates

Manifestation of exo-cyclic aromaticity in triangular heterocyclic B_2F_2X systems (X = O, S, Se, NH)

MANOSWITA HOMRAY, SATADAL PAUL and ANIRBAN MISRA*
Department of Chemistry, University of North Bengal, Darjeeling 734013, India
*Author for correspondence (anirbanmisra@yahoo.com)

MS received 14 June 2018; accepted 13 August 2018; published online 12 February 2019

Abstract. Aromaticity is an important concept in chemistry which extends over a wide range of molecular systems and imparts unique features to the molecules possessing it. In the present work, novel heteroatomic molecular systems are proposed which demonstrate non-conventional aromaticity where the molecules accomplish the aromatic sextet and hence stabilization through the conjugation of π-electrons from exo-cyclic substituents. A considerable σ-aromaticity is also observed which does not involve the exo-cyclic atoms. At first, the stability of these molecular systems is theoretically ascertained through various density functional theory and *ab-initio* calculations along with the energy decomposition analysis, *T*1 diagnostic run, estimation of ring strain energy and highest occupied molecular orbital–lowest unoccupied molecular orbital gap which indicate towards the viability of these molecular systems. Then, a detailed study of aromaticity with the aid of different computational probes such as nucleus-independent chemical shift (NICS), dissected canonical molecular orbital-NICS analysis, multi-centre bond index (MCI), adaptive natural density partitioning and theoretical tools such as aromatic stabilization energy based on a fully *ab-initio* approach are performed which establish unique exo-cyclic aromaticity in these systems.

Keywords. Aromaticity; exo-cyclic; nucleus-independent chemical shift; multi-centre bond index; aromatic stabilization energy.

1. Introduction

The idea of aromaticity is an age old concept [1–3], but its purpose and relevance is continually on the rise. Aromaticity can be considered as one of the most intriguing phenomena in chemistry which is evolving with time. The perception of aromaticity is associated with certain specific molecular characteristics, such as added stabilization, planarity of molecular systems, conjugation, electron delocalization [4–7] and most importantly, a distinct reaction to applied magnetic field [8–11]. Presently, aromaticity is not the idea involving organic systems only, but has incorporated all metal aromatic clusters [12–22] as well. Conjecture of aromaticity in planar π-electron systems by Huckel's $(4n + 2)$ rule [23] is one of the best recognized and the most functional methods. In recent times, there has been augmented interest in understanding and development of varied criteria for defining aromaticity [24–26]. Apart from the primary measures for defining aromaticity [27–29], it has also been explained by electron density based indices [30–34]. Lately, aromaticity has become a significant tool in defining the stability and bonding in various chemical species surpassing the realm of organic chemistry [35–38] extending to inorganic moieties [20–22]. Also, acyclic compounds have been found to have aromatic stability [39] thus, implying that aromaticity can no longer be confined to the field of classical conjugated organic systems. In a recent theoretical work, it has been shown that exo-cyclic aromaticity is possible in planar systems; i.e., aromaticity is achieved through back-donation of electrons from the substituents [40]. The concept of 2p–2p orbital interaction or back-donation of fluorine has been well identified in the organic and inorganic domains [41–43]. Both the inductive effect and the resonance or the back-donation effect play a vital role when the non-bonded pair of electrons of fluorine interact with the vacant orbital of the boron atom to which it is attached. The tendency of back-donation by fluorine has been established to be greater than that of the other halogen atoms, such as chlorine and bromine, where the order of back-donation is found to be $F > Cl \gg Br$ [44]. The degree of back-donation decreases with the increase in the atomic sizes of the halogens since the 2p–2p interaction is more favourable as compared to the interaction between 3p and 4p orbitals of chlorine and bromine, respectively, with the vacant 2p orbital of boron due to mismatch in the size of the orbitals.

In this work, we theoretically propose novel heteroatomic systems where exo-cyclic aromaticity is observed which is

Electronic supplementary material: The online version of this article (https://doi.org/10.1007/s12034-018-1718-8) contains supplementary material, which is available to authorized users.

achieved through back-donation of electrons from exo-cyclic fluorine atoms. The systems studied are cyclic heteroatomic B_2F_2X (where X = O, S, Se, NH) molecules (figure 1). To understand the bonding and the structural properties of these systems, a systematic theoretical study has been performed. The molecules are optimized at different levels of theory using various density functional theory (DFT) and *ab-initio* methodologies involving coupled-cluster singles and doubles (CCSD). The stability of the molecules is validated by the absence of any imaginary frequency, energy decomposition analysis (EDA) [45] computation of the ring strain energy (RSE) [46] and higher highest occupied molecular orbital–lowest unoccupied molecular orbital (HOMO–LUMO) gaps. The aromaticity is analysed and estimated through nucleus independent chemical shift (NICS) [47], canonical molecular orbital-NICS (CMO-NICS) [48], multi-centre bond index (MCI) [31], adaptive natural density partitioning (AdNDP) [49] and aromatic stabilization energy (ASE) [50]. As a whole, this work elucidates exo-cyclic aromaticity in novel systems with three-membered heteroatomic rings.

2. Computational details

Gaussian 09W suite of software was used for the minimum energy search and frequency calculation at various DFT (UB3LYP, UB3PW91, UPBEPBE, UBLYP and UCAM-B3LYP) and *ab-initio* (UCISD, UQCISD and UCCSD) methodologies using the aug-cc-pvdz basis set, $T1$ diagnostic run was carried out at the UCCSD(t1diag)/aug-cc-pvdz level, computation of the HOMO–LUMO gap at the ub3lyp/aug-cc-pvdz level and NICS evaluation at various DFT levels (UB3LYP, UB3PW91, UPBEPBE, UBLYP and UCAM-B3LYP) with the aug-cc-pvdz basis set [51]. EDA at the UB3LYP/aug-ATZP level and the CMO-NICS evaluation at the LDA/DZ level are performed using the ADF program [52]. RSE is calculated using the AIM version program [53] at the UB3LYP/aug-cc-pvdz level. The chemical bonding analysis employing the AdNDP orbitals are visualized and the MCI is calculated at the UB3LYP/aug-cc-pvdz level using Multiwfn (a multifunctional wave function analysis) [54]. For the calculation of ASE, Gaussian 09W suite of software, Multiwfn and OpenMX 3.6 quantum chemistry code [55] are used.

3. Results and discussion

3.1 *Molecular geometry*

The optimized structures of the heteroatomic molecules B_2F_2X (where X = O, S, Se, NH) with their bond lengths in Å and B–X–B bond angles in degrees as computed at the uccsd/aug-cc-pvdz level of theory are given in figure 1. The greater stability of the molecular systems can be accounted from the high minimum frequency value, the viability of the molecules are further substantiated by the absence of an imaginary frequency and the existence of a low ground state minimum energy as provided in table 1 for the B_2F_2O

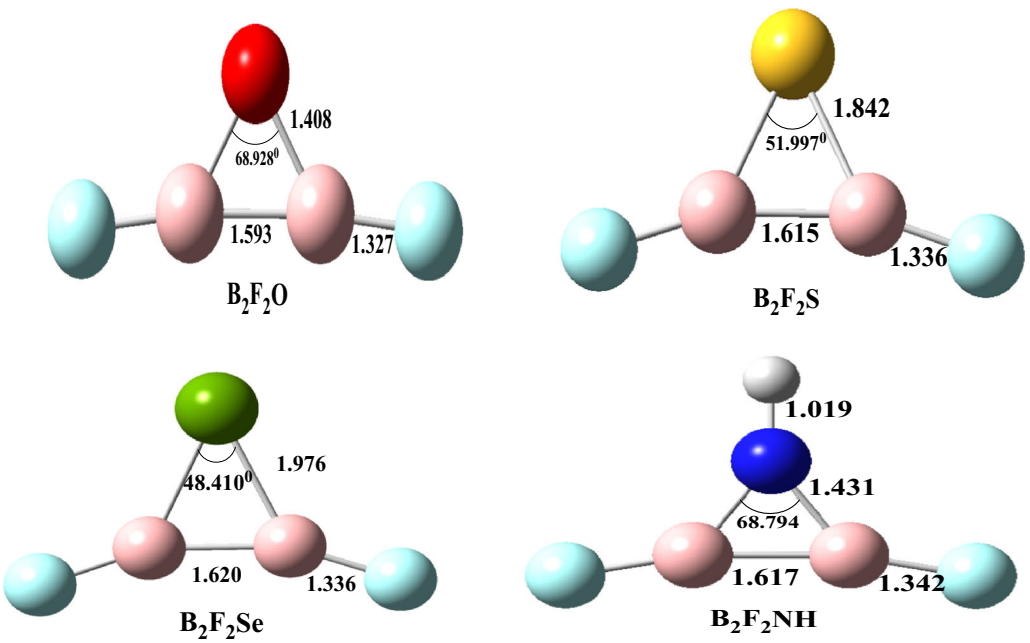

Figure 1. Optimized structures of B_2F_2O, B_2F_2S, B_2F_2Se and B_2F_2NH and their bond lengths in Å and the B–X–B bond angles in degrees computed at the UCCSD/aug-cc-pvdz level; boron, fluorine, oxygen, sulphur, selenium, nitrogen and hydrogen are represented by pink, cyan, red, yellow, green, blue and grey, respectively.

Table 1. The optimized bond lengths (Å), bond angles (°), minimum energy (a.u.) and minimum frequency (cm^{-1}) of B_2F_2O at different unrestricted DFT and *ab-initio* methodologies using the aug-cc-pvdz basis set.

Methodology (along with aug-cc-pvdz)	B–B bond length, Å	B–O bond length, Å	B–F bond length, Å	∠B–O–B, ∘	Minimum energy, a.u.	Minimum frequency, cm^{-1}
UCISD	1.58074	1.39251	1.31694	69.16405	−324.00	265.04
UQCISD	1.59440	1.41052	1.32888	68.82957	−324.03	251.94
UCCSD	1.59361	1.40804	1.32725	68.92894	−324.03	254.06
UB3LYP	1.57700	1.39737	1.31793	68.70360	−324.78	248.88
UB3PW91	1.57498	1.39795	1.31700	68.57105	−324.65	248.34
UPBEPBE	1.58413	1.41404	1.32735	68.13154	−324.44	236.47
UBLYP	1.58608	1.41416	1.32954	68.22043	−324.74	237.57
UCAM-B3LYP	1.57211	1.38981	1.31292	68.88600	−324.68	251.03

Table 2. Summary of energy decomposition parameters of B_2F_2O, B_2F_2S, B_2F_2Se and B_2F_2NH computed at the UB3LYP/aug-cc-pvdz level.

Molecules	ΔE_{Pauli}, kcal mol^{-1}	ΔV_{elstat}, kcal mol^{-1}	ΔE_{orb}, kcal mol^{-1}	$\Delta E_{int} = \Delta E_{Pauli} + \Delta V_{elstat} + \Delta E_{orb}$, kcal mol^{-1}
B_2F_2O	2954.85	−667.25	−2780.13	−492.53
B_2F_2S	2607.85	−612.66	−2419.45	−424.26
B_2F_2Se	2521.45	−602.87	−2380.41	−461.83
B_2F_2NH	3362.75	−717.70	−3265.88	−620.83

system. The optimization data for the other molecular systems are provided in supplementary tables S1–S3. The structural reliability of the molecular systems is further established through EDA based on the approach of Ziegler and Rauk [45]. The individual atomic fragments are taken into consideration for the EDA. In this method, the interaction energy (ΔE_{int}) is divided into three major components namely electrostatic interaction (ΔV_{elstat}), Pauli repulsive orbital interaction (ΔE_{Pauli}) and attractive orbital interaction (ΔE_{orb}) as given below:

$$\Delta E_{int} = \Delta V_{elstat} + \Delta E_{Pauli} + \Delta E_{orb}. \quad (1)$$

Here, the ΔV_{elstat} represents the classical electrostatic interaction between the fragments as they are brought together to form the final complex. ΔE_{Pauli} corresponds to the repulsive interaction between the filled orbital, generally termed as steric interaction [56]. ΔE_{orb} corresponds to the interactions between the occupied orbitals of one fragment to the unoccupied orbitals of the other fragment and also takes into account the interactions between the occupied and virtual orbitals of the same fragment [45]. The rationally high negative value of the total interaction energy as evident from table 2 advocates towards the structural integrity of the molecular systems. Also, a $T1$ diagnostic run from CCSD calculations has been performed to confirm the single-reference character of the molecules studied. The $T1$ diagnostics of species vary in the range of 0.015–0.017 as evident from supplementary table S4 which are <0.02 thus, advocating towards a single-reference character as suggested by Lee and Taylor [57].

Evaluation of their structures reveals that these heteroatomic molecules display planar geometry thereby indicating the possibility of aromatic behaviour in such systems since planarity of the system is a prerequisite for a molecule to be aromatic. We intuit that these molecules may have achieved the aromatic sextet as a consequence of back-donation of paired electrons from the substituent fluorine atoms to the vacant orbitals of the boron atoms according to the scheme described in figure 2 which agrees with Huckel's $(4n+2)$ rule for aromaticity.

The B_2F_2X molecular systems possessing the group 16 heteroatoms O, S and Se consisting of two lone pairs of electrons occupying two orthogonal orbitals, so only one lone pair of electrons represented by blue pair of arrows are likely to be responsible for aromaticity which lies in plane with the plane of the vacant orbital of the boron atoms which are in turn being filled by back-donating pair of electrons from the fluorine atoms as depicted in figure 2. The other lone pair of electrons characterized by red pair of arrows of the heteroatoms O, S and Se is not involved, since it is orthogonal to the π aromatic plane. In the B_2F_2X system consisting of the group 15 heteroatom N, two lone pairs of electrons are present over the nitrogen atom. Two fluorine atoms donate

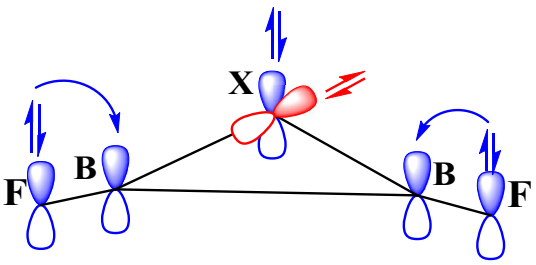

Figure 2. Orbital representation of the B_2F_2X molecules comprising 6 π-electrons showing back-donation of electrons from the fluorine atom to the vacant orbital of boron forming an aromatic π-cloud.

Table 3. RSE in kcal mol^{-1} computed at the UB3LYP/aug-cc-pvdz level.

Molecules	RSE, kcal mol^{-1}
B_2F_2O	29.22
B_2F_2S	21.20
B_2F_2Se	16.52
B_2F_2NH	28.49

two lone pairs, i.e., four electrons from fluorine atoms and two electrons are gained from the heteroatom thereby, achieving the 6π-electrons responsible for attaining aromaticity in accordance with Huckel's $(4n + 2)$ rule.

3.2 *Ring strain energy*

The molecules studied are planar and cyclic three-membered rings which are similar to the cyclopropane moiety where ring strain is an important parameter for their stability, so here the ring strain is calculated with the aid of Bader's quantum theory of atoms in molecules [46]. The Lagrange kinetic energy density value $G(r)$ computed at the ring critical point can be used to evaluate the ring strain in these small rings, with the application of the regression equation, RSE $= \{337.72 \times G(r) - 8.115\}$ [58]. The 'atoms in molecules' analysis is carried out using the AIM version program [53] at the UB3LYP/aug-cc-pvdz level of theory. The computed values of the RSE in kcal mol^{-1} for our studied systems are given in table 3.

The computed RSE values are in parity with the RSE values of experimentally observed stable three-membered cyclic systems [59–61], thereby indicating towards the structural stability and viability of the studied molecular systems. It also hints towards the presence of sigma aromaticity in the systems [62] which accounts for the reduced strain energy in the three-membered planar rings. The stability of the three-membered planar cyclic ring structure encourages the prospect of circular electronic delocalization which is the genesis of aromaticity.

Table 4. HOMO–LUMO gap in eV computed using UB3LYP/aug-cc-pvdz methodology.

Molecules	HOMO–LUMO gap, eV
B_2F_2O	4.43
B_2F_2S	6.637
B_2F_2Se	4.717
B_2F_2NH	6.593

3.3 *Molecular orbital analysis*

The HOMO–LUMO gap can be considered as a direct measurement of kinetic stability [63–70] as a greater HOMO–LUMO gap would mean a higher kinetic stability. The molecules studied have a reasonably high HOMO–LUMO gap (table 4) and since an appreciable HOMO–LUMO separation should be present for the molecules to be viable [71], thereby indicating that our systems are stable and also suggests of the closed shell nature of the molecules. This is a clear indication of the fact that these systems may have $(4n + 2)$π-aromatic electrons where all π-electrons are paired in bonding the molecular orbitals.

The above analysis shows that these molecular three-membered ring structures are reasonably stable, thereby encouraging us to explore the possibility of circular electronic delocalization which direct towards aromaticity.

3.4 *Aromaticity analysis employing NICS, CMO-NICS and MCI*

Quantifying aromaticity is a challenge due to its multi-dimensional nature [72–74], but the most efficient method of quantifying aromaticity is NICS, which was postulated by Schleyer and his co-workers [47]. The negative value of the absolute magnetic shielding gives the definition of NICS. A ghost atom is used for the determination of NICS through Gauge independent atomic orbital (GIAO) method [75–78]. In this work, the NICS values for the heterocyclic B_2F_2X systems are computed using UB3LYP, UB3PW91, UPBEPBE, UBLYP and UCAM-B3LYP methodologies along with the aug-cc-pvdz basis set which are presented in table 5. The NICS values are computed by placing the ghost atom at the centre of the ring [NICS(0)] to account for the contribution of the σ-electrons to aromaticity and 1 Å above and below the plane, i.e., [NICS(1)] and [NICS(−1)], respectively, to estimate the π-aromaticity of the systems. In harmony with NMR chemical shift principle, the NICS values are reported with negative signs. A positive NICS value signifies a paratropic magnetic field corresponding to antiaromatic systems, whereas a negative NICS value signifies a diatropic magnetic field which correlates with aromatic systems.

The NICS(0) and NICS(1) computed for our systems are highly negative which indicates that the heterocyclic B_2F_2X systems are strongly aromatic. If we compare for the negative

NICS (1) values, elements (O, S and Se) containing B_2F_2X systems then it is observed that the trend is O < S < Se since the order of electronegativity is just the opposite, so oxygen attracts the electrons more towards itself as compared to sulphur then selenium, so the order of electron delocalization is highest for Se, then S and then O. The NICS(1) value of nitrogen is also comparatively less owing to its higher electronegativity. The observation is in accordance with the notion that aromaticity increases with the decrease in the electronegativity difference between a heteroatom and its neighbouring atoms [79].

Dissected CMO-NICS analysis of the B_2F_2O system is carried out to classify the orbitals contributing to σ and π aromaticities, respectively. CMO-NICS calculations for B_2F_2O yield orbital contributions of −8.82 ppm from π, −17.422 ppm from valence σ towards the total of −26.242 ppm. From the orbital picture of the CMO contributing towards π-aromaticity (figure 3a), it is apparent that the p_z orbitals of all the atoms including the exo-cyclic fluorine atoms are involved in the formation of π-cloud over the molecular plane. The orbital picture of the CMO contributing towards σ aromaticity (figure 3b) reveals that the hybridized orbitals of the three atoms, i.e., the heteroatom and the two boron atoms are involved in the formation of CMO. It is also to be noted that fluorine atoms do not contribute to the σ aromaticity at all. The picture becomes much clearer if we consider the population analysis provided in supplementary table S5, where a 3-centred bond is present with the involvement of two sp^2 hybridized orbitals of boron and a pure in-plane p-orbital of the heteroatom (oxygen). Therefore, the σ aromaticity arises due to the delocalization of electrons across the trigonal ring through the planar heteroatom bonds with the participation of two sp^2 hybridized orbitals of boron and an in-plane pure p-orbital of oxygen without the involvement of the fluorine atoms. The trend of σ aromaticity is opposite to the trend of π aromaticity, it is highest for the heteroatoms that are comparatively smaller in size, i.e., the systems containing the heteroatom oxygen and nitrogen have higher NICS(0) values implying higher σ aromaticity which is also supported by the CMO-NICS analysis. A shorter bond distance between the heteroatoms (N and O) and the boron atom facilitates a greater in-plane delocalization, thereby accounting for a higher σ aromaticity in the B_2F_2O and B_2F_2NH systems. As the size of the heteroatom gradually increases down the group, the bond distance between the heteroatom and the boron atom consequently increases as evident from figure 1, thereby reducing the in-plane delocalization and correspondingly the σ aromaticity in the B_2F_2S and B_2F_2Se systems. From the observation, it is apparent that there exists an antagonistic relationship between σ and π aromaticities. The σ aromaticity accounts for the reduced strain energy in the three-membered rings [62].

Apart from NICS, we also performed calculations using the Multiwfn program [54] to generate the MCI. The MCI data for the studied molecular systems are provided in supplementary table S6. The MCI values are in the range of 0.45–0.52 which strongly indicates the presence of aromaticity in these heterocyclic moieties.

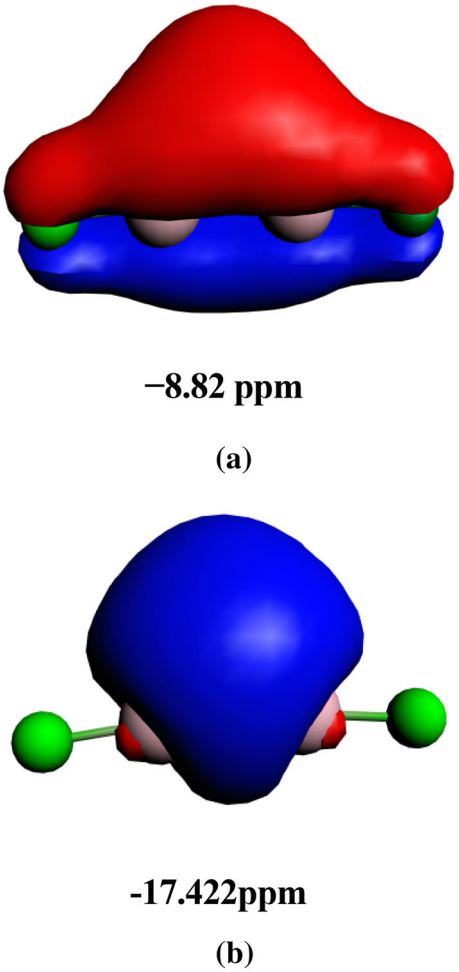

Figure 3. CMOs with maximum diamagnetic contribution to π and σ aromaticities in (**a**) and (**b**) respectively, obtained through CMO-NICS analysis at the ring, centre of the B_2F_2O molecule.

3.5 *AdNDP analysis*

Adaptive natural density partitioning (AdNDP) is a theoretical analysis which provides a very proficient and an illustrative method to understand the molecular orbital-dependent wave functions. It is a recently developed method which was proposed in 2008 by Zubarev and Boldyrev [49] for determining chemical bonding patterns in general molecular systems. This method is based on the simple Lewis concept that describes the chemical bonding with respect to the electron pair, thereby characterizing the electronic structures as *n*-centred-2 electron bonds where the value of *n* ranges from 1 to the total number of atoms present in the studied molecular systems. It figures out the elements responsible for Lewis bonding and also the elements responsible for delocalized bonding

Table 5. NICS values in ppm at the plane of the ring (NICS(0)) and at 1 Å above the plane of the ring (NICS(1)) using different DFT methodologies using the aug-cc-pvdz basis set.

Molecules	Methodology (along with aug-cc-pvdz)	NICS(0)	NICS(1)
B_2F_2O	UB3LYP	−25.8965	−9.3217
	UB3PW91	−25.4372	−9.3164
	UPBEPBE	−24.9269	−9.3870
	UBLYP	−25.1485	−9.3241
	UCAM-B3LYP	−26.2475	−9.3766
B_2F_2S	UB3LYP	−12.0535	−10.8361
	UB3PW91	−11.4657	−10.7858
	UPBEPBE	−11.5345	−10.5561
	UBLYP	−12.0159	−10.5518
	UCAM-B3LYP	−12.1434	−11.0275
B_2F_2Se	UB3LYP	−10.0864	−11.2460
	UB3PW91	−9.5752	−11.1972
	UPBEPBE	−9.8592	−10.9167
	UBLYP	−10.2615	−10.8969
	UCAM-B3LYP	−9.9759	−11.4983
B_2F_2NH	UB3LYP	−23.7343	−8.5054
	UB3PW91	−23.4382	−8.4983
	UPBEPBE	−23.2253	−8.4073
	UBLYP	−30.1548	−9.1237
	UCAM-B3LYP	−23.7884	−8.5914

which can be correlated with the concepts of aromaticity and antiaromaticity. AdNDP is an overview of natural bonding orbital (NBO) analysis as was proposed by Weinhold [80,81] from a computational view point on the basis of the diagonalization of the blocks of the first-order density matrix based on natural atomic orbitals. AdNDP bonding patterns are in consonance with the point group symmetry of the molecular systems and resonating structures are generally avoided. The main advantage of this method is that it effortlessly links the CMOs and NBOs. AdNDP orbitals for our systems are investigated using a multifunctional wave function analysis program (Multiwfn) [54].

The AdNDP analysis has been performed for all our systems as presented in figure 4. The quest for the all-centre-2 electron bond whose natural occupation number ranges from 1.99 to 2.00$|e|$ indicates a strong aromatic character in the studied systems. The visualization of the AdNDP orbitals reveals that the aromatic π cloud hovers over the molecular moiety comprising the heteroatoms (O, S, Se and N) along with the boron and the fluorine atom thereby indicating that the fluorine atoms are involved in aromaticity. This portrayal of the 5-centred 2-electron AdNDP orbital signifies the role of the substituent fluorine atoms in developing aromaticity thus, strongly establishing our notion of exo-cyclic aromaticity in these systems (figure 4).

3.6 *Aromatic stabilization energy*

In a recent work, aromaticity is quantified with respect to the energy stabilization due to circular π-electron delocalization termed as aromatic stabilization energy (ASE) [50]. The expression for ASE for conventional benzene-like systems was derived [54] as

$$\mathrm{ASE} = \sum_{i,j} \frac{t_{ij}^2}{U} \left(n_{i\sigma} n_{j\sigma'} + n_{i\sigma'} n_{j\sigma}\right) \mathrm{ELF}^2. \tag{2}$$

Therefore, from equation (2), we can relate the π-electron delocalization energy (ASE) to the inter-site hopping integral (t_{ij}) and the onsite repulsion energy (U). The electronic population engaged in delocalization is obtained as a product of spin–orbital population ($n_{i\sigma}$ and $n_{j\sigma'}$) within the unrestricted framework and the degree of delocalization, which is estimated from the electron localization function (ELF).

As already mentioned, equation (2) is applicable for benzene-like aromatic molecules, which are different from the studied system in terms of the electronic structure and aromaticity type. In the systems studied here, specifically the migration of the lone pair of electrons in between the boron and fluorine completes the loop of electronic circulation and thus, makes the pattern of electron delocalization unique and different to conventional aromatic systems. To agree with this representation of electron delocalization, equation (2) is divided into two components as given below:

$$\mathrm{ASE} = \sum_{\mathrm{B,X}} \frac{2t_{ij}^2}{U} \left(n_{\mathrm{B}\sigma} n_{\mathrm{X}\sigma'} + n_{\mathrm{B}\sigma'} n_{\mathrm{X}\sigma}\right) \mathrm{ELF}^2 + \sum_{\mathrm{F,B}} \frac{2t_{ij}^2}{U} \left(n_{\mathrm{F}\sigma} n_{\mathrm{B}\sigma'} + n_{\mathrm{F}\sigma'} n_{\mathrm{B}\sigma}\right) \mathrm{ELF}^2. \tag{3}$$

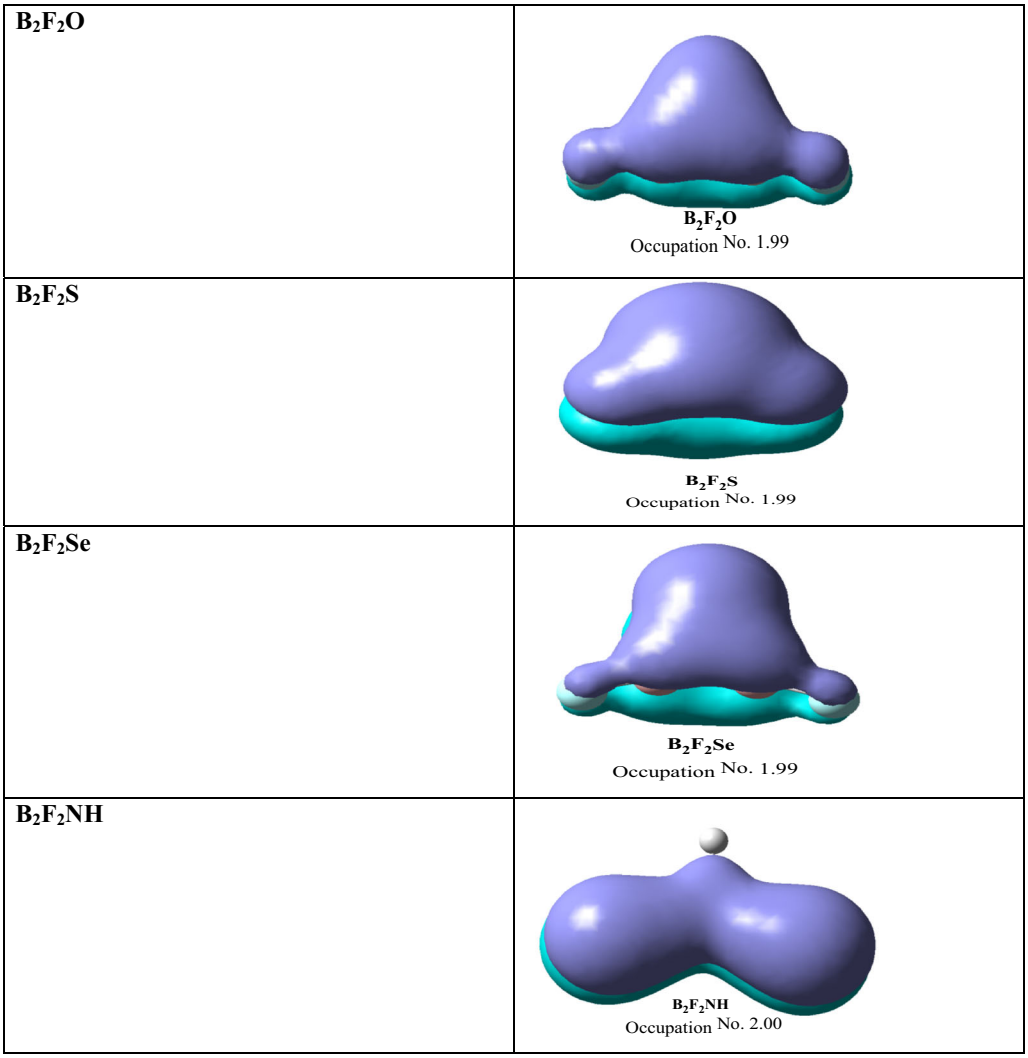

Figure 4. AdNDP orbitals of the studied systems from top view with their natural occupation numbers.

Here, the first part stands for the electron delocalization within the B–X ring, it is multiplied by two to account for two lone pairs of electrons of the heteroatom X and the second part quantifies stabilization for electron delocalization within the Lewis acid–base pair. The probability of the lone-pair transfer from F to B is taken into consideration by multiplying with two.

The high values of ASE as evident from table 6 also advocate towards a significant stabilization of the molecules as a result of aromaticity. It can also be observed that the ASE values obtained are also in accordance and are in correlation with the NICS values. The computed values are comparable to highly stable classical aromatic systems [82,83], thereby further accentuating the viability of these molecular systems. A method to localize Wannier function was given by Marzari and Vanderbilt [84] named as maximally localized Wannier function (MLWF) which provides an enhanced bonding picture.

Table 6. ASE of the studied molecular systems in kcal mol^{-1}.

Molecules	ASE, kcal mol^{-1}
B_2F_2O	17.1
B_2F_2S	22.8
B_2F_2Se	34.6
B_2F_2NH	21.1

The MLWFs obtained through OpenMX 3.6 quantum chemistry code [55] (figure 5) provide a vivid picture that the p_z orbitals perpendicular to the molecular plane of all the atoms including the exo-cyclic atoms are involved in aromaticity in accordance with our scheme described in figure 2. Similar MLWFs are obtained for the other molecular systems (Supplementary information) as well, thereby establishing our notion of exo-cyclic aromaticity where aromaticity

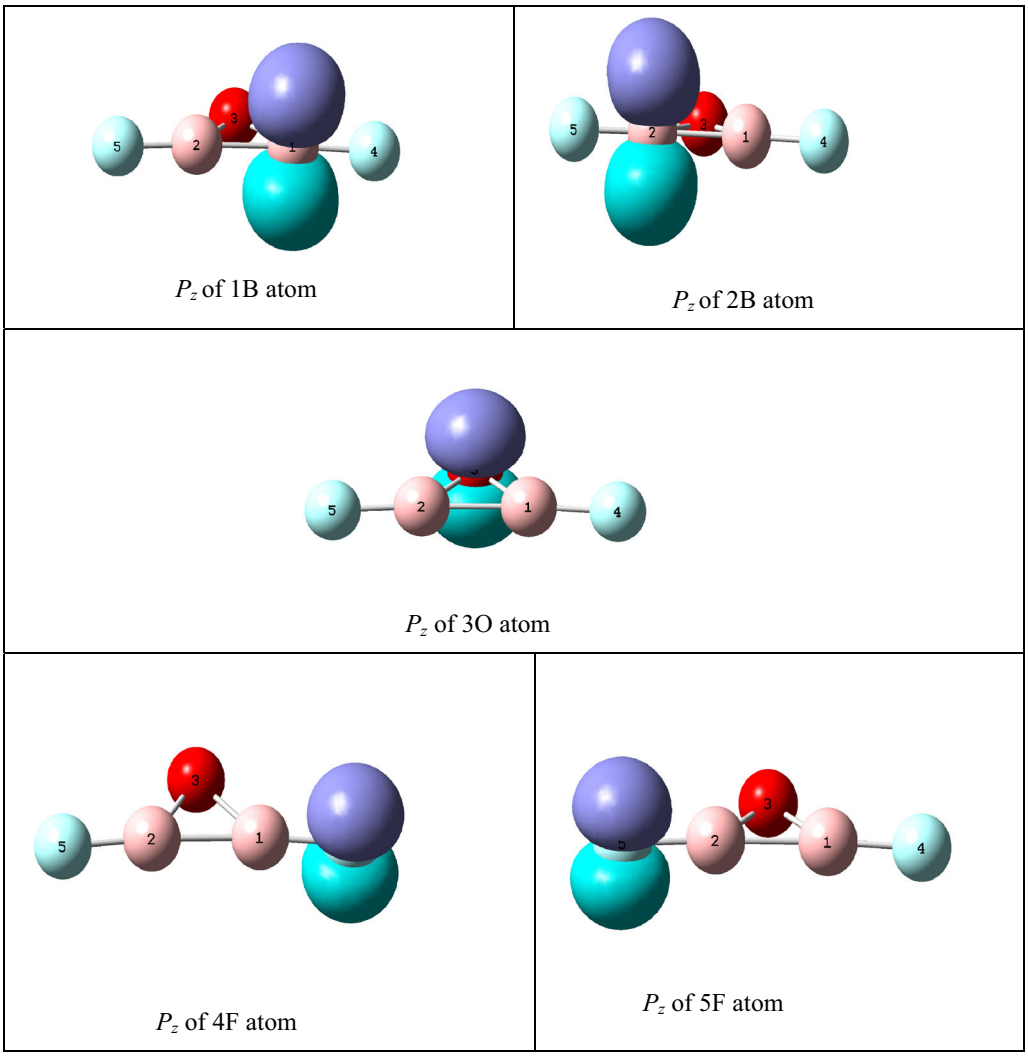

Figure 5. MLWFs in B_2F_2O.

is achieved through back-donation of electrons of the fluorine atoms to the electron-deficient p_z orbitals of the boron atoms.

4. Conclusion

The observation of unique aromaticity obtained through back-donation of 4π-electrons from substituent exo-cyclic fluorine atoms to the vacant p_z orbitals of the boron atoms make the study of these proposed novel three-membered heterocyclic planar systems an interesting addition to the domain of aromaticity. Rigorous computational study involving DFT and *ab-initio* calculations along with EDA, the evaluation of RSE and HOMO–LUMO gap indicates towards the viability of the systems. The aromaticity of the molecule is evaluated through some standard criteria, specifically, NICS and MCI. The dissected NICS analysis (CMO-NICS) presents a clear picture of the molecular orbitals contributing towards σ and π aromaticities, respectively. A coherent picture of the exo-cyclic nature of the aromatic π-cloud is viewed with the AdNDP analysis. The ASE based on a fully *ab-initio* approach is also reported which renders the proposed heterocyclic molecules to be remarkable 6π-aromatic systems where the magic number is attained through an 'exo-cyclic' conjugation. These proposed molecules are unique and distinctive due to the presence of both the σ and the π aromaticities and the antagonistic relationship existing between them makes the systems a remarkable addition to the class of aromatic molecules and provide a significant scope of future study. The high stability of the molecular systems as apparent from the various computational analysis makes us hopeful regarding the investigational reality of these molecules.

Acknowledgements

The financial support from CSIR, India, is thankfully acknowledged.

References

[1] Faraday M 1825 *Phil. Trans. R. Soc. Lond.* **115** 440
[2] Kekulé A 1865 *Bull. Soc. Chim. Paris* **3** 98
[3] Kekulé A 1866 *Ann. Chem. Pharm.* **137** 129
[4] Garratt P J 1997 *Aromaticity* (New York: John Wiley & Sons)
[5] Minkin V I, Glukhotsev M N and Simkin B Y 1994 *Aromaticity and antiaromaticity: electronic and structural aspects* (New York: John Wiley & Sons Inc.)
[6] Bickelhaupt F and de Wolf W H 1988 *Recl. Trav. Chim. Pays-Bas* **107** 459
[7] Kraakman P A, Valk J M, Niederländer H A G, Brouwer D B E, Bickelhaupt F M, de Wolf W H *et al* 1990 *J. Am. Chem. Soc.* **112** 6638
[8] Schleyer P V R and Jiao H 1996 *J. Pure Appl. Chem.* **68** 209
[9] Schleyer P V R, Jiao H, Hommes N J R V E, Malkin V G and Malkina O L 1997 *J. Am. Chem. Soc.* **119** 12669
[10] Poranne G P and Stranger A 1994 *Magnetic and structural aspects* (New York: Wiley)
[11] Homray M, Misra A and Chattaraj P K 2017 *Curr. Org. Chem.* **21** 2699
[12] Katritzky A R 2004 *Chem. Rev.* **104** 2125
[13] Aihara J I 1982 *J. Pure Appl. Chem.* **54** 1115
[14] Graovac A, Gutman L and Trinajstic 1977 *Topological approach to the chemistry of conjugated molecules* (Berlin: Springer)
[15] Nyulaszi L 2001*Chem. Rev.* **101** 1229
[16] Minkin V I and Minyaev R M 2001*Chem. Rev.* **101** 1247
[17] Katritzky A R, Jug K and Oniciu D C 2001 *Chem. Rev.* **101** 1421
[18] Li X, Kuznetsov A, Zhang H, Boldyrev A I and Wang L 2001 *Science* **291** 859
[19] Kuznetsov A E, Birch K A, Boldyrev A I, Li X, Zhai H and Wang L 2003 *Science* **300** 622
[20] Boldyrev A I and Wang L 2005 *Chem. Rev.* **105** 3716
[21] Paul S and Misra A **2011** *Inorg. Chem.* **50** 3234
[22] Chattaraj P K, Roy D R and Duley S 2008 *Chem. Phys. Lett.* **460** 382
[23] Huckel E 1931 *Z. Phys.* **70** 204
[24] Hehre W J, Radom L, Schleyer P V R and Pople J A 1986 *Ab initio molecular orbital theory* (New York: Wiley)
[25] Xie Y, Schaefer III H F and Thrasher J S 1991 *J. Mol. Struct. Theochem.* **234** 247
[26] Shaik S, Shurki A, Danovich D and Hiberty P C 1997 *J. Mol. Struct. Theochem.* **39** 155
[27] Krygowski T M and Cyraski M K 2001 *Chem. Rev.* **101** 1385
[28] Poater J, Duran M, Solà M and Silvi B 2005 *Chem. Rev.* **105** 3911
[29] Cyraski M K 2005 *Chem. Rev.* **105** 3773
[30] Matito E, Duran M and Solà M 2005 *J. Chem. Phys.* **122** 014109
[31] Bultinck P, Ponec R and Van Damme S 2005 *J. Phys. Org. Chem.* **18** 706
[32] Feixas F, Matito E, Poater J and Solà M 2008 *J. Comput. Chem.* **29** 1543
[33] Roy D R, Bultinck P, Subramanium V and Chattaraj P K 2008 *J. Mol. Struct.* **854** 35
[34] Feixas F, Matito E, Poater J and Solà M 2015 *Chem. Soc. Rev.* **44** 6434
[35] Misra A, Klein D J and Morikawa T 2009 *J. Phys. Chem. A* **113** 1151
[36] Clar E 1970 *The aromatic sextet* (New York: Wiley & Sons)
[37] Misra A, Schmalz T G and Klein D J 2009 *J. Chem. Inf. Model.* **49** 2670
[38] Bhattacharya D, Panda A, Misra A and Klein D J 2014 *J. Phys. Chem. A* **118** 4325
[39] Gund P 1972 *J. Chem. Educ.* **49** 100
[40] Goswami T, Homray M, Paul S, Bhattacharya D and Misra A 2017 *Phys. Chem. Chem. Phys.* **19** 11744
[41] Gutowsky H S and McCall D W 1953 *J. Phys. Chem.* **21** 279
[42] Onak T P, Landesman H, Williams R E and Shapiro I 1959 Paper presented to the Division of Inorganic Chemistry, 135th National Meeting of the American Chemical Society, Boston, Mass., 1959
[43] Cotton F A and Wilkinson G 1966 *Advanced inorganic chemistry* (London: Interscience) p 256
[44] Olah G A, Mo Y K and Halpern Y 1972 *J. Am. Chem. Soc.* **94** 3551
[45] Ziegler T and Rauk A 1977 *Theor. Chim. Acta* **46** 1
[46] Bader R F W 1990 *Atoms in molecules: a quantum theory* (Oxford, UK: Oxford University Press)
[47] Schleyer P V R, Maerke C, Dransfeld A, Jiao H and Hommes N J R V E 1996 *J. Am. Chem. Soc.* **118** 6317
[48] Heine T, Schleyer P V R, Corminboeuf C, Seifert G, Reviakine R and Weber J 2003 *J. Phys. Chem. A* **107** 6470
[49] Zubarev D Y and Boldyrev A I 2008 *Phys. Chem. Chem. Phys.* **10** 5207
[50] Paul S, Goswami T and Misra A 2015 *AIP Adv.* **5** 107211
[51] Frisch M J, Trucks G W, Schlegel H B, Scuseria G E, Robb M A, Cheeseman J R *et al* 2009 *Gaussian 09, Revision B.01* (Wallingford, CT: Gaussian Inc.)
[52] Amsterdam Density Functional (Theoretical Chemistry, Vrije Universitiet, Amsterdam, The Netherlands, http://www.scm.com)
[53] AIMAll (version 17.01.25), Todd A K 2017 TK Gristmill Software, Overland Park KS, USA
[54] Lu T and Chen F 2012 *J. Comput. Chem.* **33** 580
[55] DFT Code, OPENMX, is available at http://www.openmx-square.org under the GNU General Public License
[56] Pinter B, Fievez T, Bickelhaupt F M, Geerlings P and De Proft F 2012 *Phys. Chem. Chem. Phys.* **14** 9846
[57] Lee J T and Taylor P 1989 *Int. J. Quantum Chem.* **36** 199
[58] Bauzá A, Quiñonero D, Deyà P M and Frontera A 2012 *Chem. Phys. Lett.* **536** 165
[59] Cox J D and Pilcher G 1970 *Thermochemistry of organic and organometallic compounds* (London: Academic)
[60] Benson S W 1976 *Thermochemical kinetics* (New York: Wiley)
[61] Inagaki S, Ishitani Y and Kakefu T 1994 *J. Am. Chem. Soc.* **116** 13
[62] Dewar M J S 1984 *J. Am. Chem. Soc.* **106** 669
[63] Aihara J 1999 *J. Phys. Chem. A* **103** 7487
[64] Aihara J 1999 *Theor. Chem. Acc.* **102** 134
[65] Aihara J 1999 *Phys. Chem. Chem. Phys.* **1** 227
[66] Parr R G and Zhou Z 1993 *Acc. Chem. Res.* **26** 256
[67] Liu X, Schmalz T G and Klien D J 1992 *Chem. Phys. Lett.* **188** 550
[68] Haddon R C and Fukunaga T 1980 *Tetrahedron Lett.* **21** 1191
[69] Pearson R G 1973 *Hard and soft acids and bases* (Stroudsburg, PA: Dowden, Hutchinson and Ross)

[70] Manolopoulos D E, May J C and Down S E 1991 *Chem. Phys. Lett.* **181** 105
[71] Hoffmann R, Schleyer P V R and Schaefer H F 2008 *Angew. Chem. Int. Ed.* **47** 7164
[72] Katrizky A, Barczymski P, Musumarra G, Pisano D and Szafran M 1989 *J. Am. Chem. Soc.* **111** 7
[73] Schleyer P V R, Manoharan M, Jiao H and Stahl F 2001 *Org. Lett.* **3** 3643
[74] Chen Z, Wannere C S, Corminboeuf C, Puchta R and Schleyer P V R 2005 *Chem. Rev.* **105** 3842
[75] London F 1937 *J. Phys. Radium* **8** 397
[76] Cheeseman J R, Trucks G W, Keith T A and Frisch M J 1996 *J. Chem. Phys.* **104** 5497
[77] Schreckenbach G and Ziegler T 1995 *J. Phys. Chem.* **99** 606
[78] Schreckenbach G and Ziegler T 1998 *Theor. Chem. Acc.* **99** 71
[79] Simkin B Y, Minkin V I and Glukhotsev M N 1993 *Adv. Heterocycl. Chem.* **56** 304
[80] Foster J P and Weinhold F 1980 *J. Am. Chem. Soc.* **102** 7211
[81] Reed A E, Curtiss L A and Weinhold F 1988 *Chem. Rev.* **88** 899
[82] Katrizky A, Barczymski P, Musumarra G, Pisano D and Szafran M 1984 *J. Am. Chem. Soc.* **111** 7
[83] Radhakrishnan S, Anathakrishnan S J and Somanathan N 2011 *Bull. Mater. Sci.* **34** 713
[84] Marzari N and Vanderbilt D 1997 *Phys. Rev. B* **56** 12847

PCCP

PAPER

Check for updates

Cite this: *Phys. Chem. Chem. Phys.*, 2019, **21**, 7996

Bond stretch isomerism in Be_3^{2-} driven by the Renner–Teller effect†

Manoswita Homray,[ab] Sukanta Mondal,[bc] Anirban Misra *[a] and P. K. Chattaraj*[bd]

Received 1st February 2019,
Accepted 22nd March 2019

DOI: 10.1039/c9cp00643e

rsc.li/pccp

We investigate the underlying principle behind the occurrence of bond stretch isomerism in Be_3^{2-}, which has not been revealed yet. Various computational studies of the different isomers are carried out at the complete active space self-consistent field (CASSCF) level of theory in addition to the B3LYP level in conjunction with the 6-311++G(d) basis set. The potential energy surfaces linking the different isomers through transition states and conical intersections are investigated at the CASSCF level, connecting various geometrical isomers of Be_3^{2-}. The linear intermediate of the Be_3^{2-} cluster is considered to be of profound importance since its excited state is found to be degenerate and undergoing the Renner–Teller effect, producing two triangular bond stretch isomers. *Ab initio* molecular dynamics simulations based on the Atom Centered Density Matrix Propagation (ADMP) method also further elucidate the phenomenon of isomerization *via* the linear intermediate. The variation of the global reactivity descriptors and free energy profile along the bond stretch isomerization path is also investigated. The estimated aromatic stabilization energy also corroborates the stability ordering of the bond stretch isomers.

Introduction

Bond Stretch Isomerism (BSI) occurs when the isomers differ in the lengths of certain bonds. This phenomenon is intriguing due to the fact that the inter conversion between the two isomers requires only a simple compression or elongation of a bond. The idea of bond stretch isomerism was first proposed by Hoffmann and co-workers in the year 1972, where they referred to separate stable configurations whose structures vary only in the length of one (or more) chemical bond(s) where the isomers were shown to occupy different minima on their potential energy surface.[1–3] Experimental evidence of BSI was however reported in the year 1970 by Chatt,[4] prior to the theoretical proposition. Since then a range of compounds have been shown to exhibit BSI,[5–8] which was theoretically rationalized later in the year 1988.[3] In spite of increasing illustrations of BSI, both theoretically and experimentally, lack of a proper explanation behind the existence of bond stretch isomers makes the event unclear.[9–12] Despite the vagueness surrounding this phenomenon, there are a number of occurrences where BSI undoubtedly exists,[13–15] but an appropriate elucidation of the phenomenon still remains a major challenge, which sets up the objective of this present work.

BSI has been established recently in Be_3^{2-} and its unique bonding pattern is extensively discussed.[16] Be_3^{2-} is a comprehensively studied system in the field of all-metal aromatic clusters in terms of stability, aromaticity, hardness, *etc.* It has been shown to exist in a range of structural isomers including cyclic (D_{3h}, C_{2v}) and linear ($D_{\infty h}$) forms,[17–24] however, a correlation between the different isomers is yet to be realized. In numerous studies, the short-bond isomer of Be_3^{2-} with D_{3h} symmetry is reported to have a bond length of 2.078 Å;[18] on the other hand, Sola and co-workers obtained the long-bond isomer with the same D_{3h} symmetry with an optimized bond length of 2.156 Å.[24] It has been established that they lie on entirely different potential energy surfaces, occupying two different minima corresponding to the short- and long-bond isomers, respectively, since the existence of BSI requires both a double minimum on a potential energy surface and a considerable barrier between these two minima.[16] The existence of BSI is further emphasized due to the reversal of the frontier molecular orbitals, where the HOMO of the short-bond isomer is observed to be the LUMO of the long-bond isomer and *vice versa*. Hybridization isomerism due to the change in hybridization on one atom and Jahn–Teller distortions may be subtly distinguished from BSI.[25] The potential energy surfaces of these two isomers may have an intersecting point representing a Conical Intersection (CI)

[a] *Department of Chemistry, University of North Bengal, Raja Rammohunpur, Darjeeling, 734013, West Bengal, India. E-mail: anirbanmisra@yahoo.com, manosweet.homray96@gmail.com; Tel: +91-9434228745*
[b] *Department of Chemistry and Center for Theoretical Studies, Indian Institute of Technology Kharagpur, Kharagpur 721302, West Bengal, India. E-mail: pkc@chem.iitkgp.ac.in; Fax: +91-3222-255303; Tel: +91-3222-283304*
[c] *Department of Educational Science, Assam University, Silchar, Assam-788011, India. E-mail: sukanta.mondal@aus.ac.in, sukanta.mail13@gmail.com; Tel: +91-7797951118*
[d] *Department of Chemistry, Indian Institute of Technology Bombay, Powai-400076, Mumbai, India*

† Electronic supplementary information (ESI) available. See DOI: 10.1039/c9cp00643e

This journal is © the Owner Societies 2019

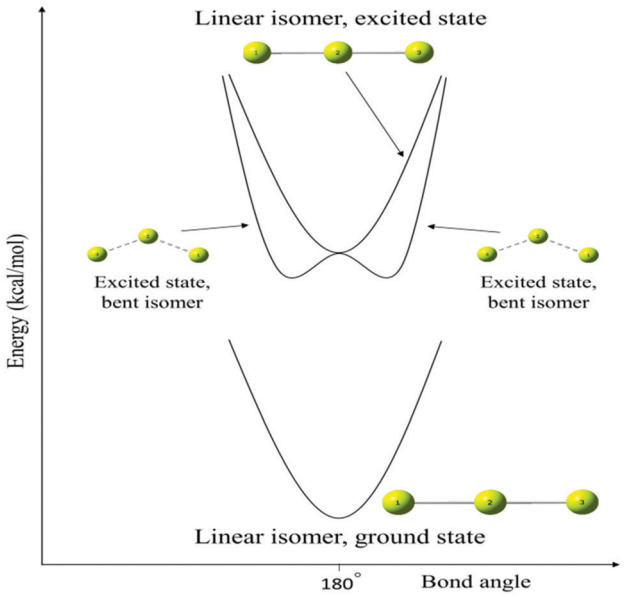

Scheme 1

to obtain a degenerate state. All these factors instigate the present study to find a connection between the two D_{3h} BSIs in Be_3^{2-}. In this paper we try to understand the underlying mechanism which leads to the presence of two bond stretch isomers. The primary force behind the presence of two different isomers of the Be_3^{2-} molecule may be the Renner–Teller effect,[26–28] which identifies the prospect of a triatomic molecule present in a degenerate electronic state to split into two when the molecule is bent. The Renner–Teller effect occurs in its simplest form in open shell linear triatomic molecules (Scheme 1). The Be_3^{2-} molecule has a linear geometrical isomer possessing $D_{\infty h}$ symmetry; as a result the electronic states may be two-fold degenerate, thereby causing the breakdown of the adiabatic (Born–Oppenheimer) approximation, which lifts the degeneracy of a linear molecule. The linear triatomic molecule is electronically non-degenerate in its ground state, but its excited state is degenerate, thereby forcing bending of the linear structure to produce two lower energy ground state equilateral triangular D_{3h} bond stretch isomers *via* conical intersections.

Computational details

According to our previously reported results,[16,23] all the isomers of the Be_3^{2-} cluster are modeled in this work. For the preparation and study of different input and output geometries, graphical software GaussView 5[29] is used. All the optimizations, frequency calculations and molecular dynamics simulations are done using the Gaussian 09 package.[30] As beryllium exhibits multi-reference behavior (due to the near degeneracy of s and p orbitals), T_1 diagnostics of the system to check the multireference issue were done in previous work.[23] Here it was shown that the values of T_1 are 0.08496, 0.08827 and 0.08108 for the D_{3h}, C_{2v} and $D_{\infty h}$ isomers, respectively, which are much greater than the 0.02 threshold. The occupation of higher energy molecular states is preferential due to the presence of two additional electrons in the Be_3 moiety. The higher influence of non-dynamical electron correlation accounts for the higher values of T_1. Large values of T_1 evidently point towards the insufficiency of single-reference methods, which suggests the requirement for multi-reference methods to predict the energy and equilibrium structure of Be_3^{2-} more precisely. The modeled structures are optimized at the complete active space self-consistent field (CASSCF) level of theory in addition to the B3LYP level in conjunction with the 6-311++G(d) basis set.[23] Harmonic vibrational frequencies are computed at the same levels of theory, and the obtained results confirm that the structures correspond to minima on the potential energy surfaces for the cyclic (D_{3h}) and linear ($D_{\infty h}$) isomers. The transition state search, excited state search, conical intersection search and intrinsic reaction coordinate (IRC) calculations are carried out at different theoretical levels, which are mentioned in the appropriate places. During the CASSCF calculations, all the valence electrons are taken into active space consideration due to the smaller size of the molecule. CASSCF(8,6) takes into account 8 electrons in the active space and 6 orbitals in the active space. The σ MOs corresponding to the 1s orbitals of the constituent Be atoms are not assigned to the active space. The σ and π MOs resulting from the 2s and 2p orbitals of the Be atoms are assigned to the active space. The orbital set used to construct the active space along with the percentages of leading configurations in wavefunctions is given in Fig. S1 (ESI†). Since the CASSCF method lacks dynamic correlation, an MP2 level electron correlation correction to the CASSCF energy is computed which incorporates the dynamic correlation.[31–33]

The dynamics of the Be_3^{2-} isomers are studied through an Atom Centered Density Matrix Propagation (ADMP)[34–37] technique as included in the Gaussian 09 program package. Simulations are done at the B3LYP/6-311++G(d) level of theory at several temperatures and it is noted that at 700 K the short-bond Be_3^{2-} isomerizes to form the long-bond analogue *via* the linear $D_{\infty h}$ isomer. The Boltzmann distribution is used to generate the initial nuclear kinetic energy of the systems. The temperature is maintained throughout the simulation by using a velocity scaling thermostat. Simulations are carried out keeping the fictitious electronic mass at 0.1 amu.

The variation of hardness (η) and electrophilicity (ω) along the isomerization path is evaluated at the B3LYP/6-311++G(d) level of theory. It is established that η and ω can predict the stability of molecular systems in conjunction with the associated electronic structure principles, *viz.*, the maximum hardness principle (MHP)[38–43] and the minimum electrophilicity principle (MEP).[43–46] The electronegativity (χ),[47–49] hardness (η)[50,51] and electrophilicity (ω)[52] of an *N*-electron system can be defined as follows:

$$\chi = -\mu = -\left(\frac{\partial E}{\partial N}\right)_{\upsilon(\vec{r})} \quad (1)$$

$$\eta = \left(\frac{\partial^2 E}{\partial N^2}\right)_{\upsilon(\vec{r})} \quad (2)$$

$$\omega = \frac{\mu^2}{2\eta} = \frac{\chi^2}{2\eta} \quad (3)$$

E, μ, and $v(\vec{r})$ are the total energy of the N-electron system, chemical potential and external potential respectively.

Employing a finite difference approximation to eqn (1) and (2) one can achieve:

$$\chi = \frac{I + A}{2} \tag{4}$$

and

$$\eta = I - A, \tag{5}$$

where I and A indicate the ionization potential and electron affinity of the cluster, respectively, and they are calculated using Koopmans' theorem.[53,54]

The aromaticity of the two cyclic D_{3h} BSIs is calculated using a recently proposed theoretical model[55–57] where quantification of aromaticity is done with respect to the energy stabilization owing to the circular π-electron delocalization, termed the Aromatic Stabilization Energy (ASE). In this theoretical model, the ASE is related to the molecular energy stabilization due to electron delocalization in the framework of second order perturbation theory consequential from atom to atom charge transfer.[58–61]

The theoretical model proposes the inter-site hopping integral (t_{ij}) and the onsite repulsion energy (U) to be responsible for the electron delocalization. The population of the electrons participating in delocalization is obtained as a product of the spin-orbital population ($n_{i\sigma}$ and $n_{j\sigma'}$) within the unrestricted framework and the level of delocalization is projected from the electron localization function (ELF) as

$$\mathrm{ASE} = \sum_{i,j} \frac{t_{ij}^2}{U}\left(n_{i\sigma}n_{j\sigma'} + n_{i\sigma'}n_{j\sigma}\right)\mathrm{ELF}^2 \tag{6}$$

For the estimation of the ASE, the Gaussian 09 suite of software is used to calculate the onsite repulsion energy (U) and the spin-orbital population ($n_{i\sigma}$ and $n_{j\sigma'}$). The ELF value is obtained utilizing the Multiwfn code[62] and the OpenMX 3.6 quantum chemistry code[63] is used to estimate the inter-site hopping integral (t_{ij}).

Results and discussion

Optimized structures of the two cyclic BSIs and linear Be_3^{2-} are given in Fig. 1 along with their varying bond lengths. The energies and bond lengths of the ground state (the short-bond isomer, the linear isomer and the long-bond isomer) are given in Table 1. All the optimized structures are devoid of any imaginary frequency but the linear isomer has a higher ground state energy compared to the cyclic isomers as anticipated from the perspective of aromaticity at various levels of theory.[23]

A transition state[64] search reveals the presence of an optimized C_{2v} transition state (TS1) connecting the D_{3h} short-bond isomer to a linear $D_{\infty h}$ Be_3^{2-} intermediate. TS1 has one imaginary frequency and from the atomic displacement vectors it is evident that TS1 facilitates the formation of the linear intermediate from the short-bond isomer. A similar C_{2v} transition state (TS2) is also observed to be present and connecting the linear $D_{\infty h}$ intermediate to the D_{3h} long-bond isomer with one negative frequency and showing atomic displacement vectors in a direction which indicates the formation of the long-bond isomer from the linear intermediate. Both the C_{2v} transition states satisfy the aforementioned criteria and their optimized structures are given in Fig. 2. The energies and the bond lengths of the transition states (TS1 and TS2) are given in Table 2. The Intrinsic Reaction Coordinate (IRC) plots showing the path from the short-bond isomer to the linear intermediate *via* TS1 and the path from the linear intermediate

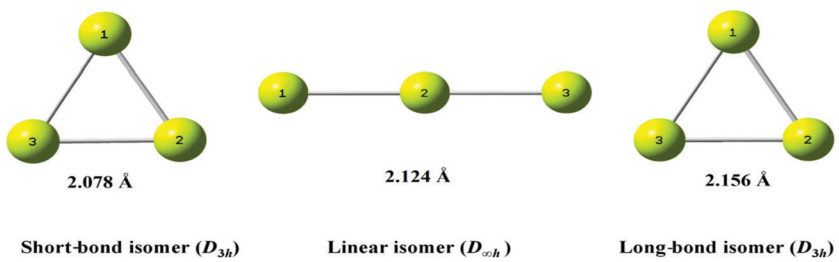

Fig. 1 Optimized bond lengths of the short-bond, linear and long-bond isomers at the B3LYP/6-311++g(d) level of theory.

Table 1 Energy (E in a.u.) and bond length (r in Å) of the ground state isomers of Be_3^{2-} at DFT, CASSCF and CASSCF MP2 levels of theory and their relative stability in kcal mol^{-1} with respect to the lower energy long bond isomer is also reported

Ground state	B3LYP/6-311++G(d)	Relative stability (kcal mol^{-1}) B3LYP/6-311++G(d)	CASSCF/6-311++G(d)	Relative stability (kcal mol^{-1}) CASSCF/6-311++G(d)	CASSCF MP2	Relative stability (kcal mol^{-1}) CASSCF MP2
Short-bond isomer	E = −44.00343 r = 2.078	4.4	E = −43.66049 r = 2.220	5.9	E = −43.80883 r = 2.218	4.3
Linear isomer	E = −43.98421 r = 2.124	16.4	E = −43.65011 r = 2.158	12.5	E = −43.79084 r = 2.159	15.6
Long-bond isomer	E = −44.01043 r = 2.156	0	E = −43.67001 r = 2.312	0	E = −43.81582 r = 2.320	0

This journal is © the Owner Societies 2019

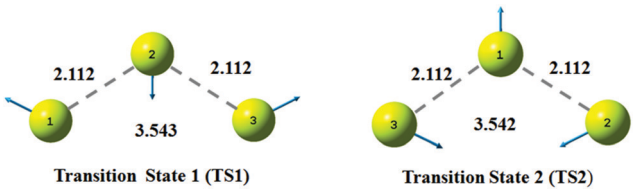

Fig. 2 Optimized structures of the transition states with their atomic displacement vectors and the respective bond lengths in Å at the B3LYP/6-311++g(d) level of theory.

to the long-bond isomer *via* TS2 are given in Fig. 3. From these observations, one can infer that the linear intermediate is a vital connector between the two bond-stretch isomers. A similar observation is also made using *ab initio* molecular dynamics simulations through the ADMP technique. In a five picosecond simulation run at 700 K, it is noted that the D_{3h} short-bond form of Be_3^{2-} isomerizes to the $D_{\infty h}$ structure at 3387 femtoseconds, which thereafter passes through a TS2 like geometry to form the long-bond isomer. To help the reader in understanding this isomerization process a graphics interchange format (GIF) video of the simulation is provided (see Video S1) in the ESI.†

From the molecular orbital analysis, a MO flip was observed for the two minimum equilateral structures as reported in one

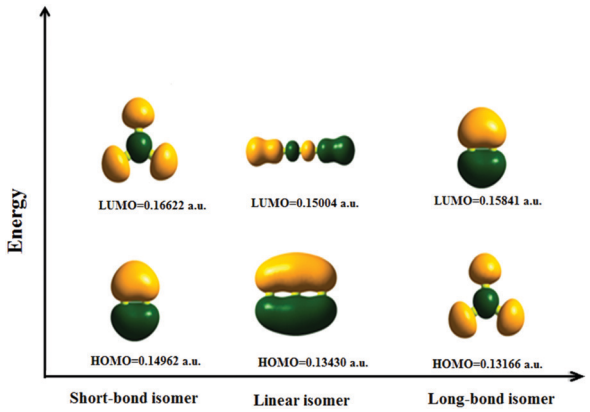

Fig. 4 The HOMO and LUMO of the ground state isomers along with their energy eigenvalues obtained at the UB3LYP/6-311++G(d) level of theory.

earlier study,[16] where the HOMO (LUMO) of the short-bond (long-bond) isomer is mainly comprised of p_z orbitals of Be atoms and the LUMO (HOMO) of the short-bond (long-bond) isomer is composed of p_x and p_y orbitals as shown in Fig. 4. Moreover, the Frontier Molecular Orbital (FMO) diagram[65] indicates that there is a reversal of the highest occupied and lowest unoccupied molecular orbitals during the passage from the short-bond isomer to the long-bond isomer *via* the linear

Table 2 Energy (E in a.u.) and bond length (r in Å) of the transition states of Be_3^{2-} at DFT, CASSCF and CASSCF MP2 levels of theory and their relative stability in kcal mol^{-1} with respect to the lower energy TS2 is also reported

Transition state	B3LYP/6-311++G(d)	Relative stability (kcal mol^{-1}) B3LYP/6-311++G(d)	CASSCF/6-311++G(d)	Relative stability (kcal mol^{-1}) CASSCF/6-311++G(d)	CASSCF MP2	Relative stability (kcal mol^{-1}) CASSCF MP2
TS1	E = −43.97723 r[Be(1)–Be(2), Be(2)–Be(3)] = 2.112 r[Be(1)–Be(3)] = 3.543	0.5	E = −43.62712 r[Be(1)–Be(2), Be(2)–Be(3)] = 2.118 r[Be(1)–Be(3)] = 3.452	5.2	E = −43.78339 r[Be(1)–Be(2), Be(2)–Be(3)] = 2.172 r[Be(1)–Be(3)] = 3.574	5.7
TS2	E = −43.97801 r[Be(1)–Be(2), Be(1)–Be(3)] = 2.112 r[Be(2)–Be(3)] = 3.542	0	E = −43.63542 r[Be(1)–Be(2), Be(1)–Be(3)] = 2.118 r[Be(2)–Be(3)] = 3.451	0	E = −43.79254 r[Be(1)–Be(2), Be(1)–Be(3)] = 2.170 r[Be(2)–Be(3)] = 3.572	0

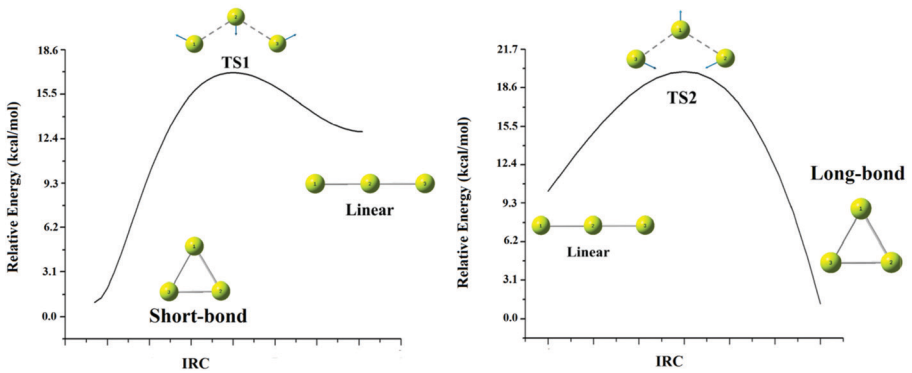

Fig. 3 IRC plots showing the path from the short-bond isomer to the linear intermediate *via* TS1 and the linear intermediate to the long-bond isomer *via* TS2 at the UB3LYP/6-311++G(d) level of theory.

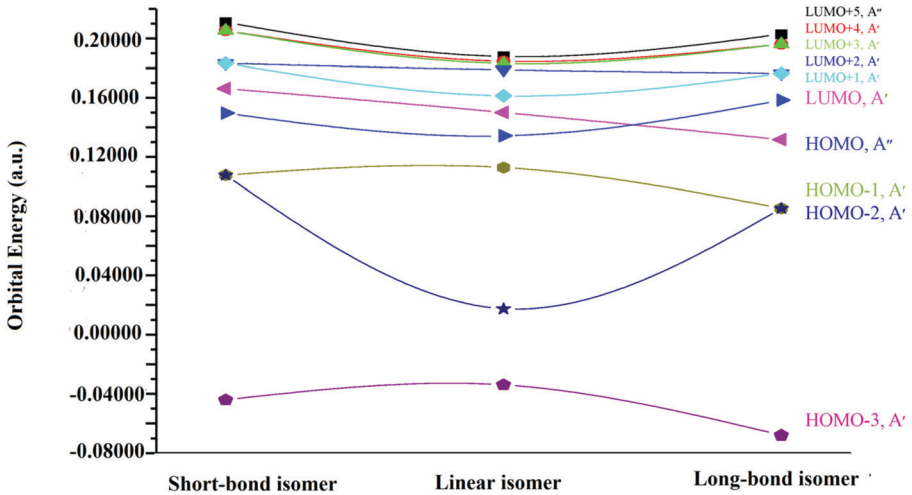

Fig. 5 Frontier Molecular Orbital (FMO) diagram for the isomerization pathway, the D_{3h} short-bond isomer to the linear $D_{\infty h}$ Be_3^{2-} intermediate to the D_{3h} long-bond isomer at the UB3LYP/6-311++G(d) level of theory.

intermediate (Fig. 5). So, there must be a point where the HOMO and the LUMO become degenerate; that point of degeneracy was observed in the first excited state of the linear isomer, which is very similar to the ground state, possessing $D_{\infty h}$ symmetry. The major difference between them is a shrinkage in the Be–Be bond length in the excited state from 2.158 Å to 2.140 Å and the energy difference between the two structures is about 9.2 kcal mol^{-1} at the CASSCF(8,6)/6-311++G(d) level of theory, where the excited state energy is −43.63545 a.u. (Fig. 6). At the CASSCF MP2 level, there is also a reduction of the bond-length from 2.159 Å to 2.157 Å in the excited state and here the excited state energy considering the dynamic correlation is −43.78145 a.u. So the difference in energy between the two structures at the CASSCF MP2 level is 6.3 kcal mol^{-1}. The degenerate orbitals of the excited state are given in Fig. 7. The different modes of vibration of the linear excited $D_{\infty h}$ state are provided in Table 3. The bending mode at a frequency of 198.15 cm^{-1} is responsible for the Renner–Teller effect. The total energy of linear molecules with three or more atoms is reduced by bending the molecule so that the degeneracy is lifted to produce two non-degenerate components.[66] Here, the breakdown of the Born–Oppenheimer approximation is the Renner–Teller effect,[26] which lifts the degeneracy as the molecule bends. This leads to a conical intersection which ultimately forms two bond stretch isomers *via* their respective transition states. The conical intersections have slightly bent structures with an angle of 167.65°, a Be–Be bond length of 2.141 Å and an energy of −43.63462 a.u. at the CASSCF(8,6)/6-311++G(d) level of theory. At the CASSCF MP2

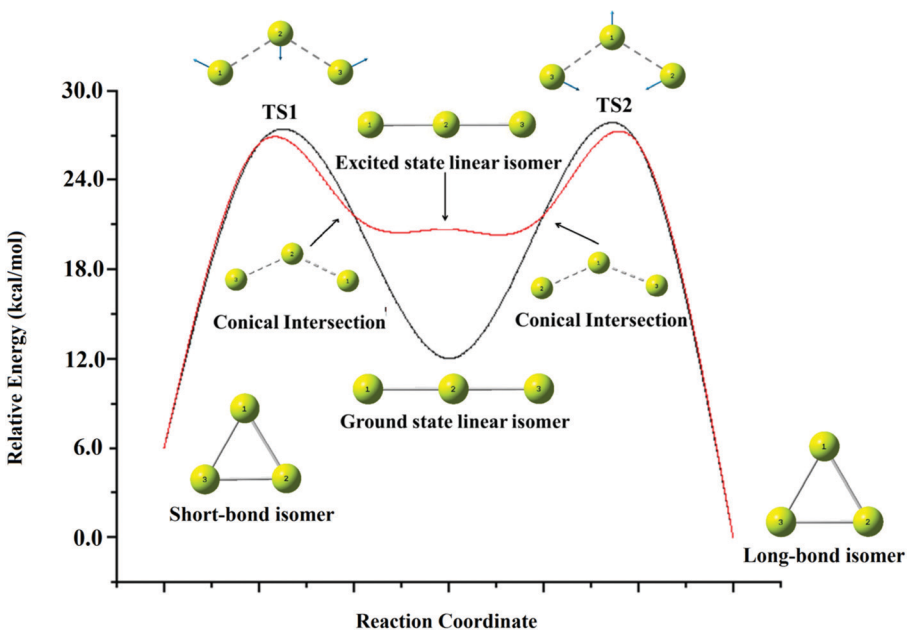

Fig. 6 Schematic representation of the bond stretch isomerism in the Be_3^{2-} molecule at the CASSCF(8,6)/6-311++G(d) level of theory.

 This journal is © the Owner Societies 2019

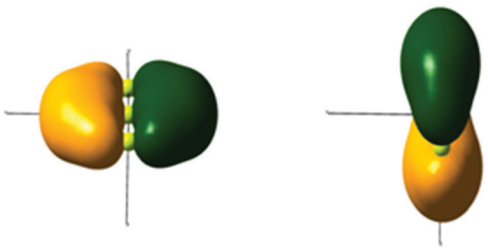

Fig. 7 The SOMOs of the linear excited state of Be_3^{2-}.

Table 3 The modes of vibration of the excited state $D_{\infty h}$ Be_3^{2-} along with the vibrational energy in cm^{-1} obtained at the CASSCF/6-311++G(d) level

Energy of the vibration of linear $D_{\infty h}$ in cm^{-1}	Assignment of the vibration
198.15	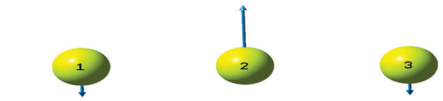 BENDING
433.29	SYMMETRIC STRETCHING
721.31	ASYMMETRIC STRETCHING

level the energy computed is −43.78145 a.u. considering the dynamic correlations with an angle of 172.02° and a bond length of 2.138 Å. A schematic representation of the phenomenon is provided in Fig. 6.

The intermediate linear isomer is non-degenerate in its ground state (Fig. 4), but the excited state is found to possess a degenerate HOMO and LUMO as shown in Fig. 7, which goes through slightly bent geometries at the conical intersections to reach the ground state potential energy surface. So this explains the underlying mechanism for the presence of two bond stretch isomers in Be_3^{2-}, which had remained an intriguing question since the observation of the phenomenon of bond stretch isomerism in the Be_3^{2-} molecule.

The variation of the hardness (η), electrophilicity (ω), chemical potential (μ) and relative energy (ΔE) is studied along the conversion pathway from the short-bond isomer to the linear isomer *via* TS1 and from linear to long-bond *via* TS2. It is noted that the hardness and electrophilicity are not a minimum and a maximum, respectively, at TS1 and TS2. The conversions from reactant to intermediate and intermediate to product *via* TS1 and TS2 are not through the constant chemical potential path,[50,67] thus they are not corroborating the MHP and MEP. Isomerization processes are often accompanied by drastic changes in the external potential as well. Moreover, it is reported that the pseudo Jahn–Teller effect is the reason behind several exceptions found to the MHP[68,69] and here the bond stretch isomerism in the molecule arises due to Renner–Teller effect, which is a specific case of the Jahn–Teller effect. Thus, the divergence from the MHP and MEP is not unexpected here; rather this deviation, in turn, corroborates the occurrence of the Renner–Teller effect. However, in both the above cases it is evident that these indices are rapidly varying near the stationary points[70] (ESI,† Fig. S2 and S3). The free energy profile of the isomerization process (Fig. 8) shows the schematic path from the short-bond isomer to the linear intermediate *via* TS1 and the path from the linear intermediate to the long-bond isomer *via* TS2. From this plot we can infer that the energy barrier between the short-bond isomer and the intermediate is

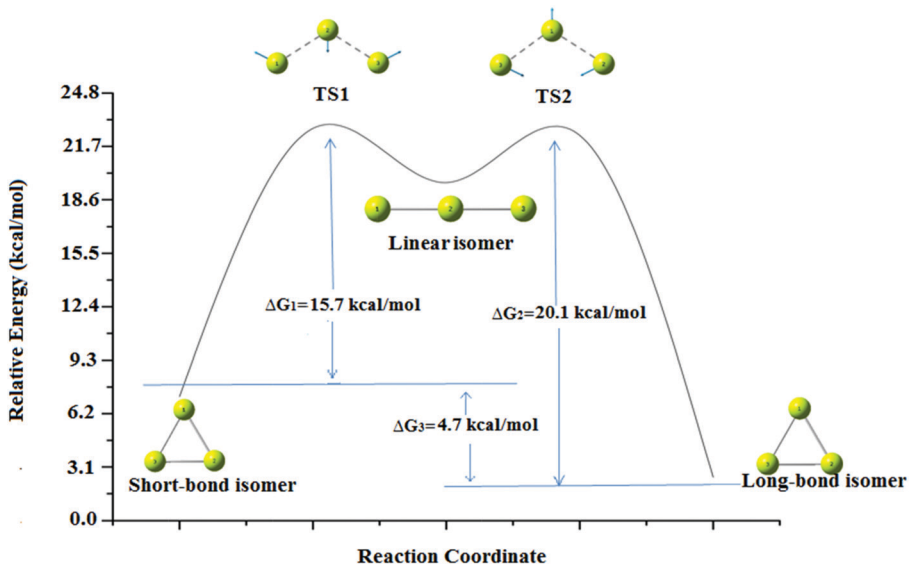

Fig. 8 Free energy profile showing the path from the short-bond isomer to the intermediate *via* TS1 and from the intermediate to the long-bond isomer *via* TS2.

Table 4 Aromatic stabilization energy of the two D_{3h} isomers in kcal mol^{-1}

ASE for the short-bond isomer of Be_3^{2-} (kcal mol^{-1})	ASE for the long-bond isomer of Be_3^{2-} (kcal mol^{-1})
8.5	9.7

comparatively smaller than the energy gap between the long-bond isomer and the intermediate.

The aromaticity of a molecule is inherently associated with its stability. As Be_3^{2-} is a simple aromatic moiety with 2-electron aromaticity, the aromatic stabilization energies of the two D_{3h} isomers are calculated (Table 4) using a recently proposed theoretical model.[55–57] The long-bond isomer has been computed to have a higher ASE as compared to the short-bond isomer, thereby correlating to the order of the ground state stability of the respective D_{3h} bond stretch isomers.

Conclusion

In the present work, comprehension of the inter-conversion between the bond stretch isomers of Be_3^{2-} is unveiled. We illuminate the underlying rationale for the phenomenon of bond stretch isomerism in Be_3^{2-} and suggest that the Renner–Teller effect of the degenerate excited state linear intermediate is the main driving force behind the occurrence of bond stretch isomerism in Be_3^{2-}. The potential energy surfaces connecting different isomers through transition states and conical intersections are elucidated. Simulations based on the ADMP method support the fact of isomerization through the linear intermediate. The hardness and electrophilicity profiles also support the occurrence of the Renner–Teller effect in this bond stretch isomerism. The stability ordering of the bond stretch isomers is in consonance with the calculated aromatic stabilization energy. Thus, as a whole this work provides an explanation for the intriguing phenomenon of bond stretch isomerism in Be_3^{2-}.

Conflicts of interest

There are no conflicts to declare.

Acknowledgements

MH & SM thank the Center for Theoretical Studies for the CTS Visitor program. In addition, SM would like to thank the Department of Educational Science, Assam University, Silchar. AM thanks CSIR, Government of India, for financial support. PKC thanks DST, New Delhi for the J. C. Bose National Fellowship. The authors are thankful to Dr Satadal Paul for his insightful suggestions.

References

1 W. D. Stohrer and R. Hoffmann, *J. Am. Chem. Soc.*, 1972, **94**, 779–786.
2 W. D. Stohrer and R. Hoffmann, *J. Am. Chem. Soc.*, 1972, **94**, 1661–1668.
3 Y. Jean, A. Lledos, J. K. Burdett and R. Hoffmann, *J. Am. Chem. Soc.*, 1988, **110**, 4506–4516.
4 A. V. Butcher and J. Chatt, *J. Chem. Soc. A*, 1972, 2652–2656.
5 M. M. Goodgame and W. A. Goddard III, *Phys. Rev. Lett.*, 1985, **54**, 661.
6 M. Moskovits, W. Limm and T. Mejean, *J. Chem. Phys.*, 1985, **82**, 4875.
7 M. M. Rohmer and M. Benard, *Chem. Soc. Rev.*, 2001, **30**, 340–354.
8 K. Wieghardt, G. Backes-Dahmann, B. Nuber and J. Weiss, *Angew. Chem., Int. Ed. Engl.*, 1985, **24**, 777–778.
9 G. Parkin, *Acc. Chem. Res.*, 1992, **25**, 455–460.
10 G. Parkin, *Chem. Rev.*, 1993, **93**, 887–912.
11 M. M. Rohmer, A. Strich, M. Benard and J. P. Malrieu, *J. Am. Chem. Soc.*, 2001, **123**, 9126–9134.
12 J. Song and M. B. Hall, *Inorg. Chem.*, 1991, **30**, 4433–4437.
13 P. Comba, A. Hauser, M. Kerscher and H. Pritzkow, *Angew. Chem., Int. Ed.*, 2003, **42**, 4536–4540.
14 I. Antol, M. Eckert-Maksić, H. Lischka and Z. B. Maksić, *Chem. Phys. Chem.*, 2004, **5**, 975–981.
15 K. T. Petrov, B. Pinter and T. Veszpremi, *J. Organomet. Chem.*, 2012, **706**, 84–88.
16 T. Goswami, S. Paul, S. Mandal, A. Misra, A. Anoop and P. K. Chattaraj, *Int. J. Quantum Chem.*, 2015, **115**, 426–433.
17 P. K. Chattaraj, D. R. Roy, M. Elango and V. Subramanian, *J. Phys. Chem. A*, 2005, **109**, 9590–9597.
18 P. K. Chattaraj and S. Giri, *THEOCHEM*, 2008, **865**, 53–56.
19 S. Giri, D. R. Roy, S. Duley, A. Chakraborty, R. Parthasarathi, M. Elango, R. Vijayaraj, V. Subramanian, R. Islas, G. Merino and P. K. Chattaraj, *J. Comput. Chem.*, 2010, **31**, 1815–1821.
20 D. R. Roy and P. K. Chattaraj, *J. Phys. Chem. A*, 2008, **112**, 1612–1621.
21 B. G. A. Brito, G. Q. Hai and L. Candido, *Chem. Phys. Lett.*, 2013, **586**, 108–110.
22 S. Paul and A. Misra, *Inorg. Chem.*, 2011, **50**, 3234–3246.
23 S. Mondal and P. K. Chattaraj, *Chem. Phys. Lett.*, 2014, **593**, 128–131.
24 J. O. C. Jiménez-Halla, E. Matito, L. Blancafort, J. Robles and M. Solà, *J. Comput. Chem.*, 2011, **32**, 372–373.
25 F. P. Di Nicola, M. Lanzi, F. Marchetti, G. Pampaloni and S. Zacchini, *Dalton Trans.*, 2015, **44**, 12653–12659.
26 R. Renner, *Z. Phys.*, 1934, **92**, 172–193.
27 G. Herzberg and E. Teller, *Z. Phys. Chem. B*, 1933, **21**, 410–446.
28 G. Herzberg, *Molecular Spectra and Molecular Structure*, Krieger, Malabar, Reprint edn, 1991, vol. III.
29 R. Dennington, T. Keith and J. Millam, *GaussView, Version 5*, Semichem Inc., Shawnee Mission KS, 2009.
30 M. J. Frisch, G. W. Trucks, H. B. Schlegel, G. E. Scuseria, M. A. Robb, J. R. Cheeseman, G. Scalmani, V. Barone, B. Mennucci, G. A. Petersson, H. Nakatsuji, M. Caricato, X. Li, H. P. Hratchian, A. F. Izmaylov, J. Bloino, G. Zheng, J. L. Sonnenberg, M. Hada, M. Ehara, K. Toyota, R. Fukuda, J. Hasegawa, M. Ishida, T. Nakajima, Y. Honda, O. Kitao, H. Nakai, T. Vreven, J. A. Montgomery, Jr., J. E. Peralta, F. Ogliaro, M. Bearpark, J. J. Heyd, E. Brothers, K. N. Kudin,

 This journal is © the Owner Societies 2019

V. N. Staroverov, T. Keith, R. Kobayashi, J. Normand, K. Raghavachari, A. Rendell, J. C. Burant, S. S. Iyengar, J. Tomasi, M. Cossi, N. Rega, J. M. Millam, M. Klene, J. E. Knox, J. B. Cross, V. Bakken, C. Adamo, J. Jaramillo, R. Gomperts, R. E. Stratmann, O. Yazyev, A. J. Austin, R. Cammi, C. Pomelli, J. W. Ochterski, R. L. Martin, K. Morokuma, V. G. Zakrzewski, G. A. Voth, P. Salvador, J. J. Dannenberg, S. Dapprich, A. D. Daniels, O. Farkas, J. B. Foresman, J. V. Ortiz, J. Cioslowski and D. J. Fox, *Gaussian 09, Revision C.01*, Gaussian, Inc., Wallingford CT, 2010.

31 J. J. McDouall, K. Peasley and M. A. Robb, *Chem. Phys. Lett.*, 1988, **148**, 183–189.

32 F. Bernardi, A. Bottoni, M. J. Field, M. F. Guest, I. H. Hillier, M. A. Robb and A. Venturini, *J. Am. Chem. Soc.*, 1988, **110**, 3050–3055.

33 G. Tonachini, H. B. Schlegel, F. Bernardi and M. A. Robb, *J. Am. Chem. Soc.*, 1990, **112**, 483–491.

34 *Proceedings of Modern Methods and Algorithms of Quantum Chemistry*, ed. D. Marx, J. Hutter and J. Grotendorst, John von Neumann Institute for Computing, Jurich, Germany, 2000.

35 H. B. Schlegel, J. M. Millam, S. S. Iyengar, G. A. Voth, A. D. Daniels, G. E. Scuseria and M. J. Frisch, *J. Chem. Phys.*, 2011, **114**, 9758–9763.

36 S. S. Iyengar, H. B. Schlegel, J. M. Millam, G. A. Voth, G. E. Scuseria and M. J. Frisch, *J. Chem. Phys.*, 2011, **115**, 10291–10302.

37 H. B. Schlegel, S. S. Iyengar, X. Li, J. M. Millam, G. A. Voth, G. E. Scuseria and M. J. Frisch, *J. Chem. Phys.*, 2002, **117**, 8694–8704.

38 R. G. Pearson, *J. Chem. Educ.*, 1987, **64**, 561–567.

39 R. G. Parr and P. K. Chattaraj, *J. Am. Chem. Soc.*, 1991, **113**, 1854–1855.

40 P. W. Ayers and R. G. Parr, *J. Am. Chem. Soc.*, 2000, **122**, 2010–2018.

41 P. K. Chattaraj and S. Sengupta, *J. Phys. Chem.*, 1996, **100**, 16126–16130.

42 P. Fuentealba, Y. Simon-Manso and P. K. Chattaraj, *J. Phys. Chem. A*, 2000, **104**, 3185–3187.

43 S. Pan, M. Solà and P. K. Chattaraj, *J. Phys. Chem. A*, 2013, **117**, 1843–1852.

44 R. Saha, S. Pan and P. K. Chattaraj, *Molecules*, 2016, **21**, 1477–1493.

45 E. Chamorro, P. K. Chattaraj and P. Fuentealba, *J. Phys. Chem. A*, 2003, **107**, 7068–7072.

46 R. Parthasarathi, M. Elango, V. Subramanian and P. K. Chattaraj, *Theor. Chem. Acc.*, 2005, **113**, 257–266.

47 P. Geerlings, P. F. De and W. Langenaeker, *Chem. Rev.*, 2003, **103**, 1793–1874.

48 P. K. Chattaraj, *J. Indian Chem. Soc.*, 1992, **69**, 173–183.

49 R. G. Parr, R. A. Donnelly, M. Levy and W. E. Palke, *J. Chem. Phys.*, 1978, **68**, 3801.

50 P. K. Chattaraj, U. Sarkar and D. R. Roy, *Chem. Rev.*, 2006, **106**, 2065–2091.

51 P. K. Chattaraj and D. R. Roy, *Chem. Rev.*, 2007, **107**, PR46–PR74.

52 R. G. Parr, L. v. Szentpaly and S. Liu, *J. Am. Chem. Soc.*, 1999, **121**, 1922–1924.

53 T. A. Koopmans, *Physica*, 1933, **1**, 104–113.

54 J. F. Janak, *Phys. Rev. B: Condens. Matter Mater. Phys.*, 1978, **18**, 7165.

55 S. Paul, T. Goswami and A. Misra, *AIP Adv.*, 2015, **5**, 107211.

56 T. Goswami, M. Homray, S. Paul, D. Bhattacharya and A. Misra, *Phys. Chem. Chem. Phys.*, 2017, **19**, 11744–11747.

57 M. Homray, S. Paul and A. Misra, *Bull. Mater. Sci.*, 2019, **42**, 46.

58 P. W. Anderson, *Phys. Rev.*, 1950, **79**, 350.

59 P. W. Anderson, *Phys. Rev.*, 1959, **115**, 2.

60 P. W. Anderson, Theory of the magnetic interaction: exchange in insulators and superconductors, in *Solid State Physics*, ed. F. Turnbull and F. Seitz, Academic Press, New York, 1963, vol. 14, p. 99.

61 S. Paul and A. Misra, *J. Chem. Theory Comput.*, 2012, **8**, 843–853.

62 T. Lu and F. Chen, *J. Comput. Chem.*, 2012, **33**, 580–592.

63 The DFT code, OPENMX, is available at http://www.openmx-square.org under the GNU General Public License.

64 M. J. S. Dewar, E. F. Healy and J. J. Stewart, *J. Chem. Soc., Faraday Trans. 2*, 1984, **80**, 227–233.

65 A. D. Walsh, *J. Chem. Soc.*, 1953, 2260–2266.

66 M. Peric, E. Engles and S. D. Peyerimhoff, in *Quantum Mechanical Electronic Structure Calculations with Chemical Accuracy*, ed. S. R. Langhoff, Kluwer, Dordrecht, 1995, p. 261.

67 T. Kar and S. Scheiner, *J. Phys. Chem.*, 1995, **99**, 8121–8124.

68 M. Torrent-Sucarrat, L. Blancafort, M. Duran, J. Luis and M. Solà, in *Theoretical Aspects of Chemical Reactivity*, ed. A. Toro-Labbe, Elsevier, Amsterdam, 2007.

69 M. Torrent-Sucarrat, J. M. Luis, M. Duran and M. Solà, *J. Chem. Phys.*, 2002, **117**, 10561.

70 P. K. Chattaraj, P. Pérez, J. Zevallos and A. Toro-Labbé, *J. Phys. Chem. A*, 2001, **105**, 4272–4283.